Aprovechamiento del calor residual a baja temperatura mediante bombas de calor para la producción de agua caliente

PhD Thesis

Estefanía Hervás Blasco

Supervisors

Dr. D. José Miguel Corberán Salvador

Dr. D. Emilio Navarro Peris

Enero 2020

Low temperature waste water heat recovery for Domestic Hot Water production based on heat pumps

PhD Thesis

Estefanía Hervás Blasco

Supervisors

Dr. D. José Miguel Corberán Salvador

Dr. D. Emilio Navarro Peris

January 2020

Endless energy exists in humans driven

by their passions

Acknowledgments

En primer lugar me gustaría mencionar a mis directores de Tesis, José Miguel y Emilio, sin ellos, este trabajo sencillamente no se hubiera podido llevar a cabo. Gracias por darme la oportunidad de trabajar en el IIE y de hacerlo dentro del proyecto "APROVECHAMIENTO DEL CALOR RESIDUAL A BAJA TEMPERATURA MEDIANTE BOMBAS DE CALOR PARA LA PRODUCCION DE AGUA CALIENTE" a través de una beca FPI del Ministerio de Economía y Competitividad. También, gracias por todo el tiempo dedicado, las ideas, lo que me habéis enseñado y el apoyo moral recibido, especialmente, en los momentos donde todavía no estaba cerrado el problema y en esta última etapa de redacción, donde habéis realizado un esfuerzo extra por ayudarme. A José Miguel, por su paciencia, su tiempo (no sé cómo lo lograba, pero siempre encontraba un hueco para mirar lo que fuera) y su sabiduría. Trabajar con él es simplemente un placer. A Emilio, por su forma de pensar, por su mente imparable e incansable a la vez, y por su tozudez, que han resultado en horas y horas de discusiones y aprendizaje realmente interesantes. Trabajar con él es todo un lujo.

Otra persona imprescindible en este trabajo ha sido Miquel, a partir de cuya tesis comenzó la mía. Gracias por estar siempre disponible y dispuesto (desde cualquier parte del mundo) a ayudar, contribuir y a compartir tu visión de la vida en todas las horas que hemos pasado Emilio, tú y yo. Será inevitable que el término exergía me recuerde a vosotros.

Gracias a todos los compañeros del IIE que están o han estado a lo largo de mi estapa, todos sois la esencia del instituto y hacéis que trabajar, se lleve con más alegría. A todas las personas que de una forma u otra han participado en este trabajo, especialmente, a los incondicionales, Álex y Rafa, por estar siempre dispuestos a ayudarme y por lograr convivir con mi obsesión por el orden, a Antonio, Alberto y Paloma, por su disponibilidad en el laboratorio, a Javi Marchante, por escucharme, ayudarme y por su trabajo de correlaciones, a Toni y Joan, por introducirme y asesorarme con Trnsys y R y a Fernando, por los findes y *deshoras* compartidas durante esta etapa final. A título más personal, no podría dejarme a mis compañeras de despacho, Bárbara y Laeti, una me incitó a cocinar, y la otra me introdujo en el mundo de correr, pero sobre todo, las más de ocho horas diarias compartidas hace que sean, amigas.

A todos los que comenzamos y vivimos la etapa universitaria juntos, por continuar creyendo siempre en mi (Fer, Cris, Alba, Empar, Antonio, Peremen, Ru, Huertas, David, Javi, Truji, Vir, Irene y Ale), que nunca dejemos de disfrutar de esas conversaciones *mundanas*.

A las imprescindibles en mi vida, María, Elisa, Irene, Susi, Ara y Chiquen, porque sin ellas, simplemente no sería "yo". Gracias por estar siempre conmigo.

A Jesús, por ser y estar. Por su paciencia, respeto, disposición, y por compartir su inteligencia y puntos de vista conmigo, la vida contigo es un aprendizaje continuo que, espero, sea *eterno*.

Por último, quería agradecer a mi familia todo el tiempo robado, el apoyo incondicional y confianza que tienen en mi, no únicamente en la etapa de la tesis, sino a lo largo de toda la vida. A mis tíos, porque son como mis padres y siempre están ahí cuando se les necesita. A mi padre, por su cabezonería, perseverancia, resiliencia y *patiment*. A mi madre, por su punto de locura, frescura, incoherencia y alegría. Mi existencia y forma de ser, os la debo a vosotros. A mi hermana, por ser la persona más afín a mi, por las innumerables horas de teléfono que hacen que a pesar de la distancia, sigas siendo mi compañera por excelencia. Y a mis abuelos, a los que se fueron y de los que tanto aprendí, y a Carmen, porque como siempre dice: "la mejor herencia que pueden dejarte tus padres es la educación". Gracias.

Abstract

A significant percentage of energy is destined to Domestic Hot Water (DHW) production in the building sector. Furthermore, most of that energy contained in the water is wasted to the ambient after its use.

Heat pumps have been clearly identified as an efficient technology for DHW production, as a main technology towards future de-carbonization of cities. In addition, they could use the heat from the wastewater as a heat source. Thus, contributing in two ways towards a more environmentally friendly energy sector.

However, the use of heat pumps for DHW based on heat recuperation from wastewater faces several challenges that require further analysis and development:

1. A heat pump design capable to operate with high performance when variable secondary temperature lifts at the heat sink take place.
2. A heat pump design capable to operate with high performance when variable secondary temperature lifts at the heat source take place.
3. The integration of the heat pump within a system (heat recovery strategies, components, sizing, operation strategy).

Usually, transcritical cycles have been considered the most suitable for DHW production (high temperature lifts of the heat sink, 10-60°C). However, these cycles involve several drawbacks as for instance the requirement of high pressures in the installation or a significant reduction of the performance with the increase of water inlet temperature at the condenser. Instead, subcritical cycles have demonstrated great potential for DHW applications if a proper control of subcooling is performed.

The objective of this thesis is to investigate the most efficient water-to-water heat pump working with a subcritical cycle for DHW production using as a heat source wasted heat at medium-low temperature and to determine the most efficient system based on heat pumps for this application.

The work is divided in two differentiated parts:

- Heat pump concept

This development is a continuation from the PhD work of M. Pitarch [1]. In that PhD work, the role of subcooling in the performance of a subcritical heat pump for DHW applications was investigated. Two different configurations of a heat pump prototype were designed based on the way subcooling was made. Results showed that a subcooling optimized subcritical heat pump was able to provide comparable performances than present HPs employing transcritical cycles. However, both configurations required an additional component compared to usual heat pumps. Thus, a new prototype based only on the typical components (compressor, condenser, expansion valve and evaporator) was proposed as future work.

In this thesis, a theoretic analysis of the heat pump was done. A subcooling control methodology was developed and tested. The proposed prototype in [1] has been built and characterized. From all the results, the most convenient heat pump design was obtained.

- Integral Heat pump-DHW system

The integration of the most convenient HP prototype within a system for DHW production based on heat recovery from wastewater has been analyzed. The research has included the development of a model of the entire system in Trnsys and the optimization of the main components of the system. That is, their sizing and their operation in order to reach the maximum global efficiency of the complete system. Due to the complexity of the problem, the analysis was performed in three main steps: first, a study of the direct heat exchange, second, an study focusing on the condenser side, that is, assuming an infinite heat source (large availability of sewage water for instance) and third, the focus was done on the evaporator side. That is, the optimization of the complete system in which a finite heat source is considered (grey water collected from buildings for instance).

The simplest and most efficient system required in DHW production and heat recuperation from wastewater has been determined. It consists of one heat exchanger (recuperator), one subcooled heat pump and two storage tanks. Regardless the dependence of its performance on external conditions (temperatures and profiles of the heat source and sink), the system is able to provide all the required DHW for instance in a building with 20 dwellings with an annual COP of the system of 6.7 by only using their self-greywater.

Resum

Un percentatge significatiu de l'energia es destina a la producció d'Aigua Calenta Sanitària (ACS) en el sector comercial i residencial. A més, la major part de l'energia que conté l'aigua es malgasta en l'ambient després del seu ús.

Les bombes de calor han sigut identificades per la seua capacitat de produir ACS amb una alta eficiència i són una gran alternativa cap a la descarbonització de les ciutats. A més, són capaços d'utilitzar com a font de calor, el calor contingut en l'aigua que actualment es desaprofita. Contribuint així, a aconseguir un sector energètic més respectuós amb el Medi Ambient.

No obstant això, l'aplicació de l'ús de bombes de calor per a ACS recuperant el calor de les aigües residuals presenta unes característiques diferents de les usuals en bombes de calor. Per tant, és necessari una anàlisi del problema més profund i es requereix una major investigació al respecte amb la finalitat d'aconseguir una alta eficiència:

1. Un disseny de bomba de calor capaç d'operar amb alta eficiència davant dels grans salts de temperatura presents en aquesta aplicació (ACS).
2. Un disseny de bomba de calor capaç d'operar amb alta eficiència davant de salts de temperatura del fluid secundari variables (recuperació de calor).
3. La integració d'aquesta bomba de calor en un sistema d'ACS complet (estratègies de recuperació de calor, components, grandària i estratègia de control).

Normalment, els cicles transcrítics han sigut considerats com una de les millors solucions per a la producció d'ACS (on es tenen grans salts de temperatura en l'aigua, 10-60°C). No obstant això, aquest tipus de cicle presenta dos desavantatges principals, la necessitat d'altes pressions en la instal·lació i la dependència de l'eficiència amb el salt de temperatura de l'aigua en el condensador i evaporador. Concretament, s'observa una reducció significativa de l'eficiència quan la temperatura de l'aigua a l'entrada del condensador augmenta. No obstant això, els cicles subcrítics han demostrat un gran potencial per a salts de temperatura de l'aigua variables si s'aplica un control del subrefredament adequat.

L'objectiu d'aquesta tesi és investigar la bomba de calor aigua-aigua més eficient treballant amb un cicle de refrigerant subcrític per a la producció d'ACS utilitzant com a font de calor el calor disponible en les aigües residuals (a baixa-mitja temperatura) per a determinar el sistema més eficient en aquest tipus d'aplicació.

El treball es dividix en dos parts diferenciades:

- Disseny de la bomba de calor

El desenvolupament de la bomba de calor és una continuació del treball realitzat en la tesi de M. Pitarch [1]. En aquella tesi, es va investigar el paper del subrefredament en una bomba de calor subcrítica per a l'apliació d'ACS. Es va desenvolupar un prototip de bomba de calor amb el disseny de dues configuracions distintes en funció de la manera en què es realitzava el subrefredament. Els resultats van permetre concloure que aquests tipus de bombes de calor (subcrítiques) eren capaços d'operar amb eficiències semblants a les de les bombes de calor basades en cicles transcrítics si s'opera amb un grau de subrefredament òptim. No obstant això, en ambdues configuracions es requereix un component més que en les bombes de calor convencionals. Per tant, es proposa el disseny d'un nou prototip basat únicament en els components típics (compressor, condensador, vàlvula d'expansió i evaporador) com a treball futur.

En la present tesi, es va realitzar un estudi i anàlisi teòric de la bomba de calor. Es va desenvolupar i implementar una estratègia de control per al subrefredament i es va construir el prototip de bomba de calor proposat en [1]. De tot aquest treball s'ha obtingut el disseny de bomba de calor basada en cicles subcrítics més interessant per aquest tipus d'aplicacions.

- Disseny i integració de la Bomba de Calor i el sistema d'ACS

La integració del prototip seleccionat en un sistema per a la producció d'ACS amb recuperació de el calor de les aigües residuals ha sigut analitzada. En aquesta investigació s'inclou el desenvolupament d'un model del sistema complet en Trnsys i l'optimització dels components principals del sistema: la seua dimensió i la seua operació amb l'objectiu d'aconseguir una eficiència global màxima del sistema complet. Donada la complexitat del problema, l'anàlisi s'ha dut a terme en tres passos principals: primer, l'estudi d'un intercanvi de calor directa, segon, s'ha focalitzat en la part del costat del condensador, és a dir, considerant una font de calor infinita (gran disponibilitat d'aigua, per exemple, en desaigües comuns) i finalment, el focus s'ha realitzat en la part de l'evaporador, és a dir, s'ha dut a terme l'optimització del sistema complet en què es té una disponibilitat de calor limitada (per exemple, les aigües grises d'un edifici).

El sistema més simple i eficient necessari per a aquest tipus d'aplicacions (producció d'ACS amb recuperació de el calor provinent d'aigües grises) està compost per un bescanviador de calor (recuperador), una bomba subrefredada i dos depòsits d'emmagatzemament. A pesar de la dependència de l'eficiència del sistema amb la temperatura i disponibilitat de la font de calor, així com de la demanda d'ACS, per exemple, el sistema és capaç de produir la demanda requerida d'ACS per a un edifici de 20 habitatges amb un COP anual de 6.7 a partir de el calor continguda en les aigües grises generades pel propi edifici.

Resumen

Un porcentaje significativo de la energía se destina a la producción de Agua Caliente Sanitaria (ACS) en el sector comercial y residencial. Además, la mayor parte de la energía que contiene el agua se desperdicia en el ambiente tras su uso.

Las bombas de calor han sido identificadas por su capacidad de producir ACS con una alta eficiencia y son una gran alternativa hacia la descarbonización de las ciudades. Además, son capaces de utilizar como fuente de calor, el calor contenido en el agua que actualmente se desperdicia. Contribuyendo así a conseguir un sector energético más respetuoso con el Medio Ambiente.

Sin embargo, la aplicación del uso de bombas de calor para ACS recuperando el calor de las aguas residuales presenta unas características diferentes a las usuales en bombas de calor. Por tanto, es necesario un análisis del problema más profundo y se require mayor investigación al respecto con el fin de lograr un desarrollo eficiente de la misma:

1. Un diseño de bomba de calor capaz de operar con alta eficiencia ante los grandes saltos de temperatura que tienen lugar en esta aplicación (ACS).
2. Un diseño de bomba de calor capaz de operar con alta eficiencia ante saltos de temperatura del fluido secundario variables (recuperación de calor).
3. La integración de esta bomba de calor en un sistema de ACS completo (estrategias de recuperación de calor, componentes, tamaño y estrategia de control).

Normalmente, los ciclos transcríticos han sido considerados como una de las mejores soluciones para la producción de ACS (donde se tienen grandes saltos de temperatura en el agua, 10-60°C). Sin embargo, este tipo de ciclo presenta dos desventajas principales, la necesidad de altas presiones en la instalación y la dependencia de la eficiencia con el salto de temperatura del agua en el condensador. Concretamente, se observa una reducción significativa de la eficiencia cuando la temperatura del agua a la entrada del condensador aumenta. Sin embargo, los ciclos subcríticos han demostrado un gran potencial para saltos de temperatura del agua variables si se aplica un control del subenfriamiento adecuado.

El objetivo de esta tesis es investigar la bomba de calor agua-agua más eficiente trabajando con un ciclo de refrigerante subcrítico para la producción de ACS utilizando como fuente de calor el calor disponible en las aguas residuales (a baja-media temperatura) para determinar el sistema más eficiente para este tipo de aplicación.

El trabajo se divide en dos partes diferenciadas:

- Diseño de la bomba de calor

El desarrollo de la bomba de calor es una continuación del trabajo realizado en la tesis de M. Pitarch [1]. En dicha tesis, se investigó el papel del subenfriamiento en una bomba de calor subcrítica para la apliación de ACS. Se desarrolló un prototipo de bomba de calor con el diseño de dos configuraciones distintas en función del modo en el que se realizaba el subenfriamiento. Los resultados permitieron concluir que este tipo de bombas de calor (subcríticas) eran capaces de operar con eficiencias similares a las de las bombas de calor basadas en ciclos transcríticos si se opera con un grado de subenfriamiento óptimo. Sin embargo, en ambas configuraciones se requiere un componente más que en las bombas de calor convencionales. Por tanto, se propone el diseño de un nuevo prototipo basado únicamente en los componentes típicos (compresor, condensador, válvula de expansión y evaporador) como un trabajo futuro.

En esta tesis, se ha realizado un estudio y análisis teórico de la bomba de calor. Se ha desarrollado e implementado una estrategia de control para el subenfriamiento y se ha construído el prototipo de bomba de calor propuesto en [1]. De todo este trabajo se ha obtenido el diseño de bomba de calor basada en ciclos subcríticos más interesante para este tipo de aplicaciones.

- Diseño e integración de la Bomba de Calor y el sistema de ACS

La integración del prototipo seleccionado en un sistema para la producción de ACS con recuperación del calor de las aguas residuales ha sido analizada.

En esta investigación se incluye el desarrollo de un modelo del sistema completo en Trnsys y la optimización de los componentes principales del sistema: su tamaño y su operación con el objetivo de lograr una eficiencia global máxima del sistema completo. Dada la complejidad del problema, el análisis se ha llevado a cabo en tres pasos principales: primero, el estudio de un intercambio de calor directo, segundo, se ha focalizado en la parte del lado del condensador, es decir, considerando una fuente de calor infinita (gran disponibilidad de agua, por ejemplo, en desagües comunes) y por último, el foco se ha realizado en la parte del evaporador, es decir,

se ha llevado a cabo la optimización del sistema completo en el que se tiene una disponibilidad de calor limitada (por ejemplo, las aguas grises de un edificio).

El sistema más simple y eficiente necesario para este tipo de aplicaciones (producción de ACS de la recuperación del calor proveniente de aguas grises) está compuesto por un intercambiador de calor (recuperador), una bomba subenfriada y dos depósitos de almacenamiento. A pesar de la dependencia de la eficiencia del sistema con la temperatura y disponibilidad de la fuente de calor, así como de la demanda de ACS, por ejemplo, el sistema es capaz de producir la demanda requerida de ACS para un edificio de 20 viviendas con un COP anual de 6.7 a partir del calor contenido en las aguas grises generadas por el propio edificio.

Contents

List of figures

Figure B.1: Experimental and theoretic performance variation with the secondary temperature lift at the evaporator for zero superheat (0K1V) and 10K of superheat (10K2V) for different evaporating temperatures.

Figure B.2: Picture of a frontal view of the evaporator (face used for thermography) and a transversal view with the location of the refrigerant and water inlet/outlet ports. Thermography of the evaporator at different superheats and water temperature glides for the same water inlet temperature at the evaporator and water conditions in the condenser.

Figure B.3: Evaporating pressure and temperature variation with the water temperature glide at the evaporator for different superheats and the measured points of Figure B.2

List of tables

Nomenclature

COP	Coefficient of Performance, [-]
c_p	Specific heat capacity [kJ kg^{-1} K^{-1}]
DT	Temperature difference [K]
h	Specific enthalpy [kJ kg^{-1}]
$\dot{m}$	Mass flow rate [kg s^{-1}]
p	Pressure [bar]
$\dot{Q}$	Rate of heat transfer, [kW]
R	Calculated variable
s	Specific entropy [kJ kg^{-1} K^{-1}]
S	Sample standard deviation
Sc	Subcooling, [K]
Sh	Superheat, [K]
$S.Fluid$	Secondary Fluid
t	Student multiplier
T	Temperature [°C]
U	Uncertainty
$\dot{V}$	Volumetric flow rate [m^3 s^{-1}]
$\dot{W}$	Rate of work, power [kW]
X	Measured variable

Greek symbols

δ	differential
Δ	Variation
η	Efficiency

Subscripts

aux	Auxiliary (Such as the water pumps)
Carnot	Ideal cycle with infinite reservoirs
comp	Compressor
evap	evaporator
h	Heating
H	Heat sink
in	inlet
infinite	Infinite heat transfer area assumption
Lorenz	Ideal cycle for variable temperatures
LR	Liquid Receiver
norm	Normalized
opt	Optimal
out	Outlet
pinch	pinch point
refer	Reference conditions
rev	Reversible Cycle
sub	Subcooler
w	Water
w,ci	Water condenser/subcooler inlet
w,co	Water condenser outlet
w,ei	Water evaporator inlet

Acronyms and abbreviations

BPHE	Brazed Plate Heat Exchanger
EU	European Union
EV	Expansion Valve
GHG	Green House Gas
GWP	Global warming potential
HP	Heat Pump
HE	Heat Exchanger
LCCP	Life-Cycle Climate Performance
LR	Liquid Receiver
Max.	Maximum
ODP	Ozone depletion potential
PID	Proportional Integral Derivative control
DHW	Domestic Hot Water
TV	Throttling Valve

Chapter 1

Introduction

1.1 Motivation

Immersed in the current scenario, where the global energy consumption has been increasing along time and, according to the U.S. Energy Information Administration (EIA) [2], the raise will be at least 28% by 2040, the scarcity and the management of the resources become a real challenge for the world.

However, not only the scarcity is the focus of the energy sector. Beyond that, aspects such as the impact of the Energy sector on the environment, on the planet and on the Society also represent an important challenge. Actually, the extraordinary high CO2 concentration in the atmosphere (the highest in History), the proven sea level and temperature increase, ice melting or the ocean acidification, evidence the strong impact of human activities on Climate change and the Planet global warming [3], and a large part of this impact is due to energy consumption.

Consequently, a transformation of the energy sector towards a more sustainable and cleaner environment is necessary.

In average, approximately 40% of the energy consumption is attributed to the building sector (3/4 from residential and 1/4 from commercial). According to Figure 1.1, the energy consumption varies among countries being greater obviously in developing countries [4]. In the European Union (EU), the residential sector represents 25.4% of the final energy consumption (excluding electricity for powering the main heating, cooling or cooking systems) [5].

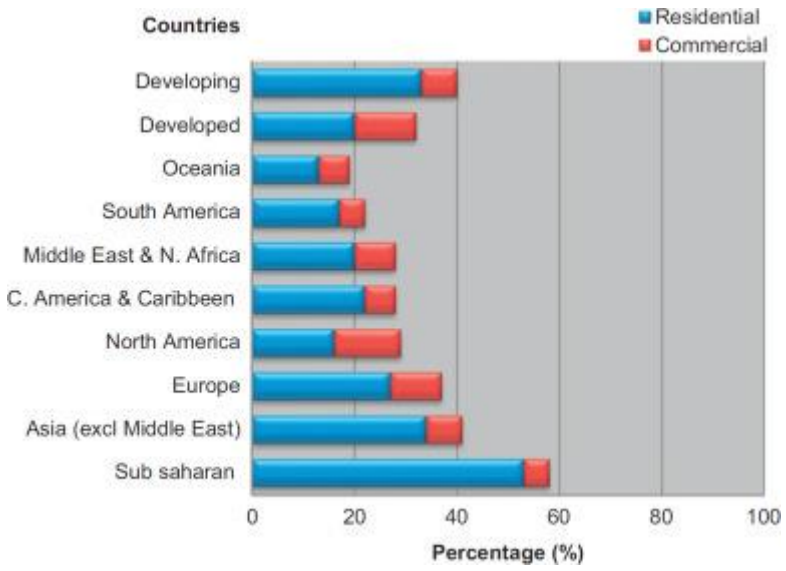

Figure 1.1: Percentage of energy consumption in building sector globally [4].

Furthermore, buildings are responsible of 1/3 of the total GHG emissions, being CO2 the main contributor. According to the European Environment Agency, in Europe the residential sector accounts for 11.5% of the CO2 emissions [6]. Hence, this sector has a direct impact on the world environment.

The commitment of the European Union in order to slow down climate change dates from 1992 after the Rio Conference. From that time, they have developed different plans based on timeframes. Currently, we are about to end the 20/20/20 plan and the new strategies will have impact on the 2030 and 2050 horizon plans. Figure 1.2 shows the European targets for 2020 and 2030 in the energy sector.

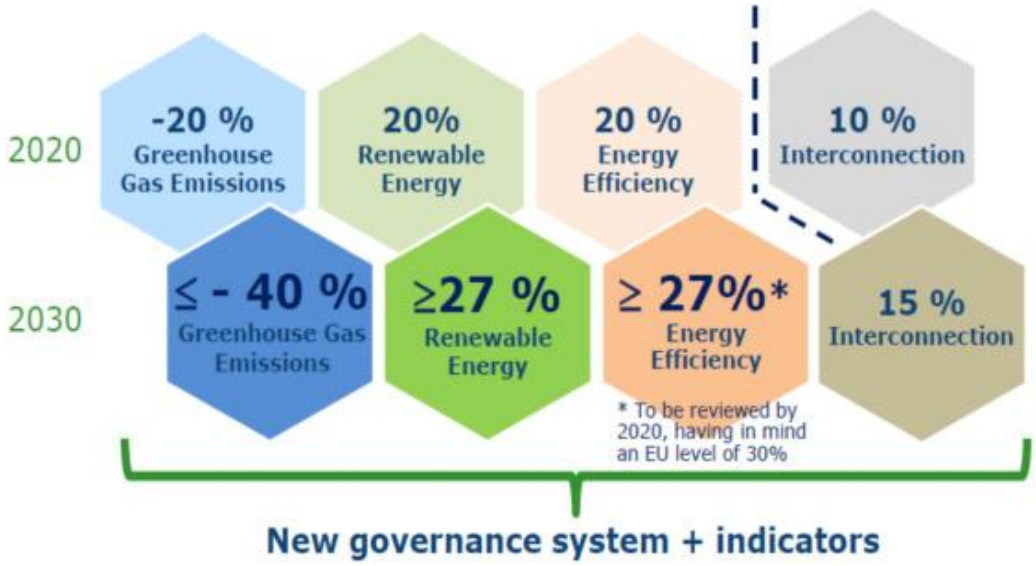

Figure 1.2: 2020 and 2030 energy targets of the European Union [7].

The main energy end-uses in the residential sector are space heating (64.7%) and water heating (14.5%)[5]. To decarbonize the sector, in the last years the focus has been mainly put on the reduction of the space heating energy consumption. The "Near Zero Energy Building and Passive House" are mandatory by the ED 2010/31/EU from 2018 in new constructions. However, while this concept significantly reduces the space heating demand through adequate insulation, orientation and air control, the water heating demand will remain very similar to the present one since it is basically dependent on the user habits. Roughly, the same domestic hot water (DHW) profiles and a constant demand is expected.

Figure 1.3 represents the energy consumption by end-use in an average house and in a passive house. As it can be observed in the figure, although the demand for hot water (DHW) will remain the same, the share in the energy consumption will dramatically increase up to almost 50% of the total house energy consumption since the energy required for the heating will substantially decrease. In addition, it should be pointed out that around 85-90% of the thermal energy employed for the DHW production is wasted through the sewage to the ambient. This loss has not been contemplated by the passive house concept yet [8] but it will have to be in the near future. Therefore, the reduction of the impact on the CO2 emissions by the residential sector will have to include in the future a significant reduction of the energy consumption for the DHW production. One of the most promising ways to do this is by recovering the heat from the waste water and by employing high efficient heat pumps. This is the main aim the present thesis points to.

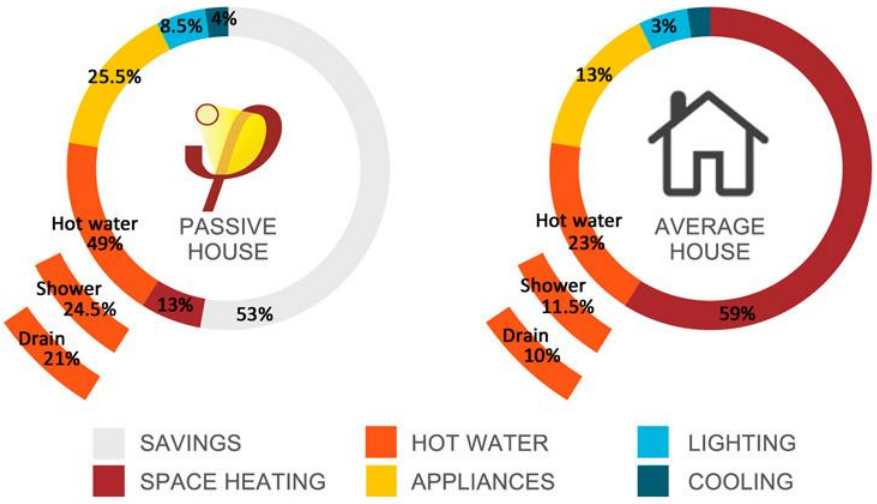

Figure 1.3: End-use energy consumption in a Passive and an average house [8]

The main technologies used to warm water or for heating applications in the building sector rely either on technologies that use fossil fuels as primary energy

source or on renewables energies (mostly solar thermal) with a back-up technology usually based on fossil fuels as primary energy as well [9]. It is worth it to remark that the electric-boilers (widest technology employed) has very low efficiency resulting in high electric consumptions. Thus, contributing to CO2 emissions increase.

On the one hand, Heat pumps (HPs) are the technology capable to overcome the main problems arisen in other technologies: they require significant less electricity to produce the same heat than electric solutions due to its much higher efficiency and they could use renewable electric sources as primary energy for their operation. In fact, heat pumps having an estimated average seasonal performance factor higher than a reference value (SPF>2.5) are recognized in the European Directive 2009/28/EC by the *"European Parliament and Council of 23 April 2009 on the promotion of the use of energy from renewable sources*" as if the energy captured by a heat pump were obtained from renewable energy sources.

On the other hand, most grey water from dwellings is directly thrown to the sewage and its heat (usually at temperature slightly higher than the ambient-25-35°C- and roughly constant through the day and year) is wasted. Moreover, this heat source is at temperature quite constant along the year, with less fluctuations and considerably higher temperature than ambient air. Hence, wastewater is a valuable source that could be effectively used as heat source for heat pumps.

The European Directive 2009/125/CE deals with the eco-design (ErP) and the energy labelling, which is mandatory for appliances with nominal capacity under 400kW is already setting very high values of global efficiency for new equipment. Figure 1.4 shows the efficiencies of the main technologies used in heating applications for the building sector and the minimum performance allowed for labelling and commercialization from 2015 onwards.

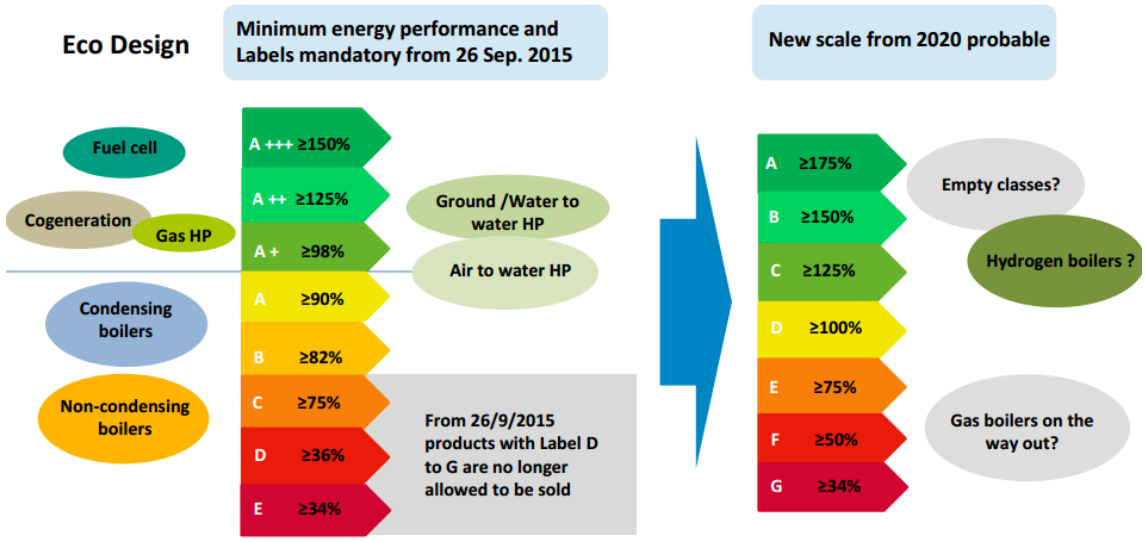

Figure 1.4: Minimum requirements of efficiency and labelling mandatory from 2015 and projection by 2020 [10].

The important role that heat pumps will play in the future of the heating and DHW production Sector is already reflected on the recent heat pump volume sales worldwide which can be seen in Figure 1.5.

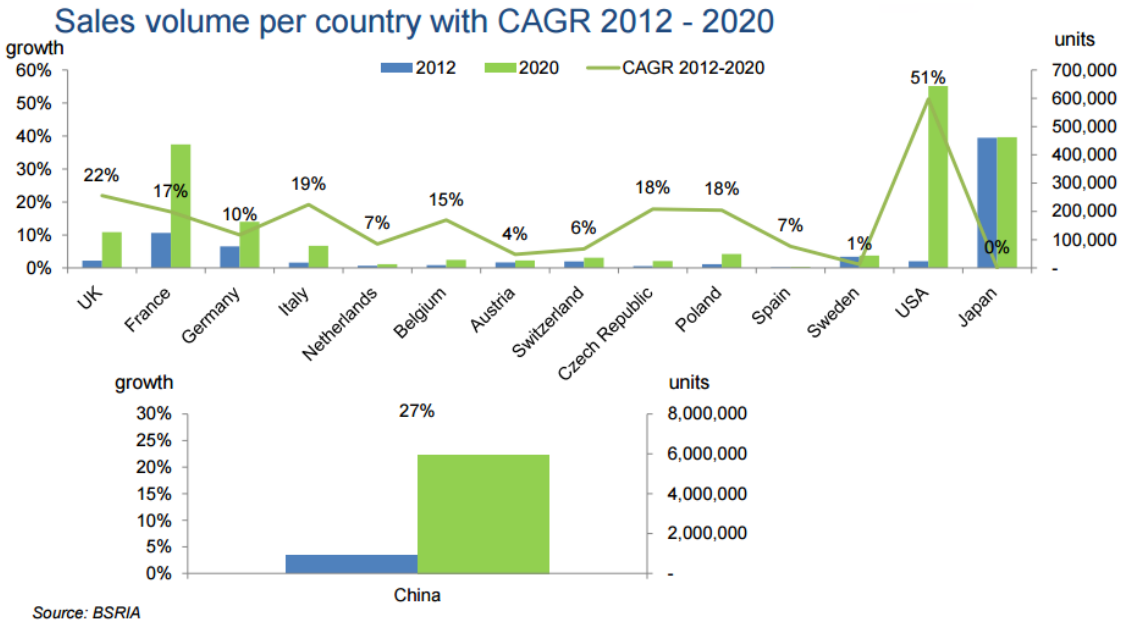

Figure 1.5: Sales volume of heat pumps to produce domestic hot water in 2012 and expected in 2020 [11].

Heat pumps to produce DHW are an efficient, reliable, committed to the environment, safe and economically affordable technology, and therefore will play

a major role in the evolution of the DHW equipment in the next future. Figure 1.6 summarizes the main advantages of the heat pump technology in the building sector.

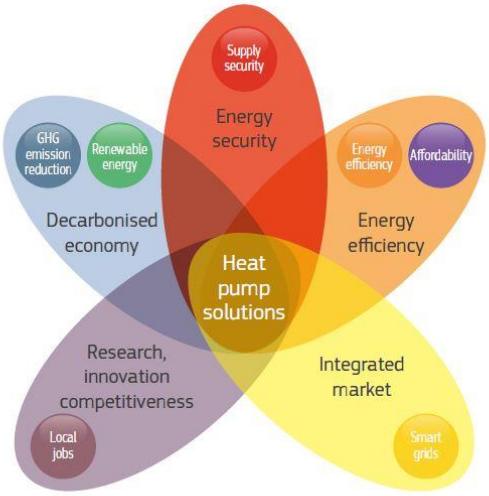

Figure 1.6: Heat pumps advantages for society [12].

In order to benefit the most from the use of heat pumps, a deep understanding of the technology and its interaction within a system for the DHW production recovering wastewater heat needs to be addressed.

Finally, the potentiality of heat pumps goes beyond the mentioned applications. Instead, it also can contribute to the global electricity supply de-carbonization. In this sense, renewables are naturally the alternative adopted by developed countries and an increase of their share in the future electric generation mix is expected. Nevertheless, renewables come with a tradeoff, the need to match production and demand. If more electric share is given to renewables, de-coupling demand and production is another challenge to overcome in order to keep the same supply quality. Thermal storage, if connected to a heat pump, could also contribute to flex the electric system allowing the reliability and efficiency of smart grids. Notwithstanding the solutions of these applications should rely on a clean, free and variable available electric energy, having a good understanding of the heat pump technology integration within systems could be valuable in order to determine an efficient solution.

The aim of this thesis is:

1. First, the optimization of a heat pump design for a water-to-water heat pump for hot water production using a natural refrigerant, with the highest possible efficiency, and the heat recuperation from grey water
2. Second, the analysis and optimization of this heat pump design, integrated within a system for DHW production and wastewater heat recuperation, from the energy point of view and the residential sector.

1.2 Background and research context

This section highlights the main challenges derived from the use of heat pumps for DHW production and the recuperation of wastewater heat under a general point of view. A specific state of art review is presented in each chapter of this thesis.

As commented in the motivation, heat pumps are a potential technology for that purpose. In fact, independently from the application, heat pumps are interesting for any heating/cooling process due to their capacity to supply more useful energy than the electric energy consumed. However, the external conditions (heat sink and source temperatures and availability) linked to the operation control strategy implemented determine the final performance of a heat pump system. In order to obtain the most from the use of heat pumps, its design and control must be adapted to the specific application.

In this section, an analysis of the highest theoretical efficiency for a heating process is pointed out in a first place. Second, the main characteristics of the heat sink and heat source for this application are described. Third, the main challenges for a heat pump derived from the heat sink (DHW production) and source (wastewater heat recovery) characteristics are investigated and finally, some insights related to the integration of heat pumps within a system are addressed.

1.2.1 Maximum performance of a heating process

The main objective of DHW production is to elevate the temperature of a determined water mass flow (at an initial temperature equal to the city network water temperature, usually around 10°C) to the adequate water temperature for DHW storage (usually 60°C).

This work considers the possibility to use wastewater as a very convenient heat source since it is always at a considerable higher temperature than the city water

and most of the winter above the outdoor air temperature. In addition, the effectiveness of a water heat exchanger is always much higher than the one exchanging heat with air, even more, it is much more compact, and has a much lower cost.

Nevertheless, in DHW applications, high temperatures are required and a direct heat exchange with waste water or air is not sufficient at all. Thus, to supply the rest of the heat, the use of external work is necessary. The minimum external work required to supply the rest of the heat is given by an ideal thermal machine (heat pump).

The highest theoretical performance obtained for the generation of a temperature difference (heat sink and source) by the application of work is provided by the reversed Carnot cycle (minimum work required to obtain a temperature difference). This ideal cycle is independent from the working fluid and it is based on four ideal transformations: two isothermal where the heat is exchanged (infinite capacitance) and two isentropic (adiabatic and reversible compression and expansion) [13].

In vapor compression systems, the ideal Carnot cycle represents the maximum efficiency that could be achieved when pumping heat from the evaporation and condensation temperatures [14]. The ideal cycle is independent from the working fluid and only the external heat sink and source temperatures (with infinite capacitance) influences on the ideal upper limit performance.

Heat pumping cycles performance is usually characterized by the Coefficient of Performance (COP), which is defined according to Eq. 1.1.

$$COP_{\mathrm{h}} = \frac{\dot{Q}_{\mathrm{h}}}{\dot{W}_{comp}} \tag{1.1}$$

Where $\dot{Q}_{\mathrm{h}}$ and $\dot{W}_{comp}$ are the heating capacity and the compressor power input of the heat pump.

The heating COP corresponding to the Carnot cycle operating between two constant temperatures: heat sink temperature (T_H) and heat source temperature (T_C) is described in Eq. 1.2. [15].

$$COP_{Carnot} = \frac{\dot{Q}_{\mathrm{h}}}{\dot{W}_{comp}} = \frac{\dot{Q}_{2-3}}{\dot{W}_{1-2}} = \frac{T_H \cdot (s_2 - s_1)}{(T_H - T_C) \cdot (s_2 - s_3)} = \frac{1}{1 - {T_C}/{T_H}} \tag{1.2}$$

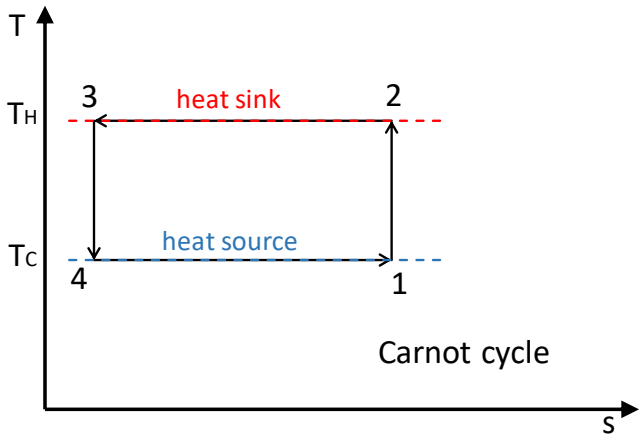

Figure 1.7: T-s diagram for Carnot cycle

The Carnot cycle is a good reference whenever the heating and cooling processes are isothermal, what would require a heat sink and a heat source with infinite capacitance.

In cycles where the heat transfer processes take place with a temperature glide (in the sink, the source or in both), the Lorenz cycle is a better reference of the ideal performance [16].

The heating COP of the Lorenz cycle with heat sink temperatures varying from $T_{3'}$ to T_H, and heat source temperature from T_C to $T_{4'}$) is described in Eq. 1.3. [17]

$$COP_{Lorenz} = \frac{\dot{Q}_h}{\dot{W}_{comp}} = \frac{\dot{Q}_{2-3'}}{\dot{W}_{1'-2}} = \frac{\overline{T}_H \cdot (s_2 - s_3)}{(\overline{T}_H - \overline{T}c) \cdot (s_2 - s_3)} = \frac{1}{1 - \overline{T}_c / \overline{T}_H} \tag{1.3}$$

Where the temperatures $\overline{T}_H$ and $\overline{T}_C$ are the entropy-averaged temperatures (average temperature in the temperature-entropy diagram) corresponding to the temperature variation. For the case of constant capacitance rate ($\dot{m}c_p$) and constant pressure process, the entropy-averaged temperature can be written as:

$$\overline{T}_H = \frac{h_2 - h_{3'}}{s_2 - s_{3'}} = \frac{T_2 - T_{3'}}{\ln(T_2 / T_{3'})} \tag{1.4}$$

$$\overline{T}_C = \frac{h_{1'} - h_{4'}}{s_{1'} - s_{4'}} = \frac{T_1 - T_{4'}}{\ln(T_1 / T_{4'})} \tag{1.5}$$

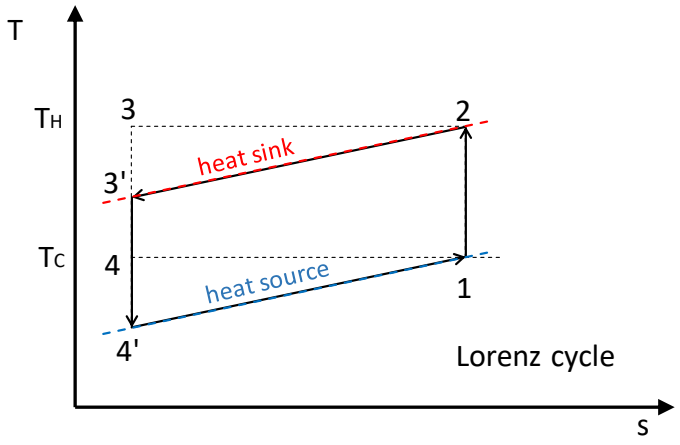

Figure 1.8: T-s diagram for Lorenz cycle

As it is in Carnot cycle, in Lorenz cycle these temperatures refer always to external conditions (heat sink and source) and are independent from the refrigerant working fluid.

This heating process is the reference one to be used when there is a limited capacitance (mc_p) on the heat sink as it is the case of heating for DHW production where the water temperature is going to suffer a large temperature lift.

The production of DHW with a heat pump based on the vapor compressor cycle usually approaches better a hybrid case since the heating is along a large temperature lift but the evaporation is more similar to an ideal isothermal process. Therefore, the reference cycle in that case approaches better a hybrid Carnot-Lorentz cycle. Figure 1.9 shows this reference cycle of a heat pump machine for a DHW production, and leads to the ideal minimum work required to heat a finite capacitance sink from a heat source of infinite thermal capacity (reservoir).

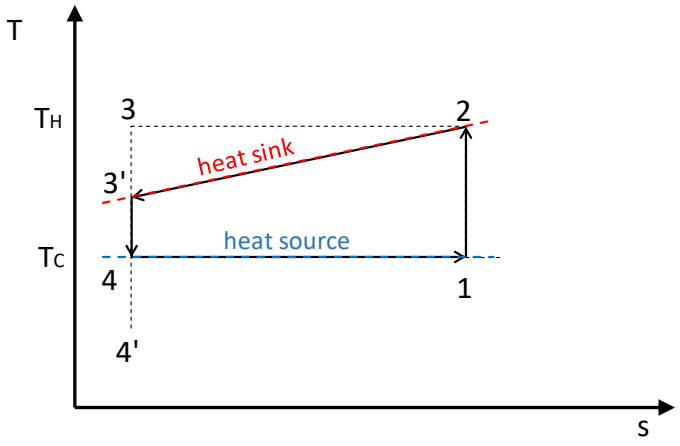

Figure 1.9: T-s diagram for the reference cycle for a heating process

The COP of this cycle operating between a variable temperature heat sink and constant temperature heat source: heat sink temperatures ($T_{3'}$-T_H) and heat source temperature (T_c) is given in Eq. 1.6.

$$COP_{ref\_heating} = \frac{\dot{Q}_h}{\dot{W}_{comp}} = \frac{\dot{Q}_{2-3'}}{\dot{W}_{1-2}} = \frac{\overline{T}_H \cdot (s_2 - s_3)}{(\overline{T}_H - Tc) \cdot (s_2 - s_3)} = \frac{1}{1 - {T_C}/{\overline{T}_H}} \quad (1.6)$$

Where the temperature $\overline{T}_H$ is the entropy-averaged temperature (average temperature in the temperature-entropy diagram) calculated according to Eq. 1.4

In real applications, irreversibility exists and the perfect match between the working fluid and the heat source/heat sink does not take place. However, the closer the working fluid can be to the heat sink/source temperature profiles, the higher the performance of the heat pump would be. In other words, the characteristics of the heat sink and source determine the design of a heat pump and the corresponding heat exchangers.

1.2.2 Characteristics of the heat sink (DHW production)

Domestic Hot Water (DHW) refers to the hot water used in sinks, showers and baths of any type of building. Specifically, this work focuses on domestic dwellings (centralized DHW production for different number of dwellings). The main characteristics of the hot water required in medium-big installations are:

(a) If the production is done instantly, a temperature usually lower than 45°C - 40°C is required. However, if the hot water is stored, a minimum temperature of 60°C needs to be maintained in order to prevent from the growth of Legionella bacteria [18].
(b) Low inlet temperatures (temperature of the water from the net service, it usually has a mean value around 10°C but seasonal effects vary its value around +/-3K, or more depending on the climate and location) [19].
(c) Highly variable requirements of water mass flow rate through the day, week and period of the year. Socio-economic factors, number of houses, type of building, occupancy, number and kind of appliances, seasonal effects or location are most of the factors influencing the variability of DHW flowrate demand [20][21].

(d) Peaky water demand. Quite often there are short peaks, which last even less than a minute.
(e) High comfort required by the user, especially for shower. Failing on the proper supply temperature can make the user not satisfied at all with the system.

1.2.3 Characteristics of the heat source (wastewater heat recovery)

Any type of wastewater at temperature higher than the ambient can have potentiality as a heat source for DHW production. The main characteristics of these water sources are:

(a) The temperature of the waste heat. This temperature depends on the type of source. Common values for the industrial and commercial sectors are: 40°C in supermarkets and industries with high demand of refrigeration[22][23], 30-40°C in hotels [24], 50°C in hospitals[25], in low-temperature district heating the water is supplied at 30-50°C[26][27]. While most common temperatures in water sources from the building are: 20-30°C in sewage water reservoirs[28] and 30-65°C at the drain in greywater, based on the draw-off origin[21].
(b) The minimum temperature of the heat source after the recuperation must not exceed 0°C in order to prevent from freezing (usually, 2°C is set as lowest limit).
(c) The availability in terms of time and quantity. In applications where a large reservoir is available, the availability is not an issue. However, in applications where there is a limited amount of water, its availability becomes essential. For instance, the availability of greywater may not be sufficient for the total DHW production [24] in some cases, or it may follow a similar pattern as DHW requirements (highly variable), in others (when the main composer of the greywater is the wastewater from DHW)[21]. Furthermore, the quantification of potentiality of a limited heat source is nowadays an opened topic (since most works treat specific sources).

Both, the temperature and the availability, determine the potentiality of low-grade water streams as heat source for DHW production.

1.2.4 Main challenges of DHW production based on heat pumps with wastewater heat recovery

The focus of this thesis is the application of DHW production in the residential sector with subcritical heat pumps using wastewater as a heat source to maximize energy efficiency. The main challenges by this application are discussed in the following.

1.2.4.1 Heat pump design

According to the maximum performance analysis, the heat sink and source characteristics define the ideal upper limit performance of a heat pump.

A heat pump needs a working fluid (Refrigerant) in order to exchange heat from source to the sink. The heat pumping is done by means of a vapor compression cycle (in this work) and the real efficiency of the heat pump depends on its design and on the characteristics of the heat sink and source. Depending on how far the refrigerant cycle is from the ideal reference cycle (that is, how close to the heat sink and source heat transfer processes), there will be more or less room for improvement.

On the one hand, a heat pump for DHW requires to overcome high temperature lifts (usually around 50K) and the working fluid would need to adapt as much as possible the heat transfer process to the heat sink in order to reach the highest efficiency.

CO2 Transcritical cycle is nowadays the most commonly employed solution for high temperature glides [29][30]. As the heat rejection process follows a profile closer to the heat sink temperature glide, efficiencies are higher than efficiencies obtained with subcritical systems where the main heat exchange on the refrigerant side takes place isothermally (condensation). Conversely, in applications with relatively small temperature lifts take place, subcritical cycles offer a better match with the secondary fluid temperature variation profile.

Figure 1.10 depicts the temperature profiles of the secondary fluid (water), along the condenser area for CO2 (R744) and propane (R290) under both cases: transcritical and subcritical cycles, as well as the COP variation with the water inlet temperature at the condenser, for different refrigerants and water outlet temperature of 60°C. Figure 1.10a corresponds to the case of high temperature lifts (10 °C to 60°C), Figure 1.10b corresponds to the case of low temperature lifts (40°C to 60°C) and Figure 1.10c shows the COP variation of different refrigerants with the temperature lift.

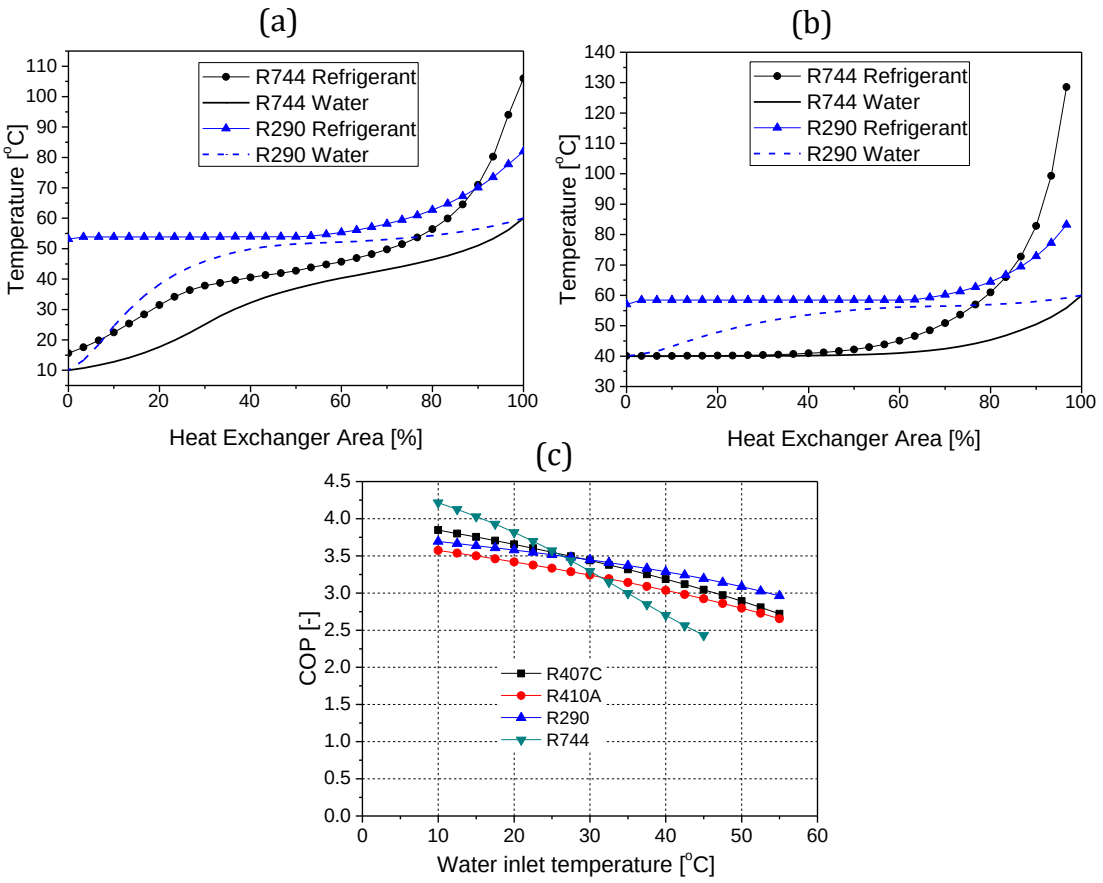

Figure 1.10: Temperature profiles of the secondary fluid (water), transcritical and subcritical cycles along the heat exchanger area and performance variation with the temperature lift for different refrigerants (water outlet temperature of 60°C). (a) high temperature lift (10°C-60°C), (b) low temperature lift (10°C-60°C); (c) COP variation of different refrigerants with the water inlet temperature for water outlet temperature of 60°C. [31]

As it can be observed in Figure 1.10, the match of the temperature between the secondary fluid and the refrigerant is better in transcritical cycles when there are high temperature lifts and the opposite when the temperature lift is small. Consequently, transcritical cycles present greater performance than subcritical for DHW application.

However, it also can be seen that the performance of transcritical cycles significantly diminishes with low temperatures lifts what happens in heat recovery applications. In addition, the performance strongly depends on the rejection pressure. An optimal rejection pressure in the gas cooler exists and needs to be controlled [32]. Another characteristic is that R744 has a low critical temperature (30.98°C), what limits its use within high evaporating temperature applications (as

it could be the case of wastewater heat recovery)[33]. Furthermore, these heat pumps are relatively expensive due to the need of using especial components (compressor, valves, and heat exchanger) to address properly transcritical conditions and the high pressures required in the circuit. Thus, researchers have been struggling in order to enhance the performance of subcritical cycles for high temperature lifts.

A better match of the temperature profiles between the water and the subcritical refrigerant for high temperature lifts can be obtained if a certain degree of subcooling is applied without compromising efficiency from the reduction of the condensation area[34]. This issue has been investigated from the refrigerant charge point of view (which is indirectly related to subcooling) [35][36], and more directly it has been addressed by some authors [30][37][1]who found that similar performances to those obtained with transcritical cycles. The dependency of the performance in subcritical cycles with subcooling lead to determine an optimal degree of subcooling that maximizes COP. In fact, for refrigeration applications (low temperature lifts), a theoretical optimal degree of subcooling was found [1][38].The only study published regarding to high temperature lifts refer to the authors of [34]. In that paper an optimal degree of subcooling based on the external temperatures was experimental and theoretically found. The authors pointed out an increase of COP up to 30% in regard to the case with negligible subcoolingfor a 50K temperature glide at the secondary fluid in the condenser (10°C to 60°C).

Therefore, since the optimal subcooling depends on the external temperatures and they vary with the operation of the heat pump, an appropriate control that enables its adaptation is required.

In order to control the subcooling degree, the design must have an extra degree of freedom (common designs use a liquid receiver at the outlet of the condenser what does not allow subcooling). Some heat pump designs were investigated in [39][40] with that purpose, and based on those studies, the authors of [41] implemented a subcooling control by means of an expansion valve using a similar heat pump design as it is used in transcritical cycles but with R410A and a liquid receiver placed at the outlet of the evaporator. However, no information about the outlet temperature was reported. Other subcooling controls rely on sophisticated algorithms (extremum seeking control) able to implement the optimal subcooling for any external condition[42]. However, the proposed algorithm needed a very long time (around three hours) to reach the optimum and accuracy was compromised if there was a change in an external variable (simulation case study). Furthermore, most of the works dealing with the improvement of efficiency with

subcooling and its control are focused on applications with small temperature lifts at the secondary fluid and optimal values are found between 5K-10K.

The only works addressing the study of subcooling for the case of high water temperature lifts are the PhD Thesis [1]. This thesis was framed in the European project: “Next Generation of Heat Pumps working with Natural fluids" (NxtHPG) and had the objective of developing a set of safe, reliable, high efficiency and high capacity heat pumps working with Natural Refrigerants.

The main aim of that thesis was to develop a prototype of a propane water-to-water heat pump capable of reaching a high COP for DHW production, in the application of heat recovery from a potential water source. Therefore, the investigation of the role of subcooling in the performance as well as different designs of heat pumps were the focus. An optimal degree of subcooling was found and localized for the infinite heat transfer area[34], from that study, a control methodology was proposed. Two different configurations designs were developed based on how subcooling is made and which variables can be controlled (subcooling and/or superheat)[43][44]. Similar performances were obtained with both configurations [45] and they were even able to exceed the performances obtained with transcritical cycles. More details about the configurations developed in this work can be found in Appendix A.

The control of subcooling was not implemented experimentally and was based on ideal studies (infinite heat transfer area). In addition, both configurations constructed had more components than typical components of a heat pump, which, if commercialized, may result an economic barrier.

On the other hand, the temperature and availability of wastewater used as the heat source influences the performance of the heat pump.

The working fluid (refrigerant) used needs to be capable to overcome possible high evaporating pressures derived from heat sources at 30°C-40°C. This condition makes less interesting transcritical cycles (CO2) due to its low critical point. Instead, subcritical cycles become more interesting as in most cases, this is not an issue[46][47].

Regarding to the availability, two different cases of the application of heat recuperation in a heat pump can be distinguished: infinite and finite heat source reservoir.

For infinite reservoirs, the closest heat transfer process to the ideal reference cycle (Lorenz and Carnot combination) takes place isothermally. In this sense, the highest the area of the heat exchanger dedicated to only evaporation, the better.

Ensuring zero/low superheats in this type of heat pump designs will lead to better performances. In fact, most of works dealing with heat pumps employ small temperature glides at the secondary fluid of the heat source and consider superheat undesirable from the perspective of the heat exchange process. Only small degrees of it are used to ensure the compressor reliability and allow the refrigerant flow control by sensing the superheat [48]. The control is done by the expansion valve, which ensures a constant (low) superheat regardless the external conditions.

However, with finite heat sources, a temperature lift takes place (higher lifts as the limitation increases). For instance, in heat recovery applications such as from grey water (secondary temperature glides up to 30-40K[49]). In these cases, the best heat exchange transformation has the reference on the Lorenz cycle and, following a similar reasoning that in the subcooling case, one could think that superheat may improve performance when dealing with high temperature glides. Few studies are available on literature about this topic, only in [49] the authors mention the problematic of a limited heat source but it is only seen under the perspective of a heat pump performance decrease and propose an operation control in order to minimize the temperature lift of the secondary fluid. Nothing related to improve the design of heat pumps to avoid the mentioned loss of efficiency is commented.

Finally, if the production of DHW relays only on a heat pump and the heat exchanger, instant production is required. As both, heat sink and heat source (when limited) present variability and short duration, instant production is only possible if the capacity of the heat pump can be regulated and the number of starts does not risk the compressor life. An inverter heat pump instead of the use of a constant speed compressor could be a solution. However, when the conditions move from the designed ones, a significant decrease of the efficiency is observed in this kind of compressors [50][51]. Nevertheless, the modulating capacity in current inverters is not sufficient to satisfy the highly variable mass flow rate typical of instantaneous DHW production, and in the end also a great number of ON/OFF cycles are required, and hence the use of storage tanks is required [52][53]. Therefore, DHW production based on heat pumps from heat recuperation will require the use of one storage tank for the heat sink side and, in the case of having limited/variable availability of the heat source, another storage tank for the he source side. The best performance of this application will be the result of the heat pump integration with the rest of the components, the optimal sizing of each component and the optimal operation of the system.

1.2.4.2 Heat pump integration within a system

Heat recovery heat exchanger

The use of a heat exchanger to take profit from wastewater streams (from different sources) by a direct exchange of heat with the water from the net has been implemented in a wide range of projects covering many applications.

Their designs an applications within DHW sector vary. The simplest design is a tube rolled to the pipe (gravity film heat exchanger) invented by [54] currently commercialized offering paybacks around 2.5 years [55]. From it, a new design based on two concentric pipes was invented [56]. Other designs such as a shell and tube heat exchangers directly placed in the drain pipe [57] found energy savings up to 20%[58] or brace plate heat exchangers are also employed to this aim within more complex systems [59]. In fact, there is a vast commercial models available with high effectivity if properly maintained. The only particularity attributable to DHW, is the double wall requirement in order to prevent mains water from possible refrigerant leakages.

Therefore, the advantageous results from the use of heat recovery heat exchangers under a system point of view is evident. However, its use combined with heat pumps penalize the heat pump performance. In fact, according to transcritical tradeoffs presented in the heat pump design analysis, CO2 becomes not appropriate when low temperature lifts at the condenser take place. Despite the important relation between these two components and the wide use of heat exchangers and heat pumps in DHW systems, there are no works analyzing their optimal sizing, based not only on the components themselves, but on the global performance of the system.

DHW Storage tank

Similar to heat exchangers, storage tanks are widely used, especially, within DHW applications based on heat pumps or solar thermal. However, from the energy point of view, the addition of a buffer tank introduce irreversibility to the system due to heat losses from the storage, and if they are of the stratified type to the mixing and heat transfer between the hot part and the cold part. Hence, their design and the operation with the heat pump plays a key role in order to minimize the losses.

In the applications with heat pumps, based on the mass balance, two main types of storage tanks are employed:

(a) Equal mass balance between inlets/outlets: the most commonly used for DHW. These types of tanks are always full, that is, maintain the volume of the stored water constant. The philosophy is to have always water available for the user (regardless the temperature). Based on how water is stored, two main types can be highlighted:

a. Fully mixed storage tanks: in which the water from the net is heated up in sequences of small temperature lifts (around 5K-10K) until the tank is full, thanks to recirculation techniques. The main disadvantage of this strategy is that the water cannot be directly supplied to the user. This type of storage tank has been used mostly with subcritical cycles (without subcooling) and there are commercial heat pumps following this principle as for instance Quantum[60] or Nibe [61].

b. Stratified storage tanks: in which the stored water is a combination of the hot water produced and the cold water coming from the net in order to ensure constant volume. A clear differentiation of the temperatures is forced in order to minimize irreversibility from mixing. The study of different geometries and the design of sophisticated techniques that favor stratification have been the focus of many researchers[62][63]. The advantage is that the heat pump can directly supply hot water to the user although only the supply of small water mass flow rates are possible. However, besides the irreversibility originated by not having perfect stratification, these tanks also involve other irreversibility, as over-using electric resistances for extra heat storage or back-up, and oversizing, what contributes to the increase of thermal losses. This solution has been commonly employed with transcritical cycles since it promotes high temperature lifts [64]. Probably this may be the reason why they are the most used tanks in DHW applications with heat pumps.
However, if a heat exchanger pre-heats the water from the net, temperature lifts across the gascooler becomes significantly lower.

(b) Variable mass balance between inlets/outlets: in which the water from the net does not mixes with the hot water. Instead, only hot water (at required levels) enters to the tank. The main advantage is that irreversibility from water mixing can be avoided. The philosophy in this case is to have the minimum energy stored. The design and control of the tank must ensure reliability to the user. Apparently, they are the most energyally convenient tanks. However, only few works use this type of storage tanks [46].

Although almost every system for DHW based on heat pumps use storage tanks, the coupling of both components is driven mainly by economic factors that are specific of the application itself. Furthermore, economic aspects depend on politics and can vary along the system-life. Hence, proper control strategies employed one year may not be the best for instance, the next year. Examples of common strategies based on electric tariffs are night production [65][66], and off-peak production [67].

More recently, controls are based on the integration within smart grids by assuming the electric grid as it is nowadays [68] or assuming renewable energy production from photovoltaics [11]. However, there are not works addressing strategies from the energy point of view. This aspect is the only aspect that remains the same and allows generality. The knowledge of a control strategy based on that would be useful in order to minimize irreversibility of a system when coupled with for instance economic factors, self-consumptions or other specific factors.

In most controls, a determined level of the user satisfaction is ensured based on energy percentages[69]. However, with this strategy, having complete comfort (24 per 365 days) all over the year is not fully guaranteed although very probably satisfied.

Wastewater Storage tank

Variability appears with limited available wastewater. In these cases, a buffer to hold the variation an ensure continuity in the production is required. Few works present details about these components within a system. If a tank is used, it is considered as a simple reservoir of variable volume [70][71][72], only in some works point out the importance of the wastewater temperature on the performance and recommend the insulation of the storage tank [49].

In regard to control strategies, it is worth underlying that the heat pump needs to be controlled by the DHW side rather than by the grey water side. That is to say: if water needs to be stored longer, it is preferable to happen in the grey water storage tank due to lower heat losses [21]. Apart from that, most strategies integrating a system composed by two storage tanks, a heat pump and a heat exchanger also rely on electric tariffs as it was the case of the DHW storage tank-heat pump side [46].

Finally, since these systems involve many variables, the development of models can help to address optimization problems considering all required interactions. This is the case of most of the papers referred in this section. However, all of them use hourly-based inputs and time-steps, what undermines the precision of the

optimization and leads to components oversizing. DHW demand is characterized by short/highly peaky demands (lasting minutes) and in order to obtain proper results, capturing the variability is crucial, therefore adequately low time-step integration needs to be used [67].

1.2.5 Identified gaps and research goals

Once some background and a general research context have been provided, the motivation of the goals addressed in this thesis based on the identified gaps are presented in the following.

1.2.5.1 Heat pump design

Identified gaps:

- The use of high efficient subcritical heat pumps for DHW requires the capability to overcome high temperature lifts. Optimal degrees of subcooling based on external temperatures have been found to improve the efficiency. Similar, or even better, performances than the ones obtained with transcritical cycles have been measured. However, the design of this type of heat pump requires more components what could increase the heat pump cost.

- Subcritical heat pumps capable to efficiently deal with both, small and high temperature lifts require a precise control of the subcooling. Few research works dealing with this control have been found in the Literature. Further, they focus on other applications (such as HVAC) and are based on complex algorithms. More recently, a control based on the external temperatures and a control based on a temperature difference were theoretically proposed; yet, not experimentally tested.

- Little attention has been paid to the evaporator side where superheat has been undesirable. However, within heat recovery applications, significant temperature glides may take place and it is possible that superheat could be also optimized in a similar way to the subcooling.

Research goals:

1) Investigate a high efficient heat pump configuration for subcritical cycles with subcooling based only on the typical components (compressor, expansion valve, condenser, evaporator and liquid receiver).

2) Study and test a control methodology of the subcooling based on a temperature difference.

3) Evaluate the role of superheat in applications where high temperature glides can take place in the secondary fluid (limited heat recovery).

1.2.5.2 Heat pump integration within a system

Identified gaps:

- In water heat recovery applications, whenever the temperature of the waste heat stream is higher than the city water temperature, the placement of a recovery heat exchanger to directly recover part of the heat to pre-heat the water from the net is desirable. Although there are works including a heat exchanger with this purpose, the interaction with a heat pump and their combined optimization have not been investigated.

- Constant volume storage tanks are usually employed with heat pumps for DHW production. However, from an energy point of view, the use of a variable volume storage tank seems to be more interesting. Studies related to sizing and coupling that type of storage tanks with heat pumps are not available.

- Very scarce works dealing with the recuperation of limited wastewater streams in order to satisfy the total DHW demand with heat pumps can be found in the literature. In addition, there is not a clear approach of the whole integration of the components in these systems in terms of sizing, control strategies, and the potential of heat recovery.

Research goals:

4) Analyze the integration of a recovery heat exchanger (recuperator) together with a heat pump in order to determine optimal sizing guidelines.

5) Investigate a proper methodology that allows designing a heat pump system with a variable volume storage tank and define an operation strategy that maximizes energy efficiency.

6) Evaluate the potentiality of the wastewater heat within residential applications in order to satisfy the total DHW demand. Define a control strategy to maximize the efficiency of the system from the heat recovery. Define a methodology to size and control the system for minimum CO2 emissions considering the integration of all the elements that compose the system (wastewater storage tank, DHW storage tank, heat recovery heat exchanger and heat pump).

1.3 Objectives

The main objective of this thesis is the design of an optimal heat recovery system for DHW production based on the use of a heat pump. To this purpose, the focus has been first aimed to the optimal design of a subcritical heat pump for DHW and heat recovery and second, to the optimal integration of the heat pump design within the whole DHW system.

The starting point of this thesis is the continuation of the work performed in the PhD done by Pitarch [1]. That thesis was framed in the European project: "Next Generation of Heat Pumps working with Natural fluids" (NxtHPG) and had the main objectives of developing a set of safe, reliable, high efficiency and high capacity heat pumps working with Propane and CO_2. In that thesis, the focus was to investigate the role of subcooling in the performance of a propane water-to-water heat pump for DHW production, in the application of heat recovery from a low temperature water source.

Two different concepts were built and tested and both were able to operate with efficiencies comparable to transcritical cycles thanks to the application of high degrees of subcooling. A dependency of the performance function of the degree of

subcooling was obtained and they found an optimal degree of subcooling based on external conditions.

In one of the investigated heat pump concepts, a dedicated heat exchanger for subcooling was required. Thus, the control of the subcooling was not possible (so called 10K1V). In the other concept, subcooling was done in the condenser. In this case, the control was done by an additional electronic throttling valve (named 10K2V). An optimal subcooling, mainly dependent on the external conditions, was found (theoretically and experimentally). Both configurations of the studied subcritical heat pump are described in Appendix A.

Similar performance were obtained with both designs concluding that economic factors would be decisive for the choice of one. A new design concept composed only by the typical components of a heat pump at the expense of not controlling superheat (set to zero) was proposed as future work (so called 0K1V).

According to the identified gaps and the work performed in the previous PhD [1], the main objectives related to the design of the heat pump in this thesis are:

a) Theoretically study the most efficient heat pump working with a subcritical cycle based on the heat sink and source characteristics.
b) Study the dependency of the optimal subcooling with superheat.
c) Analyze the role of superheat in applications where temperature lifts take place in the secondary fluid (i.e. heat recovery applications).
d) Evaluate the consequences on the performance derived from the loss of one control variable (superheat) that could take place in the proposed heat pump configuration in the PhD [1] based only on common HP components.
e) Identify possible room for improvement taking into account subcooling and superheat from a heat pump system point of view based on the heat sink and source characteristics.
f) Design and test a subcooling control methodology based on the findings found in [1].
g) Develop a new heat pump concept composed only by one expansion valve, one compressor, an evaporator, a condenser and a liquid receiver.
h) Experimentally evaluate the reliability of the concept developed and compare the performance with the performance obtained from the existing designs. Determine the most convenient configuration of the heat pump out of the three designs.

From this part, an optimized water to water heat recovery heat pump for DHW production based on the optimization of subcooling will be proposed.

The main objectives related to the integration of the optimal subcooled heat pump (SHP) within a system are based on the gaps identified previously:

i) Determine a proper sizing of a heat recovery heat exchanger (recuperator) to maximize energy efficiency from the coupling with the subcooled heat pump.
j) Define and design the components required to maximize the efficiency of a system for DHW production in the residential sector.
k) Design the most energy efficient system for DHW production in the residential sector based on heat recovery from low temperature sources capable to satisfy a residential sector demand with high comfort
l) Analyze the potential energy available in wastewater heat sources at low temperature and determine a control strategy to maximize the efficiency of the DHW production system from waste heat recovery.

Results obtained from this work could be useful for installations dealing with DHW production in the medium-long run as they go in line towards an energy sector more committed to the environment, which needs to be the society commitment for next future.

1.4 Structure

The work performed in order to achieve the proposed objectives is presented following a compilation thesis structure where the first chapter is introductory, chapters 2 to 7 are composed by one publication each, chapter 8 collects a discussion of the results, general conclusions and possible future works arisen from this study and the scientific contributions of the thesis. Finally, Appendix A describes the different heat pumps configurations developed in the work done in [1] and in this thesis, Appendix B contains a qualitative study of the fluids distribution in the evaporator of the heat pump, which was performed under the frame of the present PhD, and Appendix C shows the uncertainty of all measured points.

A more extended description of the contents in chapters 2-7 is given at the following:

Chapter 2:

PAPER 1: Exergy analysis on a heat pump working between a heat sink and a heat source of finite heat capacity rate

The main objective of this chapter is to theoretically study and determine the most efficient heat pump working with subcritical cycles based on the heat sink and source characteristics and under a general point of view.

That is, to identify the optimization of the control variables taking into account the interaction among all the components as well as to find possible improvements out of the integration of the heat pump components (that is, finding possible gaps of improvement from the coupling of the system composed by a compressor, an expansion valve, an evaporator, a condenser and a liquid receiver).

The role of subcooling and superheat are theoretically analyzed for DHW production applications based on heat recovery sources. Heat recovery applications may lead to high temperature glides in the evaporator and, contrary to common procedures, an optimal degree of superheat (not zero) could exist.

In the heat pump configuration proposed in the PhD. of Pitarch [1], the superheat control is lost (so called 0K1V). Instead, zero superheat takes place. Therefore, the influence and quantification of this effect in the heat pump performance is investigated in this paper.

Furthermore, even though the existence of an optimal degree of subcooling based on the external conditions was known, its dependence with superheat and the influence on the performance of other heat pump components was not. Thus, it is also analyzed in this chapter.

Results highlight the main components that contribute to the improvement of the heat pump efficiency depending on the external conditions. In addition, an optimal degree of superheat based on the temperature evolution of the secondary fluid at the evaporator was found, its impact on the overall performance is lower than the subcooling influence. However, a control of superheat similar to the one implemented with subcooling could be worthy in applications with large secondary fluid temperature glides.

Chapter 3

PAPER 2: Study of different subcooling control strategies in order to enhance the performance of a heat pump

In [1], the control of subcooling was done manually. However, if commercialized, an automatic control of the subcooling had to be included. In this chapter, a theoretical study of possible subcooling control strategies with 10K2V configuration is performed. From the strategies described, the control of subcooling based on a temperature difference (control of the temperature approach: difference between water temperature at the inlet of the condenser and the refrigerant temperature at the outlet of the condenser) resulted the most interesting and effective strategy. It was implemented in the laboratory in order to experimentally test its stability and results are collected in this chapter.

Chapter 4

PAPER 3: Improved water to water heat pump design for low-temperature waste heat recovery based on subcooling control

Following the aim for a possible commercialization, the development of a new propotype composed by the minimum components was encouraged [1].

This chapter deals with aspects from the new design concept and the comparison with the existing ones.

1. It describes the main characteristics and the motivation for the new configuration developed: the heat pump concept is similar to common designs used with transcritical cycles in which a liquid receiver is placed at the outlet of the evaporator (forcing superheat to be close to zero) and the control of the optimal rejection pressure is done by the expansion valve. However, although this type of control works well in transcritical cycles, where high variations of the rejection pressure take place, it needs to be tested with subcritical heat pumps. In subcritical systems, the expansion valve needs to control a temperature difference instead pressures. In addition, in subcritical systems, small changes on the condensing pressure have a significant impact on subcooling.
2. It compares the results of 0K1V configuration with the results obtained in the 10K2V existing configuration for typical conditions of DHW and heat

recovery applications. Thereafter, it shows the results from the experimental tests with both concepts under extreme conditions in order to determine the temperature working range of the heat pump.

3. It extends results available to a new campaign in order to determine optimal water mass flow rates at the evaporator and it tests the penalty of losing superheat control in the 0K1V design within heat recovery applications where high temperature glides take place in the secondary fluid of the heat source.

Results showed higher efficiencies in the 0K1V than in the 10K2V configuration independently from external conditions, that is, always.

However, the experimental observation did not agree with theory. Based on the theoretical exergy analysis performed in chapter 1, better performances when high temperature glides take place in the evaporator were expected in the 10K2V design. That is, with the application of a certain degree of superheat.

Hence, further studies regarding to the distribution of the fluids in the evaporator were performed. A qualitative analysis on this topic is presented in Appendix B.

Based on experimental results, the new configuration, 0K1V, was concluded to be the most suitable configuration for subcritical heat pumps working with subcooling control even though both designs are capable to operate with high coefficient of performance under both, low, medium and high secondary fluid temperature glides at the condenser and evaporator.

Next chapters deal with the integration of the developed heat pump within the DHW production system.

Chapter 5

PAPER 4: Optimal sizing of a heat pump booster for sanitary hot water production to maximize benefit for the substitution of gas boilers

From experimental results, a validated model of the heat pump was developed with the commercial software IMST-ART [73]. From this model, preliminary correlations including a wider range of conditions were extracted and integrated with a brazed plate heat exchanger model obtained from SWEP design software.

The combined BPHE and HP system model was developed in EES software [74] and included an economic assessment in order to determine the convenience of the heat pump inclusion.

Results evidence the energy advantage of the additional component from a system point of view and the recommendation of 5K as temperature approach (temperature difference between the wastewater stream at the inlet of the heat exchanger and the water from the net at the outlet of the heat exchanger) as a good compromise between effectivity and size. Around 20-30% of the heating required can be obtained from it leading to required smaller heat pumps.

The addition of a recuperator before the heat pump makes inlet conditions at the condenser considerably variable. While this effect strongly penalizes transcritical heat pumps, subcritical heat pumps with an optimal subcooling control are capable to adapt and operate under high efficiencies independently.

Chapter 6

PAPER 5: Optimal design and operation of a central domestic hot water heat pump system for a group of dwellings employing low temperature waste heat as a source

One-step further contemplates the optimization of the system composed by the subcooled heat pump (SHP) with the heat exchanger and the storage tank for the satisfaction of DHW production within the residential sector assuming the heat recovery from an infinite heat source in order to minimize associated C02 emissions.

A model of the system in Trnsys [75] is developed. It includes a new type containing an extension of the heat pump model used on the previous chapter. In addition, types already available in the software for the heat exchanger and the storage tank based on variable volume were used.

Different DHW demand profiles under a time step of one minute were estimated and employed in the sizing and optimization study. Moreover, a sensitivity analysis with different wastewater and net water temperatures is also performed. The wastewater stream was optimized taking into account the auxiliary pumps consumption (the pressure drop across the heat exchangers were taken into account for this; while pressure drop along the length of the pipes were neglected).

Comfort standards based on a percentage of energy and also based on the moment of the hot water shortfall are considered as well.

A definition of the main parameters to take into account in order to get a successful integration of the subcooled heat pump within a system is provided.

Results showed the inexistence of just an optimal solution. Instead, a combination of storage tank-heat pump sizes result in similar annual performances. This issue entails the use of parametric studies rather than optimization solvers.

A design and a control strategy approach are provided in this paper. The strategy is based on minimizing the energy stored (maximizing energy efficiency).

Chapter 7

PAPER 6: Closing the residential energy loop: grey-water heat recovery system for Domestic Hot Water production based on heat pumps

The final contribution of this work focuses on the evaporator side. That is, on the heat source: wastewater heat recovery.

A study of the wastewater potential (sewage water for instance) as well as possible control strategies dealing with the maximization of the benefit from the heat recovery are first addressed.

Thereafter, a complete integration of the subcooled heat pump, two storage tanks and the heat exchanger is performed in the system Trnsys model [75].

Sizing criterion based on the relationship between the hot water and the available wastewater is given.

The impact of the available heat source in the system performance is quantified, and adequate control strategies are developed for a specific case and greywater availability profile.

As an application of the above, an example of real profiles (DHW demand and grey water availability) obtained with stochastics models for 20 multifamily houses has been analyzed.

To evaluate the impact of the grey water availability, three main cases were analyzed and compared: Infinite availability of heat source, finite availability but constant and with a real variable grey water profile.

As it was the case in chapter six, a set of heat pump-storage tanks sizes lead to similar energy efficiencies and the use of optimizing solvers do not lead to an optimum. Thus, parametric studies are conducted.

Results showed that highest performance is obtained with an infinite availability (i.e. sewage, district heating). If mean average values from a real profile (constant) and limited are used, a decrease on the performance up to 20% is obtained. Finally, if a real-variable grey water profile is used and its design dynamically adapted to this conditions, 22% loss of performance compared to infinite availability is obtained. Nevertheless, it is possible to satisfy the DHW demand of a typical multifamily house only with 60% of the heat recuperation from the greywater and the optimized heat pump with lower associated emissions than current technologies (high efficiencies).

Chapter 2
Exergy analysis on a heat pump working between a heat sink and a heat source of finite heat capacity rate

Miquel PITARCH(a), Estefanía HERVAS-BLASCO(a), Emilio NAVARRO-PERIS(a)*, José M. CORBERÁN(a)

(a) Institut Universitari d'Investigació d'Enginyeria Energètica, Universitat Politècnica de València, Camí de Vera s/n, València, 46022, Spain

Tel: +34 963879123

enava@ter.upv.es

2.1 Abstract

The optimum performance of a pure subcritical refrigeration cycle depends significantly on the temperature lift of the heat source and sink. Therefore, the maximization of the system efficiency has to be linked to them. This paper shows an exergy analysis of each heat pump component (condenser, evaporator, expansion valve and compressor) considering that the heat source and sink are not at constant temperature. The performed study shows the components with more possibilities for improvement. Based on this analysis, the optimization of cycle parameters like subcooling and superheat as a function of the external conditions have been done. In addition, this work has demonstrated that the components having a higher influence in the system irreversibility's depends significantly on the temperature lift of the secondary fluids. Finally, the obtained results show potentials improvements of the efficiency up to 23% if the system is able to operate in the optimal subcooling and superheat.

Keywords: exergy; heat pump; optimal working point; subcooling; superheat

2.2 Nomenclature

COP: Coefficient of Performance, [-]

$\dot{(Ex)}$_ : Rate of exergy [kW]

ex_ : Specific exergy [kJ kg-1]

h: Specific enthalpy [kJ kg-1]

$\dot{m}$_ : Mass flow rate [kg s-1]

p: Pressure [bar]

$\dot{Q}$_ : Rate of heat transfer, [kW]

RI: Relative irreversibility [%]

s: Specific entropy [kJ kg-1 K-1]

Sc: Subcooling, [K]

Sh: Superheat [K]

S.Fluid: Secondary Fluid

T: Temperature [°C]

$\dot{W}$_ : Rate of work, power [kW]

Greek symbols

ϕ : Exergy efficiency [%]

Δ : Variation

Subscripts

0: Reference environment

1,2,3,4: State points of the cycle (Figure 1b)

comp: Compressor

cond: Condenser, or gas cooler

des: Destruction

evap: evaporator

EV: Expansion Valve

h: Heating

H: Heat sink

i: Refers to either the condenser, gas cooler or the expansion valve

in: inlet

opt: Optimal

out: Outlet

ref: Refrigerant

sf: Secondary fluid

hs: Heat Source

2.3 Introduction

Heat pumps are widely used for cooling and heating applications. Researchers are struggling to optimize the heat pump system for each application in order to obtain the maximum possible performance. There are three main ways to improve the performance of a heat pump working at a given external conditions. The first is to design more efficient heat pump components, such as the heat transfer in the heat exchangers or the efficiency of the compressor. The second is to modify the heat pump cycle according to the external conditions, so it works more efficiently, for instance, the two-stage cycle. The third is the optimization of the working cycle conditions such as subcooling, superheat, or the rejection pressure in a transcritical cycle depending on the external conditions (Inokuty, 1928), (Cecchinato et al., 2010). No matter how much the heat pump performance is improved, there will be a limit that cannot be exceeded. The maximum possible performance depends on the external conditions, and it is often defined by the ideal refrigerant cycle of Carnot or Lorentz, depending on the application (Itard and Machielsen, 1994), (van de Bor and Infante Ferreira, 2013).

In the most common applications for air conditioning and heat pumps, the temperature lifts of the secondary fluids usually is limited to 5-10°C .This fact has made that when exergy analysis are performed, the assumption of 0 temperature lift in the source and sink has been commonly made. Nevertheless, the increased

interest in energy efficiency has made that the potential application field of heat pumps has been extended to, for instance, sanitary hot water production, dryers or energy recovery systems. In these fields, the temperature lift could increase significantly (up to 60-80 °C) and the assumption of considering the temperature lift in the source and sink as negligible can introduce important deviations from the real optimum performance of the system.

From the point of view of the cycle, the analysis of the temperature lift can be related to the analysis of the optimum subcooling for a given temperature lift in the heat sink and the analysis of the optimum superheat for a given temperature lift in the heat source. The influence of these two parameters in the cycle has been studied previously in the literature, (Fernando et al., 2004), (Choi and Kim, 2004), (Corberán et al., 2007) analized the optimum charge of a heat pump, which is indirectly related to the degree of subcooling. Other researchers theoretically studied the effect of subcooling in an air conditioning system for different refrigerants have reported COP improvement with a certain subcooling (Hjerkinn, 2007), (Redón et al., 2014), (Xu, 2014), (Pottker and Hrnjak, 2015); they pointed out the existence of an optimal subcooling that maximizes COP for their equipment. In (Koeln and Alleyne, 2014), the authors developed a sophisticated methodology in order to look for the optimal subcooling by "try and error", since they did not found the relationship between the optimal subcooling and the external conditions.

In the same line are the works that study the influence of subcooling on vapor-compression system from the exergy point of view. (Yang and Yeh, 2015), (Selbaş et al., 2006) focus on the thermos-economic optimization of the heat exchanger, and the condensing temperature is kept constant as a function of subcooling. Thus, they do not simulate a real system as a function of subcooling (condensing temperature depends on subcooling (Yang and Yeh, 2015), (Pitarch et al., 2018)). Furthermore, they look at the system as a whole and not to each component individually. In (Yang and Yeh, 2015), the analysis of an optimal subcooling is done for different refrigerants including the transcitical, CO2. They concluded that the condensing temperature is the main influencer on the optimal degree of subcooling but the study does not consider the variation of external conditions.

In general, the studies found are focused on air conditioning and heat pump applications with small temperature lift. Although they arrive to relevant conclusions fixing the optimum subcooling to 5-10K, they lack of generality for other applications where the temperature lift could change significantly (Yataganbaba et al., 2015).

Furthermore, most of the recent studies published related to exergy analysis in vapor compression systems have been focused mainly on the performance of new refrigerants mixtures and hydrocarbons (Yataganbaba et al., 2015), (Ajuka et al., 2017), (Valencia et al., 2017) or on their integration in complex systems like solar with heat pumps, CHPs, geothermal district plants, where usually the conclusions applied to their specific application and study (Arat and Arslan, 2017), (Di Somma et al., 2017).

One of the first attempt to analyze the problem of optimal subcooling dependence with the external conditions was made by (Pitarch et al., 2018). They found that the optimal subcooling highly depends on the secondary fluid temperatures at the condenser, for instance the optimal subcooling was around 10K when heating water from 50°C to 60°C and around 42K when heating from 10 °C to 60°C with 25% of COP improvement respect to the case without subcooling. In (Pitarch et al., 2017), they theoretically showed (for an infinite condenser area assumption) that the optimal subcooling was given for the two pinch points situation. In addition, they found that the optimal subcooling mainly depends on the temperature lift of the secondary fluid at the condenser and not on the absolute inlet and outlet temperatures. In (Hervas-Blasco et al., 2017), the authors analyzed the double pinch point situation by means of experiments and a heat pump model. They confirm that in a subcritical system, there is an optimal subcooling and it is close to the double pinch point situation. They also gave a simple way to control subcooling by setting the temperature difference between the refrigerant outlet and secondary fluid inlet at the condenser approximately in 3K based on experimental results for a wide range of operating conditions.

Nevertheless, among all the works cited previously and found in literature dealing with the optimization of the subcooling, none of them investigates the influence of subcooling on the efficiency of each heat pump component and its dependence on the secondary temperature lift. This consideration is of major relevance in order to understand how the different components behave with subcooling and to show the direction for potential improvements. The only works developed related to that have been in the frame of transcritical cycles (not strictly subcooling). For instance, (Sarkar et al., 2004) and (Chen and Gu, 2005) made an exergy analysis of the CO2 transcritical cycle in order to look for improvement strategies of these cycles; they found that the expansion valve holds the highest irreversibility. Afterwards, in (Yang et al., 2005), a comparison of two transcritical cycles based on an exergy analysis, one with expansion valve and other with an expander, is done.

Regarding to superheat, it is usually considered undesirable from performance point of view, but a small amount of superheat is desirable for the compressor reliability (Jolly et al., 2000). Up to the knowledge of the authors, there is no literature available about the influence of superheat on system performance as a function of evaporator secondary fluid temperature lifts as it has been done in recent years for subcooling in the condenser. Usually, a small secondary fluid temperature lift at the evaporator is preferred. This might be the reason of the lack on superheat studies. However, there are applications where the required temperature lift at the evaporator is high. For instance, in heat recovery applications (Hervas-Blasco et al., 2017), it could be more profitable to have a high temperature lift at the heat source in order to extract as much energy as possible.

In this work, a novel exergy analysis for vapor-compression systems as a function of the temperature lift of the sink and the source is done. In order to perform this analysis, the water-to-water heat pump presented in (Pitarch et al., 2018) has been selected as reference. A model of this heat pump has been built and validated against a set of experimental test of the heat pump. The model has shown an error lower than 3% in the prediction of the relevant variables. Later on, the model has been used to analyze the system in a wide range of external conditions. From this analysis, the relative influence of each component to the losses of the system has been defined. The subcooling and superheat depending on the temperature lift of the source and the sink in order to operate at optimum COP conditions has been obtained.

This study will allow improving the performance of refrigeration systems controlling properly the subcooling and superheat degree of the system. It is important to remark that the proper control of these variables can be performed without major changes on the vapor compression system.

2.4 Methodology

2.4.1 Theoretical basis

The exergy at a given point is a measure of the maximum potential work that can be done respect to a reference state. This type of analysis is a way to evaluate the good use of the available energy. In this sense, it is possible to understand the direction for potential improvements (Yumrutaş et al., 2002). In real working cycles, several sources of irreversibility (exergy destruction) prevent achieving the maximum performance, that is, the ideal performance.

The main sources of irreversibility on a vapor compression system are:

- Compressor: The compression does not take place at constant entropy.
- Condenser: The temperature profile of refrigerant and secondary fluid does not match perfectly (finite temperature differences).
- Expansion Valve: The pressure drop is not isentropic, but isenthalpic.
- Evaporator: The temperature profile of refrigerant and secondary fluid does not match perfectly (finite temperature differences).
- For all components and in the pipe exist the irreversibility of the pressure drop due to friction.

For the exergy analysis in this study, the following assumptions have been taken into account:

- The pressure drop in the refrigerant and secondary fluid side is small enough to be negligible.
- Both, the throttling valve and the expansion valve are taken as a unique isenthalpic expansion from point 3 to 5 (Figure 1).
- The expansion and compression are considered adiabatic.
- The irreversibility at the liquid receiver are neglected.
- The kinetic, potential and chemical irreversibility are neglected.

This study evaluates the exergy destruction (irreversibility) and their corresponding exergy efficiencies component by component (Dinçer and Rosen, 2012). Eq. 1 and Eq. 2 represent respectively, the total and the specific exergy of a fluid:

$$\dot{E}x = \dot{m} \cdot ex \tag{1}$$

$$ex = (h - h_0) - T_0 \cdot (s - s_0) \tag{2}$$

Where h is the specific enthalpy, s is the specific entropy, and T0, h0 and s0 are the temperature, the enthalpy and the entropy at the dead state. T0 has been chosen as 0 °C as most of this work is focus on applications with liquid water but other reference can be selected, and the reference pressure for the refrigerant is takn as the saturation pressure at T0 (Dinçer and Rosen, 2012).

The exergy destruction for the compressor accounting with the electrical and mehanical losses can be calculated as follows:
$\dot{E}x_{des,comp} = \dot{W}_{comp} + \dot{m}_{ref} \cdot (ex_1 - ex_2) = \dot{W}_{comp} - \dot{m}_{ref} \cdot [(\mathrm{h}_2 - \mathrm{h}_1) - T_0 \cdot (s_2 - s_1)]$ (3)

Where $\dot{W}_{comp}$ is the compressor consumption of the heat pump and its value could be estimated from representative catalogue data, $\dot{m}_{ref}$ the refrigerant mass flow and h_i and s_i the respective relative enthalpies and entropies of the refrigerant at the inlet and outlet of the compressor according to Figure 1.

The exergy destruction of the condenser and evaporator is obtained from Eq. 4 and Eq. 5. It has been calculated accounting with the electrical and mechanical losses, but neglecting the heat interaction with the ambient (adiabatic):

$$\dot{E}x_{des,cond} = \dot{m}_{ref} \cdot [(\mathrm{h}_2 - \mathrm{h}_3) - T_0 \cdot (s_2 - s_3)] - \dot{Q}_\mathrm{h} \cdot \frac{\bar{T}_H - T_0}{\bar{T}_H} \tag{4}$$

$$\dot{E}x_{des,evap} = \dot{Q}_c \cdot \frac{\bar{T}_C - T_0}{\bar{T}_C} - \dot{m}_{ref} \cdot [(h_1 - \mathrm{h}_5) - T_0 \cdot (s_1 - s_5)] \tag{5}$$

Where and are the heating and cooling capacity of the heat pump. The temperatures and the entropy-averaged temperatures (average temperature in the temperature-entropy diagram) of the secondary fluid at the condenser and evaporator respectively. For constant heat capacity rate and constant pressure processes, the entropy-averaged temperature can also be written as in Eq. 6 and 7 (Hasan et al., 2002).

$$\overline{T}_H = \frac{h_{Sfcondout} - h_{Sfcondin}}{s_{Sfcondout} - s_{Sfcondin}} = \frac{T_{Sfcondout} - T_{Sfcondin}}{\ln(T_{Sfcondout} / T_{Sfcondin})} \tag{6}$$

$$\overline{T}_C = \frac{h_{Hsevapin} - h_{Hsevapot}}{s_{Hsevapin} - s_{Hsevapout}} = \frac{T_{Hsevapin} - T_{Hsevapout}}{\ln(T_{Hsevapin} / T_{Hsevapout})} \tag{7}$$

The exergy destruction at the expansion valve is:

$$\dot{E}x_{des,EV} = \dot{m}_{ref} \cdot T_0 \cdot (s_5 - s_3) \tag{8}$$

Based on the previous expressions, the exergy efficiency for each component is defined according to the Eq. 9-12.

$$\psi_{comp} = \frac{\dot{m}_{ref} \cdot [(\mathrm{h}_2 - \mathrm{h}_1) - T_0 \cdot (s_2 - s_1)]}{\dot{W}_{comp}} \tag{9}$$

$$\psi_{cond} = \frac{\dot{Q}_h \cdot \frac{\bar{T}_H - T_0}{\bar{T}_H}}{\dot{m}_{ref} \cdot [(h_2 - h_3) - T_0 \cdot (s_2 - s_3)]} \tag{10}$$

$$\psi_{evap} = \frac{\dot{m}_{ref} \cdot [(h_1 - h_5) - T_0 \cdot (s_1 - s_5)}{\dot{Q}_C \cdot \frac{\bar{T}_C - T_0}{\bar{T}_C}} \tag{11}$$

$$\psi_{EV} = \frac{ex_5}{ex_3} = \frac{(\mathrm{h}_5 - \mathrm{h0}) - T_0 \cdot (s_5 - s_0)}{(\mathrm{h}_3 - \mathrm{h}_0) - T_0 \cdot (s_3 - s_0)} \tag{12}$$

The total exergy efficiency of the heat pump defined in Eq. 13.

$$\psi_{HP} = \frac{\dot{W}_{comp} - \dot{E}x_{des,tot}}{\dot{W}_{comp}} \tag{13}$$

Where $\dot{E}x_{des,tot}$ is the total exergy destruction or irreversibility, i.e. the sum of exergy destruction of the heat pump components. And the total energy efficiency of the system is based on the heating COP defined in Eq. 14.

$$COP_{\mathrm{h}} = \frac{\dot{Q}_{\mathrm{h}}}{\dot{W}_{comp}} \tag{14}$$

Another important parameter to analyze the system is the relative irreversibility of each component. That is, the irreversibility contribution of each component over the system or total. The relative irreversibility for the component *i* is defined as:

$$RI_i = \frac{\dot{E}x_{des,i}}{\dot{E}x_{des,tot}} \tag{15}$$

This ratio is since a component could have the highest exergy efficiency and still could account with the major part of the system irreversibility (highest potential of improvement regardless the exergy efficiency).

2.4.2 Case study

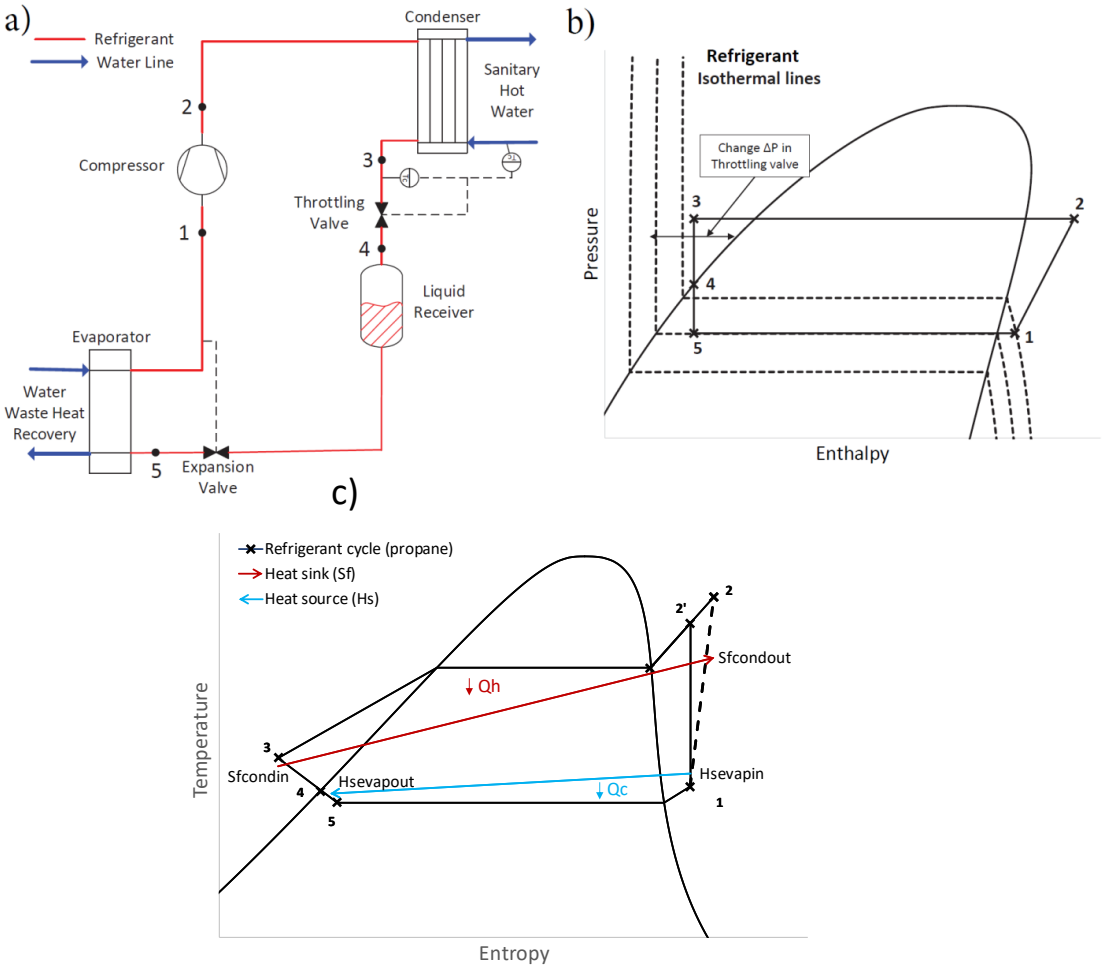

Figure 1: Heat Pump with subcooling at the condenser controlled by a throttling valve a) Scheme of the real system, b) P-h diagram and c) T-s diagram of the heat sink, heat source and refrigerant.

2.4.2.1 Description of the analyzed system

This work is done based on the water-to-water heat pump able to control the subcooling in the condenser and the superheat at the evaporator (see Figure 1). The heat pump is provided with two expansion devices: a throttling valve, located between the condenser and the liquid receiver, and an expansion valve, placed between the liquid receiver and the evaporator. The liquid receiver is used to accommodate the changes in the active charge in the system derived from the variations in the degree of subcooling at the condenser. The throttling valve is the active control component that allows setting the subcooling at the condenser independently from the external conditions. This is made as a consequence of the fact that the liquid receiver at outlet of the throttling valve forces the refrigerant to

be in saturated liquid conditions. Therefore, a change in the pressure drop in the valve will produce a change in the subcooling at the outlet of the condenser.

The expansion valve is the active control component that allows setting the superheat at the evaporator outlet. Therefore, in this system, it is possible to control subcooling and superheat independently at any external conditions.

For more information about the system, please refer to (Pitarch et al., 2018).

Table 1 shows the characteristics of each component.

Table 1: Components of the HP system

Component	Type	Size
Compressor	Scroll (2900 rpm)	29.6 m^3h^{-1}
Condenser	BPHE Counterflow	3.5 m^2
Evaporator	BPHE Counterflow	6 m^2
Liquid Receiver	-	7 l
Expansion Valve	Electronic EX-6	93 kW
Throttling Valve	Electronic EX-5	39 kW

2.4.2.2 Model Validation

A model of the heat pump has been developed using the commercial software IMST-ART (IMST-ART v3.80) in order to study the influence of subcooling and superheat at different external conditions. IMST-ART [76] is a dedicated software for modeling heat pump systems as a whole, according to the state-of-the-art. It incorporates a number of sub-models representing the different parts of the heat pump: compressor, condenser, evaporator and expansion valve.

Compressor model

The compressor model used in IMST-ART is based on the manufacturer AHRI curves for the used compressor working with the used refrigerant.

Expansion valve

The expansion valve includes both, the throttling and the expansion valve according to Figure 1a and it is modeled as an isenthalpic pressure drop in order to fulfill the desired superheat.

Condenser and evaporator

The selected condenser has a horizontal port distance and vertical port distance of 60 mm and 470 mm respectively and 62 plates.

The selected evaporator has 120 plates and a horizontal port distance and vertical port distance of 50 mm and 466 mm respectively.

IMST-ART is able to consider most of the geometrical and operation parameters of current evaporators and condensers. The global solution method employed is called SEWTLE (Semi-Explicit method for Wall Temperature Linked Equations)[77].

The model of this heat pump was already validated in terms of heating COP, capacity and condensing pressure in [78].

The experimental results are based on the measures detailed explained [78]. Table 2 collects the main sensors with the relative and absolute uncertainty intrinsic to the sensor. Please, for more information regarding to uncertainties and error studies, refer to [78].

Table 2: Sensors and uncertainties of the experimental results

Magnitude	Model	Relative uncertainty	Absolute uncertainty	Units
Pressure	*Differential 1151 Smart Rosemount*	*0.1256 % of Span*	*4.684E-04*	*bar*
	Differential P Siemens Sitrans P	*0.1417 % of Span*	*3.542E-04*	*bar*
	Differential P Setra	*0.25 % of Span*	*1.723E-03*	*bar*
	P 1151 Smart GP7 Rosemount	*0.1239 % of Span*	*2.602E-02*	*bar*
	P 1151 Smart GP8 Rosemount	*0.1547 % of Span*	*7.889E-02*	*bar*

Temperature	*P 3051 TG3 Rosemount*	*0.1351 % of Span*	*3.782E-02*	*bar*
	Thermocouple T Type		*1*	*K*
	RTD		*0.06*	*K*
Flow	*Coriolis SITRANS F C MASS 2100*	*0.29 % of Reading*		
	Magnetic SITRANS FM MAG5100 W	*0.36 % of Reading*		
Power	*DME 442*	*0.3 % of Reading*		

Figure 2 compares the model results with the experiments, for the relative irreversibility of each component and their respective exergy efficiency as well as the efficiency of the heat pump system. The results are presented as a function of subcooling for the external conditions at the condenser (Tw,c) from 10°C to 60°C, and at the evaporator an inlet water temperature (Tw,ei) of 20°C with a mass flow rate of 7000 kg/h. Table 1.3 collects the experimental test point used in the validation.

As it can be seen in Figure 2, the highest discrepancies are found for the relative irreversibility at the condenser and evaporator. Nevertheless, all the deviations are below 5%. The optimal subcooling (maximum exergy efficiency of the heat pump) takes place around 42 K for both, the experimental, and the model heat pump.

One should notice that, for this particular case (validation), the secondary fluid outlet temperature at the evaporator changes as a function of subcooling. The heat pump capacity is affected by the subcooling and the secondary fluid mass flow rate through the evaporator is fixed to 7000 kg/h. For the rest of the points showed in the results, the secondary fluid outlet temperature at the evaporator is fixed to a given value and the secondary fluid mass flow rate through the evaporator will depend on the heat pump capacity. In this way, it is easier to extend the results to other heat pump sizes and situations.

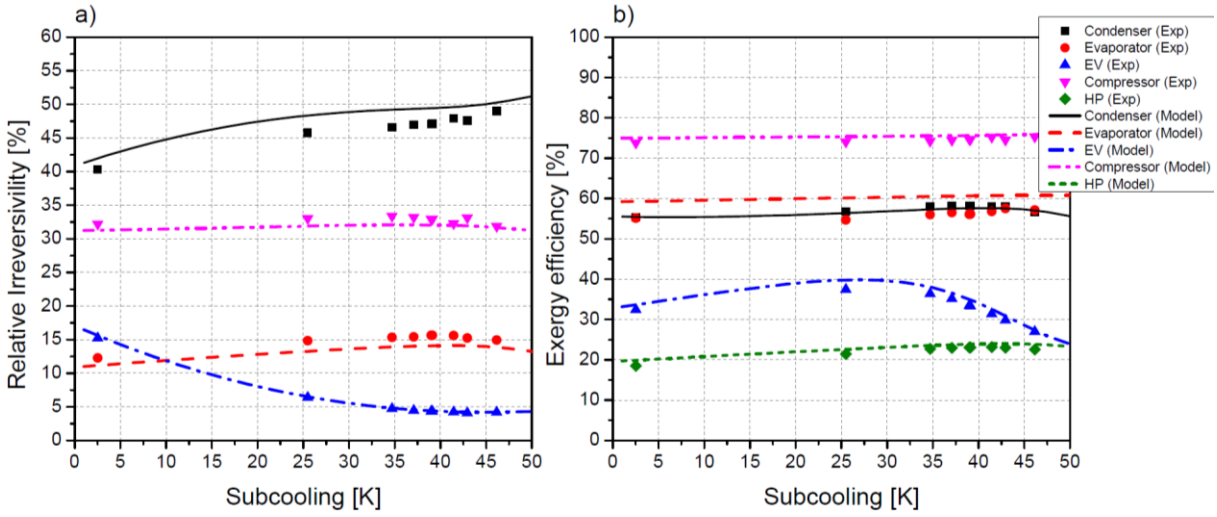

Figure 2. a) Relative irreversibility of each heat pump component. b) Exergy efficiency for each heat pump component and the heat pump system. Water temperatures at the inlet/outlet of the condenser 10°C/60°C. The inlet water temperature at the evaporator inlet 20°C, with a mass flow rate of 7000 kg/h.

2.5 Results and discussion

This section is divided in four parts. The first one analyses the exergy destruction of each component and their respective exergy efficiency as a function of the temperature lift in the condenser for different subcoolings. The secondary fluid temperatures at the evaporator are fixed to 20°C and 15°C for the inlet and outlet, respectively. The refrigerant superheat at the evaporator outlet is fixed to 10 K. The second part focuses on the exergy destruction of each component and their respective exergy efficiency as a function of the temperature lift in the evaporator for different superheats. Based on the previous sections, the third part analyses the influence of both secondary fluids combined with subcooling and superheat. Finally, the last part supplies some examples of different applications where this study can be used in order to improve the efficiency of the system. Table 1.3 summarizes all the conditions used in the performed study.

Table 3: Temperatures of the secondary fluids at the evaporator and condenser superheat and subcooling used

	Evaporator		DT evap [K]	Sh [K]	Condenser		DT cond [K]
	Tin [ºC]	Tout [ºC]			Tin [ºC]	Tout[ºC]	
1st PART	20	15	5	10	10 30 50	60	50 30 10
					30 50 70	80	50 30 10
2nc PART	20	1 5 10 15	19 15 10 5	0-20	10	60	50
		5 10 15	15 10 5		50		10
3rdPART	20	5 15	15 5	0-20	10 50	60	50 10

The outlet water temperature in the condenser has been selected in order to cover some applications were the use of heat pumps is not currently widespread. For instance, in domestic hot water production, or in the production of water up to 80°C that could be interesting for the substitution of boilers in systems using high temperature radiators as terminal units.

2.5.1 Exergy analysis as a function of temperature lift in the condenser

In previous works it has been demonstrated that for a given temperature lift in the condenser secondary fluid and for a heat exchanger of infinite area there is an optimum subcooling which is found where the condenser has two pinch points where the temperature difference between both fluids is 0K. For heat exchangers of finite area this relation is approximately maintained but the temperature difference is higher than 0K. Nevertheless, the influence of the temperature lift in the condenser secondary fluid in the whole system is not obvious.

Figure 1.3 shows the relative irreversibility of each component and their exergy efficiency as a function of subcooling for different water inlet temperatures at the condenser. The water outlet temperature is fixed to 60°C and the evaporator water inlet and outlet temperatures are 20°C and 15°C respectively. Looking at the total exergy efficiency of the heat pump, the optimal subcooling when heating water

from 10°C to 60°C (50K water temperature lift) is around 42K. The efficiency of the compressor and the evaporator remains almost constant with subcooling, the efficiency of the condenser slightly increases up to a maximum around 42K. The maximum efficiency of the expansion valve is around 27K of subcooling, having a lower efficiency at the optimum point of the heat pump. As it can be seen in the relative irreversibilities, the condenser is the component with the highest irreversibilities followed by the compressor, which account with around the 32% from the total irreversibility. This is in agreement with the fact that the curve of heat pump exergy efficiency follows the shape of the curve of the condenser efficiency.

When heating water from 30°C to 60°C, the optimal subcooling is around 26K. The total exergy efficiency is higher than in the case 10°C to 60°C, this means that the heat pump is working closer to the maximum performance for this condition. The condenser efficiency has increased significantly (up to 80%) and it is practically constant until 26K of subcooling. The efficiency of the evaporator and compressor have similar values to the observed previously and the expansion valve have a maximum efficiency approximately 26K of subcooling. Now the compressor has the highest irreversivilities of the system, followed by the condenser.

When heating water from 50°C to 60°C, the optimal subcooling is found around 10K. The condenser efficiency is higher than in the previous case but decreases slightly with subcooling. The expansion valve has its maximum efficiency at 11K of subcooling and it is the element accounting for higher relative irreversivilities after the compressor. This result is the opposite the result found for heating water from 10°C to 60°C.

Figure 4 shows the relative irreversibility of each component and their exergy efficiency as a function of subcooling for different water inlet temperatures at the condenser. The water outlet temperature is fixed to 80°C and the evaporator water inlet and outlet temperatures are 20°C and 15°C respectively. Therefore, it has the same conditions at the evaporator and the same water temperature lift at the condenser than in figure 3, but with a higher outlet temperature. Comparing both figures, it can be stablished that optimal subcooling depends mainly on the secondary fluid temperature lift in agreement with the experimental results presented in (Pitarch et al., 2018). From these figures, it can be concluded that the most influent variable on the expansion valve irreversibility is the refrigerant outlet temperature at the condenser, which is directly related to the subcooling and it is limited by the inlet temperature of the secondary fluid at the condenser.

The condenser exergy efficiency depends mainly on the temperature difference between the refrigerant and the secondary fluid at the condenser, hence it is affected mainly by the temperature profile of the secondary fluid (temperature lift) and refrigerant (subcooling). The evaporator is not affected significantly by neither the temperature lift nor the absolute value of the secondary fluid temperature in the condenser. Finally, the compressor efficiency depends on the condensing pressure, which is related to the absolute temperatures of the secondary fluid at the condenser. The compressor efficiency remains almost constant below the optimal subcooling, but it slightly decreases from this point due to an increase of the condensing pressure.

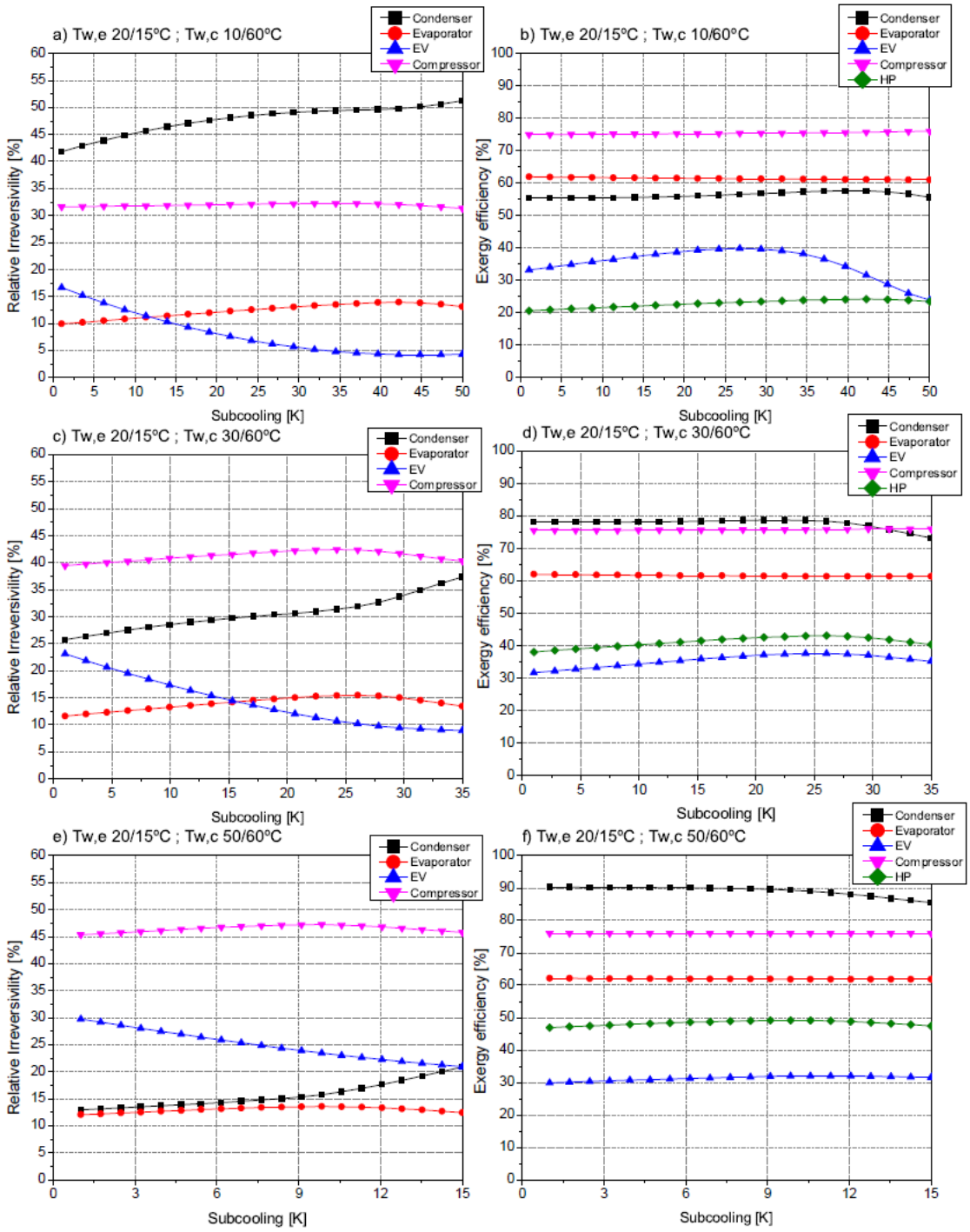

Figure 3. a), c) and e) Relative irreversibility of each heat pump component. b), d) and f) Exergy efficiency for each heat pump component and the heat pump system. Water temperatures at the inlet/outlet of evaporator 20°C/15°C, and water at the condenser outlet 60°C

Table 4 contains the absolute irreversibility of each component for the studied external conditions working at the optimal subcooling. It also shows the exergy efficiency and heating COP improvement respect to the case without subcooling. One should notice the difference between the definitions of COP and exergy efficiency. The exergy efficiency gives information about the external conditions, since it measures how well the heat pump is working in comparison to the reference reversible cycle.

Finally, it can be commented that for low and medium condenser temperature lift, the main component that contributes to the heat pump improvement with subcooling is the expansion valve, which efficiency always increases with subcooling up to a maximum, followed by the condenser, which efficiency only increases at a certain external conditions. For high condenser temperature lift, the condenser can have a higher influence than the expansion valve.

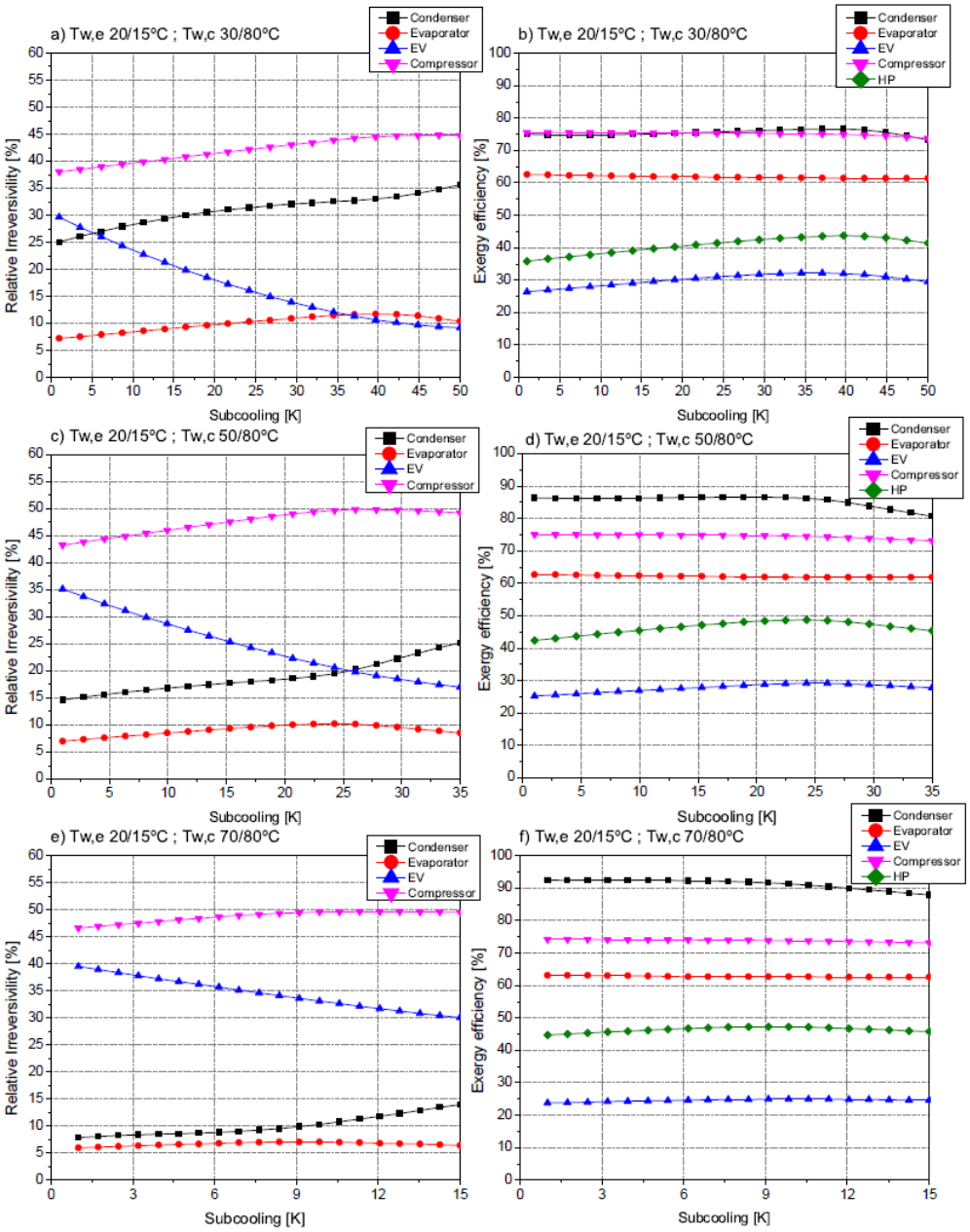

Figure 4. a), c) and e) Relative irreversibility of each heat pump component. b), d) and f) Exergy efficiency for each heat pump component and the heat pump system. Water temperatures at the inlet/outlet of evaporator 20°C/15°C, and water at the condenser outlet 80°C

Table 4: Exergy destruction of each component COP and heat pump efficiency improvement for different external conditions working at the optimal subcooling. Tw,e from 20°C to 15°C.

External condition [°C]	Sb_{opt} [K]	W_{com} [kW]	$\dot{E}x_{des,cond}$ [kW]	$\dot{E}x_{des,evap}$ [kW]	$\dot{E}x_{des,EV}$ [kW]	$\dot{E}x_{des,comp}$ [kW]	$\dot{E}x_{des,tot}$ [kW]	ψ_{HP} [%] (0K Subcool-Opt. Subcool)	COP_h [-] (0K Subcool-Opt. Subcool)
10 to 60	42.36	8.56	3.23	0.90	0.28	2.08	6.49	(20.7-24.2)	(4.46-5.54)
30 to 60	26.05	8.80	1.60	0.78	0.51	2.12	5.01	(38.1-43.1)	(4.17-4.82)
50 to 60	9.84	9.17	0.73	0.63	1.09	2.20	4.66	(47.0-49.2)	(3.82-4.02)
30 to 80	39.68	11.25	2.09	0.74	0.68	2.82	6.33	(35.8-43.7)	(3.06-3.87)
50 to 80	24.26	11.68	1.17	0.61	1.23	2.97	5.98	(42.4-48.8)	(2.81-3.30)
70 to 80	9.11	12.32	0.64	0.46	2.18	3.21	6.50	(44.7-47.3)	(2.49-2.66)

Although it is necessary to study the particularity of each case, from the previous analysis the following rules of thumb can be applied:

- For low inlet temperatures and high temperature lifts of the secondary fluid at the condenser, the components that account with higher irreversibility are the condenser and the compressor. Hence, these are a good place to look for improvement. For instance, it could be discussed if a refrigerant mixture with a high temperature glide and working with subcooling could improve performance in these cases.
- For high inlet temperatures and low temperature lifts of the secondary fluid at the condenser, the components that account with higher irreversibility are the expansion valve and the compressor. In this case, it could be discussed the use of a liquid-suction heat exchanger or doing mechanical subcooling to improve the efficiency in the expansion valve. In [79] it is proposed to use an expander in order to recover part of the energy lost in the expansion valve in a transcritical system.

2.5.2 Exergy analysis as a function of temperature lift in the evaporator

In a similar way to the condenser, considering an evaporator of infinite area, the performance of the evaporator for a heat source of finite capacity and a temperature lift of ΔT is found for an evaporating temperature equal to Tw,e,in.+ΔT and a superheat equal to ΔT. When the evaporator has a finite area, the results are not so direct. This section will show a study in order to give some insight in that respect.

Figure 5a) shows the exergy efficiency of the heat pump as a function of superheat for four different temperature lifts of the evaporator secondary fluid. Tw,ei is fixed to 20°C and the water is heated from 10°C to 60°C in the condenser. For all conditions, the exergy efficiency slightly increases with superheat up to a maximum. From this point, the exergy efficiency decreases at a higher rate. For the condition Tw,e from 20°C to 15°C, the optimal superheat is 6 K, while the optimal superheat if the conditions at the evaporator are Tw,e from 20°C to 1°C is 16 K (with more than 3% of performance improvement). The degree of improvement with superheat is not so important as the one observed with subcooling. The dependency of the optimal superheat with the secondary fluid temperature lift can be seen better in figure 5b), where it has been included the results for a different conditions on the condenser (Tw,c from 50°C to 60°C).

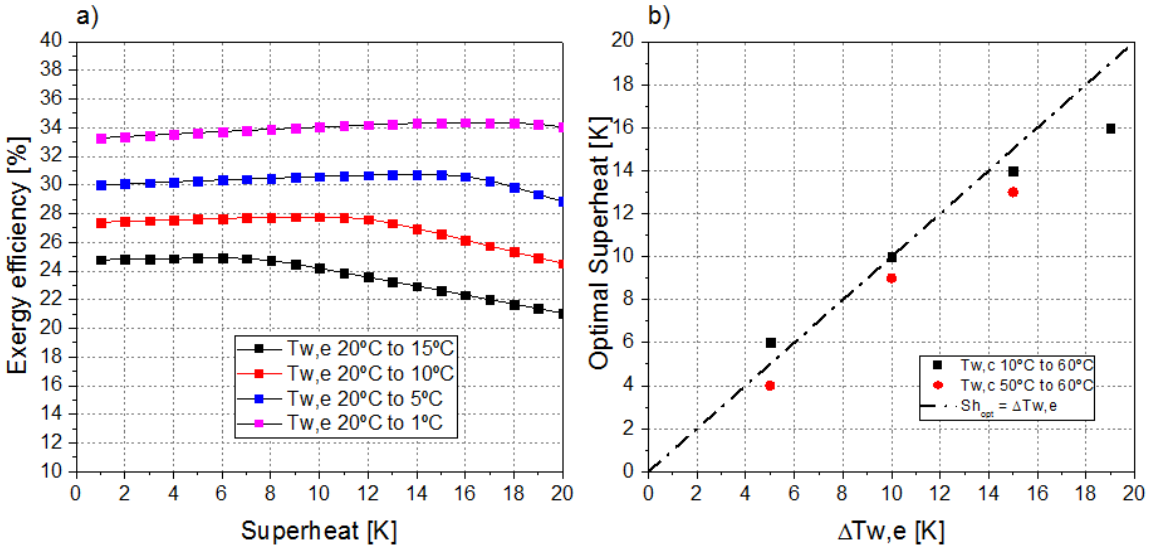

Figure 5. a) Exergy efficiency as a function of superheat, Tw,c from 10°C to 60°C b) Optimal superheat as a function of the secondary fluid temperature lift at the evaporator, Tw,ei=20°C

Figure 6 shows the relative irreversibility of each component and their exergy efficiency as a function of superheat and for different water outlet temperatures at the evaporator. Tw,ei is fixed to 20°C and the condenser water inlet and outlet temperature are 10°C and 60°C respectively. The maximum efficiency when cooling from 20°C to 5°C is given at 14 K of superheat (optimal superheat). At this point, the efficiency (exergy or COP) of the system has increased around 3% respect to the case without superheat (Table 4). Below the optimal superheat, the efficiencies of the condenser, the evaporator and the compressor slightly increase with superheat, being the compressor the one that experiences a bigger change. After the optimal superheat, the efficiency of condenser and compressor slightly decreases, while the efficiency of the evaporator decreases significantly. The efficiency of the expansion valve always decreases with superheat. The efficiency of the compressor and condenser has a similar trend for the other two conditions in the evaporator (20°C to 10°C and 20°C to 15°C). The compressor still has its maximum around 14 K or 15 K of superheat and the condenser maximum is now around 18 K, even though the optimal superheat of the system decreases with Tw,e (for instance, the optimal superheat for Tw,e from 20°C to 15°C is around 6 K). While the efficiency of the evaporator, contrary to the first condition, always decreases with superheat. This trend was similar to the observed for the condenser as a function of subcooling in the previous section.

Regarding to the relative irreversibility of each component, while the superheat is maintained below the optimum value, the superheat or the evaporator water temperature lift do not affect them significantly.

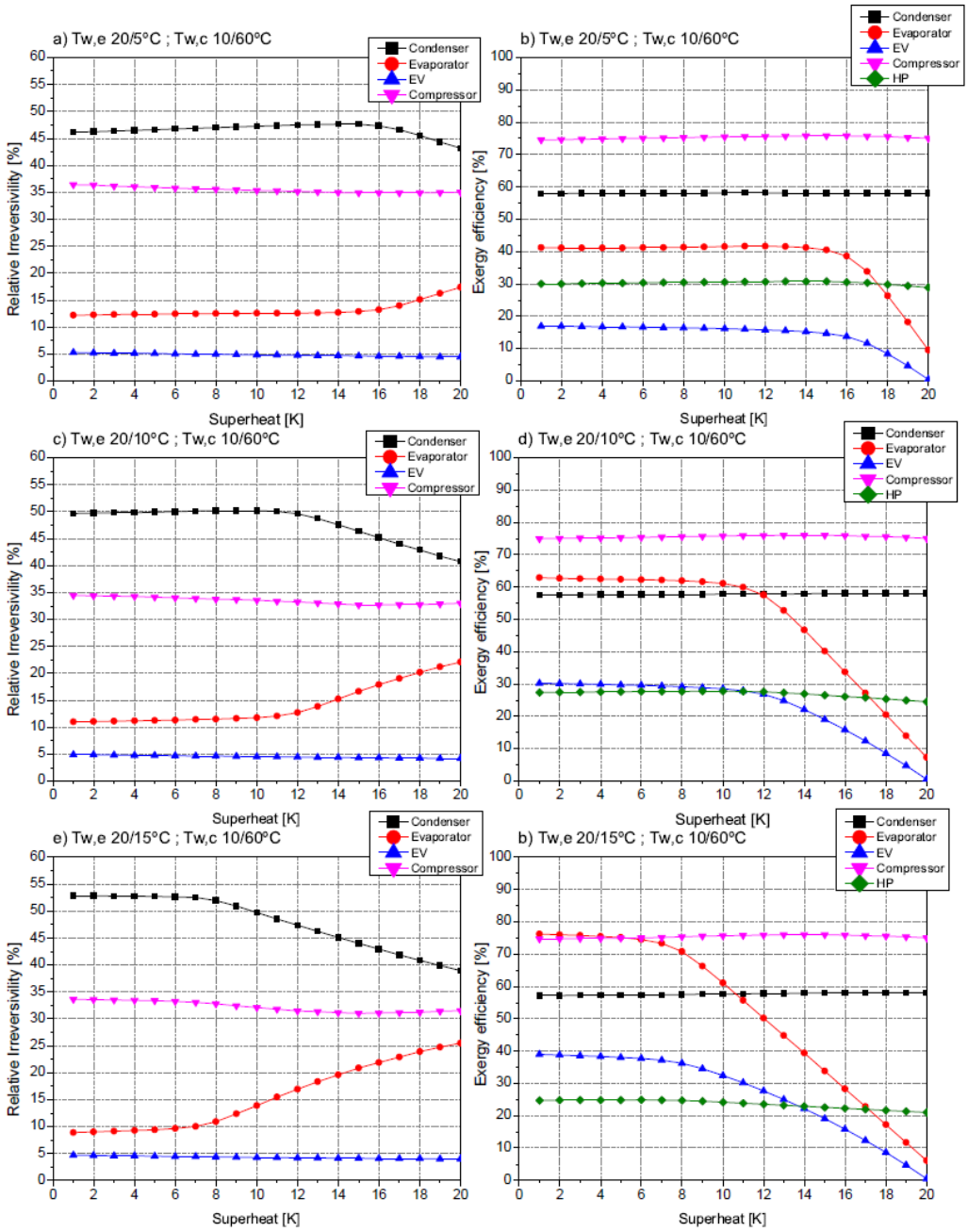

Figure 6. a), c) and e) Relative irreversibility of each heat pump component. b), d) and f) Exergy efficiency for each heat pump component and the heat pump system. Tw,ei= 20°C and Tw,c from 10°C to 60°C

Figure 7 is similar to Figure 6 but the condenser is heating the secondary fluid from 50°C to 60°C. The optimal superheat is slightly lower than in the previous case (10°C to 60°C). On the one hand, the evaporator, the compressor and the expansion valve efficiencies have a similar trend than in Figure 6 (case 10°C to 60°C at the condenser). On the other hand, the efficiency of the condenser always decreases with superheat for the three considered secondary fluid temperatures

at the evaporator. This behaviour is different from the observed in Figure 6 and can be understood as:

The discharge temperature increases with superheat and, even though the condenser needs to use more area for the de-superheating region, the condensing pressure decreases. This is due to the internal pinch point, which is limiting the condensing pressure and it is relocated to a lower temperature when the condenser has a higher a higher area for de-superheating. The effect of superheat on the discharge temperature and the condensing pressure is the same for the cases of Figure 6 and 7. Nevertheless, as it has been seen, it affects the condenser differently: for high temperature lifts at the condenser (10°C to 60°C, Figure 6), the efficiency increases with superheat up to a maximum, while for low temperature lifts (50°C to 60°C, Figure 7), the efficiency decreases with superheat.

Regarding to the relative irreversibility of each component, below the optimal value of superheat, they are not significantly affected by superheat or the secondary fluid temperature lift at the evaporator. The major part of the irreversibility takes place in the compressor, followed by the expansion valve. Similar simulations have been carried out for Tw,ei of 10 °C and 30 °C obtaining similar conclusions to the ones presented in this article.

Therefore, it has been proved that an optimal superheat exists, and it depends mainly on the secondary fluid temperature lift at the evaporator but the temperature lift in the condenser should be considered as well. The main component that contributes to the heat pump irreversivilities is the compressor. The condenser and evaporator efficiencies only increase at a certain external condition, while the expansion valve efficiency always decreases. It is worth it to remark that the degree of improvement is lower than the one achieved with subcooling.

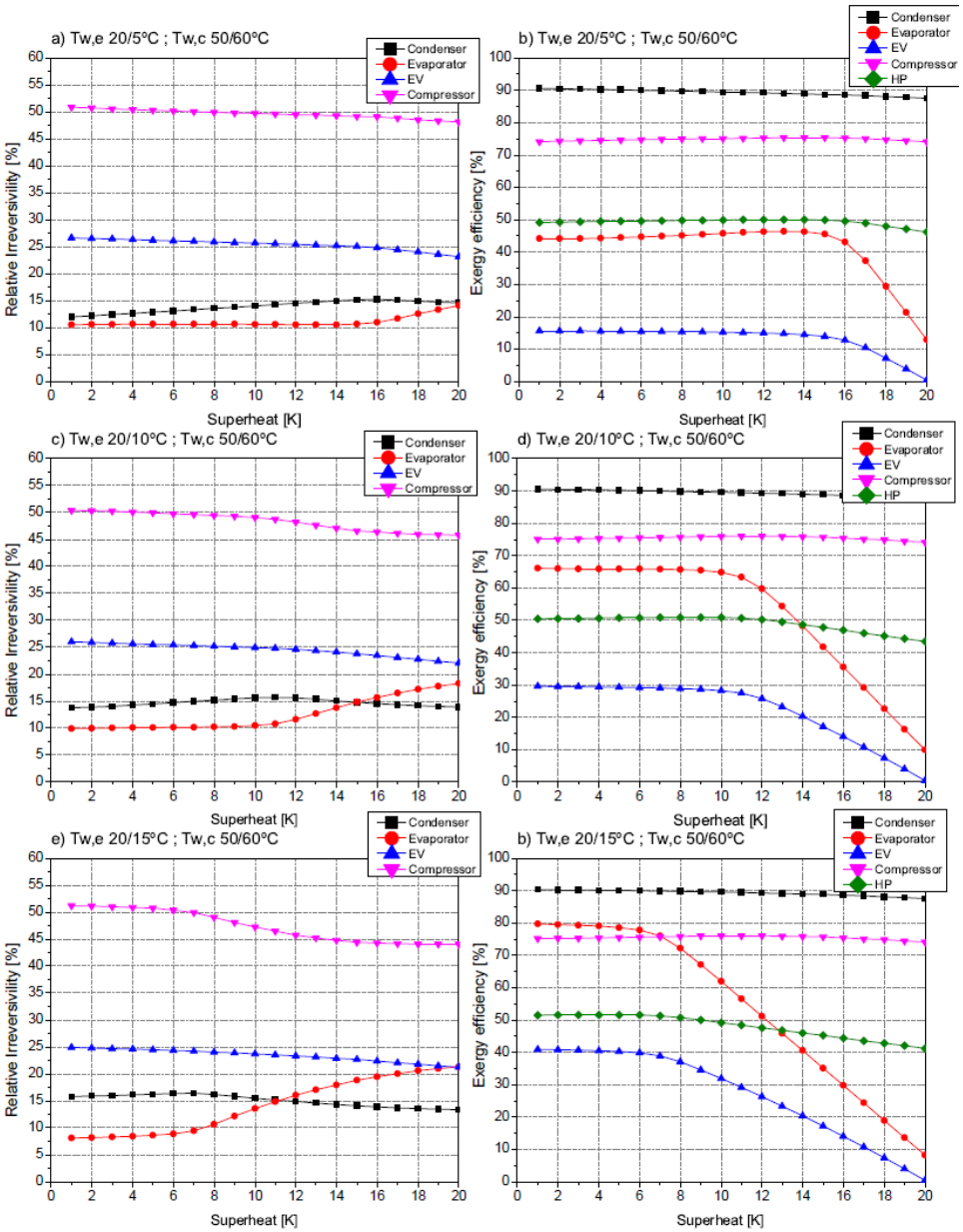

Figure 7. a), c) and e) Relative irreversibility of each heat pump component. b), d) and f) Exergy efficiency for each heat pump component and the heat pump system. Tw,ei= 20°C and Tw,c from 50°C to 60°C

Table 5: Exergy destruction of each component and heat pump efficiency improvement for different external conditions working at the optimal superheat and subcooling.

External condition [°C]	Sh_{opt} [K]	W_{comp} [kW]	$\dot{E}x_{des,cond}$ [kW]	$\dot{E}x_{des,evap}$ [kW]	$\dot{E}x_{des,EV}$ [kW]	$\dot{E}x_{des,comp}$ [kW]	$\dot{E}x_{des,tot}$ [kW]	ψ_{HP} [%] (0K SH-Opt. SH)	COP_h[-] (0K SH-Opt. SH)
20to1 &10 to 60	16	7.89	2.40	0.55	0.26	1.96	5.18	(33.3 - 34.4)	(4.43-4.58)
20 to 5 &10 to 60	14	8.09	2.67	0.71	0.26	1.96	5.61	(30.0-30.7)	(4.80-4.93)
20 to 10 &10 to 60	10	8.42	3.05	0.72	0.28	2.04	6.08	(27.4-27.8)	(5.27-5.35)
20 to 15 &10to 60	6	8.77	3.47	0.63	0.29	2.19	6.58	(24.8-24.9)	(5.72-5.75)
20 to 5 &50to 60	13	8.86	0.65	0.47	1.12	2.19	4.43	(49.2-50.0)	(3.51-3.58)
20 to 10 &50 to 60	9	9.09	0.69	0.46	1.12	2.20	4.46	(50.4-50.9)	(3.88-3.92)
20 to 15 &50 to 60	4	9.33	0.73	0.38	1.11	2.30	4.52	(51.5-51.6)	(4.24-4.25)

Although it is necessary to study the particularity of each case, from the previous analysis the following rule of thumb can be applied:

The optimum superheat in the evaporator increases as increases the temperature lift in the evaporator. This optimum superheat constitutes a value that the system never has to overcome as from this value there is an important reduction of system efficiency.

2.5.3 Exergy analysis of the whole system as a function of subcooling and superheat

In the previous two sections, it has been shown that there is an optimum subcooling and superheat in vapor compression cycles working between a heat sink and a heat source of finite capacity. It has been shown also that the optimum subcooling depends mainly on the temperature lift of the heat sink and the optimum superheat depends mainly on the temperature lift of heat source. However, it has been also seen that the heat sink has an influence in the optimum superheat and the heat source has an influence in the optimum subcooling. In order

to understand properly the combined effect of both variables from the point of view of the system figure 8 shows the counterplot of the heat pump exergy efficiency as a function of superheat and subcooling for different conditions in the evaporator and the condenser. The efficiency degradation above the optimal subcooling is slightly higher than below this point. The efficiency degradation above the optimal superheat is considerably higher than below this point. The efficiency improvement obtained when superheat increases from 0 up to the optimum is not very significantly (this behavior is significantly different for subcooling). This might be the reason why most of the works and technical papers recommendations is to keep low superheat.

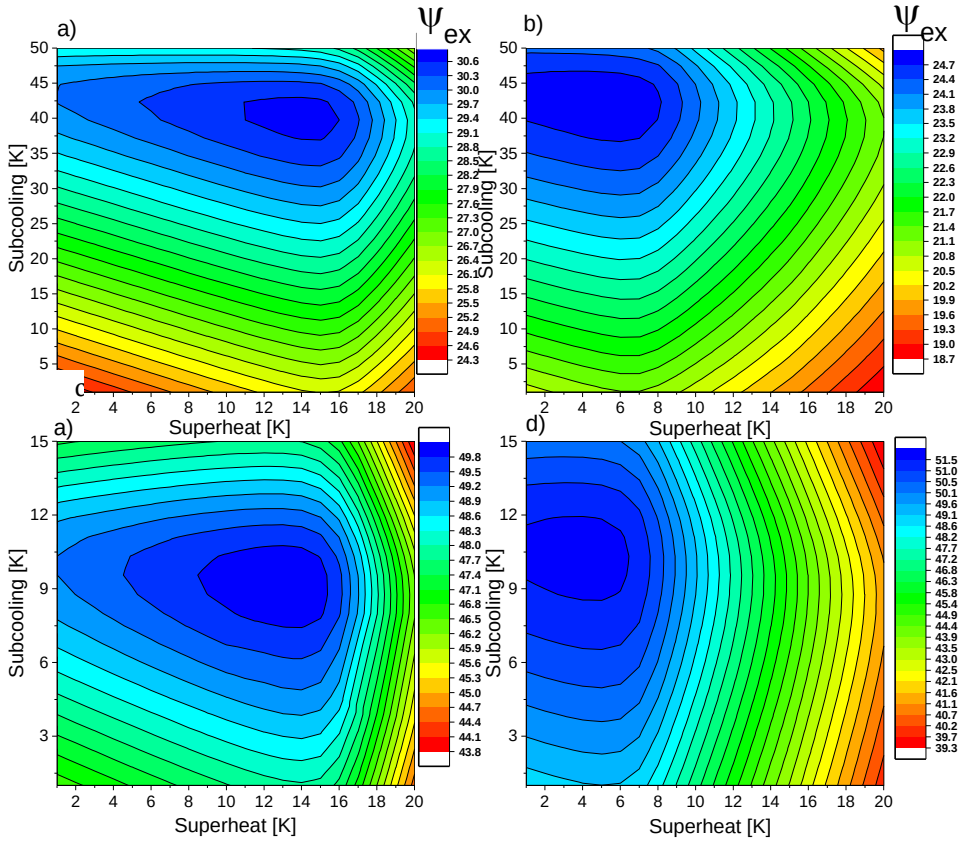

Figure 8. Heat pump exergy efficiency as a function of subcooling and superheat a) Tw,e from 20°C to 5°C and Tw,c from 10°C to 60°C; b) Tw,e from 20°C to 15°C and Tw,c from 10°C to 60°C; c) Tw,e from 20°C to 5°C and Tw,c from 50°C to 60°C; d) Tw,e from 20°C to 15°C and Tw,c from 50°C to 60°C

From Figure 8, it is seen that optimum subcooling depends on temperature lift of the heat source and heat sink, nowadays there are some authors that are focusing in developing models in order to predict the charge of the system and based on that be able to predict the subcooling [80]. With the approach shown here, that kind of models can be used in the other way around, the prediction of the charge of the system corresponding to the optimum subcooling which provides the optimum COP for a given temperature lift in the heat source.

2.5.4 Optimal operation for different applications

From all this work, the optimum superheat and subcooling of a single stage vapor compression system is obtained as a function of the external conditions (temperature lift of the source and sink).

From the heat pump design, these results are useful from the point of view of defining the setting of the subcooling and superheat of a vapor compression system depending on the application field.

Table 6: Optimal subcooling and superheat for different HP applications

Application	Heat source Tin-Tout [°C]	Heat sink Tin-Tout [°C]	Heat source DT [K]	Optimal superheat [K]	Heat sink temp.lift [K]	Optimal subcooling [K]
DHW production	15 -10	10-60	5	~ 7 (min)	50	43
Dryer	47 - 40	40-75	7	~ 7 (min)	35	31
Heating	15 - 10	40-45	5	~ 7 (min)	5	8
Heat recovery	35 - 5	10-60	30	28	50	43
Heat recovery	20 - 5	10-60	15	16	50	43

As a rule of thumb, it is described that heat pumps for heating and cooling have an optimum subcooling between 5K and 10K and the superheat should be maintained as low as possible in order to optimize the performance of the systems. (~7 K due to temperature measure complexity of satured conditions and the safety of the compressor) (Pottker and Hrnjak, 2015). While these rules are close to optimal values for applications where the temperature lifts at the heat source or sink are small (typical HP applications until recent years such as heating applications), they

are only valid for the specific application in which they were obtained. In fact, the results presented in the previous sections shows that the optimum subcooling depends mainly on the temperature lift of the secondary fluid in the condenser and that the superheat depends mainly on the temperature lift of the secondary fluid of the evaporator.

Table 6 shows some application examples of heat pump systems with different temperature lift in the secondary fluids and supply the optimum subcooling and superheat for them.

2.6 Conclusions

A heat pump has been analyzed component by component (exergy analysis) as a function of subcooling and superheat for several external conditions at the condenser and evaporator.

The main conclusions extracted from the subcooling analysis are:

•The components that contribute most to the heat pump exergy efficiency improvement with subcooling are the expansion valve and the condenser. The most influent one will depend on the external conditions in the condenser.

•For low secondary fluid inlet temperatures and high temperature lifts of the secondary fluid at the condenser, the components that account with higher irreversibility are the condenser and the compressor. Hence, if looking for improvements, these components are the first to look at. For instance, it could be discussed if a refrigerant mixture with a high temperature glide and working with subcooling could improve performance in these cases.

•For high secondary fluid inlet temperatures and low temperature lifts of the secondary fluid at the condenser, the components that account with higher irreversibility are the expansion valve and the compressor. In this case, it could be discussed the use of a liquid-suction heat exchanger or doing mechanical subcooling to improve the efficiency in the expansion valve.

Regarding to the superheat study, there is an optimal superheat, and it depends mainly on the secondary fluid temperature lift in the evaporator as subcooling does in the condenser. Other relevant results are:

•Working at the optimal superheat, the efficiency of the heat pump for the condition 20°C to 5°C in the evaporator (optimal superheat 14K) increases 3%

compared to the case without superheat. This improvement is lower than the one observed for subcooling for the same temperature lift.

•The compressor is the most influent component in the observed improvement of the heat pump performance with superheat.

•Below the optimal superheat, the relative irreversibility of each component is not affected significantly by superheat or by the secondary fluid temperature lift at the evaporator. Hence, the irreversibility distribution in the components will depend mainly on the conditions at the condenser.

Therefore, based on the temperature lift of the working sources and sinks of a heat pump, it seems necessary to design heat pumps able not only to control subcooling, which has already proved to have a high influence on the heat pump performance, but also able to control the degree of superheat, which can push a bit higher the heat pump performance. As it is show in the heat pump system presented in this paper, subcooling and superheat are the two variables that can be controlled at the will of the engineer in a heat pump of single stage cycle working between a heat source and a heat sink. The rest of the parameters of the system like condensing temperature, evaporating temperature and the like usually are more fixed once the compressor and the heat exchangers are selected.

2.7 Acknowledgements

Part of the results of this study were developed in the mainframe of the FP7 European project 'Next Generation of Heat Pumps working with Natural fluids' (NxtHPG). Part of the work presented was carried by Miquel Pitarch-Mocholí with the financial support of the Phd scholarship from the Universitat Politècnica de València. Part of the work presented was carried by Estefanía Hervás Blasco with the financial support of a PhD scholarship from the Spanish government SFPI1500X074478XV0. The authors would like to acknowledge the Spanish 'MINISTERIO DE ECONOMIA Y COMPETITIVIDAD', through the project ref-ENE2014-53311-C2-1-P-AR "Aprovechamiento del calor residual a baja temperatura mediante bombas de calor para la produccion de agua caliente" for the given support.

2.8 References

Ajuka, L., Odunfa, M., Ohunakin, O., Oyewola, M., Oyewola, M., 2017. Energy and exergy analysis of vapour compression refrigeration system using selected eco-friendly hydrocarbon refrigerants enhanced with tio2-nanoparticle. Int. J. Eng. Technol. 6, 91. doi:10.14419/ijet.v6i4.7099

Arat, H., Arslan, O., 2017. Exergoeconomic analysis of district heating system boosted by the geothermal heat pump. Energy 119, 1159–1170. doi:10.1016/j.enery.2016.11.073

Bahman, A., Ziviani, D., Groll, E., 2018. Development and Validation of a Mechanistic Vapor-Compression Cycle Model.

Cecchinato, L., Corradi, M., Minetto, S., 2010. A critical approach to the determination of optimal heat rejection pressure in transcritical systems. Appl. Therm. Eng. 30, 1812–1823. doi:10.1016/j.applthermaleng.2010.04.015

Chen, Y., Gu, J., 2005. The optimum high pressure for CO2 transcritical refrigeration systems with internal heat exchangers. Int. J. Refrig. 28, 1238–1249. doi:10.1016/j.ijrefrig.2005.08.009

Choi, J., Kim, Y., 2004. Influence of the expansion device on the performance of a heat pump using R407C under a range of charging conditions. Int. J. Refrig. 27, 378–384. doi:10.1016/j.ijrefrig.2003.12.002

Corberán, J.M., Martínez, I.O., Gonzálvez, J., 2007. Charge optimisation study of a reversible water-to-water propane heat pump Etude sur l'optimisation de la charge d'une pompe à chaleur ré versible eau-eau au propane. doi:10.1016/j.ijrefrig.2007.12.011

Corberan, J.M., Gonzalvez, J., Montes, P., Blasco, R., , 2002. Purdue 'ART' A Computer Code To Assist The Design Of Refrigeration and A/C Equipment R9-4 ".

Corberán, J.M., Fernández de Cordoba, P., Gonzalvez, J., Alias, F., 2001. Semiexplicit method for wall temperature linked equations (sewtle): a general finite-volume technique for the calculation of complex heat exchangers. Numer. Heat Transf. Part B Fundam. 40, 37–59. doi:10.1080/104077901300233596

Di Somma, M., Yan, B., Bianco, N., Graditi, G., Luh, P.B., Mongibello, L., Naso, V., 2017. Multi-objective design optimization of distributed energy systems through cost

and exergy assessments. Appl. Energy 204, 1299–1316. doi:10.1016/j.apenergy.2017.03.105

Dinçer, I., Rosen, M. (Marc A.., 2012. Exergy : Energy, Environment and Sustainable Development. Elsevier Science.

Fernando, P., Palm, B., Lundqvist, P., Granryd, E., 2004. Propane heat pump with low refrigerant charge: design and laboratory tests. Int. J. Refrig. 27, 761–773. doi:10.1016/j.ijrefrig.2004.06.012

Hasan, A.A., Goswami, D.Y., Vijayaraghavan, S., 2002. First and second law analysis of a new power and refrigeration thermodynamic cycle using a solar heat source. Sol. Energy 73, 385–393. doi:10.1016/S0038-092X(02)00113-5

Hervas-Blasco, E., Pitarch, M., Navarro-Peris, E., Corberán, J.M., 2017. Optimal sizing of a heat pump booster for sanitary hot water production to maximize benefit for the substitution of gas boilers. Energy 127. doi:10.1016/j.energy.2017.03.131

Hjerkinn, T., 2007. Analysis of Heat Pump Water Heater Systems for Low-Energy Block of Flats. Master thesis at the Norwegian University of Science and Technology (NTNU), Dept. of Energy and Process Engineering. EPT-M-2007-24.

Inokuty, H., 1928. Graphical method of finding compression pressure of CO2 refrigerating machine for maximum coefficient of performance, in: The Fifth International Congress of Refrigeration, Rome. pp. 185–192.

Itard, L.C.., Machielsen, C.H.., 1994. Considerations when modelling compression/resorption heat pumps. Int. J. Refrig. 17, 453–460. doi:10.1016/0140-7007(94)90005-1

Jolly, P.G., Tso, C.P., Chia, P.K., Wong, Y.W., 2000. Intelligent Control to Reduce Superheat Hunting and Optimize Evaporator Performance in Container Refrigeration. HVAC&R Res. 6, 243–255. doi:10.1080/10789669.2000.10391261

Koeln, J.P., Alleyne, A.G., 2014. Optimal subcooling in vapor compression systems via extremum seeking control: Theory and experiments. Int. J. Refrig. 43, 14–25. doi:10.1016/j.ijrefrig.2014.03.012

Pitarch, M., Hervas-Blasco, E., Navarro-Peris, E., Gonzálvez-Maciá, J., Corberán, J.M., 2017. Evaluation of optimal subcooling in subcritical heat pump systems. Int. J. Refrig. 78. doi:10.1016/j.ijrefrig.2017.03.015

Pitarch, M., Navarro-Peris, E., Gonzálvez-Maciá, J., Corberán, J.M., 2018. Experimental study of a heat pump with high subcooling in the condenser for sanitary hot water production. Sci. Technol. Built Environ. 24, 105–114. doi:10.1080/23744731.2017.1333366

Pottker, G., Hrnjak, P., 2015. Effect of the condenser subcooling on the performance of vapor compression systems. Int. J. Refrig. 50, 156–164. doi:10.1016/j.ijrefrig.2014.11.003

Redón, A., Navarro-Peris, E., Pitarch, M., Gonzálvez-Macia, J., Corberán, J.M., 2014. Analysis and optimization of subcritical two-stage vapor injection heat pump systems. Appl. Energy 124, 231–240. doi:10.1016/j.apenergy.2014.02.066

Sarkar, J., Bhattacharyya, S., Gopal, M.R., 2004. Optimization of a transcritical CO2 heat pump cycle for simultaneous cooling and heating applications. Int. J. Refrig. 27, 830–838. doi:10.1016/j.ijrefrig.2004.03.006

Selbaş, R., Kızılkan, Ö., Şencan, A., 2006. Thermoeconomic optimization of subcooled and superheated vapor compression refrigeration cycle. Energy 31, 2108–2128. doi:10.1016/j.energy.2005.10.015

Valencia, G., Beltrán, J., Romero, O., Cabrera, J., 2017. Comparative Evaluation of Different Refrigerants on a Vapor Compression Refrigeration System via Exergetic Performance Coefficient Criterion. Contemp. Eng. Sci. 10. doi:10.12988/ces.2017.7763

van de Bor, D.M., Infante Ferreira, C.A., 2013. Quick selection of industrial heat pump types including the impact of thermodynamic losses. Energy 53, 312–322. doi:10.1016/j.energy.2013.02.065

Xu, L., Hrnjak, P.J., 2014. Potential of controlling subcooling in residential air conditioning system. Purdue conference. Conference paper 1465.

Yang, J.L., Ma, Y.T., Li, M.X., Guan, H.Q., 2005. Exergy analysis of transcritical carbon dioxide refrigeration cycle with an expander. Energy 30, 1162–1175. doi:10.1016/j.energy.2004.08.007

Yang, M.-H., Yeh, R.-H., 2015. Performance and exergy destruction analyses of optimal subcooling for vapor-compression refrigeration systems. Int. J. Heat Mass Transf. 87, 1–10. doi:10.1016/j.ijheatmasstransfer.2015.03.085

Yataganbaba, A., Kilicarslan, A., Kurtbaş, İ., 2015. Exergy analysis of R1234yf and R1234ze as R134a replacements in a two evaporator vapour compression refrigeration system. Int. J. Refrig. 60, 26–37. doi:10.1016/j.ijrefrig.2015.08.010

Yumrutaş, R., Kunduz, M., Kanoğlu, M., 2002. Exergy analysis of vapor compression refrigeration systems. Exergy, An Int. J. 2, 266–272. doi:10.1016/S1164-0235(02)00079-1

LIST OF FIGURES

Tw,c from 10°C to 60°C; c) Tw,e from 20°C to 5°C and Tw,c from 50°C to 60°C; d) Tw,e from 20°C to 15°C and Tw,c from 50°C to 60°C

Chapter 3
Study of different subcooling control strategies in order to enhance the performance of a heat pump

Estefanía HERVAS-BLASCO[(a)], Miquel PITARCH[(a)], Emilio NAVARRO-PERIS[(a)], José M. CORBERÁN[(a)]

[(a)] Institut Universitari d'Investigació d'Enginyeria Energètica, Universitat Politècnica de València, Camí de Vera s/n, València, 46022, Spain

Tel: +34 963879123

enava@ter.upv.es

3.1 Abstract

The performance of vapor-compression systems working with subcritical refrigerants varies with the degree of subcooling. There is an optimal subcooling that maximizes efficiency. However, it depends on the operating conditions and the control of the system needs to be adapted. Most of the works available in literature are able to operate in optimal conditions only at the design point or if a system is designed to be able to adapt its subcooling, only complex control algorithms which usually are difficult to set and time-costly, are used. This work focuses on the study of the main variables influencing the optimal subcooling and analyzes two different control methodologies from the theoretical point of view. Based on the theoretical study a final control strategy is selected and tested experimentally. The reliability, stability and robustness of the selected strategy is experimentally demonstrated for a wide set of operating conditions.

KEYWORDS: Heat pump, natural refrigerant, subcritical refrigerant, optimal subcooling, control

HIGHLIGHTS

- Subcooling enhances heat pump performance up to an optimal value
- Two methodologies to control the optimal subcooling are studied
- Optimal subcooling control based on the secondary fluid temperature lift
- Optimal subcooling control based on a temperature approach
- Stability of the temperature approach control is experimentally proved

3.2 Nomenclature

SHW: Sanitary Hot Water

COP: Coefficient of Performance (COP=QW-1), [-]

COP_norm: COP/COP_max for the same conditions

DT: Temperature difference [K]

Q: heating capacity [W]

W: compressor power [W]

Sh: superheat

Subscripts

a: at the outlet of the heat exchanger

b: at the dew point of the heat exchanger

w: water

in: inlet

out: outlet

norm: normalized

comp: Compressor

cond: Condenser

evap: evaporator

3.3 Introduction

The growth in the awareness to respect the environment is reflected worldwide by means of an increase in the targets and policies to enhance the improvement of the energy sector towards a more sustainable way. Higher performance technologies, heat recovery, natural working fluids and electricity generated by renewables contribute to the reduction in CO2 emissions.

Heat pumps accomplish most of the current requirements for the heating and cooling fields. Hence, the interest of this technology is growing and the improvement of their efficiency would have an impact on society.

In order to optimize the efficiency of vapor compression heat pumps, most of the works used to focus mainly on heat exchangers designs, compressor's improvement, expansion process or working fluid election but the effect of the degree of subcooling on the performance has not been systematically investigated until recently. Possibly, the reason was that in the most common heat pump configurations, the liquid receiver is placed right after the condenser forcing the refrigerant to exit the condenser under saturated conditions leading to zero subcooling. However, in configurations where it is possible to have subcooling some authors demonstrate an increase of performance linked to it. For instance, an improvement of 2% in the efficiency is found for a refrigeration case working with ammonia with 4.66K of subcooling in (Jensen and Skogestad, 2007a). Moreover, a theoretical study of the potential performance improvement by the application of subcooling in an air to air heat pump for various refrigerants was done in (Pottker and Hrnjak, 2015a) resulting, for instance, in an increase of 12% for R744. Later on, in (Pottker and Hrnjak, 2015b) they experimentally demonstrated the enhancement of the COP due to subcooling for an air conditioning system working with R134a for an inlet air temperature of 35°C at the condenser and 5.3kW of cooling capacity. Furthermore, in hot water production applications with high temperature lifts and suboolings around 44K, an improvement up to 30% is experimentally proved in (Pitarch et al., 2017b). In spite of this fact, for each operating condition and size, there is an optimal subcooling that maximizes the COP as it can be seen in (Pitarch et al., 2017c) where two different configurations (a dedicated extra heat exchanger to subooling and the production of the subcooling in the condenser) are compared. The dependency of the optimal value with the working conditions is experimentally demonstrated in (Pitarch et al., 2017d) where improvements range from 7% up to 30% based 10K to 50K of secondary temperature lift. A theoretical study of the optimal subcooling for different refrigerants and heat exchangers design is performed in (Pitarch et

al., 2017a) observing a similar behavior among the subcritical refrigerants studied and the optimal subcooling main dependence on the water temperature lift for a given system.

For predefined external conditions, the subcooling of the system is controlled mainly by the amount of effective charge circulating thorugh the system as it can be seen in (Fernando et al., 2004) for propane. This type of control has some similarities with the control and optimality of the pressure in the gas cooler for transcritical cycles being an example of this the work done in (Jensen and Skogestad (2007a)by the application to CO2 and propane or in (Jensen and Skogestad, 2007b) for CO2 and ammonia. Although there is a vast literature on the thermodynamic analysis of closed refrigeration cycles, few authors discuss the control of the effective charge circulating through the systems. Some discussions are found in textbooks like (Stoecker, 1998) but these mainly deal with more practical aspects. Most of the available literature focuses on CO2 transcritical systems, heating and cooling applications (Sarkar et al., 2004), water heating applications (Stene, 2007), the design of heat exchangers (Chen and Gu, 2005) or the determination of the optimal pressure in the gas cooler (Kauf, 1999) are only a few examples of this.

For subcritical systems, the main control approaches, based on its capability of adaptation can be divided in:

- Passive control: The use of an optimal refrigerant charge based on the design point which is charged before of the system operation (Corberá et al., 2007). In this case, always that the system is not working at the design point, the external conditions vary or after a certain time, the efficiency of the system would not be the maximum.

- Active control: The use of control systems based on equations found after testing the heat pump under a wide set of conditions and for a specific refrigerant. In this type, the optimal subcooling varies based on the programmed fitting and allows the system to work with near-optimal conditions (Bauck Jensen, 2008) even though it implies the test of the heat pump under the given application conditions which could be expensive.

The use of complex controlling methods such as extremum seeking control (Koeln and Alleyne, 2014) (Zhu et al., 2016) that are based on adaptative strategies able to bring the system operating at the highest efficiency. These systems are based on one input and complex controllers that need first to be tunned in order

to determine all the values of the process (frequency, amplitude, perturbations, phases…). Once the parameters are set, its operation starts from a point and tries to converge into the solution close to the maximum COP value. This process does not allow a real understanding of the problem as well as it is time costly (around 3h are needed only to set the installation close to the optimal COP for static conditions, as it is stated in (Hu et al., 2015)).

Nevertheless, in most cases, either the optimal degree of subcooling is unknown (and only is used a certain degree of it) or it is not specified (Fernando et al., 2004) and in works where it is used, the optimal conditions are not stated clearly (Pottker et al., 2012).

Only a few works can be found in this line. In (Jensen and Skogestad (2007a)the optimal subcooling variation with the temperature lift at the secondary fluid is investigated. This dependece allows the control based on an equation for a given size of the system. Furthermore, the potential of the temperature approach as a control variable is analyzed in (Jensen and Skogestad, 2007b) and deeply studied in (Jensen and Skogestad (2007a), where, from a theoretical point of view, it was found that the optimal subcooling in an infinite area condenser takes place when there are two pinch points at the condenser: one inside (dew point) and another at the condenser outlet (approach) and for finite heat exchangers, a similar value of those leads to nearly-optimal operation conditions. Hence, the control of the system based on the temperature approach appears to be a good methodology even though, up to the knowledge of the authors, it has not been experimentally done yet.

In (Pitarch et al., 2017a), the authors analyzed under a theoretical point of view, the effect of the optimal subcooling for different refrigerants and in (Pitarch et al., 2017d) the authors experimentally demonstrated the improvement due to the effect of working with optimal subcooling for each operating and external condition in a water heating application. However, the system was maintained in steady state using a manual control system.

Therefore, according to the above literature, the subcooling problem has been evaluated by a few authors within the heat pump sector. The improvement of the heat pump performance by the implementation of a certain degree of it as well as the existance of an optimal subcooling has been demonstrated in those works for different applications. Nevertheless, it is worth to notice that the optimal subcooling depends on the external operating conditions, the heat pump design and the refirgerant used. Thus, a commercialized heat pump requires not only the knowledge of the existence of an optimum subcooling but also, the integration of a

feasible control system to allow working in these optimal subcooling based on external conditions. Some alternatives has been proposed theoretically but the estrategies experimentally tested in the literature definitively have some open issues in order to be able to implement them in commercial systems. The control is still considered an opened problem.

In this work, two different subcooling control strategies have been evaluated theoretically. The two strategies allow the system to work under optimal conditions. Based on this analysis and the comparison of them, an optimum control strategy compromising complexity-efficiency improvement has been selected. Furthermore, the strategy has been experimentally implemented and tested under a wide range of operating conditions. From the experimental tests, robustness and the characteristic times of the control response have been determined.

The work is organized as follows: first, a description of the system and a theoretical analysis, are presented. Second, the results of the study for the two control strategies considered are detailed investigated. Third, the selected control is experimentally implemented and its stability, presented. Finally, the main conclusions extracted from the work are exposed.

3.4 Methodology

3.4.1 Studied system

This study is based on a water to water heat pump that uses the HC propane (R290) as refrigerant, tap water to be heated until SHW temperatures as secondary fluid and the recuperation of the wasted heat water at temperatures close to the ambient as a heat source.

Figure 1 shows the scheme of the heat pump studied in this work and its P-h diagram.

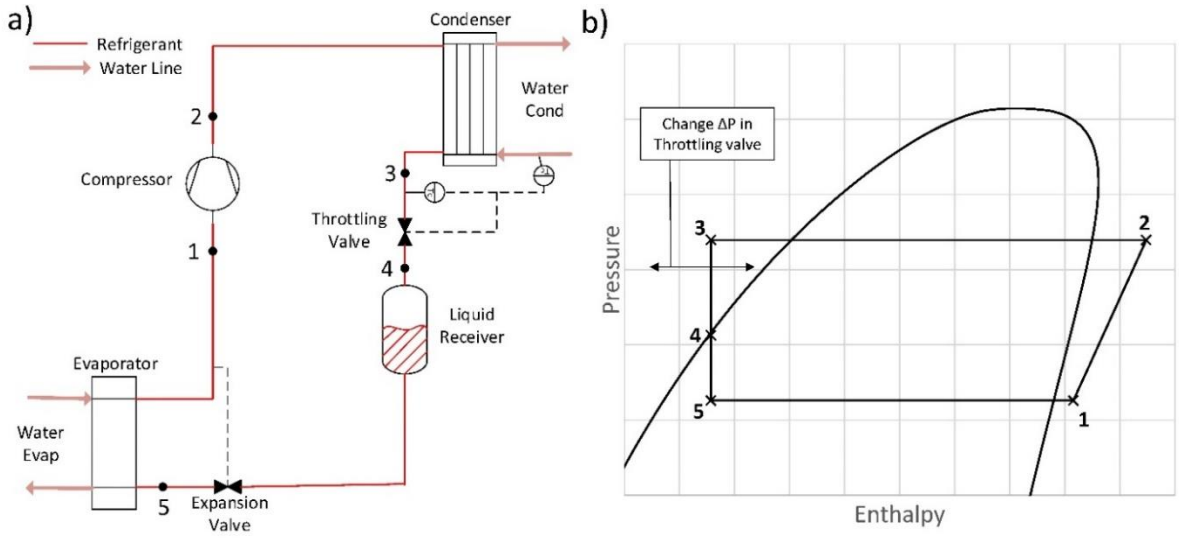

Figure 1: Water-to-water heat pump with subcooling controlled by a throttling valve. a) Scheme b) P-h diagram(Miquel Pitarch i Mocholí, 2017)

The main characteristics of this system, besides the typical components of a heat pump (condenser, evaporator, compressor and expansion valve(EV)), are the existence of a throttling valve (TV) and a liquid receiver placed respectively in series at the outlet of the condenser. In this configuration, the liquid receiver has mainly two functions: to accommodate the variation of the active refrigerant charge due to the modification of external/operation conditions and to ensure saturated liquid conditions of the refrigerant at the outlet of the throttling valve. Thus, it is possible to have a variable subcooling (for which a part of the condenser area is used) and to control it using the throttling valve

The proposed control mechanism for the subcooling will influence the control of the expansion valve (EV). This valve must ensure the desired degree of superheat. However, its pressure drop will not only depend on the condenser and evaporator pressures, but also on the degree of subcooling (pressure drop in the throttling valve). As it can be seen in Figure 2b, as the subcooling increases, the point 4 reduces its pressure and the expansion valve only introduces a small drop pressure (from 4-5) and vice versa.

For more details about the system, please refer to the doctoral thesis (Miquel Pitarch i Mocholí, 2017).

3.4.2 Theoretical analysis

In this work, two different control strategies based on the optimal subcooling are evaluated in depth. The first considered strategy is the implementation of a relation between the subcooling and of the secondary temperature lift as it was pointed to be directly related in (Pitarch et al., 2017a). The second strategy consists of the control by means of the temperature approach as it was theoretically proposed in (Pitarch et al., 2017a) and (Jensen and Skogestad, 2007b).

In order to understand better the main variables used in this work, Figure 2 has been included. Figure 2a shows the temperature profile of the secondary fluid (water) and the refrigerant working with three different subcoolings around the optimal point for finite heat exchangers. It can be seen that as the subcooling increases (reducing the temperature temperature approach, DTa), the temperature difference at the dew point (DTb), increases. Figure 2b shows the temperature differences (DTa and DTb) and the heating COP as a function of the subcooling.

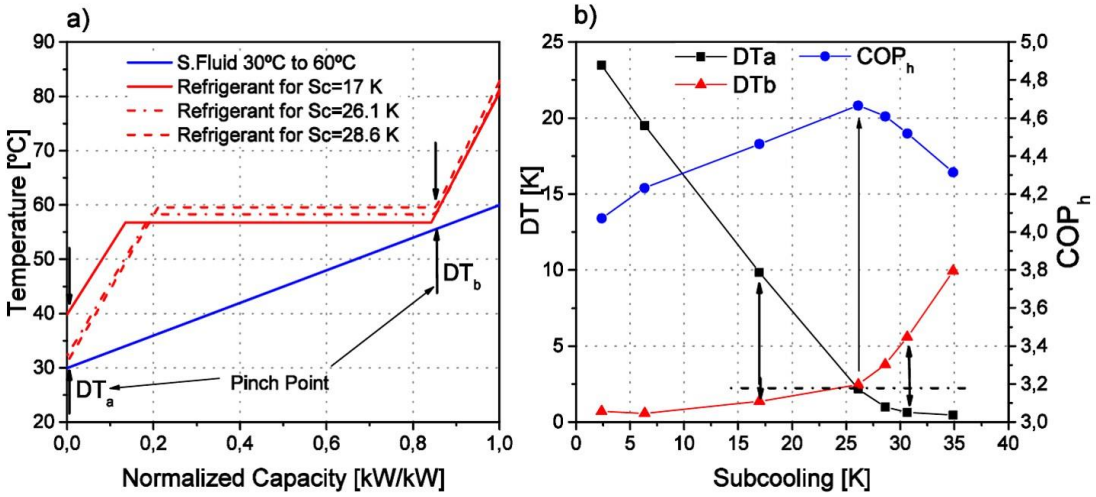

Figure 2: (a) Temperature profile vs. normalized capacity: Refrigerant R290 with different subcooling and the secondary fluid going from 30°C to 60°C (finite heat exchange area) (b) Pinch points values with different subcoolings.

For infinite heat exchangers, the optimal condition was theoretically found when two pinch points exist and they equal to zero, that is DTa=DTb=0. However, it was shown that although the difference was not too large under other operating conditions and finite heat exchangers, DTa≈DTb≠0 but not further investigations were done.

The second control strategy is based on this hypothesis. Hence, a deep analysis of the pinch points (DTa and DTb variation) in the optimal point for different operating conditions in finite heat exchangers has been done.

A model of the heat pump described in the previous section has been built using the IMSTart software (José Miguel Corberán, 2009). The model has been validated with experimental data accounting for a total of 61 points under a wide range of water temperature conditions collected in Table 1.

Table 1: Experimental water temperature range considered in the validation of the model

SHW condenser inlet temperature	10,30,50°C
SHW condenser outlet temperature	60°C
Water evaporator inlet temperature	10,20,30°C

Figure 3 represents the validation of the model for DTa, DTb and the heating COP. The experimental results are represented by dots, triangles, and crosses and the model results in lines for a water inlet temperatures of (a) 10°C (evaporating temperature 0°C), (b) 20°C and (c) 30°C and different water inlet temperatures at the condenser. The first number in the legend corresponds to the water inlet temperature at the evaporator, the second number to the water inlet temperature at the condenser and the third number, to the water temperature at the outlet of the condenser.

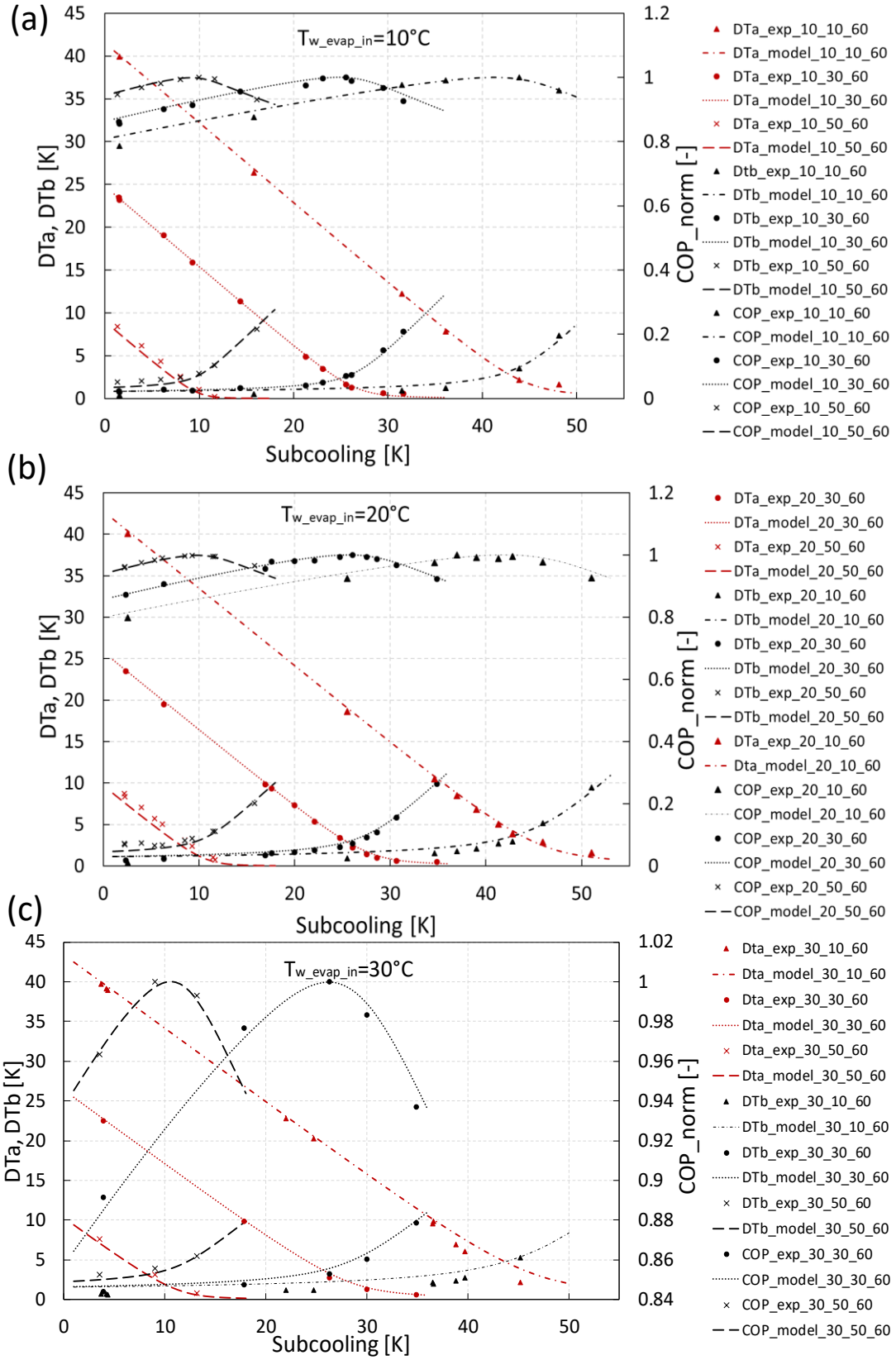

Figure 3: Model and experimental results of the normalized COP, DTa and DTb (a) for water inlet temperature of 10°C (b) for water inlet temperature of 20°C and (c) for water inlet temperature of 30°C.

According to the previous figures, it can be seen that the model captures the behavior of the real heat pump in all the conditions with an error lower than 4%.

Once the model has been validated, the number of points simulated around the maximum COP has been extended in order to be able to analyze with more detail the values of DTa and DTb around the optimal point (maximum COP). Since the study focuses mainly on the condenser, to avoid disturbances on the interpretation of the results, the efficiency of the compressor has been considered constant in all the cases.

Table 2 collects the water temperature ranges considered in this work. As it can be seen, with the mix of those temperatures, most of heating water applications range are covered.

Table 2: Water temperatures range considered in this work.

SHW condenser inlet temperature	10-50°C
SHW condenser outlet temperature	40-90°C
Water evaporator inlet temperature	10-30°C

3.5 Results

3.5.1 Optimal subcooling control based on a linear approach

According to previous works, the subcooling can be theoretically controlled by means of a linear fitting function of the water temperature lift (Pitarch et al., 2017a). Thus, this possibility is evaluated for the considered points.

Figure 4 represents the secondary temperature lift (the difference between the water temperature at the outlet and the water temperature at the inlet of the condenser) and the optimal subcooling.

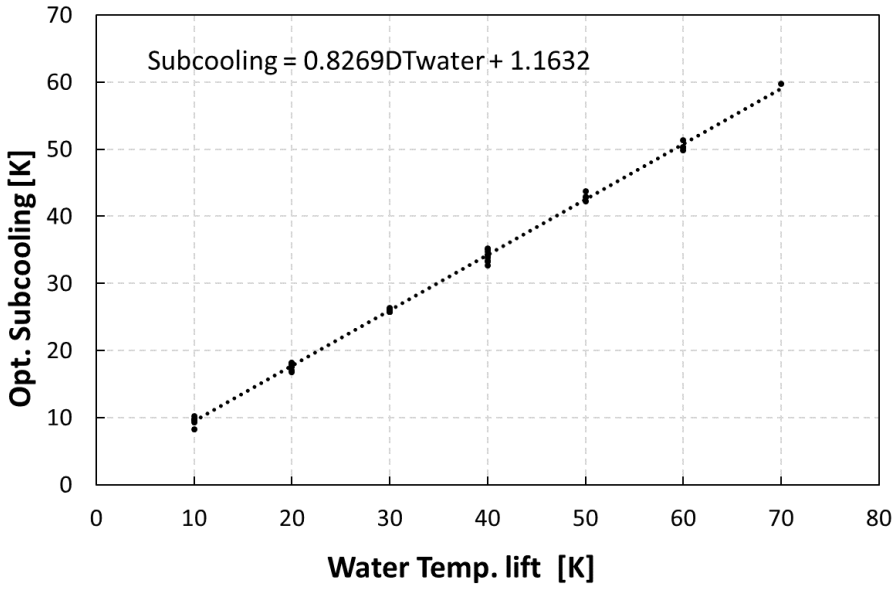

Figure 4: Optimal subcooling function of the water temperature lift for Propane. Linear fitting.

From the figure is deduced that a linear fitting function of the water temperature lift would lead to values very close to the optimal subcooling for each condition being the error lower than 1% in all the cases.

Figure 5 represents the COP calculated with the linear fitting and the optimal COP calculated with the software IMST-ART previously validated.

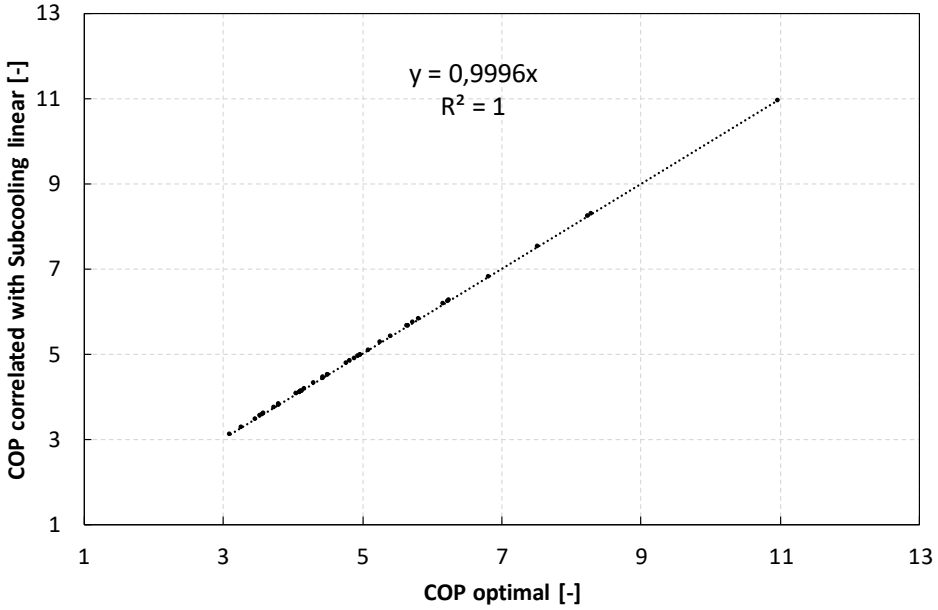

Figure 5: COP deviation from the optimal with the subcooling linear control

According to the figure, if a control of the subcooling is done by means of a linear fitting function of the secondary temperature lift (DTw), the deviation would be negligible (maximum of 0.04%) in all the cases. Nevertheless, this type of control must be adapted, and the parameters adjusted based on the refrigerant used. In addition, the error incurred by using it may differ from one to another refrigerant. In fact, for refrigerants such R32, which critical point is closer to the condensing pressure, this control would result in higher errors than for instance, propane or R1234yf [5]. In spite of it, for a given size of the heat pump components, the parameters adjustment for the linear fitting control could be found, for most refrigerants, by the testing only 6/7 points.

Another interesting consideration when using a control methodology is represented by the analysis of the maximum possible deviation (accuracy of the methodology used) in order to obtain a certain maximum decrease of the efficiency. In this case, for each DTw (water temperature lifts) considered, the most critical external conditions from the studied points have been chosen. That is, for each DTw, the point that had the sharpest COP variation with subcooling. Thereafter, if 2% is chosen as the maximum desired decrease of the optimal COP at any condition, different deviation percentages from the optimal subcooling are allowed. For all the considered points and DTw, the minimum allowed deviation is around 10%.

Figure 6 represents the variation of normalized COP with the subcooling for the most critical conditions of each DTw. Black points represent the optimal subcooling obtained with the equation of Figure 4. Red crosses represent the normalized COP when a subcooling 10% lower than the optimal is applied. Green triangles represent the normalized COP when a subcooling 10% higher than the optimal is applied. Yellow dotted line represents the 2% loss of COP from the optimal.

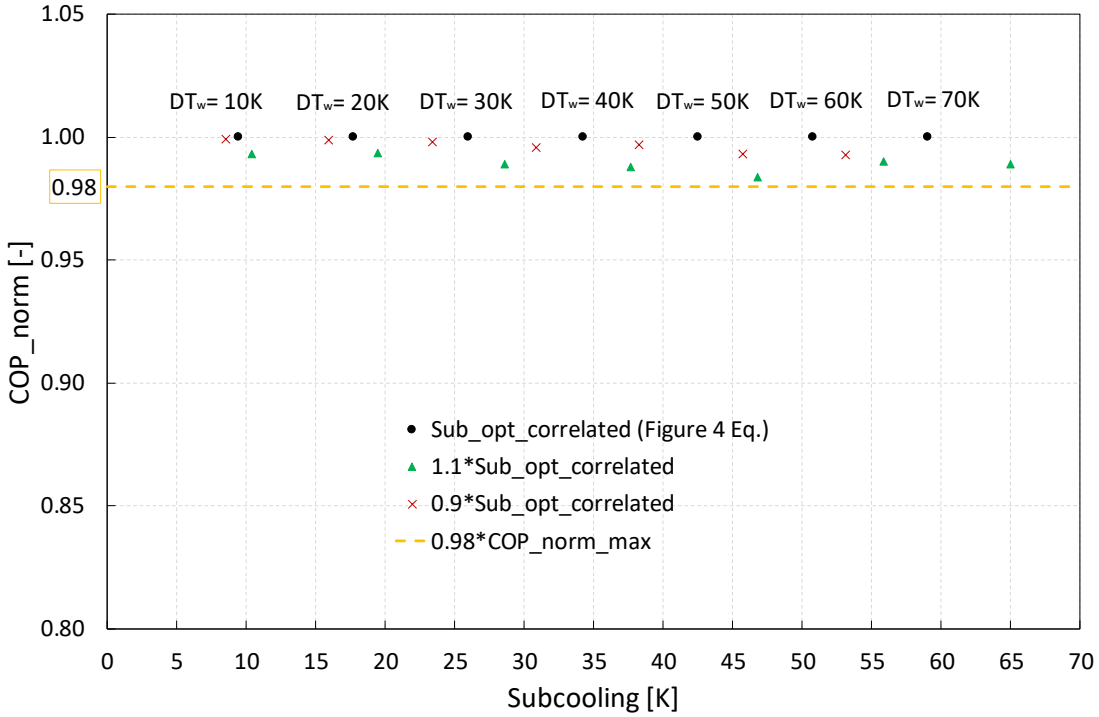

Figure 6: Optimal subcooling variation with the normalized COP based on the water temperature lift for different evaporating temperatures.

Two main conclusions can be derived from Figure 6:

- Deviations from the optimal subcooling until 10% would lead to near-optimal conditions by only decreasing in 2% the optimal COP in the worst cases. Thus, simplicity of the control approach could be a more valuable quality than precision.

- Smaller subcoolings than the optimal are preferable than higher.

3.5.2 Optimal subcooling control based on the temperature approach

In (Jensen and Skogestad, 2007b) the temperature approach at the condenser was proposed and statistically studied as a good candidate to control the subcooling. However, the reason of this choice is not analyzed in deep. In (Pitarch et al., 2017a), a theoretical analysis of this variable based on infinite heat exchanger was done. The authors found that the optimal subcooling (maximum COP) takes place when two pinch points (one at the outlet of the condenser and another at the dew point) exist and they equal to zero. Due to the impossibility of the zero pinch point value in real heat exchangers, the values of DTa and DTb (nomenclature according to Figure 2) were cursorily investigated concluding that the optimal condition is found when two pinch points exist, that is DTa≈DTb. Finally, it was assumed DTa=DTb as a good approach but not further details are given.

In this part, a detailed study of the relationship between the optimal subcooling and the temperature differences DTa and DTb values for a real heat exchanger (finite), is done. First, the representation of the DTa, DTb, COP and subcooling values for all the considered is presented.

Figure 7 shows the variation of the temperature approach (DTa), the temperature at the dew point (DTb) and the normalized COP for different water temperature lifts (DTw) and the water inlet temperature at the evaporator of (a) 10°C, (b) 20°C and (c) 30°C. The vertical lines with the arrow indicate the normalized COP correspondent to DTa=DTb.

For the three cases (a), (b) and (c), the curve represented above is the variation of the normalized COP with subcooling for different DTw while the curves represented below belong to DTa and DTb variations with subcooling. Specifically, DTa decreases as subcooling increases and DTb increases with the increase of subcooling. The yellow horizontal line corresponds to the minimum normalized COP obtained under the assumption of the equality DTa=DTb considering all the points and DTw. The COP normalized when DTa=DTb is marked with the line ended in an arrow for each case.

Dotted lines, solid lines or dash lines represent different conditions at the condenser secondary fluid with the particularity that they are grouped by temperature lifts (for instance, in Figure 7a, a water inlet evaporator temperature of 10°C is given for DTw=10K, solid line corresponds to the 30°C of water inlet temperature at the condenser and 40°C as water outlet temperature at the condenser while the dash line belongs to 10°C (evaporator water inlet temperature), 50°C of water inlet temperature at the condenser and 60 °C of water outlet temperature). It is worth it to notice that the important variable to consider is the difference between the inlet/outlet conditions of the secondary fluid at the condenser (DTw) rather than the values.

(a)

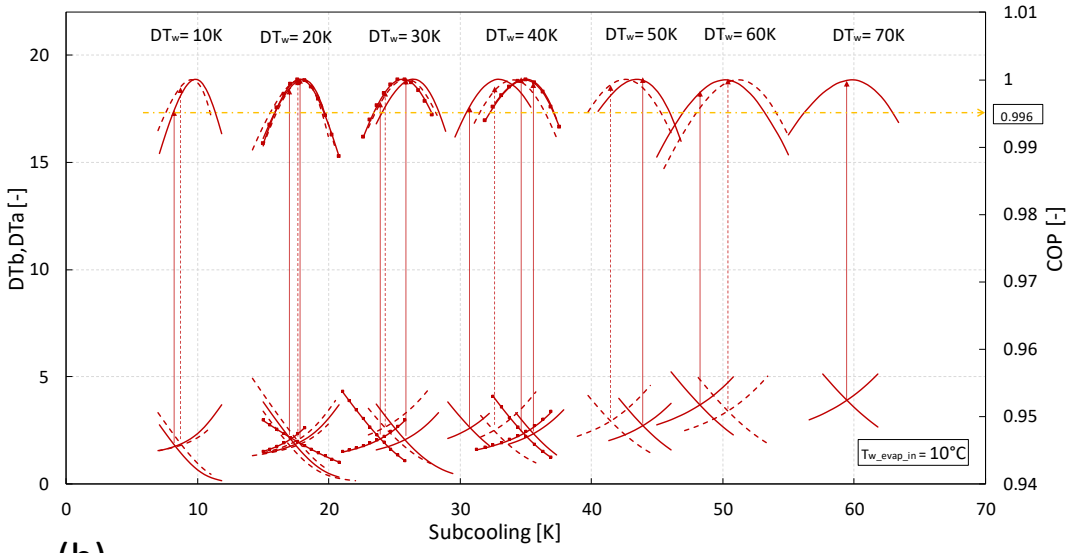
DTw= 10K
DTw= 20K
DTw= 30K
DTw= 40K
DTw= 50K
DTw= 60K
DTw= 70K
DTb,DTa [-]
COP [-]
Subcooling [K]
Tw_evap_in = 10°C

(b)

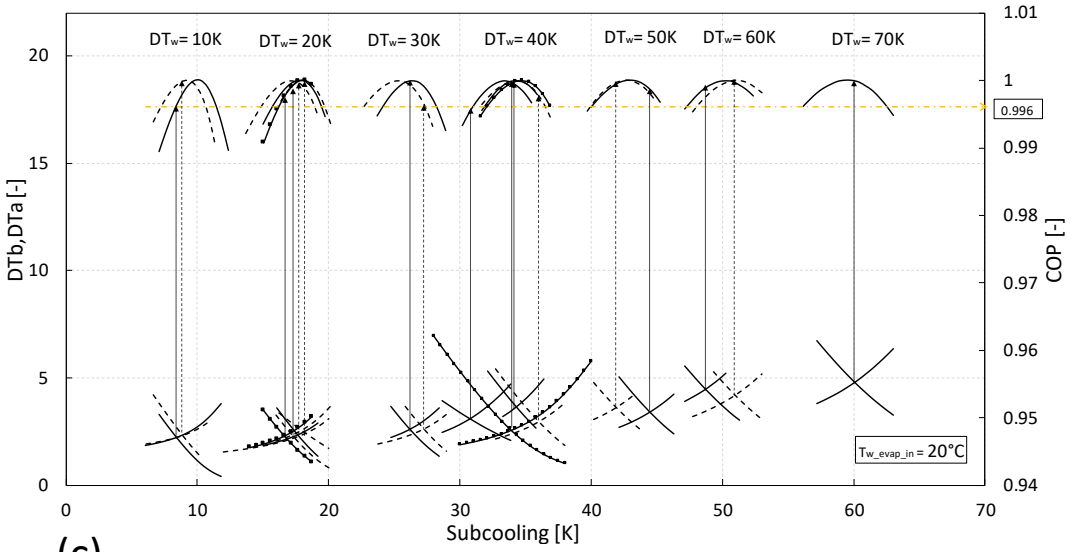
DTw= 10K
DTw= 20K
DTw= 30K
DTw= 40K
DTw= 50K
DTw= 60K
DTw= 70K
DTb,DTa [-]
COP [-]
Subcooling [K]
Tw_evap_in = 20°C

(c)

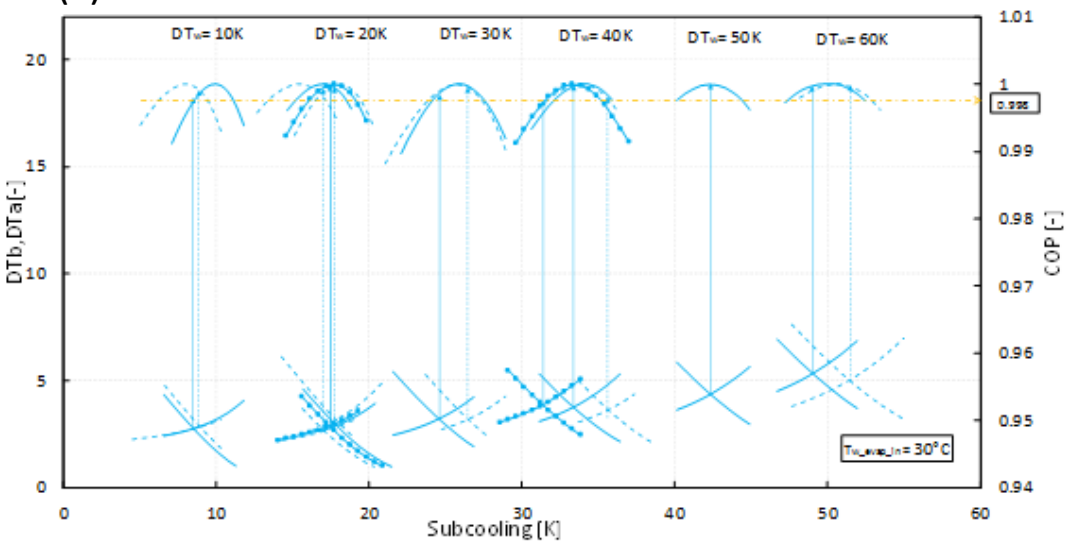
DTw= 10K
DTw= 20K
DTw= 30K
DTw= 40K
DTw= 50K
DTw= 60K
DTb,DTa [-]
COP [-]
Subcooling [K]
Tw_evap_in = 30°C

Figure 7: DTa, DTb and normalized COP variation with the subcooling for different water temperature lifts and the water temperature at the inlet of the evaporator of (a) 10°C (b) 20°C and (c) 30°C. Vertical lines with the arrow indicate the normalized COP correspondent to DTa=DTb. Yellow horizontal line corresponds to the minimum normalized COP obtained under if DTa=DTb.

As it can be seen in Figure 7, the approximation of considering in real cases (finite heat exchangers) the equality of both terms would deviate from the optimum the results only 0.4% in the worst cases. Therefore, the theoretical result found by (Pitarch et al., 2017a) in which the optimal subcooling takes place when DTa=DTb for infinite heat exchangers can be applied for finite heat exchangers for a wide range of working conditions not compromising the optimal efficiency significantly. Thus, for a given heat exchanger size, the assumption that the optimal subcooling occurs when the temperature approach and the temperature at the dew point would be equal could in practice be considered as a general design criteria, at least for a heat exchanger that has been designed considering the subcooling area and a temperature approach lower than 5K, further studies are required in order to extend this behavior to more general situations.

Figure 10 represents, the variation of the normalized COP with the temperature approach (DTa) for some of the analyzed points. Only a few points are represented in order to see the figure clearly. It should be noticed that the worst cases (the cases with higher dispersion) are represented. The first number of the legend corresponds to the water inlet temperature at the evaporator (the evaporating temperature is 10K lower than this value), the second to the water inlet temperarture at the condenser and the third, to the water outlet temperature at the condenser. Red lines correspond to points with 10°C of water temperature at the inlet of the condenser, black lines to 20°C and blue lines to 30°C. Yelow line is the average DTa and the yelow dotted lines correspond to the maximum deviation from optimal conditions if the average value is assumed in all the cases.

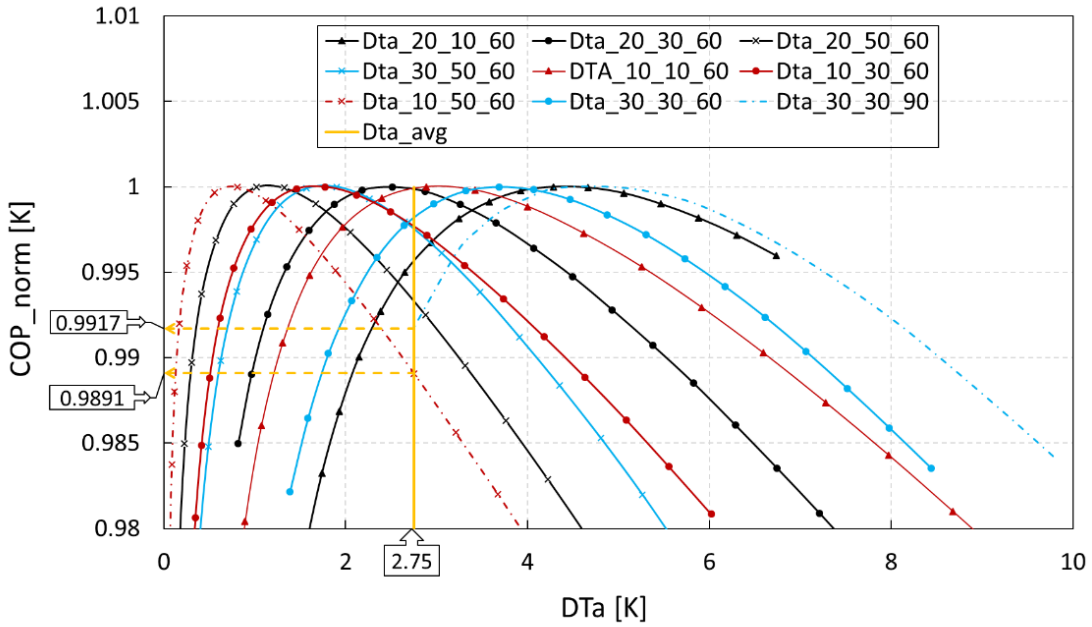

Figure 8: Temperature approach that corresponds to the optimal subcooling variation with the normalized COP based on the water temperature lift for different evaporating temperatures. The first number of the legend corresponds to the water inlet temperature at the evaporator (the evaporating temperature is 10K lower than this value), the second to the water inlet temperarture at the condenser and the third, to the water outlet temperature at the condenser. Red lines correspond to points with 10°C of water temperature at the inlet of the condenser, black lines to 20°C and blue lines to 30°C. Yelow line is the average DTa and the yelow dotted lines correspond to the maximum deviation from optimal conditions if the average value is assumed in all the cases.

As it can bee seen in the Figure, the optimal values of DTa differ as maximum approximately in 3K (from ~1.5K to ~4.5K) for the considered range of external conditions. Furthermore, the maximum performance decrease that would incur the consideration of a constant temperature approach for all the cases would be slightly higher than 1%. In this case, for any considered value of DTa from 2-4, the deviation from the optimal COP would be lower than 2%, what demonstrates that for DHW water applications, the control of the subcooling by means of the temperature approach seems to be reliable.

In this work, a constant value of the temperature approach (equal to the average value of all the analyzed points, that is, equal to 2.75K) has been considered as a control setting point for the installation regardeless the external conditions.

Figure 9 represents the COP calculated with the constant temperature approach (DTa) of 2.75K and the theoretical optimal COP calculated.

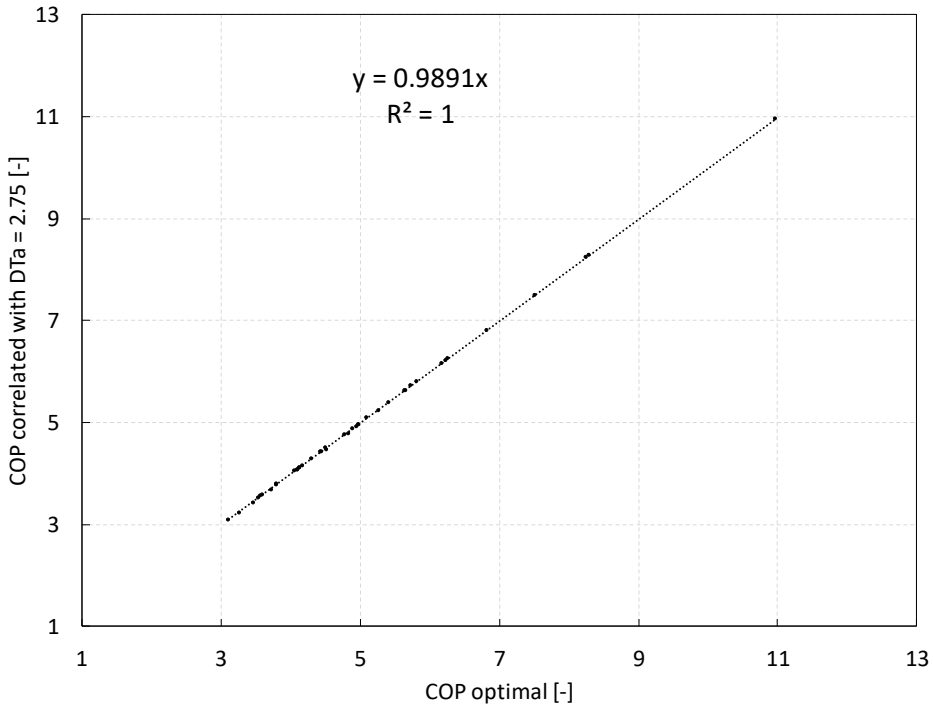

Figure 9: COP deviation from the optimal with the constant temperature approach control.

As it can be observed in the figure, if a control of the subcooling is done by means of a constant value in the temperature approach, the maximum deviation is 1.09% in all the cases.

Therefore, given condenser size and refrigerant, a good methodology in order to control the optimal subcooling would be to set a constant temperature approach at the outlet of the condenser independent of the external operating conditions. This methodology has the advantages of being simple to implement and accurate in order to operate under near-optimal conditions.

From the performed analysis, two subcooling control methodologies have been theoretically studied. Based on the results, the next part of the work will be focused on implementing the control of the subcooling from the temperature approach in a test bench. This potential strategy has not been evaluated in a real system up to the knowledge of the authors. Thus, some effects not considered on the previous theoretical analysis like the characteristic times of this control, the robustness of the strategy, the control coupling effects between subcooling and superheat and other possible factors that could appear in real systems is tested in the following part.

3.5.2.1 Stability control

In the configuration of Figure 1, the control of the superheat is done by means of the expansion valve (EV) while the throttling valve (TV) is in charge of the subcooling control.

Figure 10 is the control scheme used in the prototype experimentally tested.

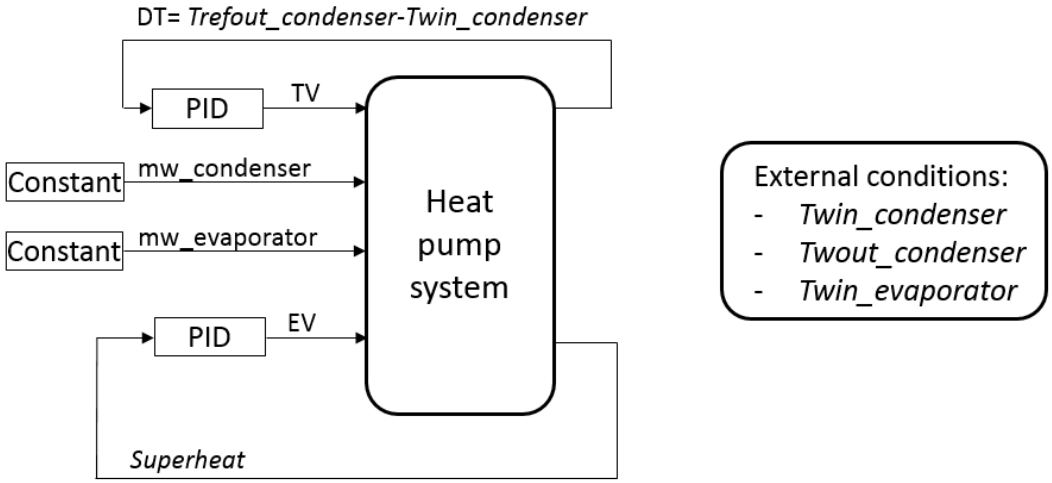

Figure 10: Heat pump control scheme

The testing conditions are attained by a certain water mass flow in the evaporator and the condenser which is defined before the experimental measurement. The control of the superheat is already automatically done. Thus, this section focuses on the control of the subcooling. In this case, the control is done by means of a PID (KS 90-1 PID from GmbH (PMA Prozeß- und Maschinen-Automation GmbH, n.d.)) that regulates the opening of the TV in Figure 1 in order to maintain a set point of DT. Only two temperature sensors were needed (one at the refrigerant condenser outlet (input 1, x1) and another at the water condenser inlet (input 2, x2)), in this case two thermocouples were used, and the PID controls the difference between both temperatures, DT (process value x1-x2). The three PID signals are connected as voltage signals (0-10V) and the control algorithm is so called "on/off controller or signaler with one output". The method of controller operation is inverse based on the process value.

The operating procedure of the PID is based on the achievement of a setting point in the temperature approach and the correspondent actuation over the throttling valve. That is, based on Figure 1, if the throttling valve is completely opened, the refrigerant would exit the condenser under saturated conditions (cero

subcooling). In this condition, the maximum temperature approach is given, DT=liquid saturated refrigerant temperature at the condenser – water inlet temperature at the condenser. Thereafter, for a certain degree of subcooling, a lower value of the temperature approach is required and the PID would make the valve closing certain percentage until the setting point is reached which would correspond to a certain degree of subcooling. For example, if one fixes the temperature approach to 3 as setting point and the water inlet temperature is 10°C, the PID would close the valve until the refrigerant exits the condenser at 13°C (difference between the refrigerant temperature at the outlet of the condenser and the water inlet temperature at the condenser is 3) which is directly translated to the existence of a certain degree of subcooling.

Finally, the other extreme would be to set the temperature approach to a very low value closed to zero. That is, maximum subcooling. In this case, the PID will be closing the valve until the approach is minimized which, in the example, implies the refrigerant to exit the condenser at almost 10°C. The refrigerant must be in subcooled conditions at the inlet of the TV in order to allow a reliable control.

To proceed with the evaluation, the stability and robustness of the system, the installation was set to equilibrium conditions for a point that was experimentally tested before (but manually controlled). The equilibrium point characteristics are collected in Table 3.

Table 3: Heat pump conditions for the PID tunning

SHW condenser inlet temperature	30°C
SHW condenser outlet temperature	60°C
Water evaporator inlet temperature	20°C
Water evaporator outlet temperature	15°C
Superheat	10K
Subcooling	12K

Once the installation was stable, the tuning of the PID was done following the heuristic method proposed by Ziegler-Nichols (Ziegler and Nichols, 1995). The critical gain for closed loops methodology was used to firstly adjust the PID parameters. First, the integral and derivative terms were set to zero. Second, the proportional gain (which value was originally zero) was incremented in order to

find the critical value that results in an output with consistent oscillation. Afterwards, based on the critical proportional term and the oscillation period, the integral, the derivative and the proportional values were calculated according to the proposed table for a classic PID by Ziegler-Nichols. The critic proportional value that leads to stable oscillations was found to be 160 with an oscillation period of 90 seconds. From those values and following the methodology, the rest of the values used in the process were set: the proportional term to 360, the integral term to 180 and derivative time set to 45.

After, in order to verify the capability and stability of the PID under other points, the modification of the main conditions and the analysis of the PID response, was done.

Figure 11 represents the variation of the main temperatures involved, the superheat, the subcooling and the temperature approach with the time. In this case, different values of DTa (temperature approach), that is, the same point as in the first phase but different subcooling values, are tested. The subcooling is represented in blue. The temperature approach (variable to control, DTa), in black. The inlet water temperature is represented in purple and the superheat in green.

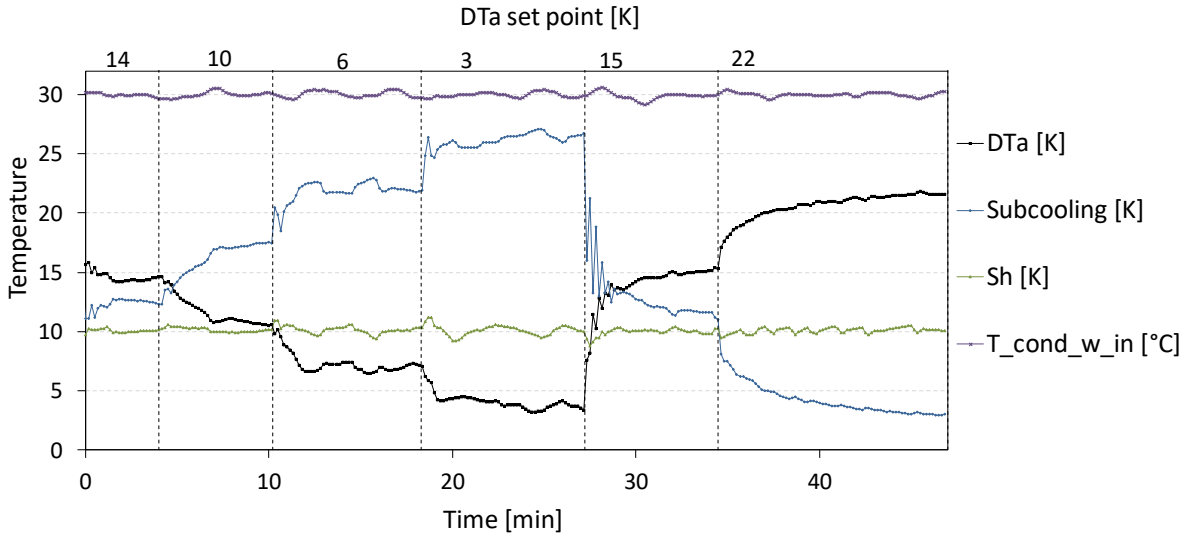

Figure 11: Verification of the PID response for different DTa setting values from a stable system condition (Twcondin=30°C, Twevapin=20°C).

From the figure can be seen the direct relation of the subcooling and the controlled variable, DTa (both curves have the same shape but opposite trend). First, DTa was set to 15K (from the equilibrium initial conditions), second, it was changed to 10K and the system was able to reach the setting in less than 5min,

afterwards, the setting value of DTa was modified to 6K, 3K, 15K and 22K. In all the cases the control converged, and the set point was attained in less than 3 min.

Furthermore, since this control could affect the control of the expansion valve, the superheat was an important value to look at. From Figrue 11 can be seen that the value of the superheat remains practically constant to the setting value of 10°C which means that the control of the DTa variable is not affecting the control of the superheat.

At this point, it has been verified that when the system is at steady state conditions, it is able to automatically attain the DTa setting value. Another important test would be the verification of this capability from a starting up of the system, the time for the system to reach stable conditions and the response of this control with the modification of external conditions.

Figure 12 represents the starting up of the heat pump until it reaches the DTa setting value of 4 and evaluates the response of the main parameters to variations at the condenser water inlet temperature (from 30°C to 40°C).

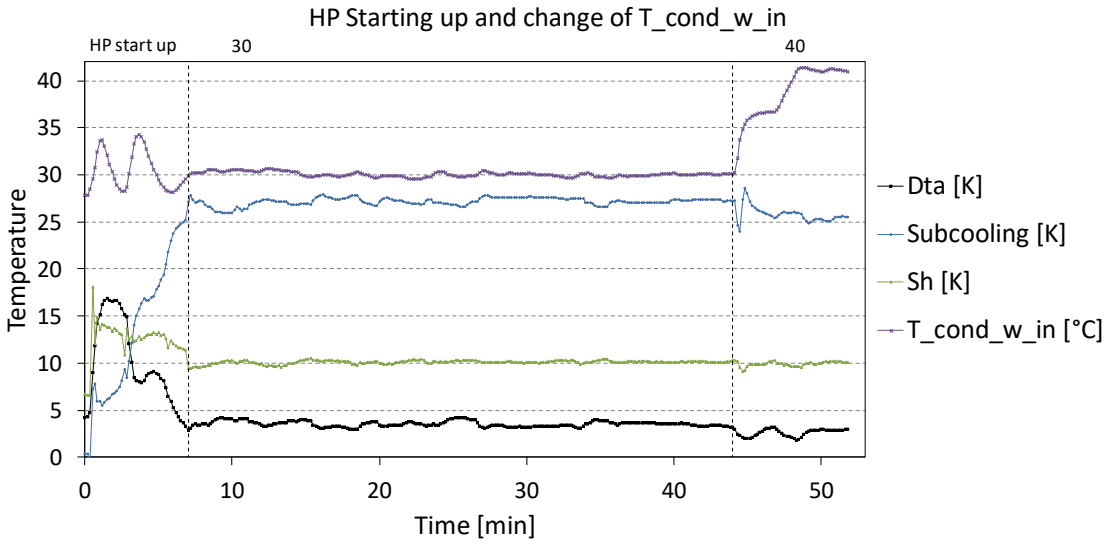

Figure 12: Heat pump starting up, control of DTa=4 and increase of the water inlet temperature at the condenser with the time.

According to the figure, the heat pump starting up approximately lasts 8 minutes. After this time, the temperatures are stable. Then, even though in real applications, the external conditions remain practically constant with time, a sudden water temperature at the inlet of the condenser of 10°C was applied considering it as worst condition to test the control. Based on the Figure, the system could absorb this modification and returned to stable conditions in less than 5 minutes.

Figure 13 is the continuation of Figure 12. It shows the response of the external condition temperatures, the subcooling and superheat with time. In this case, a decrease of the water inlet temperature at the condenser until 20°C has been tested. Thereafter, in order to obtain real conditions of the installation, the secondary mass flow has been decreased to reach 60°C at the outlet of the condenser. In the secondary axis, the outlet water temperature is represented.

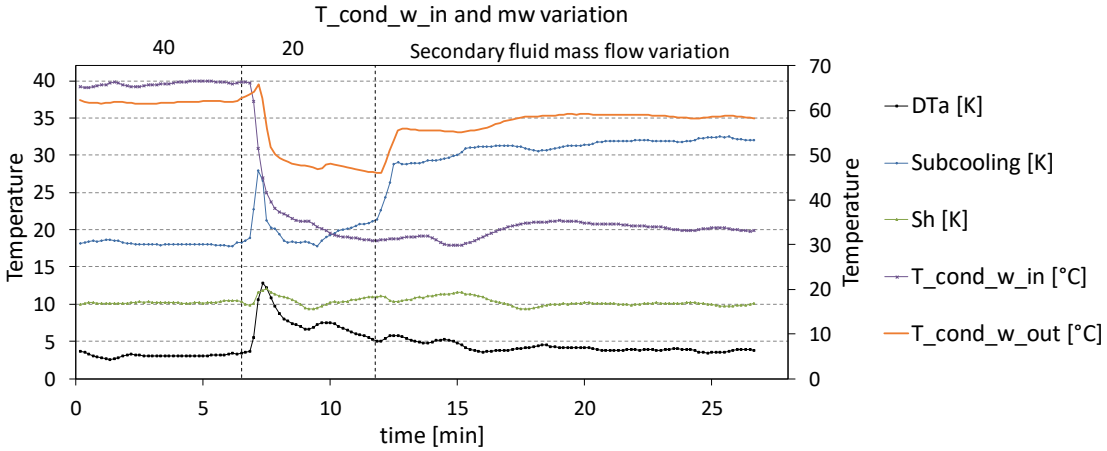

Figure 13: DTa=4 control, decrease of the water inlet temperature at the condenser and variation of the secondary mass flow in order to have the water temperature at the outlet of the evaporator at 60°C.

According to the figure, one step diminution of 20°C in the water inlet temperature can be absorbed by the installation in less than 5 minutes which is further conservative compared to real behavior of the installation. Afterwards, the system is capable of stabilizing and a subsequent reduction on the water mass flow rate is able to be captured in less than 2 minutes from when the system remains stable.

Figure 14 is the continuation of Figure 13 and evaluates the evolution of the system after the modification of the external conditions in order to have tested the range of operation in this type of applications. First, the water inlet temperature at the condenser is stable and equal to 20°C (from Figure 13), after 3 minutes, this temperature is decreased until 10°C. Thereafter the evaporating temperature is decreased in 10°C and finally, the secondary water mass flow rate at the condenser is adapted in order to obtain water at 60°C at the outlet of the condenser following the same reasoning than in Figure 13.

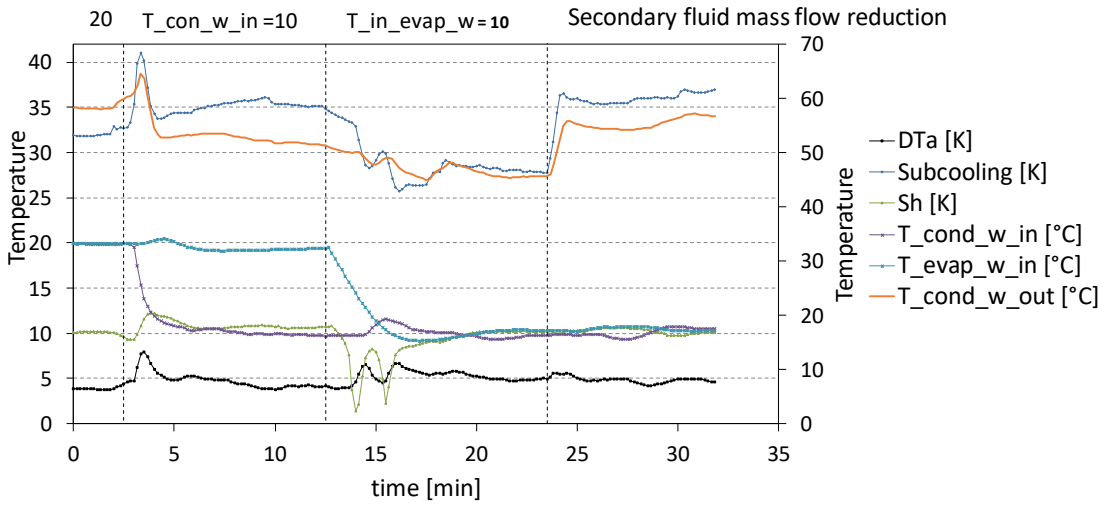

Figure 14: DTa=5 control, decrease of the water inlet temperature at the condenser, decrease of the water inlet temperature at the evaporator and reduction of the water mass flow rate.

Based on the figure, the diminution of the water temperature at the inlet of the condenser generates a transitory peak variation in almost all the variables but the system is stable in less than 3 minutes. It is important to understand that this transitory is not merely a consequence of the implemented control but of the equilibrium in the system after a variation of the conditions at the condenser and that this event would not happen in real conditions since the water inlet temperature used to be very stable across the time. Once the values are stable, a reduction of the water temperature at the inlet of the evaporator was done. This variation was interesting in order to see how the expansion valve could react in the control of the superheat as well as to extend the study under more conditions, for instance within a colder climate. Two transitory peaks were observed (green line) but again, the system is able to stabilize in around 3 minutes. Finally, the adjustment of the water mass flow rate in order to obtain 60°C in the water condenser outlet temperature was done and the system, stabilized very fast.

After the tuning of the PID and analysis of the response under different conditions, the heat pump was tested for some of the points at their optimum that were measured before the application of the automatic control. In this case, the PID used had only a unitary precision and the value chosen for the measures was 3 (the closest value to the average, 2.75). The tests were performed from the heat pump completely turned off.

Figure 15 represents the evolution of the DTa with the time for a DTa setting value of 3 from the starting up of the system for different conditions measured

before. (a) water temperature at the inlet of the condenser of 10°C, 60°C at the outlet of the condenser, 20°C at the inlet of the evaporator and 15°C at the outlet of the evaporator, (b) water temperature at the inlet of the condenser of 30°C, 60°C at the outlet of the condenser, 20°C at the inlet of the evaporator and 15°C at the outlet of the evaporator and (c) water temperature at the inlet of the condenser of 50°C, 60°C at the outlet of the condenser, 20°C at the inlet of the evaporator and a 15°C at the outlet of the evaporator.

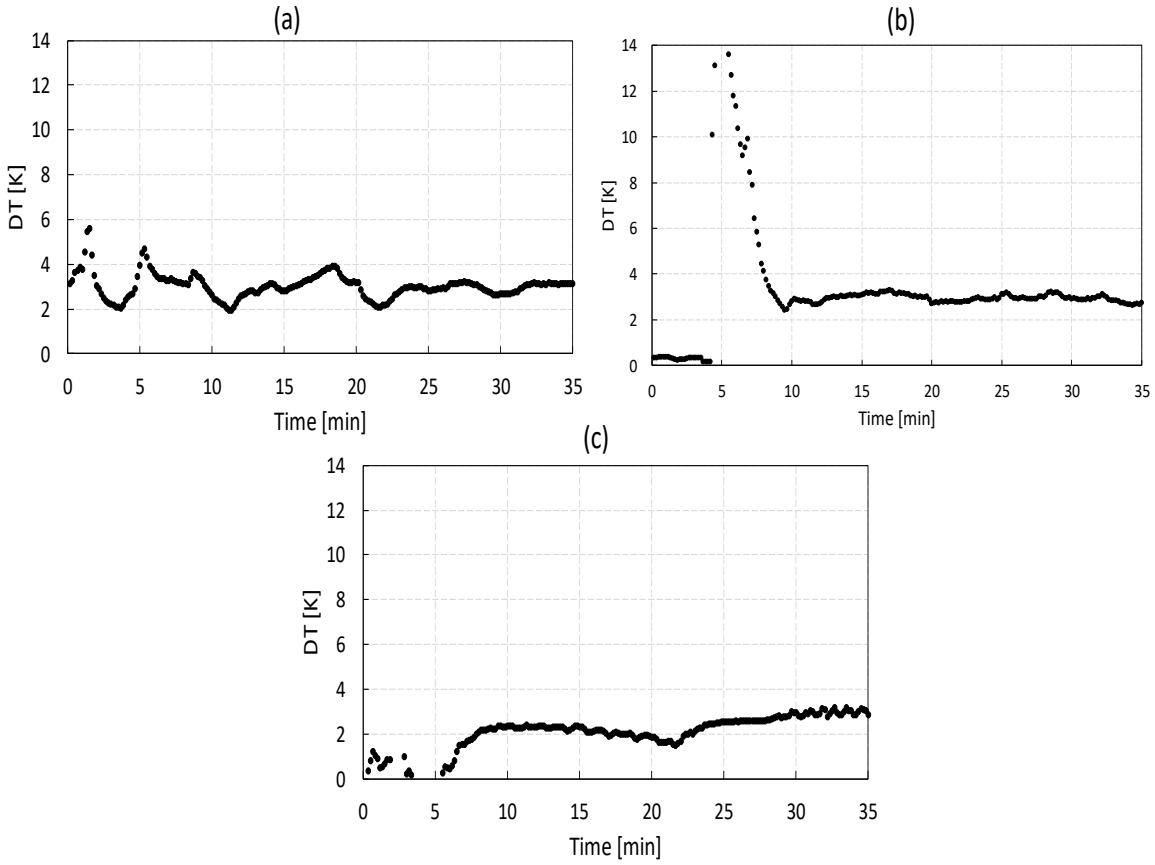

Figure 15: DTa variation (set to 3) with the time for (a) Twinevap=20°C, Twoutevap=15°C, Twincond=10°C and Twoutcond=60°C. (b) Twinevap=20°C, Twoutevap=15°C, Twincond=30°C and Twoutcond=60°C (c) Twinevap=20°C, Twoutevap=15°C, Twincond=50°C and Twoutcond=60°C.

According to figure 15a, the system is able to control the temperature approach after approximately 20 minutes from the starting up of the heat pump. Notice that the transitory is not due to the control itself but about the stabilization of the entire system after the starting up.

From Figure 15b can be inferred that the system is stable after 10 minutes from a completely stopped mode. Afterwards, the control of DTa remains within the limits for the rest of the test.

As it can be observed in Figure 15c, the system is also able to reach the equilibrium state in the setting point in a bit more than 20 minutes.

Finally, Table 4 collects the experimental results measured before the control of the subcooling and with the control of the subcooling by setting a constant value of 3 in DTa.

Table 4: Experimental values measured without the subcooling control and with the control set to DTa=3 and considering the variation of the compressor efficiency.

Water inlet temp. Evaporator °C	Water temperature lift at the condenser °C	Optimal subcooling [K]	COP heating max [-]	DTa at the maximum subcooling [K]	Subcooling for DTa=3K control [K]	COP heating for DTa=3K control [-]
20	10-60	42.77	5.46	4.77	41.45	5.46
	30-60	26.1	4.66	2.57	24.67	4.65
	50-60	9.27	3.91	2.38	8.34	3.91

From the table can be seen that even if the optimal DTa experiments a variation of 2.4K among the three measures, the control of the system through a constant value of DT=3K independently from external conditions, leads to negligible differences on the COP heating. Thus, indicating that the curve of the temperature approach (DTa) remains flat with respect the COP during a few degrees and bearing out the reliability of the subcooling control by means of the temperature approach.

3.6 Conclusions

Subcooling has demonstrated to play an important role in the heat pump efficiency. In fact, an increase of the COP up to 30% can be possible with the proper control of it for a certain conditions. However, only a few works analyze this paramenter and from the experimental point of view only complex algorithms have been implemented in order to control subcooling and operate under the optimal value. In this work, based on previous experimental and theoretical works, two potential subcooling control strategies have been evaluated under a theoretic point of view.

o Linear fitting equation: the optimal subcooling dependence mainly on the temperature lift of the secondary fluid was investigated. An approximation made by this relationship was found and the use of it leads to deviations from the

optimum COP lower than 0.04% in all the cases. As a drawback, the paramenter of the obtained equation depend on the external conditions and the obtained errors could be higher for other refrigerants like R32.

- Constant value of the approach (DTa): The temperature approach influence on the optimality of the subcooling for finite heat exchangers was studied. Results show that the optimal subcooling does not occurs when DTa=DTb=0 as in the infinite heat exchanger area case but for the analyzed cases it is true that the optimum subcooling verifies DTa≈DTb≠0. If it is assumed that the optimum is found in the equality condition (DTa=DTb), the deviations from the maximum COP are lower than 1.09% in all the cases. Thus, the assumption of considering the equality seems to be reasonable as a general rule for a given condenser size and refrigerant and temperature approaches lower than 5K.

Both strategies seem to be appropriated for the control of the subcooling. However, due to simple implementation, not compromising accuracy and applicability independent of the refrigerant, the control by means of the temperature approach was selected and the stability of it was experimentally proved for the considered system and conditions. The time from shut off to stable behavior of the system is around 20 minutes and the deviation from the optimal COP is lower than 0.2% for the measured points.

3.7 Acknowledgements

Part of the work presented was carried by Estefanía Hervás Blasco with the financial support of a PhD scholarship from the Spanish government SFPI1500X074478XV0. The authors would like also to acknowledge the Spanish 'MINISTERIO DE ECONOMIA Y COMPETITIVIDAD', through the project ref-ENE2014-53311-C2-1-P-AR "Aprovechamiento del calor residual a baja temperatura mediante bombas de calor para la produccion de agua caliente" for the given support.

3.8 References

Bauck Jensen, J., 2008. Optimal Operation of Refrigeration Cycles. Norwegian University of Science and Technology Faculty of Natural Sciences and Technology Department of chemical engineering.

Chen, Y., Gu, J., 2005. The optimum high pressure for CO2 transcritical refrigeration systems with internal heat exchangers. Int. J. Refrig. 28, 1238–1249. doi:10.1016/j.ijrefrig.2005.08.009

Corberá, J.M., Martínez, I.O., Gonzá, J., 2007. Charge optimisation study of a reversible water-to-water propane heat pump Etude sur l'optimisation de la charge d'une pompe à chaleur ré versible eau-eau au propane. doi:10.1016/j.ijrefrig.2007.12.011

Fernando, P., Palm, B., Lundqvist, P., Granryd, E., 2004. Propane heat pump with low refrigerant charge: design and laboratory tests. Int. J. Refrig. 27, 761–773. doi:10.1016/j.ijrefrig.2004.06.012

Hu, B., Li, Y., Cao, F., Xing, Z., 2015. Extremum seeking control of COP optimization for air-source transcritical CO2 heat pump water heater system. Appl. Energy 147, 361–372. doi:10.1016/j.apenergy.2015.03.010

Jensen, J.B., Skogestad, S., 2007a. Optimal operation of simple refrigeration cycles: Part I: Degrees of freedom and optimality of sub-cooling. Comput. Chem. Eng. 31, 712–721. doi:10.1016/j.compchemeng.2006.12.003

Jensen, J.B., Skogestad, S., 2007b. Optimal operation of simple refrigeration cycles: Part II: Selection of controlled variables. Comput. Chem. Eng. 31, 1590–1601. doi:10.1016/j.compchemeng.2007.01.008

José Miguel Corberán, J.G.-M., 2009. Refrigeration Technologies Software IMST-ART.

Kauf, F., 1999. Determination of the optimum high pressure for transcritical CO2-refrigeration cycles. Int. J. Therm. Sci. 38, 325–330. doi:10.1016/S1290-0729(99)80098-2

Koeln, J.P., Alleyne, A.G., 2014. Optimal subcooling in vapor compression systems via extremum seeking control: Theory and experiments. Int. J. Refrig. 43, 14–25. doi:10.1016/j.ijrefrig.2014.03.012

Pitarch, M., Hervas-Blasco, E., Navarro-Peris, E., Gonzálvez-Maciá, J., Corberán, J.M., 2017a. Evaluation of optimal subcooling in subcritical heat pump systems. Int. J. Refrig. 78, 18–31. doi:10.1016/j.ijrefrig.2017.03.015

Pitarch, M., Navarro-Peris, E., Gonzálvez-Maciá, J., Corberán, J.M., 2017b. Experimental study of a subcritical heat pump booster for sanitary hot water production using a subcooler in order to enhance the efficiency of the system with

a natural refrigerant (R290). Int. J. Refrig. 73, 226–234. doi:10.1016/j.ijrefrig.2016.08.017

Pitarch, M., Navarro-Peris, E., Gonzálvez-Maciá, J., Corberán, J.M., 2017c. Evaluation of different heat pump systems for sanitary hot water production using natural refrigerants. Appl. Energy 190, 911–919. doi:10.1016/j.apenergy.2016.12.166

Pitarch, M., Navarro-Peris, E., Gonzálvez-Maciá, J., Corberán, J.M., 2017d. Science and Technology for the Built Environment Experimental study of a heat pump with high subcooling in the condenser for sanitary hot water production Experimental study of a heat pump with high subcooling in the condenser for sanitary hot water production. Sci. Technol. Built Environ. 0, 1–10. doi:10.1080/23744731.2017.1333366

PMA Prozeß- und Maschinen-Automation GmbH, n.d. Industrial and process controller KS 90-1and KS 92-1. Operating manual.

Pottker, G., Hrnjak, P., 2015a. Effect of the condenser subcooling on the performance of vapor compression systems. Int. J. Refrig. 50, 156–164. doi:10.1016/j.ijrefrig.2014.11.003

Pottker, G., Hrnjak, P., 2015b. Experimental investigation of the effect of condenser subcooling in R134a and R1234yf air-conditioning systems with and without internal heat exchanger. Int. J. Refrig. 50, 104–113. doi:10.1016/j.ijrefrig.2014.10.023

Pottker, G., Hrnjak, P.S., Hrnjak, P., 2012. Purdue e-Pubs Effect of Condenser Subcooling of the Performance of Vapor Compression Systems: Experimental and Numerical Investigation Effect of Condenser Subcooling of the Performance of Vapor Compression Systems: Experimental and Numerical Investigation.

Sarkar, J., Bhattacharyya, S., Gopal, M.R., 2004. Optimization of a transcritical CO2 heat pump cycle for simultaneous cooling and heating applications. Int. J. Refrig. 27, 830–838. doi:10.1016/j.ijrefrig.2004.03.006

Stene, J., 2007. INTEGRATED CO 2 HEAT PUMP SYSTEMS FOR SPACE HEATING AND HOT WATER HEATING IN LOW-ENERGY HOUSES AND PASSIVE HOUSES. Int. Energy Agency.

Stoecker, W., 1998. Industrial Refrigeration Handbook. McGraw-Hill Companies.

Zhu, Y., Li, Y., Dong, L., Salsbury, T.I., House, J.M., 2016. Purdue e-Pubs Distributed Extremum Seeking Control for a Variable Refrigerant Flow System Distributed Extremum Seeking Control for a Variable Refrigerant Flow System.

Ziegler, J.G., Nichols, N.B., 1995. Optimum settings for automatic controllers. InTech. doi:10.1115/1.2899060

LIST OF FIGURES

Figure 9: COP deviation from the optimal with the constant temperature approach control.

Figure 10: Heat pump control scheme

Figure 11: Verification of the PID response for different DTa setting values from a stable system condition (Twcondin=30°C, Twevapin=20°C).

Figure 12: Heat pump starting up, control of DTa=4 and increase of the water inlet temperature at the condenser with the time.

Figure 13: DTa=4 control, decrease of the water inlet temperature at the condenser and variation of the secondary mass flow in order to have the water temperature at the outlet of the evaporator at 60°C.

Figure 14: DTa=5 control, decrease of the water inlet temperature at the condenser, decrease of the water inlet temperature at the evaporator and reduction of the water mass flow rate.

Figure 15: DTa variation (set to 3) with the time for (a) Twinevap=20°C, Twoutevap=15°C, Twincond=10°C and Twoutcond=60°C. (b) Twinevap=20°C, Twoutevap=15°C, Twincond=30°C and Twoutcond=60°C (c) Twinevap=20°C, Twoutevap=15°C, Twincond=50°C and Twoutcond=60°C.

Chapter 4
Improved water to water heat pump design for low-temperature waste heat recovery based on subcooling control

Estefanía Hervás-Blasco(a), Emilio Navarro-Peris(a), Francisco Barceló-Ruescas(a), José Miguel Corberán(a)

(a) Institut Universitari d'Investigació d'Enginyeria Energètica, Universitat Politècnica de València, Camí de Vera s/n, València, 46022, Spain

Tel: +34 963879123 enava@ter.upv.es

4.1 Abstract

Traditional heat pumps designs have been optimized for heating applications based on small secondary temperature lifts (around 5 K); however, in applications with other characteristic temperature lifts, different design criteria could be required. For instance, transcritical cycles have demonstrated to have a high efficiency for domestic hot water production with high water temperature lifts.

This work presents the experimental results of a new water-to-water heat pump composed by the basic heat pump components (condenser, compressor, evaporator, expansion valve and liquid reliever) able to adapt its performance depending on the required water temperature lift. Domestic hot water production from grey water waste heat recovery has been chosen as experimental application to test this heat pump. Results show COP values up to 5.5 at the design condition (20-15ºC at the inlet-outlet of the evaporator and 10-60ºC at the inlet-outlet of the condenser) and an optimal degree of subcooling of 47K.

Keywords: heat pump; optimal control; water heating; subcooling; superheat.

4.2 Nomenclature

10K2V: Configuration with superheat=10K/two control valves

0K1V: Configuration with superheat=0K/one control valve

Tw,ei: Water inlet temperature at the evaporator (°C)

Tw,ci: Water inlet temperature at the condenser (°C)

Tw,co: Water outlet temperature at the condenser (°C)

COP: Coefficient of Performance, [-]

p: Pressure [bar]

Sc: Subcooling, [K]

Sh: Superheat [K]

T: Temperature [°C]

Greek symbols

Δ: Variation

S*ubscripts*

comp: Compressor

cond: Condenser, or gas cooler

evap: Evaporator

in: Inlet

opt: Optimal

out: Outlet

ref: Refrigerant

4.3 Introduction

Looking for a decarbonized energy sector, the use of renewable energies as well as efficient technologies arise as focus for next decades, where a change on the energy system is required (García-Álvarez et al., 2016).

Heat pumps (HP) are a mature technology widely used due to its high performance, reliability and stability. Nowadays, they are on growing interest as alternative to conventional water heating systems (boilers, solar thermal) as the European Directive 2009/28/CE recognizes the water heated with a HP able to operate with a Seasonal Performance Factor (SPF) greater than 2.5 as if it was produced by renewable energies ("DIRECTIVE 2009/28/EC OF THE EUROPEAN PARLIAMENT AND OF THE COUNCIL" of 23 April 2009 on the promotion of the use of energy from renewable sources and amending and subsequently repealing Directives 2001/77/EC and 2003/30/EC).

As demonstrated in other works, their efficiency strongly depends on the external conditions (Pitarch et al., 2017a). Domestic Hot Water (DHW) applications deal with high secondary temperature lifts at the condenser, the tap water is around 10°C and needs to be heated up to at least 60°C, contrary to the most widespread applications of HP until the moment (heating and cooling applications with low temperature lifts at the secondary fluids) (Cecchinato et al., 2005a; Zehnder, 2004). Thus, HPs for DHW applications are still a field with room for improvement (Gunerhan et al., 2014).

Furthermore, new heat recovery applications, based on low-grade temperature mass flows currently wasted to the ambient such as heat recuperation from the sewage in residential sector or from condensing loops in commercial/industrial sectors, are gaining importance within HPs. This heat, usually at temperature slightly higher than the ambient, becomes a valuable and stable heat source in HPs that are able to elevate the temperature of the heat sink up to useful levels. Hence, high or at least different temperature lifts at the secondary fluid in the evaporator may also take place, which is a new topic that needs further research and understanding (Law et al., 2013; David et al., 2017; Meggers and Leibundgut, 2010; Cipolla and Maglionico, 2014; Shen et al., 2018).

Another issue related to HPs is the working fluid (refrigerant). In order to meet all the characteristics required, that is, good thermodynamic properties, safety and environmentally friendly, natural refrigerants (carbon dioxide –CO2 (R744), hydrocarbons (HCs) and ammonia (NH3)) are seen as the solution for now and the next future (Lorentzen, 1995; Ajuka et al., 2017).

According to the above mentioned, a research line from the last and the coming years is the study and integration of heat recovery heat pumps (HRHPs) working with natural fluids for DHW production (To, 2013) .

Among the cited refrigerants, transcritical cycles (CO2) present higher efficiency than subcritical with high temperature lifts due to a better match of the temperature profile between the secondary and the refrigerant in the condenser side (Stene, 2007; Cecchinato et al., 2005a; Yokoyama et al., 2010). For that reason, CO2 has been the most used refrigerant in DHW applications ("Eco Cute | MAYEKAWA Global (MYCOM)," 2009; Nekså et al., 1998; Nekså, 2002; Cecchinato et al., 2005b). However, subcritical refrigerants have also been used to this purpose. In these cases, to avoid the loss of efficiency, the heating process is progressive and divided in steps of around 5K until it reaches values up to 60°C (Quantum National Distributor, 2018).

Recently, researches have been dealing with the study of the benefit obtained from the application of a certain degree of subcooling in subcritical cycles (Pitarch et al., 2017b; Pitarch et al., 2018; Alonso and Stene, 2010; Pottker and Hrnjak, 2015) in order to adapt the performance of the system to the required water temperature lift. With subcooling, a better temperature profile match between the secondary fluid and the subcritical cycle is possible. Thus, improving the efficiency of the heating process. While the existence of an optimal active charge of the system (directly related to the condenser subcooling) was studied in the past (Cecchinato et al., 2005b; Corberán et al., 2008), it was mainly for applications with low water temperature lifts and the optimal subcooling was found in the interval of 5-10K only for the nominal condition. But as it has been demonstrated by Pitarch et al., (2017a), these results depend not only on the heat pump design but also on the target application. For instance, for an application with a temperature lift in the condenser of 50K the optimal degree of subcooling has been found to be around 43K and the obtained improvement for these conditions from working at 0 K of subcooling was 31% in terms of COP.

In this way, subcritical cycles working with the optimal degree of subcooling and high temperature lifts are able to operate under similar efficiencies than transcritical cycles and their design is more flexible to different operating conditions (Pitarch et al., 2017b).

The same approach could be extrapolated to the evaporator side, where superheat was only applied to ensure the reliability of the compressor, in that sense usually it has been considered as harmful and only recommendations of 5-

10K are given (Jolly et al., 2001). This point may become important within heat recovery applications.

Derived from all of the above, a heat pump system needs to have a proper control strategy that allows the adaptation to the external conditions in order to operate under the maximum performance (Stene, 2007). To that purpose, different control strategies have been used: from the analysis of the operational parameters and degrees of freedom (Kim et al., 2004; Jensen and Skogestad, 2007) to complex algorithms (Koeln and Alleyne, 2014; Hu et al., 2015) based on seeking control or to simpler controls based on the temperature approach as assessed by Hervas-Blasco et al., (2018).

In this work, a new heat pump prototype with the same components of a standard heat pump has been build. The heat pump uses the expansion valve to control subcooling instead of superheat. Superheat is fixed to 0 K placing the liquid receiver at the outlet of the evaporator. With that configuration, the heat pump is able to adapt its subcooling to the external condenser conditions resulting in an improvement of the COP without adding any additional cost to a regular system. The prototype has been tested for an application of domestic hot water production with heat recovery from the sewage water. Later, the results have been compared with the results obtained in the heat pump presented by Pitarch et al., (2018) which has been especifically designed for that target. That heat pump has been considered as the reference one as it was able to control the subcooling and the superheat independently but introducing more components in the system. Derived from that, the selected refrigerant was propane (the one used in the reference system), although the results can be generalized for other refrigerants.

4.4 Heat Pump design

The developed prototype is a water-to-water heat pump (WtWHP) for heating water from 10 ºC to 60 ºC from the heat recovery of any low temperature water source which controls the subcooling with the expansion valve in order to maximize the efficiency.

Figure 1 shows the lay-out and the refrigerant cycle of the prototype 0K1V (zero superheat, one valve).

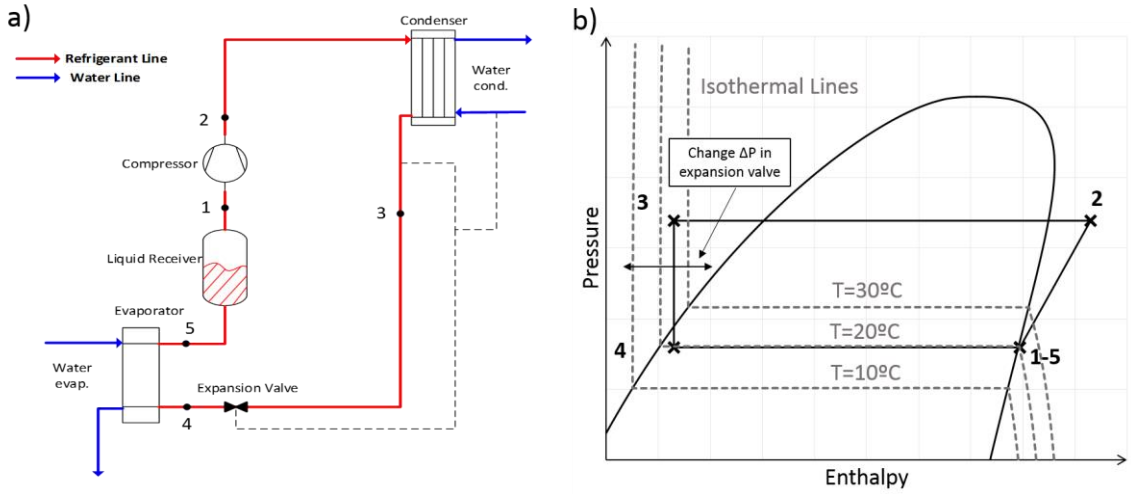

Figure 1: 0K1V configuration (a) system lay-out (b) refrigerant cycle

The objective of testing this configuration is to analyze the reliability and stability of this system that has the same components as a typical heat pump but the expansion valve (thermostatic or electronic) is dedicated to the subcooling control at the expense of losing the superheat control. In this sense, the liquid receiver is placed at the outlet of the evaporator (point 5) ensuring saturated vapor conditions (zero superheat). The evaporation pressure depends mainly on the heat process at the evaporator (points 4-5) while the condensing pressure is constrained from the heat process in the condenser (points 2-3). The pressure drop introduced by the expansion valve will determine the degree of subcooling made at the condenser. Hence, lower degrees of subcooling are obtained. In this configuration, a liquid-suction heat exchanger may be suitable for other applications where the temperature at the outlet of the condenser is not too close to the evaporation temperature. The control strategy implemented in the system is based on the temperature approach measurement following the same approach as the one performed by Hervas-Blasco et al., (2018). Please refer to it for further details.

Some aspects would need to be carefully addressed:

1) Control reliability: even though this configuration has been used with transcritical cycles before, the characteristics of both type of cycles are significantly different and the reliability and stability of the proposed heat pump must be tested. In transcritical cycles, the control of the rejection pressure by means of the drop pressure in the expansion valve is accurate and stable. However, in this case the pressure drop in the valve is going to control a temperature difference, therefore, at the beginning of this work it was unknown if this kind of control would be reliable.
2) Liquid receiver: stability and reliability problems associated to the deposit placed at the inlet of the compressor could appear.
3) Not superheat control penalty: in common heat pump applications, superheat has a negative impact on the efficiency. However, within heat recovery applications, were large secondary temperature lifts at the evaporator take place, certain degree of superheat could constitute a benefit, as it will allow the increase of the evaporating pressure. Therefore, work at 0 K superheat could constitute a penalty to the efficiency of this design that must be evaluated.

The implemented control algorithm was based on the temperature difference between the water inlet temperature and the refrigerant outlet temperature in the condenser used by Hervas-Blasco et al., (2018). Vapor conditions at the inlet of the compressor are ensured by placing a sight glass at the outlet of the liquid receiver and by removing part of the isolation in the circuit from the liquid receiver to the compressor.

Finally, the analysis of the impact on the efficiency due to the lack of superheat and its control has been addressed by comparing the experimental results to the results obtained for a HP configuration in which both, subcooling and superheat control, are possible at the expense of an extra valve. This system is referred as 10K2V and will work at 10 K of superheat. Further details of the last configuration can be found in the work by Pitarch et al., (2016).

4.5 Experimental setup and test procedure

4.5.1 Test rig

Figure 2 shows a general lay-out of the HP test rig. The rig allows the control of the water temperatures at the condenser (points 1-2) that simulate the heat sink and at the evaporator (points 3-4) simulating the water recovery mass flow.

The heat pump prototype has been designed to obtain around 50kW at the design point (20-15°C at the water inlet-outlet evaporator and 10-60°C at the water inlet-outlet condenser) and the test rig is capable to test HPs up to 70kW.

The heat pump itself is placed inside the black dotted points and the circuit of the 0K1V is represented in red. The test rig used is the same as the one used by Pitarch et al., (2016), please refer to it for a more detailed explanation. For further details on the sensors and the instrumentation used including the error analysis, please refer to the publication by Pitarch et al., (2018). The total uncertainty for COP and heating capacity is lower than ±0.08 and ±0.05 kW, respectively, for all measurements.

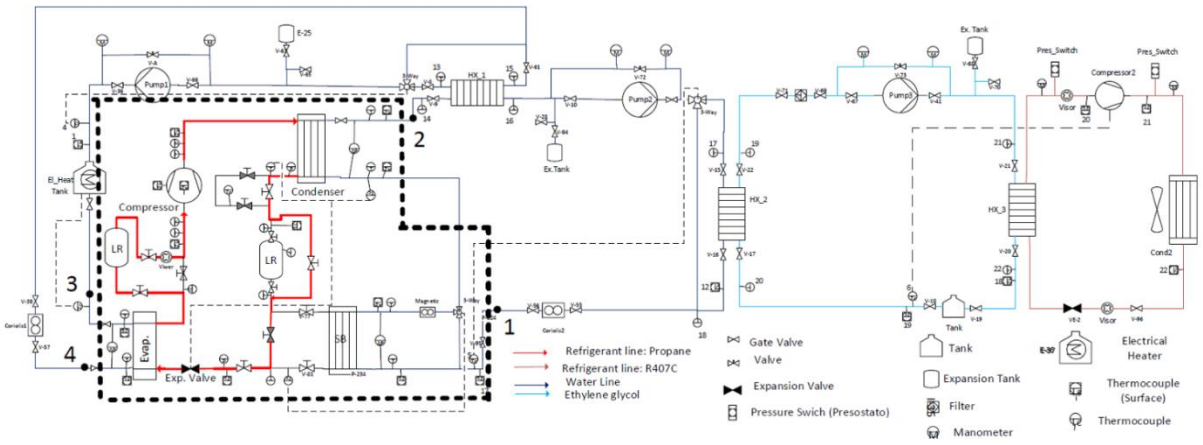

Figure 2: Overview of the HP test rig and sensors used in the experimental setup.

Table 1 shows the characteristics of the main components used in the prototype. The same size of the components as in the reference case (10K2V) has been chosen in order to obtain comparable results.

Table 1: Characteristics of the components of the HP system

Component	Type	Size
Compressor	Scroll (2900rpm)	29.6m^3h^{-1}
Condenser	BPHE Counter-flow	3.5m2
Evaporator	BPHE Counter-flow	6m2
Liquid receiver	-	8 l
Expansion valve	Electronic EV	5-60kW

4.5.2 Sensors and error analysis

The evaporator and condenser capacities of the heat pump were measured in the water side. In order to measure them as accurate as possible, six RTDs were located at inlet/outlet of each heat exchanger directly in contact with the water. To monitor and measure temperature in other points, a total number of 27 T-type thermocouples were used. The water mass flow through evaporator and condenser were measured with Coriolis mass flow meters. For the pressure, at the refrigerant side there were two pressure transducers. In the water side, there were 3 differential pressure sensors to measure the pressure drop in the heat exchangers. With these measurements and according to the norm EN 14511-3 "Test methods" (DIN EN 14511-3, 2013), the auxiliary consumption of the water pumps was calculated.

Table 2 shows these sensors with the relative and absolute accuracy for each sensor. From these sensors and the characteristics of the experimental set up the total uncertainty of the variables not measured directly like COP and heating capacity does not overpass ±0.08 and ±0.05 kW respectively for all measurements.

Table 2: Sensors and their uncertainty

Magnitude	Model	Relative Accuracy	Absolute Accuracy	Units
Pressure	Differential 1151 Smart Rosemount	0.13 % of Span	5 E-04	bar
	Differential p Siemens Sitrans	0.14 % of Span	4 E-04	bar
	Differential p Setra	0.3 % of Span	1.7 E-03	bar
	P 1151 Smart GP7 Rosemount	0.12 % of Span	0.03	bar
	P 1151 Smart GP8 Rosemount	0.15 % of Span	0.08	bar
Temperature	Thermocouple T Type		1	ºC
	RTD Class 1/10 DIN		0.06	ºC
Flow	Coriolis SITRANS F C MASS 2100	0.3 % of Reading		
Power	DME 442	0.3 % of Reading		

4.5.3 Experimental campaign

The experimental campaign is divided in three parts:

1. **Reference conditions:** A campaign including a total of 86 measurements, where most of the common DHW and the heat recovery water temperatures have been covered through it. 60ºC has been set as the condenser outlet temperature of the water. The inlet water temperature at the condenser varies from 10ºC-50ºC. The water inlet conditions at the evaporator range from 10ºC to 30ºC representing the temperature of the water in the sewage or a heat recovery process. The water mass flow rate in the evaporator was adjusted in the nominal point and it is kept constant for the rest of the test points (~7000kg/h), this procedure is described in the European Standard EN 14825. Superheat is kept always lower than 2K.

Table 2 collects the matrix of the conditions tested with 0K1V prototype. Table 2 collects the matrix of conditions tested with 0K1V prototype.

Table 2: Experimental campaign matrix with 86 measurements carried out in the OK1V configuration

$T_{in\_water\_evap}$ [°C]	$T_{in\_water\_cond}$ [°C]	$T_{out\_water\_cond}$ [°C]	Refrigerant subcooling range [K]
10	10	60	4 to 54
	30		4 to 36
	50		4 to 16
20	10		4 to 54
	30		4 to 36
	50		4 to 16
30	10		4 to 54
	30		4 to 36
	50		4 to 16

2. **Water heating limit conditions:** to test the capabilities of the prototype, 16 new measurements considering higher outlet temperatures at the condenser were performed for the OK1V prototype. In order to be able to compare the obtained results with the reference the same test campaign was repeated for 10K2V prototype.

Table 3 shows the matrix of the conditions tested with both configurations for different water temperatures at the outlet of the condenser.

Table 3: Experimental campaign matrix with 16 measurements carried out in the OK1V and 10K2V configurations

$T_{in\_water\_evap}$[°C]	$T_{in\_water\_cond}$[°C]	$T_{out\_water\_cond}$[°C]
20	30	70
		80
		90
20	40	80
		90
30	30	70
		80
		90

3. **Evaporator conditions:** An experimental campaign of 54 measured points was performed in order to study the optimal water mass flow rate through the evaporator (optimum DT). This campaign supplies very relevant information in order to understand the system behavior for energy recovery applications. As in the previous cases, the test campaign was performed for the analyzed prototype 0K1V and the reference system 10K2V.

Table 4 shows the matrix of the conditions tested with both configurations in order to obtain the optimal water mass flow rate through the evaporator.

Table 4: Experimental campaign matrix with 54 measurements carried out in the OK1V and 10K2V configurations

Tin_water_evap [°C]	DTevap [K]	Tin_water_cond-Tout_water_cond [°C]	Refrigerant subcooling range [K]
15	3.5-9	20-60	28-39
20	4-12.5		
35	5-21		

4.6 Results

4.6.1 Reference conditions

This section presents the experimental results obtained from the reference conditions campaign collected in Table 2 and the 0K1V prototype. In order to directly compare the results with the reference system (prototype in which both controls are possible), the experimental results obtained with the 10K2V prototype presented previously by Pitarch et al., (2018) have been included also here

Figure 3 shows the heating COP variation with subcooling obtained for both configurations at different water temperature conditions. (a) Evaporator water inlet temperature of 10°C, (b) Evaporator water inlet temperature of 20°C and (c) Evaporator water inlet temperature of 30°C. 10K2V configuration is represented by dots while 0K1V configuration by triangles. Filled markers belong to 0K1V and not filled markers to the reference prototype, 10K2V. Triangles represent the condenser water temperature (10-60°C), dots the water temperature at the condenser (30-60°C) and squares markers to (50-60°C).

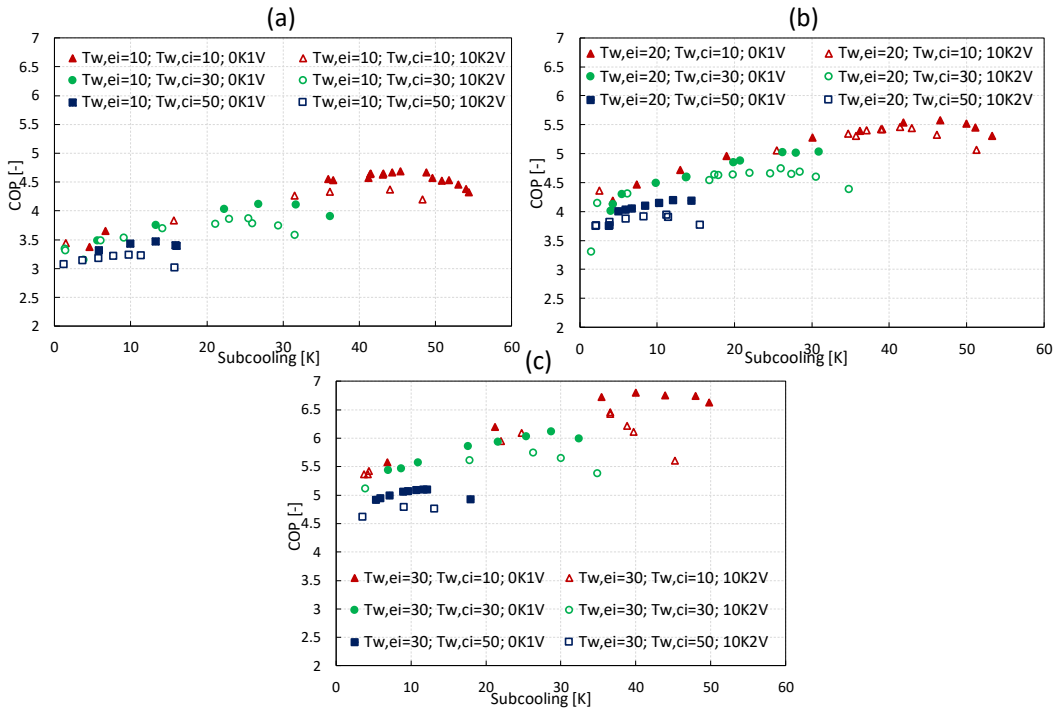

Figure 3: Heating COP variation with subcooling at different temperatures for both configurations and (a) Tevap_water_inlet=10°C (b) Tevap_water_inlet=20°C and (c) Tevap_water_inlet=30°C.

According to Figure 3:

1. The heating COP increases as the evaporating temperature and the water temperature lift at the condenser are higher.

2. The heating COP at the design point (20°C at the evaporator water inlet temperature and 10-60°C at the condenser) is 5.58 (2% higher than the one obtained with 10K2V). The application of the optimal degree of subcooling improves the efficiency up to 25% with regards not having subcooling.

3. An optimal subcooling based on the water temperature lift at the condenser is obtained. The optimal subcooling is around 5K higher in the 0K1V configuration than in the 10K2V configuration.

4. The optimal subcooling was obtained for approximately the same temperature difference between the refrigerant temperature at the outlet of the condenser and water temperature at the inlet of the condenser of the obtained for the reference system. This result is very relevant from the point of view of developing a commercial prototype as allows a very simple control strategy in order to work in the optimum subcooling.

5. The COP of 0K1V, is greater than the COP obtained with the 10K2V at any condition.

6. The 0K1V has a lower reduction in COP as a consequence of working at higher subcoolings than the optimums obtained for the10K2V system.

Figure 4 represents the suction and discharge pressures of the system for both prototypes with subcooling at different water temperature conditions (a) Evaporator water inlet temperature of 10°C, (b) Evaporator water inlet temperature of 20°C and (c) Evaporator water inlet temperature of 30°C. 10K2V configuration is represented by dots while 0K1V configuration by triangles. Filled markers belong to 0K1V and not filled markers to the reference prototype, 10K2V. Triangles represent the condenser water temperature (10-60°C), dots to (30-60°C) and squares markers to (50-60°C).

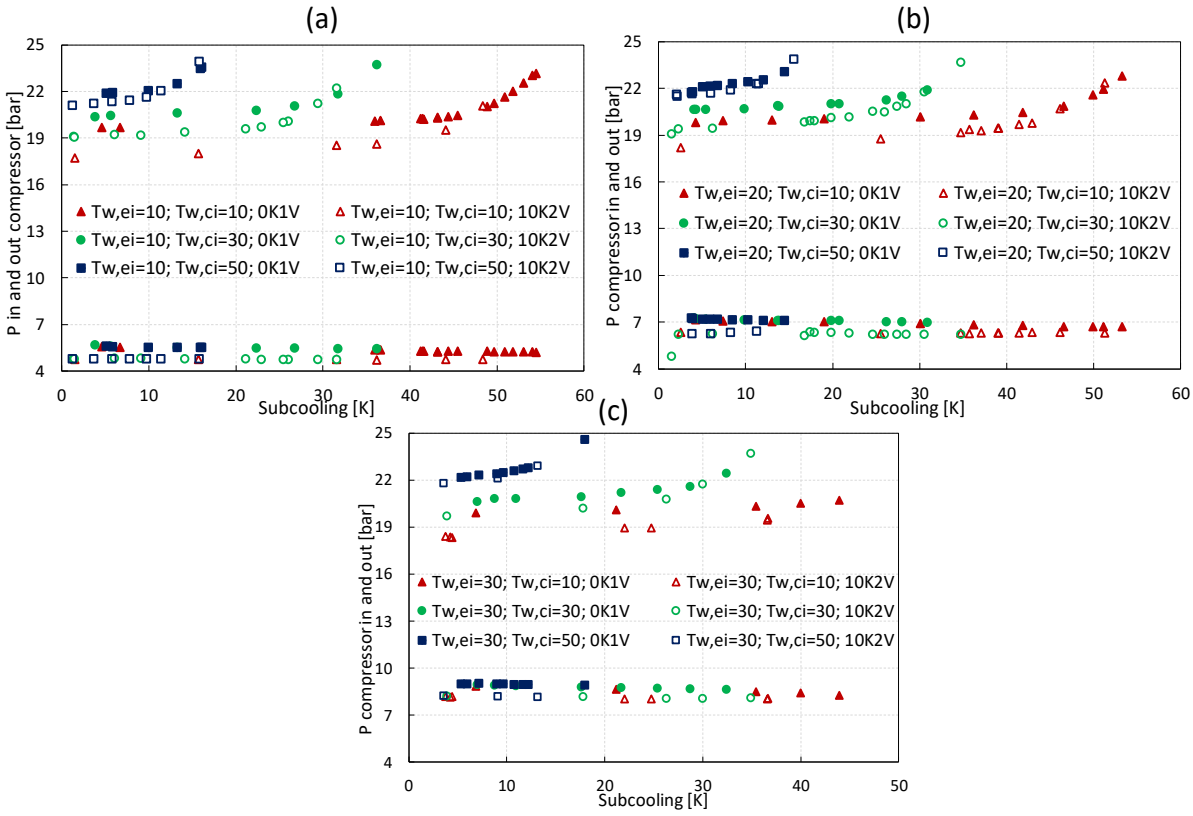

Figure 4: Compressor suction and discharge pressure variation with subcooling at different water temperatures for the 0K1V and the 10K2V configurations. (a) Tevap_water_inlet=10°C (b)Tevap_water_inlet=20°C and (c) Tevap_water_inlet=30°C.

Form Figure 4 the following comparative behavior is extracted:

1. The evaporating pressure remains similar within the same water inlet temperature at the evaporator regardless the subcooling conditions. The 0K1V has a slightly higher evaporation temperature than the 10K2V.

2. The 0K1V configuration works with slightly higher pressures than the 10K2V configuration (due to the fact of having higher subcooling). This effect becomes more important as the temperature lift in the condenser decreases and the water inlet temperature at the condenser increases.

3. The discharge pressure remains almost constant before the optimal subcooling and it is higher in the 0K1V configuration, especially when high water temperature lifts in the condenser take place (because of zero superheat, higher pressures are attained becoming a penalty for the 0K1V configuration if working with lower subcooling than the optimal). Once the optimal subcooling is reached, the discharge pressure exponentially increases not presenting significant differences between both configurations.

Figure 5 represents the compressor discharge temperature for both prototypes as a function of subcooling at different water temperature conditions (a) Evaporator water inlet temperature of 10°C, (b) Evaporator water inlet temperature of 20°C and (c) Evaporator water inlet temperature of 30°C. 10K2V configuration is represented by dots while 0K1V configuration by triangles. Filled markers belong to 0K1V and not filled markers to the reference prototype, 10K2V. Triangles represent the condenser water temperature (10-60°C), dots to (30-60°C) and squares markers to (50-60°C).

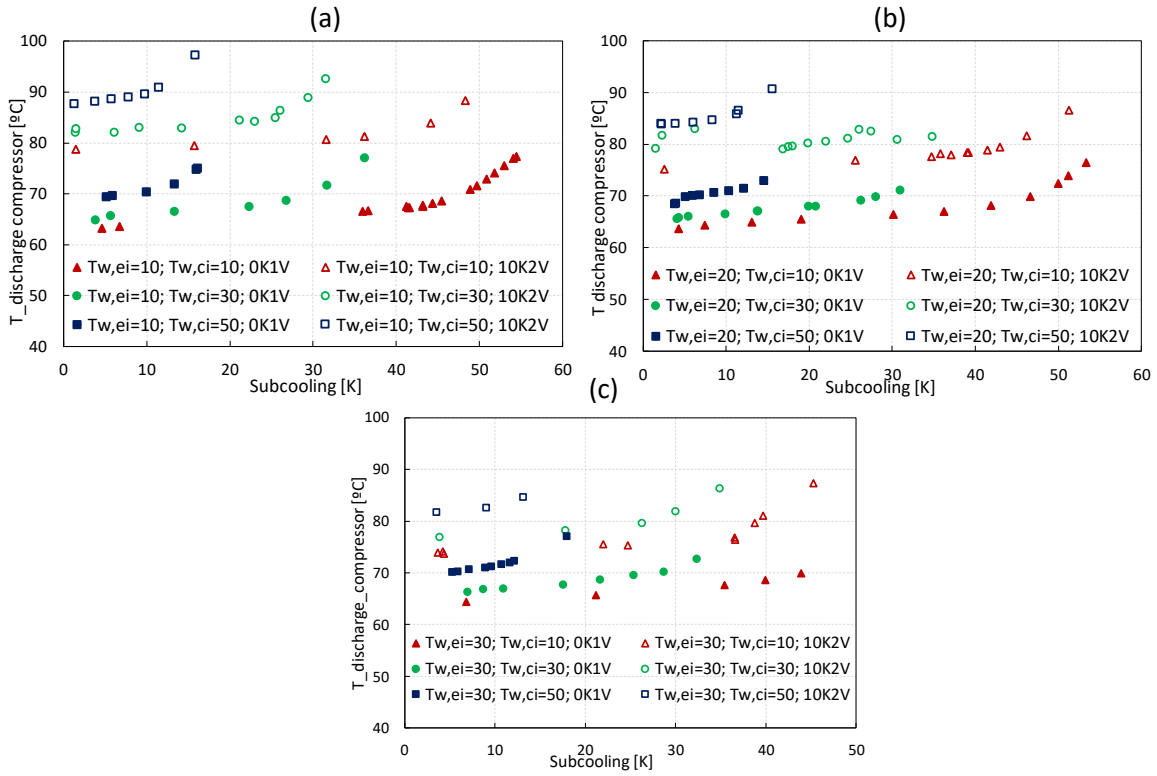

Figure 5: Discharge temperature variation with subcooling at different water temperatures for the 0K1V and the 10K2V configurations. (a) Tevap_water_inlet=10°C (b) Tevap_water_inlet=20°C and (c) Tevap_water_inlet=30°C.

As it can be seen in Figure 5, the discharge temperature is always around 10K lower in the 0K1V than in 10K2V. This is a direct consequence of the superheat degree and lead to obtain higher optimal degrees of subcooling in 0K1V.

For water heating applications, lower discharge temperatures lead to higher condensing temperatures in order to obtain the same water outlet temperatures. This effect will have a significant influence especially for high water temperatures such as 80-90 °C. Thus, it is analyzed more in deep later on.

4.6.2 Water heating limit conditions

Figure 6 represents the heating COP for the prototype as function of the water temperature in the condenser outlet at different water temperature conditions compared to the reference system. 10K2V is represented by dots while 0K1V by line markers. Red color belongs to evaporator water inlet temperature of 20°C and condenser water temperature of 30°C, green color to 20°C at the inlet of the evaporator and 40°C at the inlet of the condenser and black color 30°C evaporator

and 30°C condenser inlet water temperature.

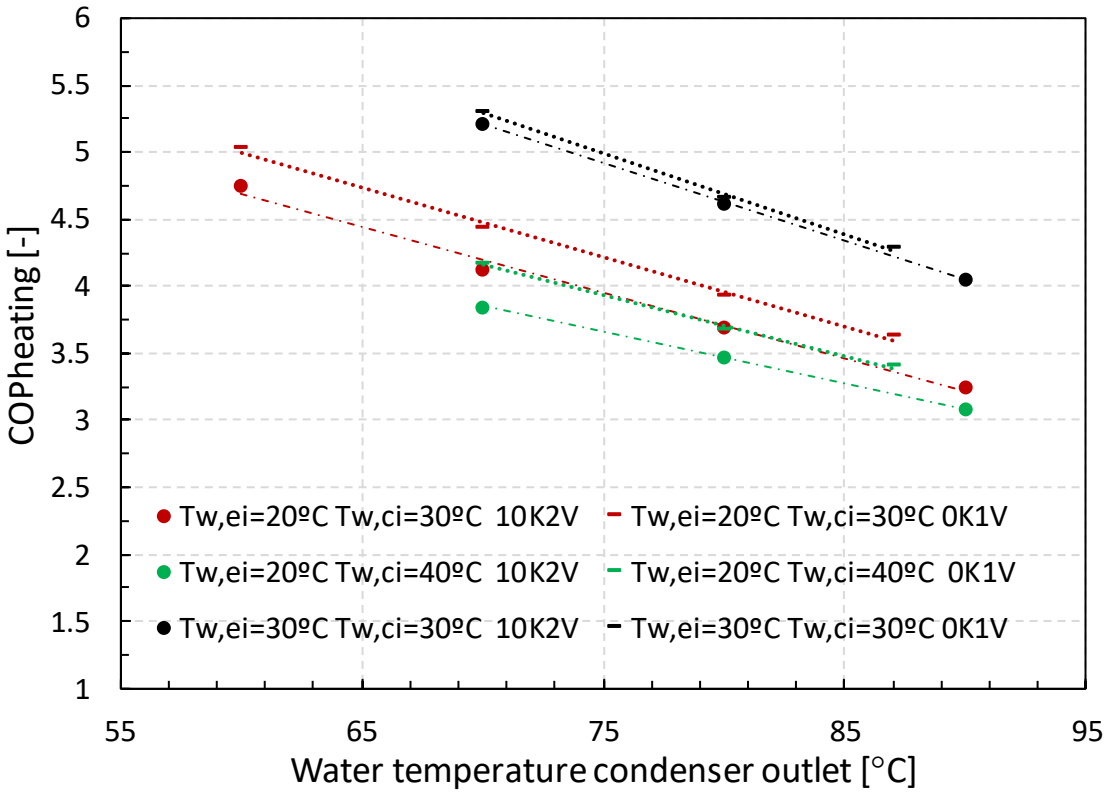

Figure 6: COP heating as a function of Tw,co for different water conditions at the inlet of the condenser and evaporator in both configurations.

As it can be seen in Figure 6, the same results are obtained with the increase of the water outlet temperature at the condenser, that is, the 0K1V maintain its better performance for all the conditions. However, it is worth it to remark that 90°C were impossible to attain with the 0K1V configuration being the maximum stable temperature 87°C due to the increase of the discharge pressure was close to the propane critical point.

Figure 7 represents discharge pressure for 0K1V as function of the water temperature in the condenser outlet at different water temperature in the condenser inlet conditions compared to the reference state. 10K2V is represented by dots while 0K1V by lines markers. Red color belongs to evaporator water inlet temperature of 20°C and condenser water temperature of 30°C, green color to 20°C at the inlet of the evaporator and 40°C at the inlet of the condenser and black color 30°C evaporator and 30°C condenser inlet water temperature.

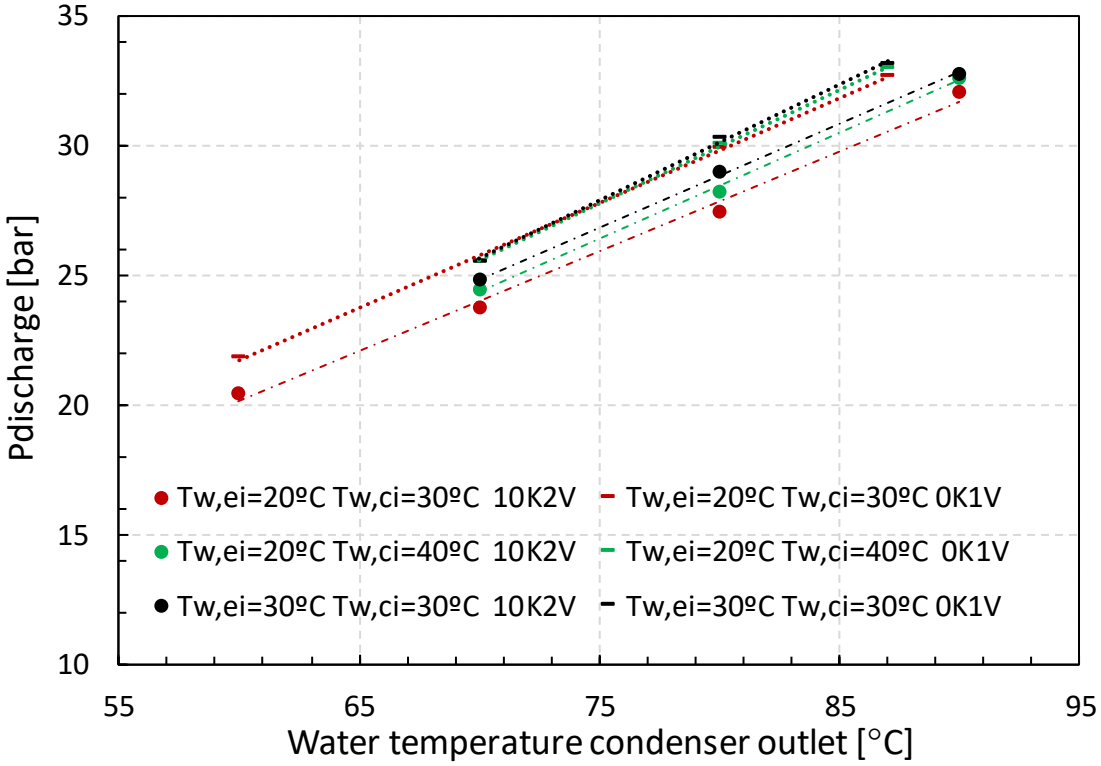

Figure 7: Discharge pressure as a function of Tw,co for different water conditions at the inlet of the condenser and evaporator in both prototypes.

According to the figure, the discharge pressure of 0K1V is always greater than the one reached with the 10K2V. This fact limits the maximum stable temperature for 0K1V system.

This effect may limit the application of the new configuration to DHW since to heat water up to 80-90°C results in a very high discharge pressure.

4.6.3 Evaporator conditions

Figure 8 shows the COP heating for both prototypes as a function of the evaporator water temperature lift for different water inlet temperatures at the evaporator with 40K of water temperature lift at the condenser (20-60 °C). Triangles belong to the 0K1V configuration and circles to the 10K2V. Black color is used for Tw,ei=35 °C, red color for Tw,ei=20 °C and green color for Tw,ei=15 °C.

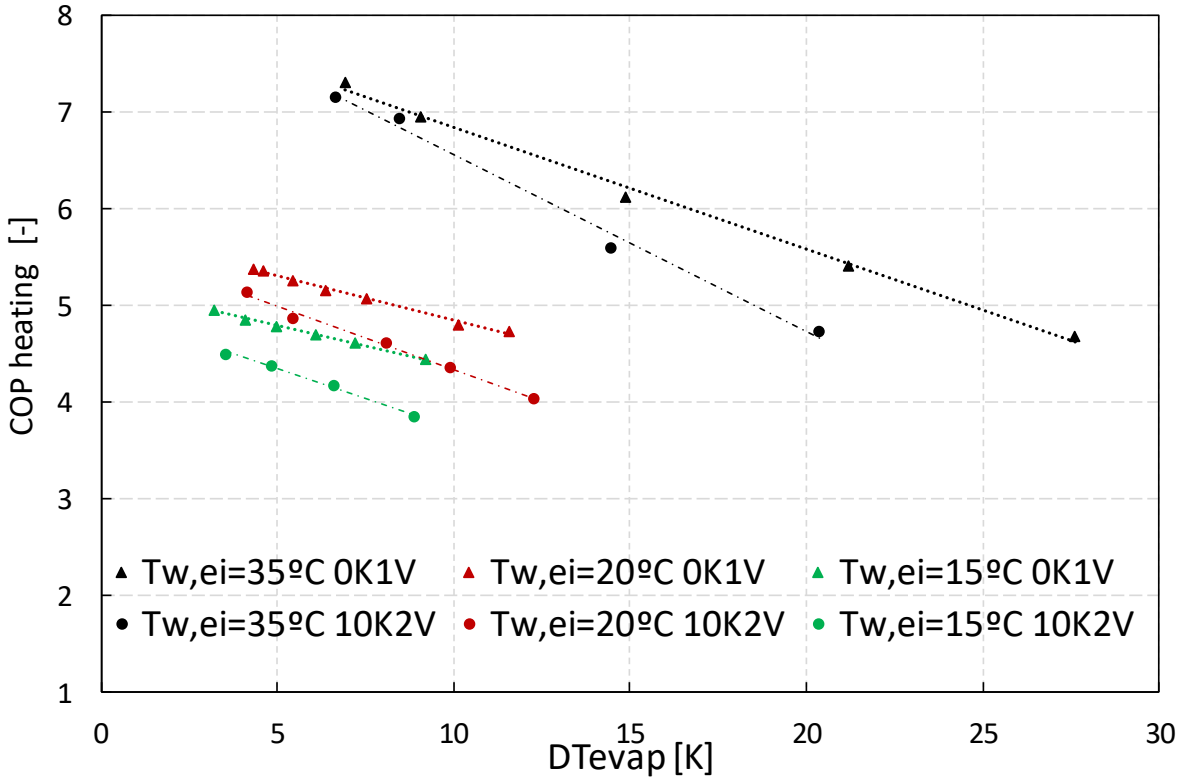

Figure 8: Heating COP variation with the water temperature lift at the evaporator. Tw,ci=20˚C and Tw,co=60˚C and different Tw,ei for 0K1V and 10K2V configurations.

According to Figure 8, it seems that the higher the mass flow, the higher the COP heating is. Hence, for the tested water mass flows, one would always use the maximum. However, it is expected that at some point, the auxiliaries would penalize more and a maximum would be found. This analysis has not been experimentally performed since the water pumps available on the test bench were not able to handle higher mass flows.

Furthermore, as it can be seen, the performance is always greater in the 0K1V regardless the water mass flow rate through the evaporator. This difference becomes more significant as the water mass flow diminishes (greater DTevap). This result is the opposite of the expected from theoretical considerations as for high DTevap having superheat should increase the evaporating temperature which would benefit the configuration with superheat (Pitarch et al.2019). According this assumption, the prototype 0K1V should show a better performance for low DTevap level but as DTevap increases the difference should be reduced up to a value were the reference system 10K2V should show a better COP.

Figure 9 represents (a) the suction pressure (related to the evaporating pressure) and (b) the compressor inlet temperature (related to the evaporating

temperature taking into account the superheat in 10K2V) function of the water temperature lift at the evaporator for different water inlet temperatures at the evaporator and 40K of water temperature lift at the condenser (20-60ºC). Triangles belong to the 0K1V configuration and circles to the 10K2V. Black color is used for Tw,ei=35ºC, red color configuration for Tw,ei=20ºC and green color for Tw,ei=15ºC.

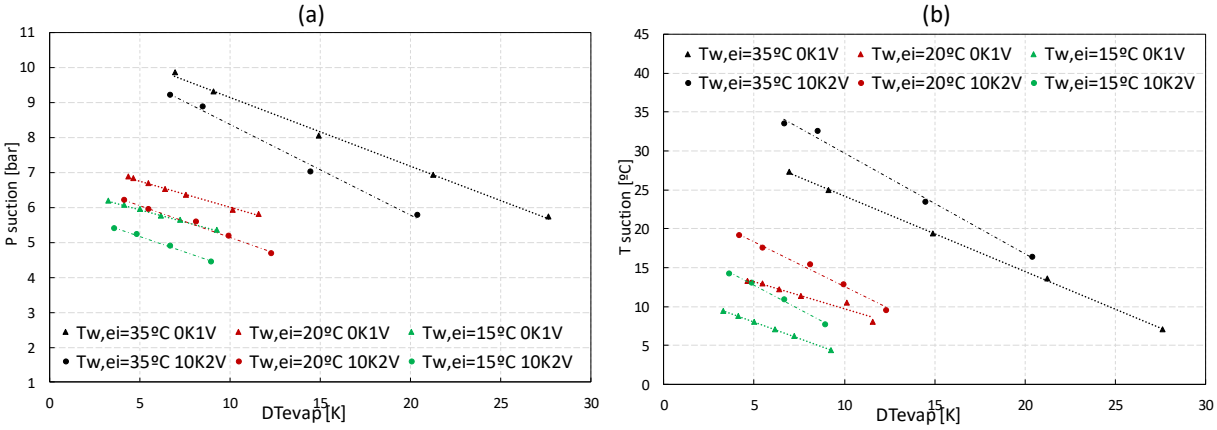

Figure 9: (a) Suction pressure and (b) Suction temperature variation with the water temperature lift at the evaporator. Tw,ci=20˚C and Tw,co=60 ˚C and different Tw,ei for 0K1V and 10K2V configurations.

According to Figure 9, the evaporating pressure has the same trend as the performance, the difference between the 0K1V and 10K2V becomes more important as DTevap increases. As it has been commented previously, it would be expected that high water temperature lifts penalize the evaporator by reducing the evaporating pressure compared to the 10K2V. However, this behavior is not observed. A possible explanation for that could be related with the different vapor qualities at the inlet of the evaporator which could induce bad refrigerant distribution within the evaporator. Nevertheless, further investigation is required in order to find an explanation for the obtained results.

4.7 Conclusions

This paper presents the performance of a new water-to-water heat pump which improves the performance of the system using the expansion valve to control the subcooling instead of the superheat. The heat pump developed has been systematically compared with a heat pump which is able to control the superheat and the subcooling showing higher performance for all the tested conditions.

From all the results, these main conclusions can be extracted:

1) The 0K1V configuration is stable and does not present control problems.
2) The 0K1V configuration without superheat has greater performance than the 10K2V configuration for all the tested conditions. The improvement is around 5%.
3) Comparing the 0K1V prototype with the reference 10K2V, the proposed system has higher discharge pressures, around 10K lower discharge temperatures and the optimal subcooling is around 5K greater. However, the reference system (10K2V) is able to reach higher water temperatures at the outlet of the condenser which could limit the application range of the 0K1V.
4) This limitation factor for the 0K1V could be solved including a liquid to suction heat exchanger after the receiver. Nevertheless, to make it effective, it should be checked that the temperature difference between the evaporator and the condenser is high enough and that it could be cost effective as an additional element is being introduced.
5) The optimum subcooling is found for a temperature difference between the refrigerant outlet and the water inlet in the condenser of 3K for both systems, therefore, to use a control strategy of a constant DT at the outlet of the condenser is reliable. This is a very important fact from the point of view of developing a commercial prototype as it will allow the use of electronic expansion valves as well as thermostatic expansion valves.
6) The evaporating pressure is slightly higher in the 0K1V configuration. The vapor quality at the inlet of the evaporator is lower which allows the evaporating pressure to vary only slightly.
7) The application of superheat at the outlet of the evaporator experimentally always penalizes the performance, contrary to the expected from a theoretical analysis. This result is experimentally obtained but further studies are required in order to be able to explain the discrepancy with the expected.

The obtained results show that the proposed heat pump configuration with the proposed control system for the expansion valve could increase significantly the efficiency of the heat pump overall when a high water temperature lift is imposed by the application. Although in the present paper the application has been mainly focused in domestic hot water production, based on the wide test matrix used which has not been limited to a water temperature lift of 50K, the proposed system with the obtained conclusions can be applied to any other application.

4.8 Acknowledgements

Part of the results of this study were developed in the mainframe of the FP7 European project 'Next Generation of Heat Pumps working with Natural fluids' (NxtHPG). Part of the work presented was carried out by Estefanía Hervás Blasco with the financial support of a PhD scholarship from the Spanish government SFPI1500X074478XV0. The authors would like also to acknowledge the Spanish 'MINISTERIO DE ECONOMIA Y COMPETITIVIDAD', through the project "MAXIMIZACION DE LA EFICIENCIA Y MINIMIZACION DEL IMPACTO AMBIENTAL DE BOMBAS DE CALOR PARA LA DESCARBONIZACION DE LA CALEFACCION/ACS EN LOS EDIFICIOS DECONSUMO CASI NULO" with the reference ENE2017-83665-C2-1-P for the given support.

4.9 References

Ajuka, L., Odunfa, M., Ohunakin, O., Oyewola, M., 2017. Energy and exergy analysis of vapour compression refrigeration system using selected eco-friendly hydrocarbon refrigerants enhanced with tio2-nanoparticle. Int. J. Eng. Technol. 6, 91. https://doi.org/10.14419/ijet.v6i4.7099

Alonso, M., Stene, J., 2010. IEA heat pump program annex 32 umbrella report: system solutions, design guidelines, prototype system and field testing-Norway, Tech. rep.

Cecchinato, L., Corradi, M., Fornasieri, E., Zamboni, L., 2005a. Carbon dioxide as refrigerant for tap water heat pumps: A comparison with the traditional solution. Int. J. Refrig. 28, 1250–1258. https://doi.org/10.1016/j.ijrefrig.2005.05.019

Cecchinato, L., Corradi, M., Fornasieri, E., Zamboni, L., 2005b. Carbon dioxide as refrigerant for tap water heat pumps: A comparison with the traditional solution. Int. J. Refrig. 28, 1250–1258. https://doi.org/10.1016/j.ijrefrig.2005.05.019

Cipolla, S.S., Maglionico, M., 2013. Heat recovery from urban wastewater: Analysis of the variability of flow rate and temperature. Energy Build. 69, 122–130. https://doi.org/10.1016/j.enbuild.2013.10.017

Corberán, J.M., Martínez, I.O., Gonzálvez, J., 2008. Charge optimisation study of a reversible water-to-water propane heat pump. Int. J. Refrig. 31, 716–726. https://doi.org/10.1016/j.ijrefrig.2007.12.011

David, A., Mathiesen, B.V., Averfalk, H., Werner, S., Lund, H., 2017. Heat Roadmap Europe: Large-scale electric heat pumps in district heating systems. Energies. https://doi.org/10.3390/en10040578

DIRECTIVE 2009/28/EC OF THE EUROPEAN PARLIAMENT AND OF THE COUNCIL of 23 April 2009 on the promotion of the use of energy from renewable sources and amending and subsequently repealing Directives 2001/77/EC and 2003/30/EC, n.d.

Eco Cute | MAYEKAWA Global (MYCOM) [WWW Document], 2009. URL http://www.mayekawa.com/products/features/eco_cute/

García-Álvarez, M.T., Moreno, B., Soares, I., 2016. Analyzing the sustainable energy development in the EU-15 by an aggregated synthetic index. Ecol. Indic. 60, 996–1007. https://doi.org/10.1016/j.ecolind.2015.07.006

Gunerhan, H., Ekren, O., Araz, M., Biyik, E., Hepbasli, A., 2014. A key review of wastewater source heat pump (WWSHP) systems. Energy Convers. Manag. 88, 700–722. https://doi.org/10.1016/j.enconman.2014.08.065

Hervas-Blasco, E., Pitarch, M., Navarro-Peris, E., Corberán, J.M., 2018. Study of different subcooling control strategies in order to enhance the performance of a heat pump. Int. J. Refrig. https://doi.org/10.1016/J.IJREFRIG.2018.02.003

Hu, B., Li, Y., Cao, F., Xing, Z., 2015. Extremum seeking control of COP optimization for air-source transcritical CO2 heat pump water heater system. Appl. Energy 147, 361–372. https://doi.org/10.1016/j.apenergy.2015.03.010

Jensen, J.B., Skogestad, S., 2007. Optimal operation of simple refrigeration cycles. Comput. Chem. Eng. 31, 712–721. https://doi.org/10.1016/j.compchemeng.2006.12.003

Jolly, P.G., Tso, C.P., Chia, P.K., Wong, Y.W., 2001. Intelligent control to reduce superheat hunting and optimize evaporator performance in container refrigeration, in: ASHRAE Transactions. p. 267. https://doi.org/10.1080/10789669.2000.10391261

Kim, M.H., Pettersen, J., Bullard, C.W., 2004. Fundamental process and system design issues in CO2 vapor compression systems. Prog. Energy Combust. Sci. https://doi.org/10.1016/j.pecs.2003.09.002

Koeln, J.P., Alleyne, A.G., 2014. Optimal subcooling in vapor compression systems via extremum seeking control: Theory and experiments. Int. J. Refrig. 43, 14–25. https://doi.org/10.1016/j.ijrefrig.2014.03.012

Law, R., Harvey, A., Reay, D., 2013. Opportunities for low-grade heat recovery in the UK food processing industry. Appl. Therm. Eng. 53, 188–196. https://doi.org/10.1016/j.applthermaleng.2012.03.024

Lorentzen, G., 1995. The use of natural refrigerants: a complete solution to the CFC/HCFC predicament. Int. J. Refrig. 18, 190–197. https://doi.org/10.1016/0140-7007(94)00001-E

Meggers, F., Leibundgut, H., 2010. The potential of wastewater heat and exergy: Decentralized high-temperature recovery with a heat pump. Energy Build. 43, 879–886. https://doi.org/10.1016/j.enbuild.2010.12.008

Nekså, P., 2002. CO2 heat pump systems, in: International Journal of Refrigeration. Elsevier, pp. 421–427. https://doi.org/10.1016/S0140-7007(01)00033-0

Nekså, P., Rekstad, H., Zakeri, G.R., Schiefloe, P.A., 1998. CO2-heat pump water heater: Characteristics, system design and experimental results. Int. J. Refrig. 21, 172–179. https://doi.org/10.1016/S0140-7007(98)00017-6

Pitarch, M., Hervas-Blasco, E., Navarro-Peris, E., Corberán, J.M., 2017a. Exergy analysis on a heat pump working between a heat sink and a heat source of finite heat capacity rate. Int. J. Refrig. 99, 337-350. https://doi.org/10.1016/j.ijrefrig.2018.11.044

Pitarch, M., Hervas-Blasco, E., Navarro-Peris, E., Gonzálvez-Maciá, J., Corberán, J.M., 2017a. Evaluation of optimal subcooling in subcritical heat pump systems. Int. J. Refrig. 78, 18–31. https://doi.org/10.1016/j.ijrefrig.2017.03.015

Pitarch, M., Navarro-Peris, E., Gonzálvez-Maciá, J., Corberán, J.M., 2018. Experimental study of a heat pump with high subcooling in the condenser for sanitary hot water production. Sci. Technol. Built Environ. 24, 105–114. https://doi.org/10.1080/23744731.2017.1333366

Pitarch, M., Navarro-Peris, E., Gonzálvez-Maciá, J., Corberán, J.M., 2017b. Evaluation of different heat pump systems for sanitary hot water production using natural refrigerants. Appl. Energy 190, 911–919. https://doi.org/10.1016/j.apenergy.2016.12.166

Pitarch, M., Navarro-Peris, E., Gonzálvez-Maciá, J., Corberán, J.M., 2016. Experimental study of a subcritical heat pump booster for sanitary hot water production using a subcooler in order to enhance the efficiency of the system with a natural refrigerant (R290). Int. J. Refrig. 73, 226–234. https://doi.org/10.1016/j.ijrefrig.2016.08.017

Pottker, G., Hrnjak, P., 2015. Effect of the condenser subcooling on the performance of vapor compression systems. Int. J. Refrig. 50, 156–164. https://doi.org/10.1016/j.ijrefrig.2014.11.003

Quantum National Distributor, 2018. Commercial Heat Pumps – Quantum [WWW Document]. URL http://quantumenergy.com.au/commercial-heat-pumps/

Shen, C., Lei, Z., Wang, Y., Zhang, C., Yao, Y., 2018. A review on the current research and application of wastewater source heat pumps in China. Therm. Sci. Eng. Prog. https://doi.org/10.1016/j.tsep.2018.03.007

Stene, J., 2007. INTEGRATED CO 2 HEAT PUMP SYSTEMS FOR SPACE HEATING AND HOT WATER HEATING IN LOW-ENERGY HOUSES AND PASSIVE HOUSES. Energy 85, 1–14.

To, E., 2013. W ASTEWATER - - - H EAT R ECOVERY TO H EAT / C OOL B UILDINGS.

Yokoyama, R., Wakui, T., Kamakari, J., Takemura, K., 2010. Performance analysis of a CO2 heat pump water heating system under a daily change in a standardized demand. Energy 35, 718–728. https://doi.org/10.1016/j.energy.2009.11.008

Zehnder, M., 2004. Efficient Air-Water pumps for high temperature lift residential heating, including oil migration aspects. ÉCOLE POLYTECHNIQUE FÉDÉRALE DE LAUSANNE.

LIST OF FIGURES

LIST OF TABLES

Chapter 5
Optimal sizing of a heat pump booster for sanitary hot water production to maximize benefit for the substitution of gas boilers

Estefanía HERVAS-BLASCO(a), Miquel PITARCH(a), Emilio NAVARRO-PERIS(a)*, José M. CORBERÁN(a)

(a) Institut Universitari d'Investigació d'Enginyeria Energètica, Universitat Politècnica de València, Camí de Vera s/n, València, 46022, Spain

Tel: +34 963879123

enava@ter.upv.es

5.1 Abstract

Heat recovery from water sources such as sewage water or condensation loops at low temperatures (usually between 10-30°C) is becoming very valuable. Heat pumps are a potential technology able to overcome the high water temperature lift of the Sanitary Hot Water (SHW) application (usually from 10°C -60°C with COPs up to 6). This paper presents a model to find the optimal size of a system (heat pump and recovery heat exchanger) based on water sources to produce SHW compared to the conventional production with a gas boiler in order to maximize the benefit. The model includes a thermal and economic analysis for a base case and analyzes the influence of a wide set of parameters which could have a significant influence. Even the uncertainties involved, results point out considerable benefits from this substitution based on the capacity of the system. Thus, demonstrating the importance of the optimal size analysis before an investment is done.

KEYWORDS: heat pumps, sanitary hot water, waste water, low grade heat recovery, optimal size

5.2 Nomenclature

m_{demand} : SHW mass flow rate capacity, tap water flow [kg s^{-1}]

m_w : wastewater mass flow rate [kg s^{-1}]

cp_w : specific water heat [J kgK^{-1}]

T_{grey} : wastewater temperature [ºC]

T_{tap} : fresh/tap water temperature [ºC]

T_{in_evap} : evaporator water inlet temperature [ºC]

T_{out_evap} : evaporator water outlet temperature [ºC]

T_{in_cond} : condenser water inlet temperature [ºC]

T_{out_cond} : condenser water outlet temperature [ºC]

T_{evap} : fluid evaporating temperature [ºC]

W_c :compressor consumption [kW]

Q_{ref} : available heat to recover assuming a lowest water temperature of 0°C [kW]

Q_{evap} : cooling capacity [kW]

Q_{heat} : heat exchanged in the heat exchanger [kW]

Q_f : fuel heating capacity [kW]

ε: heat exchanger effectiveness

DP_{evap} :water drop pressure through the evaporator [mbar]

DP_{cond} : water drop pressure through the condenser [mbar]

DP_{demand} : fresh water drop pressure through the HE [mbar]

DP_{water} : wasted water drop pressure through the HE [mbar]

$Power\_pump$: consumption of the water pump [kW]

η_{pump} :pumpefficiency[-]

ρ_w : water density [kg (m3)$^{-1}$]

η_{cald} : boiler efficiency [-]

Economic

i : bank interest rate [%]

n : annual payments [years]

r : annuity [-]

$C_{y\_total\_m}$: Annual equivalent investment cost of *m* [€ year^{-1}]

C_{a_m} : Annual cost of the element *m* [€ year^{-1}]

C_{y_m} : Yearly costs of *m* related to taxes [€ year^{-1}]

C_{i_m} : Initial investment cost of *m* function of its size [€]

C_{s_m} : Residual value of *m* after the *n* years [€]

$C_{y\_op\_m}$: Annual operating cost of *m* [€ year^{-1}]

C_{elec_energ} : electricity price (energy term) [€ kWh^{-1}]

C_{elec_pow} : electricity price (power term) [€ kW^{-1}]

$C_{ma\,int\_k}$: annual maintenance cost of *m* [€ year^{-1}]

$C_{\_fix\_gas}$: fix part of the gas price [€ year^{-1}]

$C_{\_fuel}$: gas price [€ kWh^{-1}]

t : operating hours of the installation [h]

Y: ratio annual Benefit/ Q_ref [€kW^{-1}]

Abbreviations

SHW: Sanitary Hot Water

EES: Engineering Equation Solver

EU: European Union

HP: Heat Pump

HX: Heat exchanger

NxtHPG: Next Generation of Heat Pumps working with Natural Fluids

COP: Coefficient of Performance (HP=heat pump; total=system including the recovery heat exchanger), [-]

Subscripts

HP: Heat Pump

heat: Heat Exchanger

boiler: Gas Boiler

5.3 Introduction

Sustainable energy management as well as environmental protection are two activities of major relevance nowadays. Many efforts towards these objectives have been done and an increase of share of renewable energy is crucial to keep growing in this direction [1].

Under that framework, technologies based on the recovery of low temperature energy sources are becoming an interesting alternatives in the recent years ; its availability linked to the fact that they have not been deeply exploited, make them as promising challenge to keep moving towards a more sustainable world [2]. These sources include from residential (sewage wastewater) to commercial or industrial (condensing loops, wasted heat from thermal processes, thermal power plants). In fact, at this moment most of this heat is wasted to the ambient, is removed by additional technologies (such as refrigeration towers) or is lost to the sewage.

In the residential sector, grey water heat recovery can be a profitable and reliable source of heat according to [3]. In fact, the use of wasted heat from the sewage in order to produce heating, cooling or sanitary hot water (SHW) has demonstrated to be very profitable. Examples of this are in-house or district heating projects [2],[3],[4],[5],[6] and organizations like the Japanese agency which has included it in the strategy for energy efficiency technologies in Japan [7].

Other sectors with a large potential for these type of strategies are the industrial and commercial sectors (power plants, chemical plants, almost any type of industry, hotels, supermarkets, gyms, hospitals…) where there is a huge cooling demand and the heat is dissipated in many situations through a closed condensation loops that, afterwards, needs to be dissipated to the ambient. In these cases, these strategies will lead to additional benefits as in addition to the energy direct use, less heat would be dissipated to the ambient [8],[9],[10]. In addition, the fact that for the most common situations, the heat source use to be water which has a high heat capacity and density and it is under quite constant temperatures (around 20/25 °C over the year)[11] allows an optimal sizing design, operating expenses reduction.

At present and regarding the building sector is responsible of around half of global greenhouse emissions, the consumption of two-thirds of all the electricity and one-third of global waste production [11],[12]. To reduce this impact, the main solutions have focused on the reduction of the consumption or the use of more efficient/renewable technologies but mostly regarding to cooling and heating. Prove of this is the reduction of the consumption and, in its extreme, the existence of passive houses with less than 15 kWhm-2 of space heating demand [11],[13]. Nevertheless, sanitary hot water has been underestimated and remains a significant constant demand.

In the commercial sector, the heat recovered is used in other processes within the building where there is a water heat need at higher temperature, like in swimming pools, gyms or as combination with solar heating. In this sector, the absorption heat pump -with usual heating COPs around 1.5-2.5 [14]- is one of the most established technologies. Many works are already done in this line, for instance, the use of the wasted heat from a CHP for a spa or as solar-assisted district heating [15], in a textile industry [16] or in desalination plants [17] are examples of this heat source potential.

Conventional technologies to produce SHW in the building and some commercial applications usually operate with low efficiencies or/and high pollutant emissions rate (among others, solar, electric heating, gas and oil boilers) [18]. In this sense, heat pumps are a very promising technology for this application due to its capability to operate with high levels of efficiency, the possible recognition according to the European Directive 2009/28/CE as renewable energy and the capability to use waste water at low temperature as a heat source [19],[20],[21]. Moreover, the use of natural refrigerants in heat pumps for that type of application is quite common. In fact, CO2 working in transcritical conditions has been demonstrated as a reliable alternative with high COP [20],[21]. In addition

others alternatives like propane has demonstrated high levels of performance in this type of applications [22],[23], [24].

Thermodynamically, it is well known that the substitution of the gas boiler by a heat pump is an efficient solution and has the potential of reusing some sources of waste heat. However, up to the knowledge of the authors no public research has been done related to the optimal heat pump size based on the SHW demand and on the wasted heat considering, in addition, the economic part which is determinant in the final optimal solution.

In this paper, the optimal substitution of a gas boiler by a heat pump and a recovery heat exchanger (HPR) to produce SHW is analyzed. The study assumes a sanitary hot water demand always larger than the capacity of the HPR, a constant availability and temperature of waste heat that could come from sewage water or a condensation loop. Based on those two conditions, the optimal size of the components that maximize the economic benefit has been analyzed.

The paper is organized as follows: first, a description of the model is presented. Second, the performed analysis section collects the characteristics of the base case study and a sensitivity analysis description. Third, all the results obtained from the model are presented. Finally, the conclusions are discussed.

5.4 Description of the model

5.4.1 Description of the system

Figure 1a represents the basic scheme of the water to water heat pump system alone (HPA). Based on the present application, an additional recovery heat exchanger (HPR) in order to pre-heat the water before the inlet of the condenser has been also analyzed (see Figure 1b).

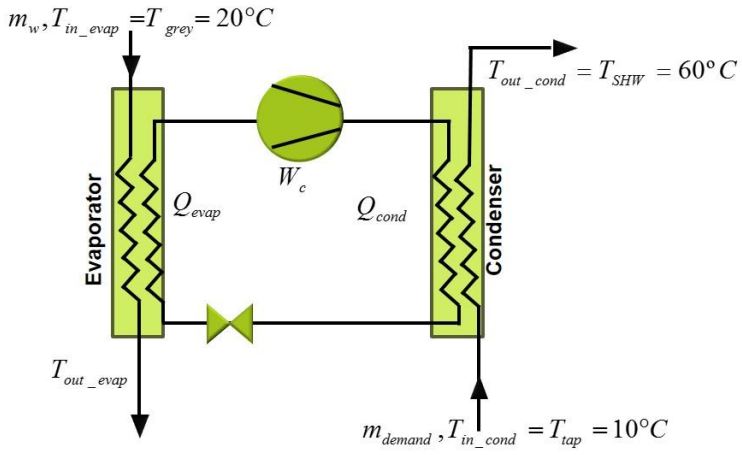

Figure 1a: Heat pump alone (HPA) system layout.

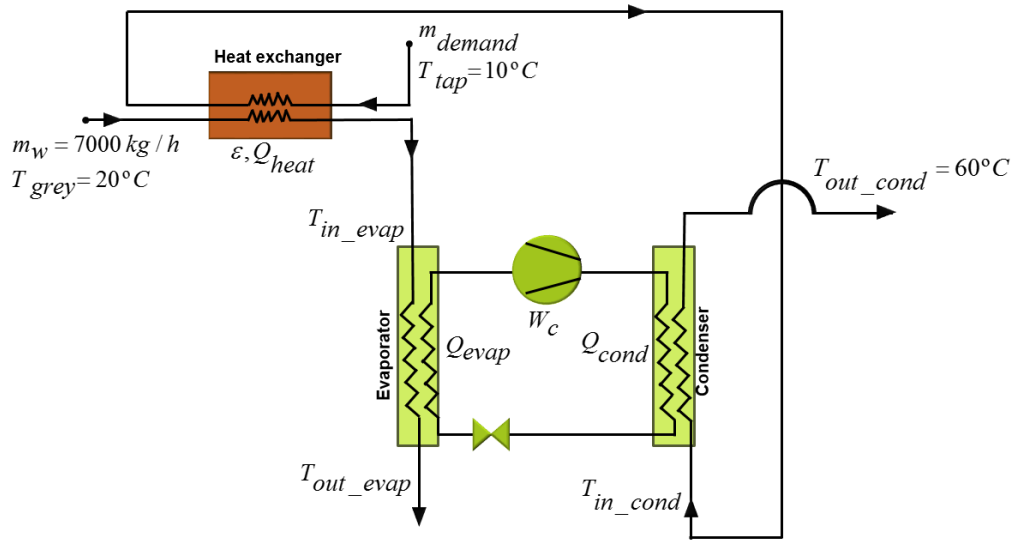

Figure 1b: System layout of the heat pump with an additional recovery heat exchanger (HPR)

Characteristics of the heat pump and boundary conditions:

- The system is based on an existing prototype of a new water to water heat pump that is able to work with subcritical conditions and high COPs thanks to the sub-cooling maximization which is adapted based on the operating conditions. Further information as well as a more detailed explanation regarding to the heat pump can be found in [22].

- The nominal heating capacity under the assumptions considered for this study is which is the size of the existing prototype used for the experimental results and the model validation. In the rest of the document, this value is used as the reference size.

- Refrigerant: the heat pump uses propane not only because of environmentally reasons but also due to interesting thermodynamic characteristics for this application [22], [24].

- Heat source: any available wasted source of energy at low temperature, for instance, sewage water or water from a condensing loop. In this case, water at 20°C and a constant available water mass flow rate of 7000kg h-1 has been considered for the base case.

- Sanitary Hot Water production: the SHW demand is assumed to be significantly higher than the production of the heat pump. The tap/fresh water is considered at 10°C and it will be heated until 60°C. These are, therefore, the temperature conditions of the condenser.

Characteristics of the recovery plate heat exchanger:

A preliminary study in order to choose a heat exchanger size was done based on the open access Sweep software [25] .

The heat exchanger was chosen with the following boundary conditions based on specifications from the manufacturer:

- Minimum number of plates due to efficient design: 10

- Maximum number of plates due to efficient design: 140

5.4.2 Model equations

5.3.2.1. Thermodynamic problem

First, the equations used for the recovery heat exchanger modeling are presented, second, the equations of the heat pump are exposed and third, a description of the model equations of the complete system is done.

The recovery heat exchanger modifies the water temperature at the inlet of the evaporator and condenser of the heat pump. Its influence on the heat pump performance has been evaluated modelling it by the following equations.

The heat rejected from the wastewater is calculated according Eq.1:

$$Q_{heat} = \varepsilon \cdot mcp_{\min} \cdot (T_{grey} - T_{tap}) \quad (1)$$

Where the effectivity has been modeled based on Sweep software[81]. According to that, an expression for the effectivity and the effective capacity as a function of the number of plates and the mass flow rate has been obtained:

$$\varepsilon = f(m_{demand}, Plates) \quad (2)$$

And $mcp_{\min} = \min(m_{demand} \cdot cp_w, m_w \cdot cp_w)$.

The new inlet temperatures are calculated according Eqs.3 and 4:

$$T_{in\_evap} = T_{grey} - (\frac{Q_{heat}}{m_w cp_w}) \quad (3)$$

$$T_{in\_cond} = T_{tap} - (\frac{Q_{heat}}{m_{demand} cp_w}) \quad (4)$$

Where T_{in_evap} the evaporator inlet temperature [K] and T_{in_cond} is the condenser inlet temperature [K].

The pressure drop has been calculated following the same methodology described previously for the heat transfer problem and it is shown in Eq. 5 and 6.

$$DP_{demand} = f(m_{demand}, Plates) \quad (5)$$

$$DP_{water} = f(m_w, Plates) \quad (6)$$

The heat pump model is based on empirical correlations for the COP and heating capacity developed from experimental results according to [22] as a function of the water temperature at the inlet of the condenser and the evaporating temperature including the auxiliaries. Eq. 7 and Eq. 8 show the fitting used in the model for an outlet condenser water temperature of 60°C:

$$COP_{hp} = -94.5966685 + 0.22736625 \cdot T_{in\_cond} + 0.39666425 \cdot T_{evap} - 0.00095157 \cdot T_{in\_cond} \cdot T_{evap} \quad (7)$$

$$T_{evap} = (-201.603822 - 17.3859437 \cdot T_{in\_evap} + 19.9534897 \cdot T_{out\_evap} - 0.13609611 \cdot T_{in\_evap}^2 - \\ - 0.20473267 \cdot T_{out\_evap}^2 + 0.33769076 \cdot T_{in\_evap} \cdot T_{out\_evap}) \quad (8)$$

$$Q_{cond} = -837.342696 + 1.79739626 \cdot T_{in\_cond} + 3.38242539 \cdot T_{evap} - 0.00725288 \cdot T_{in\_cond} \cdot T_{evap} \quad (9)$$

Where COP_{hp} is the Coefficient of Performance, T_{evap} the evaporating temperature [K], T_{out_evap} [K], the evaporator outlet temperature and Q_{cond} the heating capacity [W].

The water mass flow rate supplied at 60°C (SHW production) is calculated from heat transfer balance according to Eq. 10.

$$m_{demand} = \frac{Q_{cond}}{cp_w (T_{out\_cond} - T_{in\_cond})} \quad (10)$$

The cooling capacity is obtained according Eq. 11:

$$Q_{evap} = Q_{cond} \frac{COP_{hp} - 1}{COP_{hp}} \quad (11)$$

Where Q_{cond} is calculated in Eq.9 and the COP_{hp} from Eq.7.

The compressor capacity is, directly related to the heating capacity and the coefficient of performance according to Eq. 12.

$$W_c = \frac{Q_{cond}}{COP_{hp}} \quad (12)$$

The evaporator outlet water temperature is calculated using Eq.13.

$$Q_{evap} = \dot{m}_w \cdot cp_w \cdot (T_{in\_evap} - T_{out\_evap}) \quad (13)$$

The water pressure drop in the evaporator and the condenser has been calculated based on correlations obtained from experimental results.

The evaporator water pressure drop correlation is shown in the Eq. 14 and Eq. 15

$$DP_{evap} = 2 \cdot 10^{-6} \cdot m_w^2 + 4.1 \cdot 10^{-3} \cdot m_w + 19.962 \quad (14)$$

$$DP_{cond} = 1 \cdot 10^{-5} \cdot m_{demand}^2 + 2.9 \cdot 10^{-3} \cdot m_{demand} + 32.149 \quad (15)$$

Finally, the whole system (Fig. 2) has been defined as a function of COP and the heating capacity by coupling both, the heat exchanger and heat pump. These variables are defined as:

-COP:

The auxiliary pump consumption due to the water drop pressures (for both mass flows in the heat exchanger, the evaporator and the condenser) is calculated based on Eq. 16 according to the European standard 14511-3.

$$Power\_pump = \sum \frac{m_k \cdot DP_i}{\eta_{pump} \cdot \rho_w} \quad (16)$$

Where i =[pump_cond, pump_evap, pump_demand, pump_water], $\rho_w = 1000 kgm^{-3}$ the water density , $\eta_{pump} = 0.3$ the pump efficiency and $k = [demand, water]$ respectively.

Therefore, the COP of the HPR system is expressed in Eq.17.

$$COP_{total} = \frac{Q_{heat} + Q_{cond} + P_{pump\_cond}}{W_c + P_{pump\_cond} + P_{pump\_evap} + P_{pump\_demand} + P_{pump\_water}} \quad (17)$$

-**Total Heating Capacit**y:

The total heating capacity supplied by the HPR system is given by Eq.18

$$Q_{HPR} = Q_{heat} + Q_{cond} + DP_{pump\_cond} \quad (18)$$

Thus, the equivalent capacity supplied by the previous gas boiler -the capacity substituted by the heat pump- is calculated according to the European standard 14511-3 expressed in Eq.19

$$Q_f = \frac{Q_{cond} + Q_{heat} + P_{pump\_cond}}{\eta_{cald}} \tag{19}$$

Where $\eta_{cald} = 0.95$ is the considered boiler efficiency.

5.3.2.2. Economic problem

In order to evaluate the economic benefit, the approach followed in [28] has been used as a reference .

The annual benefit is calculated by the difference between saving and cost according to Eq. 20_considering the annual Saving and the equivalent annual Cost.

$$Benefit = Saving - Cost \tag{20}$$

The cost of an inversion can be divided into three different categories: initial cost, annual cost and operating cost.

Initial cost: includes the investment cost. In the present study, this cost is the heat pump price (function of its size) and the heat exchanger cost (function of the number of plates). Notice that the gas-boiler investment cost will not be considered since the assumption is that there is already gas-boilers operating to warm up the sanitary water and the study only considers the interest of substituting this production by recovering wasted heat through a heat pump.

To calculate the yearly benefit, the equivalent annual cost must be calculated. This term can be understood as if the capital would come from a bank loan under an interest rate, i, to be paid off (recovered) in n annual payments (years). This is the term considered in “Cost” within the Eq.20.

Annual cost: includes expenses derived from taxes and maintenance. In this work, the same tax rate will be applied annually for the whole scope as well as

a fix an annual maintenance cost applies to the heat pump, boiler and the heat exchanger, respectively.

Operating cost: costs derived from the use of the technology. The electricity price in the case of the heat pump and the Natural Gas price in the gas boiler. These prices are based on the tariffs from the company called "Gas Natural Fenosa" at date of 07/06/2016 [83].

Electric price

The price of the chosen Tariff 3.0A which includes an installed power greater than 15kW and a voltage <1kV with 3-periods distinction is expressed in Table .

Table 1: Electric tariff

Period	c€/kWh	%of time/day
1	15.5774	42
2	13.0775	33
3	9.5653	25

Another decisive parameter is the time, t, in which the system has waste heat available and when the system is running. The study has been done assuming it equal to 8.760h, considering that the wastewater mass flow rate is constant and available during all the hours of the year. The installation is running 24h every day. Hence, a weighted average price of the electricity is considered equals to $C_{elec\_energ} = 0.13249 eurkWh^{-1}$.

Natural gas price.

The price of the chosen Tariff 3.4. which includes yearly consumption higher than 100MWh is $C_{\_fuel} = 0.04239 eurkWh^{-1}$.

Finally, the term "Saving" includes the annual saving due to the sanitary water production using the heat pump system instead of the gas boiler. It is characterized by the difference between the operating cost of the gas-boiler and of the heat pump system. That is, the cost of the SHW production using a gas boiler for the considered size (natural gas cost and maintenance), the cost

of the same production using a heat pump (electric cost and maintenance) and the maintenance cost of the heat exchanger according to Eq. 21.

$$Saving = C_{y\_op\_bo} - C_{y\_op\_HP} - C_{y\_op\_heat} \tag{21}$$

5.3.2.1. System maximization equation

Once the installation has been characterized, the model optimizes the size of the components based on the maximization of the term "Benefit" presented in the economic part of the modeling in Eq. 20 where the term "Saving" considers the operating costs and the term "Cost" the equivalent annual cost due to the heat pump and the heat exchanger investment cost.

The size of the heat pump and the heat exchanger to obtain the maximum benefit is obtained according to Eq.22.

$$(size, Plates) = f(\max Benefit) \tag{22}$$

Finally, the payback period is calculated as in Eq.23. This term aims to give an overall view of the required number of years to pay the total investment cost (not only under an annual point of view) for the considered life-time of the system and the correspondent originated savings. Notice that this calculation does not include the actualization of the money but it is a ratio whose components have been previously actualized following the methodology stated in [26].

$$payback(years) = Investment\_\cos t / Saving \tag{23}$$

Where the term Saving is calculated from Eq.21 and the term Investment cost includes the total investment costs (including taxes).

5.5 Performed analysis

The main assumptions performed in the model are summarized in Table .

Table 2: Constant parameters in the present work

Wastewater temperature	20°C
Fresh/tap water temperature	10°C
Sanitary hot water demand temperature	60°C
Annual interest rate	3%
Number of plates	10 ≤ Plates ≤ 140
Maintenance gas boiler cost	100 €/year
Maint. Heat pump + heat exchanger cost	150 €/year

The study begins with the analysis of a reference heat available to recover which is calculated according to Eq. 24.

$$Q_{ref} = \dot{m}_w \cdot cp_w \cdot (T_{grey} - T_{out\_evap}) \quad (24)$$

Where $T_{grey} = 20^{o}C$ and $T_{out\_evap} = 0^{o}C$ (assumed to be the minimum possible temperature at the outlet of the evaporator in order to avoid the water freezing).

Afterwards, a parametric study including values of heat recovered from 5% to 85% of the heat reference has been done. Finally, the sizing of the system is defined by the percentage of heat recovered that leads to the maximum benefit. For that percentage, the size of the components (condenser and heat exchanger) is obtained through the sequence stated in Figure 2.

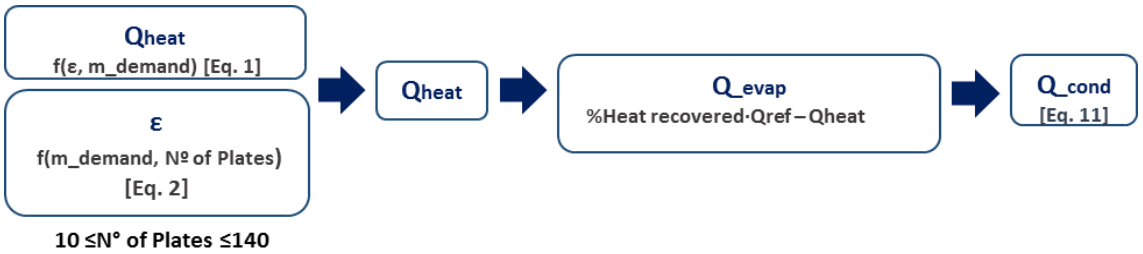

Figure 2: Followed sequence in order to size the system (heat exchanger and heat pump)

In order to dimensionless the problem, the ratio Ƴ=Benefit [eur]/Qreference [kW] has been used in the analysis.

The work is based on a "base case" and its completed with a sensitivity study varying some of the assumptions in order to evaluate different scenarios. The following paragraphs describe the sensitivity cases and the collection of all of them, including the base case, are summarized in Table 4.

- **SENSITIVITY ON THE RUNNING HOURS**

The different set of variations are the running hours. The Base Case assumes that the installation has a wastewater mass flow of 7000kgs^{-1} at 20°C and a sanitary water consumption greater than the produced by the heat pump during all the hours within a year (24h/day). The second case considers the installation to be working only 12h/day, which is 4380h/year. The third case is based on 8h/day working pattern, 2920h/years and the forth case considers the operation of the installation just 4h/day, a total of 1460h/year.

This sensitivity has been kept for the other parameters variations.

- **SENSITIVITY ON THE NUMBER OF PAY-OFF YEARS**

The base case study has evaluated the results for 15 years of investment or heat pump life-time since any value is expected afterwards. This parameter conditions the final decision. Therefore, a heat pump life-time of 10 years has also been analyzed.

- **SENSITIVITY ON THE ENERGY PRICES**

The profitability and attractiveness of this investment strongly depend on the energy prices. In the base case, the current electric and gas prices have been considered. However, the evaluation of the maximum benefit with higher electricity prices and lower gas prices is interesting.

Electric price variation: the number "1" means the value considered in the base case. An increase of the tariff price equals to the current peak price has been considered. This is, an increase of 14%.

Natural Gas price variation: the number "1" means the value considered in the base case. A decrease of the tariff price equals to 4% has been considered. This value is based on the IDAE statistics trend for the past 4 years[84]. In addition, a decrease on the price equals to 14% in order to compare with the electric price variation has been considered.

The sensitivity studies in this section are based on applying a pessimist view regarding to the attractiveness of the heat pump investment. Therefore, only an increase of the electric tariffs and a decrease on the gas prices has been done.

- **SENSITIVITY ON THE INVESTMENT COST CONSIDERING DIFFERENT RUNNING HOURS**

Finally, the last variable estimated in the study has been the cost of the heat pump and the heat exchanger. The values in the base case are based on a current manufacturer catalogue according to Eq. 26 and 27 named as "1" in the table). The sensitivity is considered as an increase of the 50% in the investment cost (cases 21-24) and a decrease of 50% (cases 25-28).

- **SENSITIVITY ON THE AVAILABLE SEWAGE WATER MASS FLOW**

In the base case, a constant total sewage water mass flow rate of 7000kg/h has been considered through the considered number of operating hours. Different water mass flow rates available would lead to different final benefits but similar sizes at the maximum benefit. In order to demonstrate this approach, the analysis of the system with a sewage water mass flow rate of 14000kg/h and 3500kg/h has been included within this work.

5.6 Results and discussion

5.6.1 Study of a heat pump vs system heat exchanger-heat pump

First, an evaluation of the ratio ʒ for the HPA considering the nominal heating capacity and the base case assumptions has been done. The first column of Table 3 collects the results of the maximum benefit case.

Second, the evaluation of the HPR has been performed. Considering the same heat pump size used in the previous case, the evaluation of the profitability by the addition of a heat exchanger based on its size has been performed. That is, the optimization of its area in order to maximize the benefit. The second column of Table 3 contains the results of this case.

Figura 3a represents the evolution of the COP_{hp} and the COP_total with the increase of the heat exchanger area (by means of the increase of the number of plates) adapting to the maximum possible subcooling for every condition. As it can be seen, the COP_{hp} decreases with the increase of the heat exchanger size. The bigger the heat exchange is, the smaller the capacity of the heat pump is.

Figure 3b shows the annual Benefit, the Cost and the Saving according to Eq. 22 and 23 versus the increase of the heat exchanger area. The grey line represents the benefit of the case considering only the heat pump (HPA).

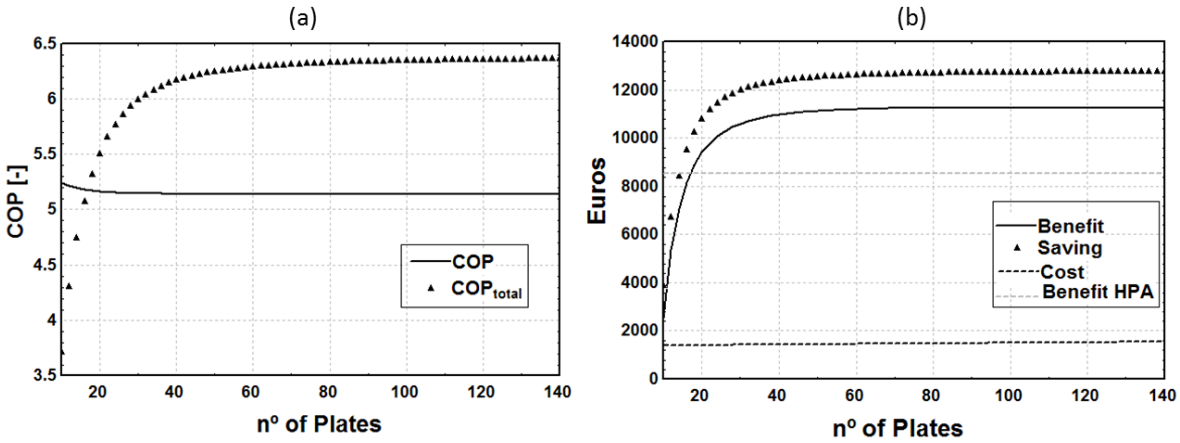

Figure 3: (a) Variation of the COP_{hp} (HPA) and the COP_total (HPR) with the n° of plates of the heat exchanger (b) Variation of the Benefit, Saving and Cost of the system with the n° of plates of the heat exchanger

From (a) and (b) can be inferred that COP_total and the Benefit increases significantly until the effectivity of the heat exchanger becomes almost one (around 80 plates). In this case, the maximum Benefit occurs when using a heat exchanger of 100 plates and it equals to 11,266€ (annually).

The influence of the number of plates in the investment cost is low because it is divided by the number of operation years considered (15years). As in Figure 3 this influence cannot be clearly appreciated due to the scale, Figure 4 represents only the term "Cost" with the addition of number of plates and it increases from 1400eur/years to 1550 eur/years. This term is an annual term that considers the investment cost, the maintenance cost and the operating cost.

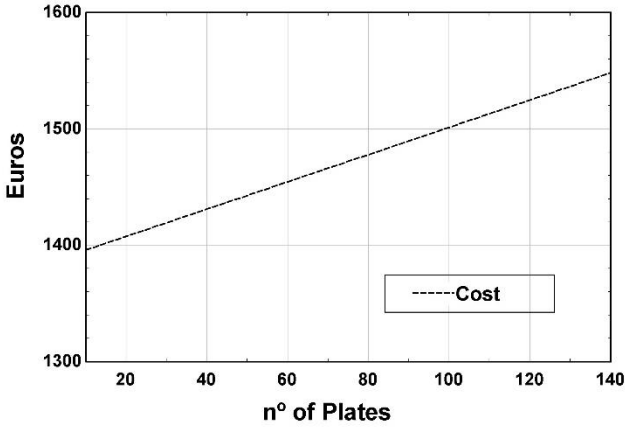

Figure 4: Cost evolution for a heat pump size of one and the variation of the number of plates of the recovery heat exchanger.

Table 3 collects the main thermos and economic parameters for the optimal case.

Table 3. Output of the system (heat pump + heat exchanger)

	Heat pump	Heat pump + Heat exchanger
Q ref (kW)	162.556	162.556
% of heat recovered	23.45 %	27.53 %
THERMODYNAMIC VARIABLES		
Tin_cond (°C)	10	19.81
Tout_cond (°C)	60	60
Tin_evap (°C)	20	18.72
Tout_evap (°C)	15.31	14.49
Q_cond (kW)	42.63	42.63
Wc (kW)	8.2	8.2
Q_heat (kW)	-	10.41
COPhp	5.66	5.142
COP_total	5.649	6.356
mw (kg/h)	7000	7000
m_demand (kgh^{-1})	798	913.68
ECONOMIC RESULTS		
Annual equivalent cost (€)	1351	1501
Annual saving (€)	9973	12767
Annual benefit (€)	8622	11266
Y (€/kW)	53.04	69.3
Payback (years)	1.62	1.37

From Table 3 can be said that the substitution of the SHW production from a gas boiler to a heat pump is very profitable. The annual benefit is 8622€ with a COP_total, of 5.649. This means that, asking for a bank loan with 3% of interest the investment cost on a heat pump, the payoff to the bank would be 1351€ annually during 15 years while you will be saving 9973€, leading to a benefit of 8622€ during the considered life-time.

The investment on the system composed by the heat pump and the heat exchanger (HPR) brings considerably more profitability than the heat pump itself. Specifically, the benefit for the best case is 23.4% higher. The benefit of the HPR is higher than the benefit of the HPA when the number of plates is greater than 18, even if it is not the optimum.

Based on these results, the HPR has demonstrated a greater performance than the HPA. Therefore, now the size of the heat pump as well as the recovery heat exchanger are studied in order to be optimized.

5.6.2 Study of the optimal size of HPR to maximize the Benefit.

The analyisis of each case consists of:

- Evaluation of the COP_total
- Estimation of the Benefit
- Optimal size that maximizes the benefit

5.5.2.1. Base Case

Figure 5a represents the COP_hp as a function of the percentage of energy recovered and the number of plates. Grey color corresponds to the highest value and it is found with low values of number of plates in the heat exchanger and relatively low percentages of heat recovered. This result can be related to the size of the heat pump. Moreover, the variation has more influence in the COP than in the number of plates. The maximum COP_hp (5.3) is found for values of heat recovered around 15% which means heating capacities around 25kW and only 20 plates considering HPR. Nevertheless, it is worthy to notice that the maximum COP_hp is 5.767 and it occurs for the HPA of the same size as the considered in the system.

Figure 5b represents the COP_total as a function of the percentage of energy recovered and the number of plates. Grey color corresponds to the highest value. The COP_total increases as the percentage of heat recovered decreases and with the addition of plates (higher UA values). It should be noticed that the

optimal number of plates depends on the heat exchanger effectivity and hence, the trend is not linear. The maximum values correspond to large heat exchangers and relatively small heat pump sizes. Thermodynamically, this can be explained as the COP_total takes into account both components of the system, the heat exchanger (which exchanged heat is given "for free") and the heat pump. The maximum COP_total is around 6.51 and occurs for the maximum heat exchanger size and the most efficient (in terms of COP) heat pump which, according to figure 5a, corresponds to a heating capacity around 25kW.

Figure 5c represents the ratio Y[€/kW] = Benefit/Qref as a function of the percentage of heat recovered and the number of plates. Grey color corresponds to the highest benefit. The maximum values of Y occur when the percentage of heat recovered is located around 50% and increases with the addition of plates to the heat exchanger until around 80 number of plates from when the ratio becomes very similar according to the effectivity of the heat exchanger curve. It is noticeable that maximum benefit ratio (Y >100€/kW) does not correspond to the maximum COP_ total, this fact means that other considerations like the investment cost and the energy produced with it, among others, must be considered in order to determinate the most profitable solution. In this case, the increase of the HPR capacity leads to higher operational savings despite of the increment of the investment.

From figure 5c it can be extracted that values of 103€/year per kW of heat recovered by the substitution of a gas boiler by a heat pump of 82.45kW and a heat exchanger of 19.6kW can be obtained.

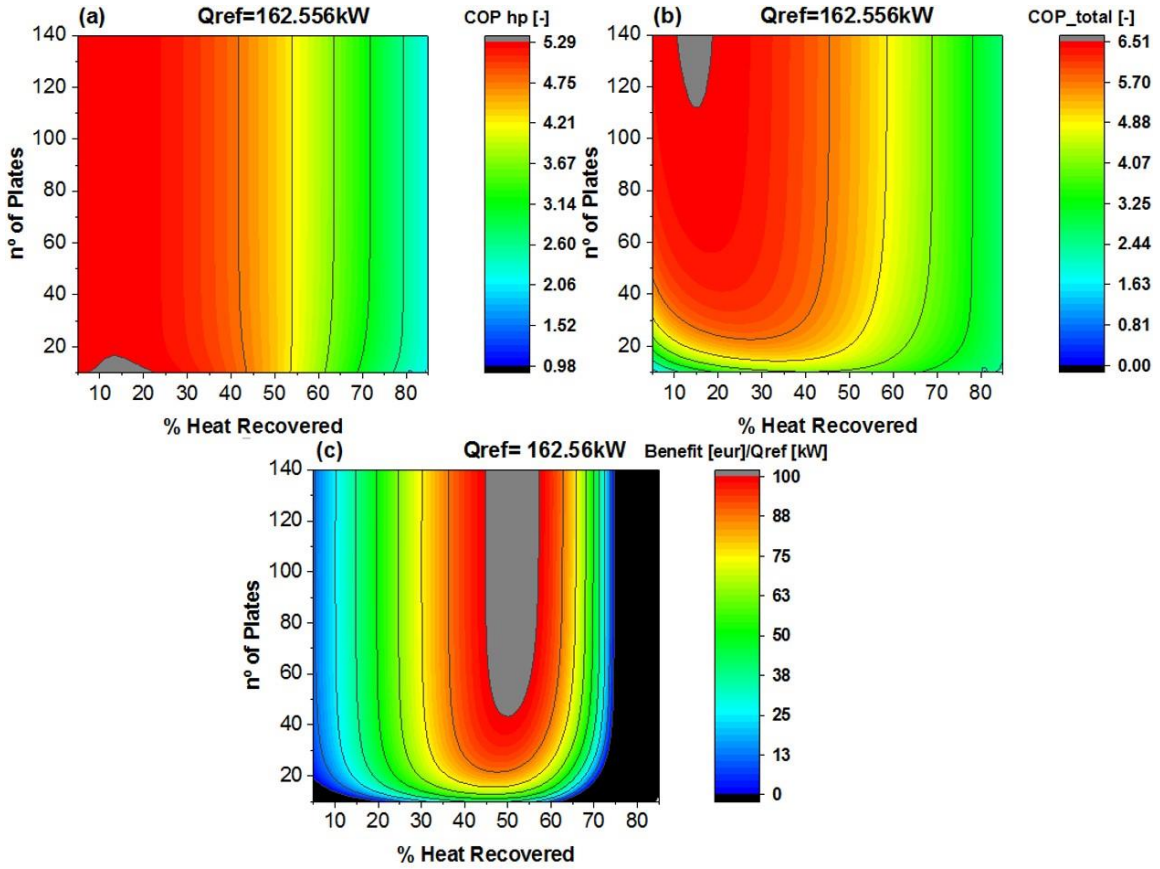

Figure 5: (a) COP variation function of the percentage of heat recovered and number of plates. Base case. (b) COP_total variation function of the percentage of heat recovered and number of plates. Base case. (c). Y=Benefit/Qref variation function of the percentage of heat recovered and number of plates. Base case.

Figure 6a presents the variation of the ratio annual investment cost of the HPR/Qref as a function of the heat pump and the percentage of heat recovered. The term annual investment cost is the total investment cost in yearly values including the annual interest rate. As it can be observed, the investment cost increases with the percentage of heat recovered (bigger HPA) and with the number of plates. The heat exchanger investment cost has major contribution as the heat pump is smaller. The total investment cost increases with the number of plates proportionally much more for values of heating recovered lower than 40% than for higher recovered values where the increase of the size in the heat exchanger becomes much less important in the total investment cost.

Figure 6b presents the variation of the ratio saving/Qref as a function of the heat pump and the percentage of heat recovered. The saving includes the operating costs of both, the HPR and the gas boiler. Similar trend as in Figure 5c for the benefit can be observed. As the percentage of heat recovered increases the saving

term rises until a maximum which corresponds to a values around 55% of heat recovered and saving rate of more than 125€/kW recovered. With the increase of the HPR size, the COP_total decreases (Figure 5b) and the consumption of the compressor with the auxiliaries increases, reaching values of the saving that can be even negative.

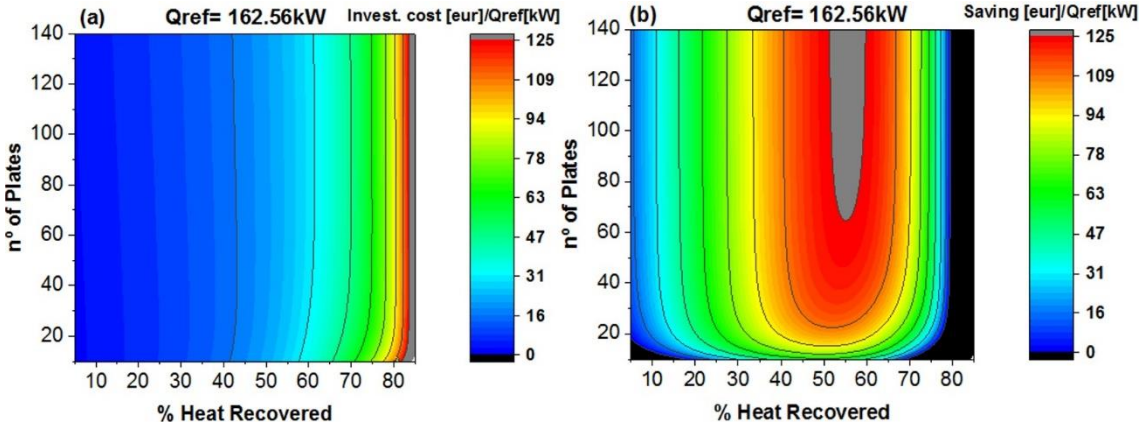

Figure 6: (a)Annual investment cost of the system/Qref function of the percentage of heat recovered and the number of plates for the base case. (b) Saving/Qref of the system function of the percentage of heat recovered and the number of plates for the base case.

Figure 7 represents the variation of the ratio heating capacity/Qref with the number of plates and the percentage of heat recovered. This figure allows to have an idea about the sizes of the heat pump for the base case. As it can be seen in the figure, the size of the HPA increases as the percentage of heat recovered increases. Regarding to the number of plates, the size of the HPA depends on the effectivity of the heat exchanger curve: being needed for the same percentage of heat recovered a larger HPA when the number of plates is low (small HE) and remaining practically constant once the effectivity achieves values close to one (from 80 plates). This effect is more important as the size of the HPA increases.

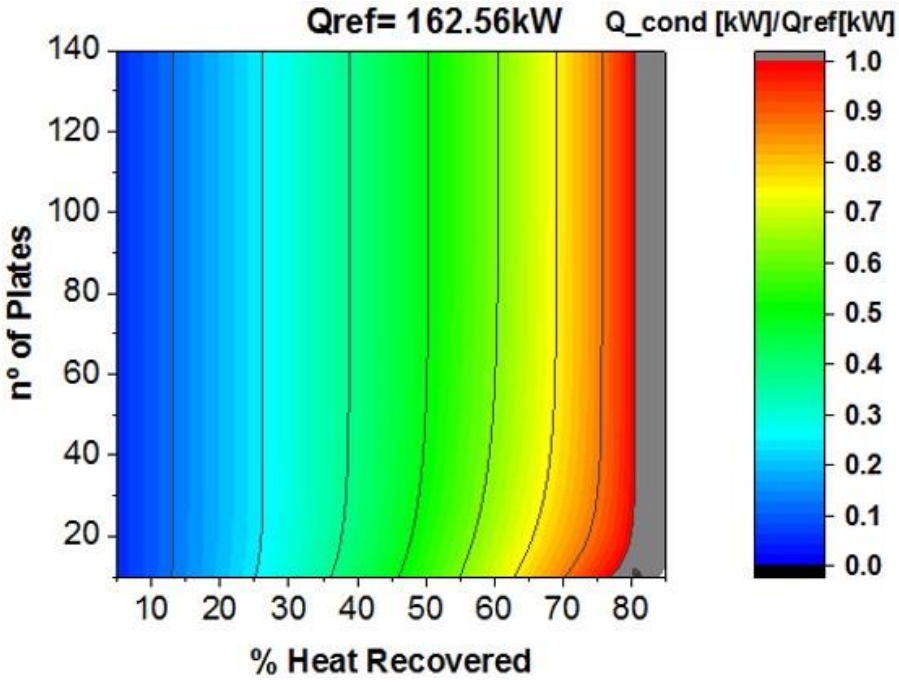

Figure 7: Heat pump size/Qref function of the percentage of heat

Cases 1-4

These cases represent the study of the operating hours influence on the final benefit. The reference heat for the cases 1-27 is 162.56kW which corresponds to an available water mass flow rate from the sewage of 7000kg/h. ***Figure*** 8 shows the variation of the ratio Y[€/kW] = Benefit/Qref with the percentage of heat recovered and number of plates of the heat exchanger for different available operating hours. Grey color corresponds to the highest benefit and black color to negative values of the benefit.

According to the figure, as the operating time is larger, the optimal size of the heat exchanger and the heat pump size increase and the annual benefit is higher. Nevertheless, in terms of percentage of heat recovered, values around 50% lead to the best solution from a certain number of operating hours. The annual investment cost becomes more important as the number operating hour decreases. The same investment size could lead to a benefit (>16000eur) if the installation is used 24h/days (51% of heat recovered) or could lead to a not profitable investment (negative benefit) for example if the installation is used only 4h/day. Therefore, the effect of the operating hours is determinant. Thus, a critical variable when trying to find the optimal size of these systems is the availability and the use that the system will have.

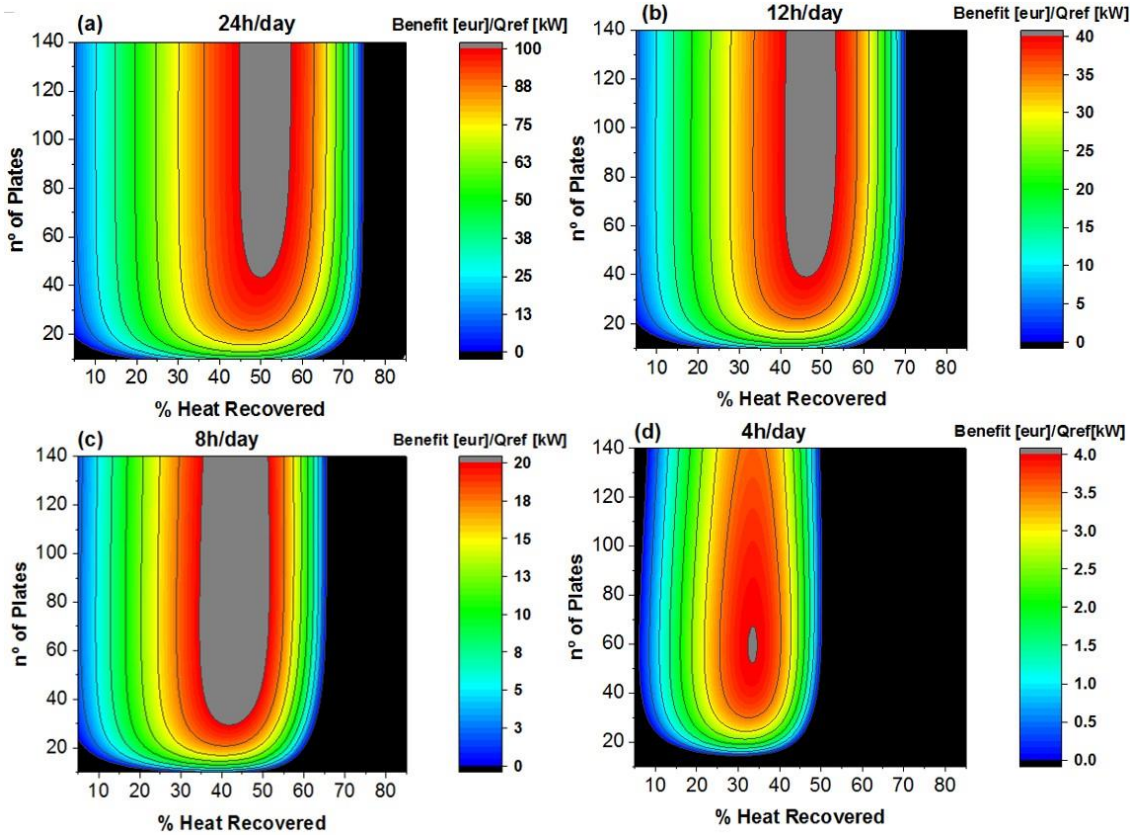

Figure 8: Y=Benefit/Qref variation function of the percentage of heat recovered and number of plates. (a) Base case (24h/day); (b) 12h/day; (c) 8h/day; (d) 4h/day. The colors of the scale have not been maintained across the graphs due to scale differences.

It should be noticed that the COP_total increases with the diminution of the HPA size. However, based on the electricity and gas price assumptions, the influence of the production volume on the annual benefit becomes more important as the size increases. While the benefit from using the installation 24h/day to the lowest use (4h/day) is reduced around 96%, the SHW production capacity reduces 37%.

Table 5 collects the main thermodynamic, economic and the optimal sizes of the maximum benefit for all the cases.

5.5.2.2. Cases 5-28

The rest of the sensitivity study is presented only for the optimal solution in order to be able to have an overall view of the results summarized in Table 5.

Figure 9 represents the maximum ratio Y=Benefit/Qref in monetary terms for each case. The horizontal lines are the maximum benefits for the operating hours considered in the base case.

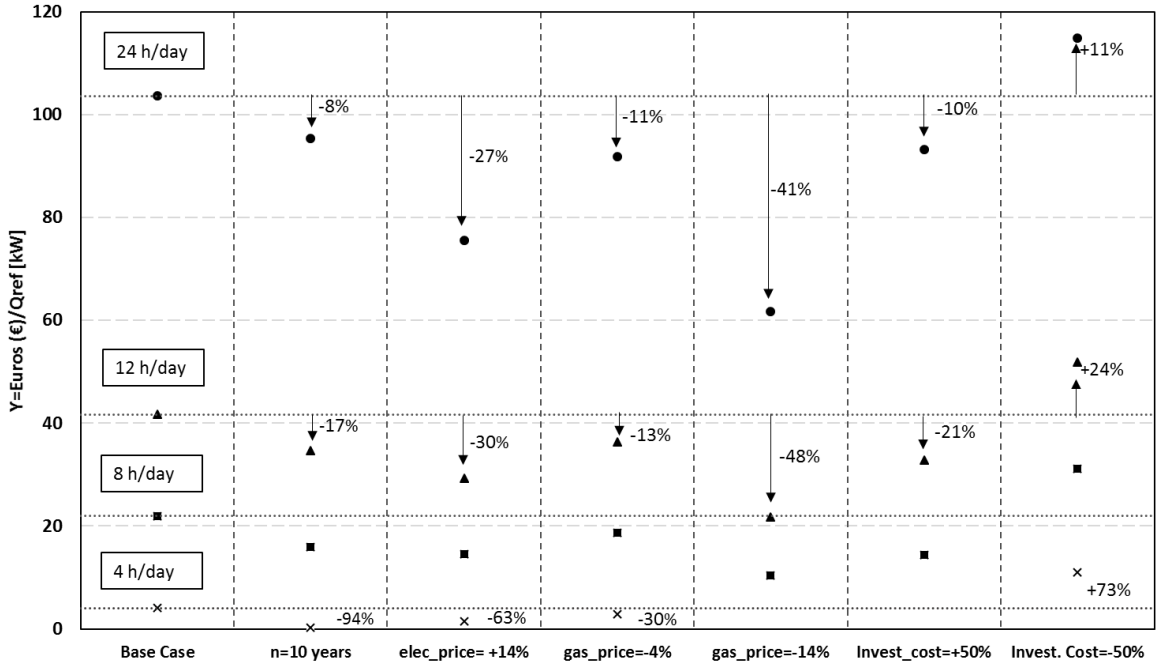

Figure 9: Maximum ratio Benefit/Qref of any studied case based on the number of operating hours.

The 14% decrease on the gas price is the most influent parameter followed by the increase on the electricity price as well as the decrease of 4% on the gas price, except for low operation hours represented by last series (4h/day). Therefore, in general, the most influent effect on the maximum benefit is the electricity/gas price. Their volatility as well as the dependency on external factors make the investment decision riskier. However, from a determined number of operating hours, all the cases experiment high benefits by the substitution of the SHW production from a gas boiler to a heat pump.

Regarding to the investment cost influence and considering that the cost of the heat pump and the heat exchanger were conservative in the base case, even increasing it by 50%, the investment would still be profitable.

According to the followed approach, the investment cost is divided by "annual equivalent" quantities as if a loan were asked to the bank. The time in which this

"loan" must be returned as well as the interest rate of it is also an important variable. In this study, a 3% of interest rate has been considered (pessimistic rate with the current bank situation) a 15 years' period (also pessimistic due to the heat pump lifetime is expected to be higher than 15). Nevertheless, even if the study is made for 10 years of lifetime, the investment reminds highly beneficial.

Figure 10a represents the optimal heat pump size (heating capacity kW) for each case and operating time.

The more operating hours, the higher savings and benefits. Thus, bigger sizes of the heat pump (it is shown by the upper dots).

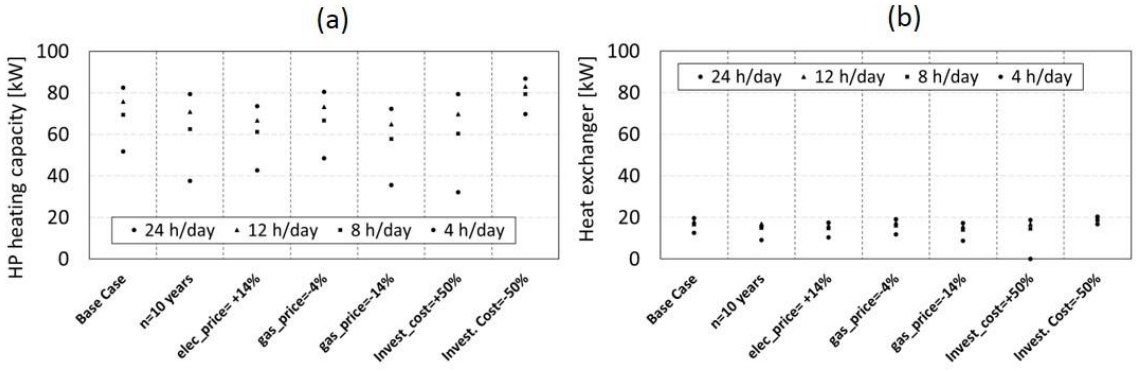

Figure 10: (a) Optimal heat pump heating capacity of every considered case (b) Optimal heat exchanger capacity for every considered case.

The optimal size of the heat pump strongly depends on external variables like the grey water temperature, the gas and electric price, the investment cost and the like. Nevertheless, if the operating hours is greater than 4.1h/day, the substitution of a gas boiler by a heat pump is profitable even under a wide range of conservative conditions according to the results of this study.

Figure 10b represents the optimal number of plates of the recovery heat exchanger for each case. The optimal number of plates of the heat exchanger is mainly influenced by the investment cost and the use of the installation. In any case, the maximum benefit occurs with a medium/high number of plates which result for the considered heat exchanger of capacities around 18kW for most of the considered cases.

It should be noticed that the optimum recovery heat exchanger depends mainly on the operation hours. Hence, defined this parameter, a good estimation of the optimal size can be done.

Finally, Figure 11 represents the payback period of the optimal investment for the considered life-time (15 years except for the case that is 10 years).

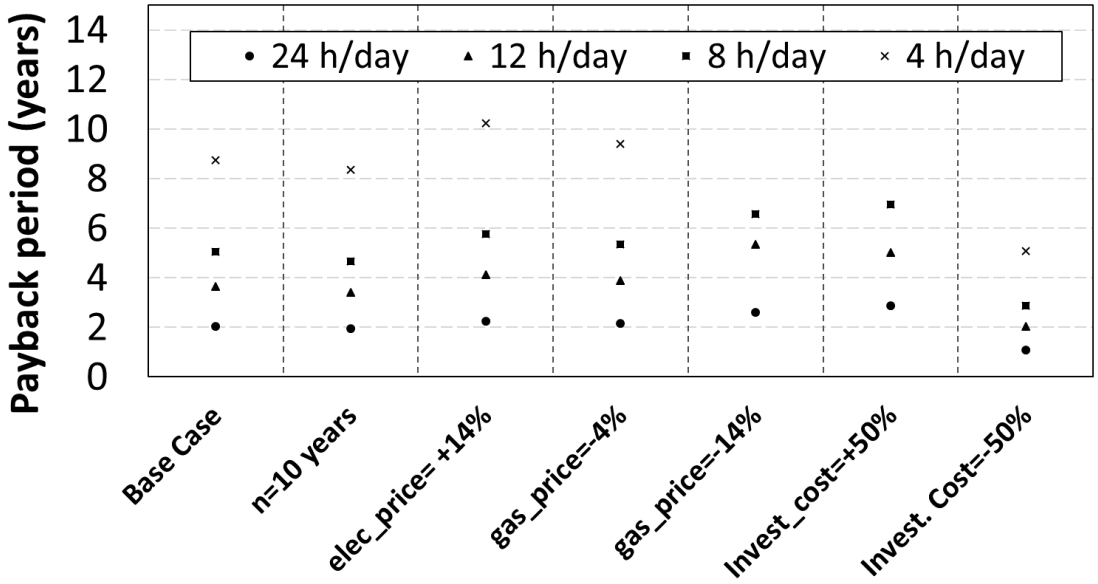

Figure 11: Payback time for every considered case

As it can be seen from the figure, the payback period depends on the number of life-time considered for the system and indirectly on the number of operating hours. However, the frame of the payback time is narrow (from a considerable number of operating hours, the expected payback time varies from 2-6 years).

5.5.2.3. Cases 29-30

The last sensitivity case is the study of the influence of the available water mass flow rate (sewage mass flow rate) in the most profitable solution. Two more available mass flow rates have been considered within this cases: half of the base case water mass flow rate (3500kg/h) and double (14000kg/h).

Figure 12 represents the rate Benefit/Qref obtained for (a) 3500kg/h and (b) 14000kg/h of available sewage mass flow rate function of the percentage of heat recovered and the number of plates.

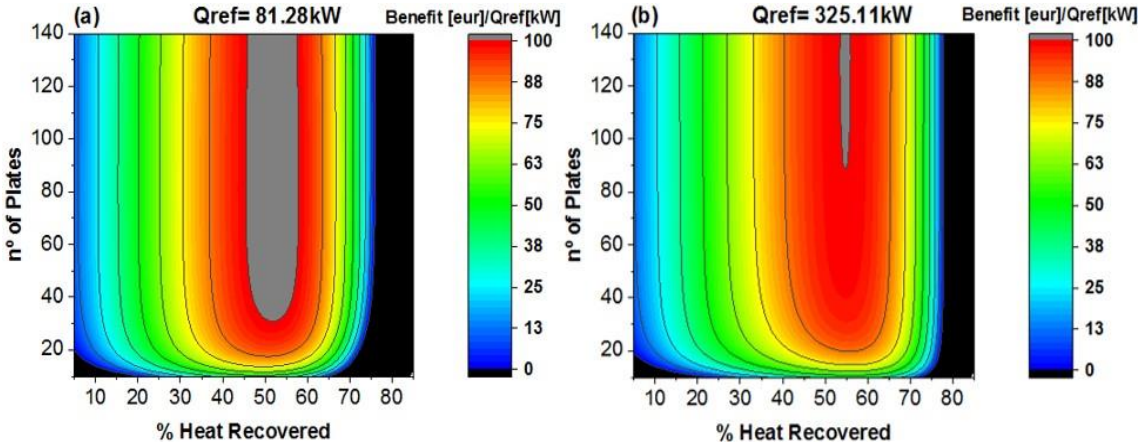

Figure 12: Ratio Benefit/Qref variation function of the percentage of heat recovered and number of plates. (a)mw= 3500kg/h,(b)mw=14000kg/h.

As it can be observed from Figure 12, the maximum benefit states around the same percentage of heat recovered (50-55%) in both cases according to what happens also for the base case (8760kg/h) in Figure 5c. Therefore, the heat available influences the final annual benefit obtained but not the ratio (which is very similar in the three cases) and not the maximum value (which is located for very similar percentages of heat recovered). The number of plates that lead to that maximum benefit states around 80 for the three cases. In addition, the variation of the benefit across the number of plates for the respective percentage of heat recovered has a very flat slope, not penalizing very much in the final benefit. This can be seen for the base case in Figure 13.

Figure 13 represents the variation of the benefit with the number of plates for the base case and the percentage of heat recovered of 51.06% which corresponds to the highest benefit.

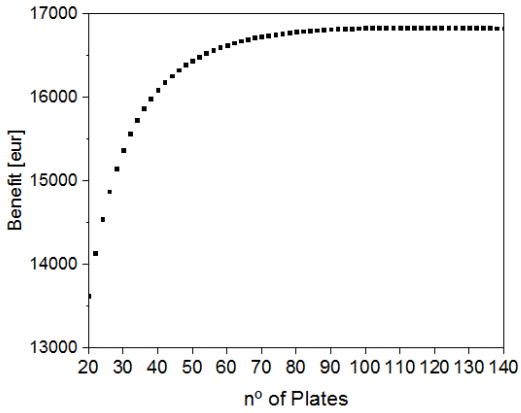

Figure 13: Benefit variation with the number of plates for the base case and 51.06% of recovered heat.

5.7 Conclusions

In this work, an analysis of the potential profitability derived from the substitution of the SHW production from a conventional technology (gas boiler) to a new heat pump booster to recover heat from a low temperature water source has been done.

This analysis consists of an optimization of the heat pump size to maximize the benefit.

The main conclusions of this work are:

- The introduction of a recovery heat exchanger is always positive.
- As a consequence of the number of external variables required in order to find the optimal solution of this kind of system, a sensitive analysis of the influence of the different variables involved in the process has been done. From that, it has been determined that as far as the number of operating hours are greater than 1500 within a year, the investment reminds clearly profitable, even under the hypothesis of considering a 14% variation in gas/electricity prices, 50% of variation in the investment cost and a 33% of the reduction in the heat system lifetime. Therefore, the heat pump demonstrates that is a very interesting and cost effective technology for this type of applications.
- The size that corresponds to the maximum benefit of the recovery heat exchanger, the heat pump as well as the payback period depends mainly on the operating hours.
- The maximum benefit of the system strongly depends on the properly sizing of it. It is worth it to notice that the maximum benefit does not take place for a heat pump size with the highest benefit but to a size that optimizes the whole system (the heat pump and the heat exchanger) for a given external conditions.
- Results for the base case show that the substitution of the gas boiler by the heat pump can lead to annual benefits of around 103€/kW of heat recovered and this ratio remains very similar with the variation of the available water mass flow rate from the sewage to recover.

Finally, from all this work it has been proved that the system composed of a heat pump booster with a recovery heat exchanger has great potential to substitute conventional technologies as for instance boilers, to produce SHW. The accurate sizing of the system is crucial to obtain the maximum benefit.

5.8 Acknowledgements

Part of the work presented was carried by Estefanía Hervás Blasco with the financial support of a PhD scholarship from the Spanish government SFPI1500X074478XV0. Part of the work presented was carried by Miquel Pitarch-Mocholí with the financial support of a PhD scholarship from the Universitat Politècnica de València. The authors would like also to acknowledge the Spanish 'MINISTERIO DE ECONOMIA Y COMPETITIVIDAD', through the project ref-ENE2014-53311-C2-1-P-AR "Aprovechamiento del calor residual a baja temperatura mediante bombas de calor para la produccion de agua caliente" for the given support.

5.9 References

[1] DIRECTIVE 2009/28/EC OF THE EUROPEAN PARLIAMENT AND OF THE COUNCIL of 23 April 2009 on the promotion of the use of energy from renewable sources and amending and subsequently repealing Directives 2001/77/EC and 2003/30/EC n.d.

[2] Alnahhal S, Spremberg E. Contribution to Exemplary In-House Wastewater Heat Recovery in Berlin , 2016;40:35–40. doi:10.1016/j.procir.2016.01.046.

[3] Kardaš D, Gvero P, Katalini M, Kotur M. Use of Sewage Water as a Heat Source for Sanitary Water Heating in Student Dormitory „ Nikola Tesla " Banja Luka n.d.:1–4.

[4] Persson U. District heating in future Europe: Modelling expansion potentials and mapping heat synergy regions. 2015.

[5] AGENCIA PROVINCIAL DE LA ENERGÍA DE BURGOS. ESTUDIO ENERGÉTICO DE UN SISTEMA CON BOMBA DE CALOR GEOTÉRMICA PARA VIVIENDA UNIFAMILIAR EN BURGOS 2011:1–12.

[6] Zhen L, Lin DM, Shu HW, Jiang S, Zhu YX. District cooling and heating with seawater as heat source and sink in Dalian, China. vol. 32. 2007. doi:10.1016/j.renene.2006.12.015.

[7] New Energy and Industrial Technology Development Organization (NEDO), Japan. 2015 Next Generation Heat Pump System Research and Development 2015.

[8] Law R, Harvey A, Reay D. Opportunities for low-grade heat recovery in the UK food processing industry. Appl Therm Eng 2013;53:188–96. doi:10.1016/j.applthermaleng.2012.03.024.

[9] Miguel M (CIAT), Zamora Z. DESHUMECTACIÓN CON BOMBA DE CALOR Y RECUPERACIÓN DE CALOR EN GIMNASIOS Y PISCINAS n.d. http://www.grupociat.es/rubrique/index/spa-grupo-CIAT-referencias/3205.

[10] Hepbasli A, Biyik E, Ekren O, Gunerhan H, Araz M. A key review of wastewater source heat pump (WWSHP) systems. Energy Convers Manag 2014;88:700–22. doi:10.1016/j.enconman.2014.08.065.

[11] Meggers F, Leibundgut H. The potential of wastewater heat and exergy: Decentralized high-temperature recovery with a heat pump. Energy Build 2011;43:879–86. doi:10.1016/j.enbuild.2010.12.008.

[12] D.M. Roodman NL. A Building Revolution: How Ecology and Health Concerns are Transforming Construction. Worldwatch Pap 24 n.d.

[13] eist W (20 de 09 de 2015). PASSIPEDIA, The Passive House Resource 2015. The world?s first Passive House, Darmstadt-Kranichstein, Germany: http://passipedia.passiv.de/passipedia_en/examples/residential_buildings/single_- (accessed July 1, 2016).

[14] Keil C, Plura S, Radspieler M, Schweigler C. Application of customized absorption heat pumps for utilization of low-grade heat sources. Appl Therm Eng 2008;28:2070–6. doi:10.1016/j.applthermaleng.2008.04.012.

[15] Srikhirin P, Aphornratana S, Chungpaibulpatana S. A review of absorption refrigeration technologies. Renew Sustain Energy Rev 2001;5:343–72. doi:10.1016/S1364-0321(01)00003-X.

[16] Pulat E, Etemoglu AB, Can M. Waste-heat recovery potential in Turkish textile industry: Case study for city of Bursa. Renew Sustain Energy Rev 2009;13:663–72. doi:10.1016/j.rser.2007.10.002.

[17] Li H, Russell N, Sharifi V, Swithenbank J. Techno-economic feasibility of absorption heat pumps using wastewater as the heating source for desalination. Desalination 2011;281:118–27. doi:10.1016/j.desal.2011.07.049.

[18] Garcia NP, Vatopoulos K, Lopez AP, Thiel C. Best available technologies for the heat and cooling market in the European Union. JRC Scientif and Policy Reports. 2012:48. doi:10.2790/5813.

[19] Hepbasli A. Exergetic modeling and assessment of solar assisted domestic hot water tank integrated ground-source heat pump systems for residences. Energy Build 2007;39:1211–7. doi:10.1016/j.enbuild.2007.01.007.

[20] Nekså P. CO2 heat pump systems. Int J Refrig 2002;25:421–7. doi:10.1016/S0140-7007(01)00033-0.

[21] Fernandez N, Hwang Y, Radermacher R. Comparison of CO 2 heat pump

water heater performance with baseline cycle and two high COP cycles Comparaison de la performance d'un systè me de chauffage d'eau à pompe à chaleur au CO 2 et celle d'un cycle de base et celles de deux cycles au COP é levé. Int J Refrig 2009;33:635–44. doi:10.1016/j.ijrefrig.2009.12.008.

[22] Miquel PITARCH, Emilio NAVARRO-PERIS, José GONZÁLVEZ-MACIÁ JMC. Evaluation of different heat pump systems for sanitary hot water production using natural refrigerants. Appl Energy 2017 (In Press).

[23] Tammaro M, Montagud C, Corberán JM, Mauro AW, Mastrullo R. A propane water-to-water heat pump booster for sanitary hot water production: Seasonal performance analysis of a new solution optimizing COP. Int J Refrig 2015;51:59–69. doi:10.1016/j.ijrefrig.2014.12.008.

[24] McLinden MO, Kazakov AF, Steven Brown J, Domanski PA. A thermodynamic analysis of refrigerants: Possibilities and tradeoffs for Low-GWP refrigerants. Int J Refrig 2014;38:80–92. doi:10.1016/j.ijrefrig.2013.09.032.

[25] SWEP. SWEP. (s.f.). SSP G7 version 7.0.3.53. n.d.

[26] Mills AF. Heat Transfer. Concord, MA 01742: Richard D. Irwnin Inc.; n.d.

[27] gasnaturalfenosa n.d. http://www.gasnaturalfenosa.es/es/Empresas/Electricidad_o_gas/Contratar_electricidad_o_gas/Tarifa_Fija.html (accessed February 6, 2016).

[28] IDAE. Regulated tariffs in Spain, IDAE. 2016.

Chapter 6
Optimal design and operation of a central domestic hot water heat pump system for a group of dwellings employing low temperature waste heat as a source

Estefanía Hervás-Blasco[a], Emilio Navarro-Peris[a], José Miguel Corberán[a]

[a] Institut Universitari d'Investigació d'Enginyeria Energètica, Universitat Politècnica de València, Camí de Vera s/n, València, 46022, Spain

Tel: +34 963879123 enava@ter.upv.es

6.1 Abstract

In this work, a study of an energy recovery system from a low-grade temperature source based on heat pumps for domestic hot water is done. The main components of the system are a pre-heating heat exchanger, an optimized heat pump for domestic hot water production, and a variable-volume storage tank. A model has been developed in TRNSYS to analyse the best configuration and control strategy of the system in order to satisfy the profile demands of 10, 20, and 30 multifamily houses, which are considered as a representative target market for this type of application. From this analysis, the influence of the design/sizing parameters on the system CO2 emissions has been obtained and a design criterium for their minimization has been supplied. Finally, a sensitivity analysis based on different net and heat source temperatures has been done in order to estimate the generalizability of the proposed solution. The obtained results show that this kind of system, with the proper design, sizing, and operation, offers potential CO2 emissions reductions by a factor of almost five compared to a conventional gas boiler system but a bad system selection could reduce this potential benefit up to 25%.

6.2 Nomenclature

20H: twenty multifamily-houses

10H: ten multifamily-houses

30H: thirty multifamily-houses

DHW: domestic hot water

Tei: water inlet temperature at the evaporator [°C]

Teo: water outley temperature at the evaporator [°C]

Tci: water inlet temperature at the condenser [°C]

Tco: water outlet temperature at the condenser [°C]

Tnet: water mains/net temperature [°C]

Tsource: water heat recovery(district heating) temperature [°C]

T_{st}: water stored temperature

Thot= water temperature at the system conditins [°C]

Tuser= water temperature supplied to the user [°C]

Tdemanded=water demand temperature [°C]

Qcond=Heat pump heating capacity [kW]

COP_{hp}: Heat pump Coefficient of Performance, [-]

COP_{sys}: System Coefficient of Performance, [-]

α: control level rate [-]

Tset= water stored control temperature

Subscripts

ST: storage tank

HP: Heat pump

SHP: Water to water high efficiency heat recovery heat pump optimized for water heating applications (up to 90 °C)

6.3 Introduction

6.3.1 Motivation

As corporate, national, and international goals move towards reducing carbon footprints and the effects of global warming, renewables and low-carbon solutions will replace current fossil fuel alternatives within the energy sector [1].

The building sector accounts for 21% of the total energy consumption, and almost 15% of that percentage is related to water heating for domestic hot water (DHW) (with a significant increase of that share being projected as room heating loads decrease) [2]. In addition, according to the European Environment Agency (EEA), the residential sector is responsible for 11.5% of total CO2 emissions. Thus, improving water heating production within this sector is becoming unavoidable for a sustainable future, overall, considering that the employment of more efficient technologies and the introduction of passive houses mean that DHW becomes the most important thermal need of a building.

Most residential water heaters are equipped with conventional boilers that use electricity or fossil fuels. Despite their simplicity and affordability, they are neither energyally nor environmentally desirable. Compared to these solutions, Heat Pumps (HPs) are seen as a potential alternative for water heating [3] as: they have demonstrated high efficiency, can operate in standalone form, avoid the need for a back-up technology and are the best solution in order to recover waste energy or use heat from a low temperature district heating network. Therefore, they will constitute in the following years a key system in order to reduce the current emissions associated to this type of application.

HPs have been widely used within many heating and cooling applications. However, most applications are characterized by low secondary fluid temperature lifts. In applications where high secondary fluid temperature lifts are required, an efficient alternative is the use of transcritical cycles capable to operate with high temperature lifts [4]-[7]. Nevertheless, these heat pumps are not so flexible and show a poor efficiency when the temperature lift is reduced. Another more “traditional” solution using subcritical systems consist of using a progressive water heating processes of the water contained in a tank [8]. This alternative has the inconvenient of not being able to produce water at the temperature required by the demand conditions directly and from the efficiency point of view is not so optimal but in the other side this kind of systems are less expensive.

Recently, researchers have been working on the optimization of subcritical HPs for that kind of applications and HPs with coefficients of performance (COPs) similar that those found with transcritical cycles at high secondary fluid temperature lift have been obtained. This is possible thanks to the applications of high (optimal) degrees of subcooling [9], [10] and the proper redesign of the HP. This kind of HP has been called a "Subcooled Heat Pump" (SHP).

In addition, DHW production have a high variability in profile demand along the day. This characteristic change significantly the sizing criteria of heat pumps for this application compared to the criteria followed for HP in heating and cooling systems where a constant demand profile is common.

In that sense, one of the most difficult tasks linked to the sizing of DHW installations is the characterization of a representative demand profile, especially within the building sector, where DHW can vary significantly from hour-to-hour and high peaks are expected not only during the day but also during different days of the week and through the year. The geographical situation, social and economic factors, type of building, and number of users, among others, are some of the factors that condition the DHW demand. The efficiency of the system is highly dependent on the DHW profile. Thus, having a representative load profile is crucial in order to achieve high user satisfaction and a proper and efficient sizing of the rest of the components. [11] reviews several approaches used in order to estimate representative DHW load profiles.

Once this representative DHW load profiles are defined, and as a consequence of their variability, one-step further deals with the integration of the HP with a water storage tank (ST). This point becomes essential in order to avoid oversizing of the system and allows the decoupling of DHW consumption from DHW production [12]. However, it will add irreversibility's to the system as the temperature water production in the heat pump must be higher in order to compensate the ST thermal losses [13], cost and control complexity.

One step further is related to the integration of the HPs within a recovery system in order to satisfy the DHW demand. In that sense, a holistic approach is essential as optimize the system performance means more than optimize its components individually. Most of the works found in the literature dealing with DHW production [14] - [20] from heat recovery uses a specific system configuration but it is difficult to find general information about the sensitivity of the obtained results to the selected configuration (size, control strategy, system topology…).

This paper analyses heat recovery systems for DHW production in the residential sector in order to supply gidelines to define the optimum system configuration and estimate which could be the penalty in the efficiency obtained from a bad design. The basic components of the system are the new designed SHP working with propane, a heat-recovery heat exchanger (HE) and a variable-volume storage tank (ST). The selection of the components has been done in order to maximize the efficiency of the application. In addition, the sizing of the components and the definition of the operating control strategy in order to minimize the global energy consumption of the system are investigated.

The results presented shows the influence of the proper sizing and the control strategy in the final system performance and they can yield valuable information for the next years, guiding the proper system design when the substitution of common DHW production technologies by HPs takes place in order to meet the requirements of new policies aimed towards a decarbonized energy sector. In this point it should be noted that the obtained differences could be higher if a conventional subcritical heat pump were used.

The main characteristics of the considered system are:

- The DHW load demand: it is based on stochastic models and has been obtained with DHWcalc software and validated with the profile obtained with SynPro [21] [22]. Different profiles considering 10, 20, and 30 multifamily houses are included. A yearly one-minute step profile is used.
- Heat Source: sufficient availability of the heat source is assumed (as it is the case in district heating or sewage water).
- Direct heat recovery system: Heat exchanger preheat initially the tap water.
- Heat pump: the SHP is able to modulate the subcooling in order to maximize the efficiency as a function of the condenser secondary fluid temperature lift. SHP have performances comparable to transcritical HPs at high condenser water temperature lift while it maintains common high performances of subcritical systems when operating under low secondary temperature lifts.
- Storage tank: variable volume ST has been employed, that is, a fully-mixed tank with all the water stored at the same temperature. This type of tank reduces the losses compared to stratified tank. One-step further deals with the integration of these SHPs within a complete system for DHW production.

6.4 Developed Model

This section describes the model developed in TRNSYS [23] in order to perform the analysis of this work. The section is divided in three parts, in the first one the description of the external model conditions is done, in the second one the type created for SHP model integrated in TRNSYS is explained and finally, the developed system model is described in detail.

6.4.1 Heat source and heat sink characterization

The study considers enough availability of the heat source. This situation could correspond to low-temperature district heating or heat recovery from sewage water. The temperature of this water service could be from 40°C in the first case up to temperatures slightly higher than the ambient like sewage water heat source. Based on that, the design temperature has been set to 20 °C that could be considered a critical temperature for these applications.

Regarding the heat sink, the DHWcalc tool [21] has been used to generate the profiles. In order to validate the generated profiles a one-minute resolution DHW load profile facilitated by the developers of the software SynPro [22] was used. This profile was based on 20 apartments with an average occupancy of 1.95 persons/house (39 people in total) and the agreement between both profiles was good. The considered annual average energy consumption is 804 kWh per person, which is based on a total hot water consumption (at 45 °C) of 54.1 litres per person per day and a net water temperature equal to 10 °C.

Four categories of tapping are considered. The mean flow rates and the volumes (durations) per tapping are based on VDI 2067 [24] and have been set as follows:

- Hand-washing/cleaning: this is a small fraction which groups all the water mass flow rate usages of around 3 lpm with a duration of up to 5 min.
- Shower: this category includes medium flow rate tapping (9 lpm) and durations of up to 10 min
- Bath: includes consumption with medium hot water flow rates (9 lpm) but long durations (more than 25 min).
- Cooking: this category refers to low water mass flow rates and medium durations (15 min).

The probability of each event (tapping) considers socio-economic factors and is based on data presented in [22].

Table 1 collects the main characteristics of the draw-offs considered in the profile used as the base of this work.

Table 1: Draw-off types and characteristics based on [24]

Type of draw-off	Temperature [°C]	Mean flow [lpm]	Probability [%]	Duration [min]	Standard deviation σ [l/h]
Handwash/cleaning	45	3	45	5	2
Shower	45	9	17	10	2
Bath	45	9	5	25	2
Cooking	45	3	33	15	2

DHWcalc tool applies probability distribution based on a Gaussian distribution to generate the profiles of the different days. The weekend–weekday variation is set to 120% and the seasonal variations are obtained with a sinusoidal function with a maximum in the day 45 and a sine amplitude equal to 10%.

Figure 1 represents the DHW demand load at 45 °C for 20 multifamily houses based on the above. The demand is shown under a daily scale instead of the used minute scale due to resolution reasons.

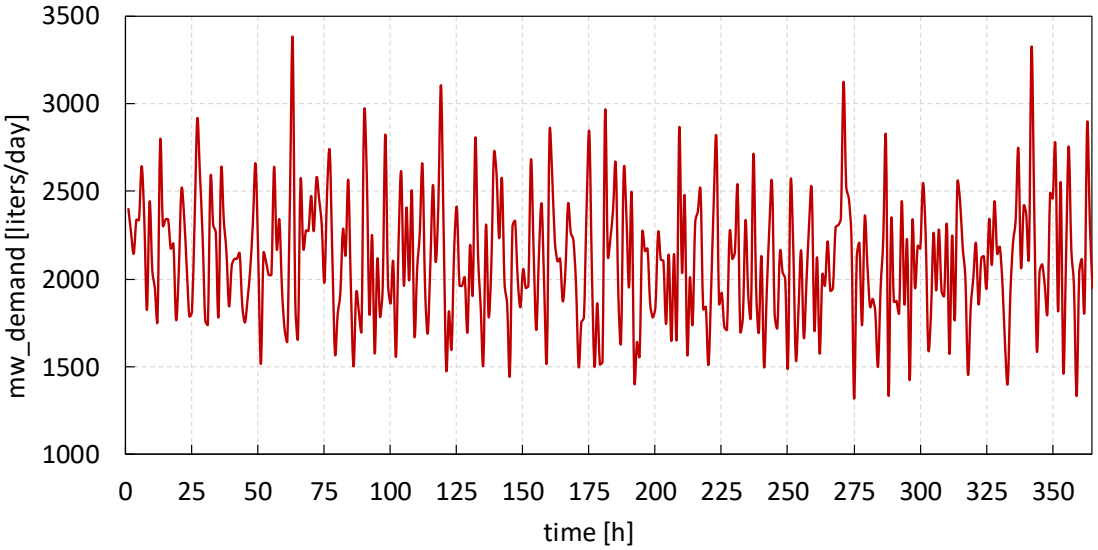

Figure 1: DHWcalc generated daily- profile for a 20 multifamily-houses DHW consumption at 45°C and Tmains 10°C

The work presented considers 20 multifamily houses (20H) as the base case. Additionally, a sensitivity analysis of the number of houses, types of draw-offs, and the timeframe used in the generation of the profiles is included.

Table 2 collects the main characteristics of the DHW profiles used in this study for hot water consumption at 45 ºC and a mains temperature of 10 ºC. These cases correspond to the following profiles:

a) Reference case (20H)
b) Demand for 10 houses (10H)
c) Demand for 30 houses (30H).
d) Demand for 20 houses during 10 consecutive years (20HY)
e) Demand determined by the software default draw-off values and the same average consumption as 20H (20Hdef).
f) Application of the solution for one third of the 20H demand, which could happen on holidays (20HL).

Table 2: Main DHW load characteristics of the profiles used in the study

DHW load profile	20H	10H	30H	20HY	20HL	20Hdef
Annual Energy demand [kWh]	31283.2	15641.6	46924.8	31283.2	10427.7	31283.2
Daily DHW demand at 45 ºC [l/day]	2110	1055	3165	2110	703.33	2110
Instant peak at 45 ºC [l/min]	36.1	24.08	33.05	(max. 50.5, 8th year)	12.03	48.68
Profile timeframe	1 year	1 year	1 year	10 years	1 year	1 year

6.4.2 Model of the SHP

The considered SHP used in the study is a high-efficiency heat-recovery water-to-water HP working with propane for water heating applications (up to 90 ºC). The SHP is composed of the typical HP components including a liquid receiver placed between the evaporator and the compressor (ensuring zero-superheat conditions). The expansion valve controls the subcooling, which is optimized based on external conditions. Thanks to the variable subcooling application, this SHP is capable of operating under high COPs for high and low temperature lifts (see figure

2) [25]. This characteristic is especially relevant for energy recovery applications where a HE is placed before the HP condenser and the water inlet temperature to the heat pump can change significantly.

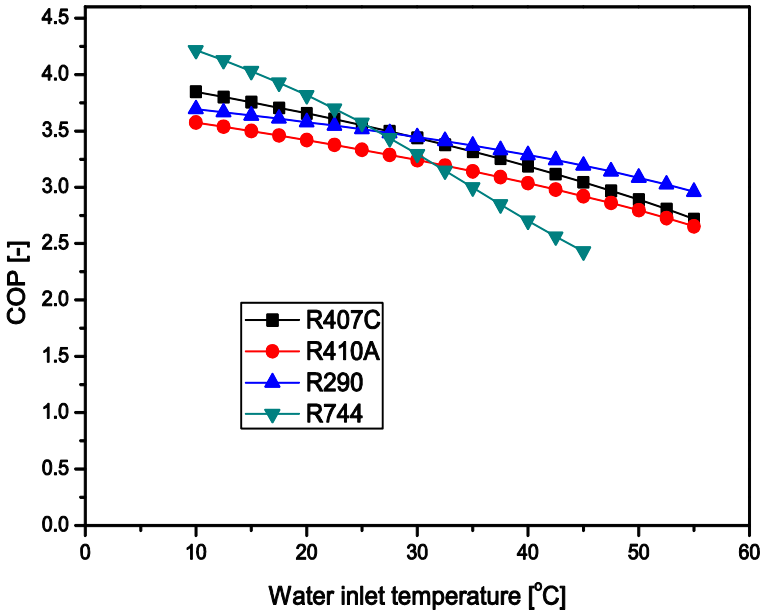

Figure 2: Typical HP performances as a function of the refrigerant used with variation of the inlet water temperature for water heating at 60°C. The heat pumps working in subcritical conditions works with constant subcooling of 5K. The line without marks correspond to the expected performance of the subcooled heat pump.

A new TRNSYS type has been implemented in order to describe properly the behaviour of this heat pump. To build the model, the following procedure has been followed:

1. A prototype of the SHP has been experimentally tested in more than 50 different experimental conditions [26].
2. IMST-ART software [27] has been used in order to develop a SHP model.
3. The developed model has been validated with the experimental campaign.
4. Once the model has been validated, it has been used as a virtual lab in order to simulate 3569 operating conditions of the heat pump.
5. A correlation has been obtained from these 3569 cases. This correlation is the one used in the developed TRNSYS type.

Table 3 collects the range of temperatures of the secondary fluid (sink and source) included in the study. Notice that only the feasible cases have been considered (for instance, the outlet water temperature at the evaporator is always lower than the

inlet water temperature at the evaporator). Furthermore, superheat is fixed to zero and the optimal subcooling is calculated as a linear function of the water temperature lift at the condenser according to [28].

Table 3: External conditions simulated in IMST-ART to obtain the type of the HP for Trnsys

	Temperature Range [°C]
Evaporator water inlet temperature	5-45
Evaporator water outlet temperature	2-42
Condenser water inlet temperature	5-60
Condenser water outlet temperature	40-90

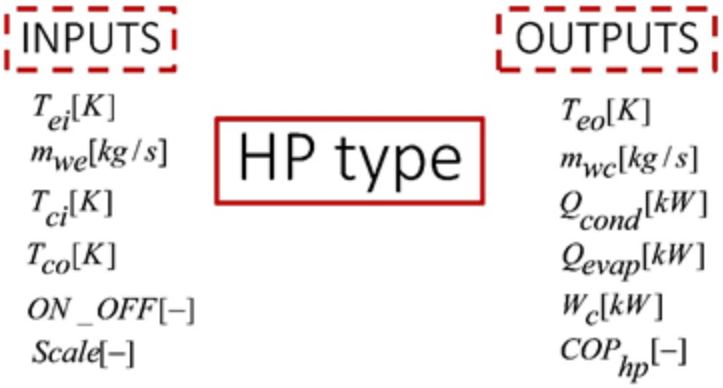

Figure 3. HP type inputs and outputs

Figure 3 shows the inputs and outputs of the HP model. Tei is the water inlet temperature at the evaporator (the district heating/wasted temperature after the HE), mwe is the water mass flow rate through the evaporator (the district heating/wasted mass flow rate), Tci is the water inlet temperature at the condenser (the mains temperature after the HE), Tco is the water outlet temperature at the condenser (the temperature that goes to the ST), and Control is the ON/OFF signal given from the operation control of the installation (further detailed in the control section).

Teo is the evaporator water outlet temperature, mwc is the hot water mass flow rate produced by the HP, Qcond is the heating capacity of the HP, Qevap is the heat

recuperated by the HP in the evaporator, and Wc is the electric compressor consumption.

Scale is set as a parameter and represents the heating capacity size of the HP. It is the parameter used in the optimization.

The obtained correlations for the cooling capacity is given by Eq. 1:

$$Q_{evap\_corr} = f(T_{eo},T_{ei},T_{ci},T_{co}) = c_0 + c_1T_{ei} + c_2T_{eo} + c_3T_{co} + c_4T_{ci} + c_5T_{ei}^2 + c_6T_{eo}^2 + c_7T_{ci}^2 + c_8T_{ei}T_{eo} + c_9T_{ei}T_{ci} + c_{10}T_{eo}T_{co} + c_{11}T_{eo}T_{ci} + c_{12}T_{co}T_{ci} \quad (1)$$

Nevertheless, from a practical point of view, it would be more practical to write down the equation (1) in terms of the evaporator water mass flow rate instead of the evaporator outlet temperature. In order to do that, the outlet evaporator temperature can be expressed according Eq. 2.

$$T_{eo} = T_{ei} - \frac{Q_{evap}}{m_{wevap}cp} \quad (2)$$

And solving using an computer algebraic system "CAS" Eq. 3 is obtained:

$$Q_{evap\_corr} = f(m_{we},T_{ei},T_{ci},T_{co}) = \\ = \frac{1}{c_6}\cdot\left[\sqrt{\left(\frac{-m_{we}\cdot cp}{2}\right)\cdot(A1\cdot cp - 4\cdot A2 - 4A3)} - \left(m_{we}\cdot cp + c_{10}T_{co} + c_{11}T_{ci} + c_2 + 2\cdot(c_6 + {}^{c_8}\!/_{2})\cdot T_{ei}\right)\right] \quad (3)$$

where:

$$A1 = \left(m_{we}^2\cdot cp^2 + 2\cdot m_{we}\cdot\left(c_{10}T_{co} + c_{11}T_{ci} + c_2 + 2\cdot(c_6 + {}^{c_8}\!/_{2})\cdot T_{ei}\right)\right.$$

$$A2 = \left(\begin{array}{l} c_0c_6 + c_1c_6T_{ei} - {}^{1}\!/_{4}\cdot(c_{10}^2T_{co}^2 + 2c_{10}(c_{11}T_{ci} + c_2 + c_8T_{ei})\cdot T_{co} + \\ + c_{11}^2T_{ci}^2 + 2c_{11}(c_2 + c_8T_{ei})\cdot T_{ci}) \end{array}\right.$$

$$A3 = \left(\begin{array}{l} (c_{12}c_6T_{ci}T_{co} - {}^{1}\!/_{4}\cdot(c_2^2 + 2c_2c_8T_{ei} - 4\cdot(c_3c_6T_{co} + c_4c_6T_{ci} + \\ + c_5c_6T_{ei}^2 + c_6(c_7T_{ci} + c_9T_{ei})\cdot T_{ci} - \frac{c_8^2T_{ei}^2}{4})) \end{array}\right.$$

c0 = 273.4477, c1 = –7.406263d-0, c2 = –4.687551, c3 = 0.2076619, c4 = 2.646866, c5 = –2.310626e-03, c6 = 1.010544e-02, c7 = –1.053072e-03, c8 = 9.182375e-03, c9 = 1.296127e-03, c10 = –1.655369e-03, c11 = –7.495019e-03 and c12 = 6.849771e-04

Only the relevant terms in order to reproduce the heat pump behaviour have been maintained.

Thereafter, the heating capacity is obtained from the correlation in Eq. 4.

$$Q_{cond\_corr} = f(T_{eo},T_{ei},T_{ci},T_{co}) = c_0 + c_1 T_{ei} + c_2 T_{eo} + c_3 T_{ci} + c_4 T_{ei}^2 + c_5 T_{eo}^2 + c_6 T_{ci}^2 + c_7 T_{ei} T_{eo} + c_8 T_{ei} T_{ci} + c_9 T_{eo} T_{co} + c_{10} T_{eo} T_{ci} + c_{11} T_{co} T_{ci} \quad (4)$$

where *c0 = 3.2379e02, c1 = –7.439879e-01, c2 = –4.946912, c3 = 0.2076619, c4 = 2.645119, c5 = 9.859616e-03, c6 = –9.507318-04, c7 = 9.589339-03, c8 = –1.344549e-03, c9 = –5.224201e-03, c10 = –7.669214e-03, c11 = 7.365229e-03.*

The HP hot water mass flow rate capacity is obtained from Eq. 5:

$$m_{wcond} = \frac{Q_{cond\_corr}}{cp \cdot (T_{CO} - T_{Ci})} \cdot Scale \quad (5)$$

The compressor consumption is calculated from Eq. 6:

$$W_{c\_corr} = f(T_{eo},T_{ci},T_{co}) = c_0 + c_1 \cdot (T_{co} - T_{ci}) + c_2 T_{eo} + c_3 T_{co} + c_4 T_{eo}^2 + c_5 T_{co}^2 + c_6 T_{co}^3 + c_7 T_{co} T_{eo}^2 + c_8 T_{eo} T_{co}^2 \quad (6)$$

co=-2.345e+02;c1=-1.320e-02;c2= 3.663;c3=-1.035;c4=-1.284e-02; c5=2.801e-03;c6=6.055e-06;c7=3.717e-05;c8=-3.018e-05

The HP performance (COP_{hp}) calculation is done directly from the above correlations according to Eq. 7.

$$COP_{corr} = Q_{cond\_corr} / W_{c\_corr} \quad (7)$$

Summing up, equations (2), (3) (5) (6) and (7) describe the heat pump.

Finally, the real values of the variables are calculated by applying the scale factor as shown in Eqs. 8 to 11.

$$Q_{evap} = Q_{evap\_corr} \cdot Scale \quad (8)$$

$$Q_{cond} = Q_{cond\_corr} \cdot Scale \quad (9)$$

$$W_c = W_{c\_corr} \cdot Scale \tag{10}$$

$$COP_{hp} = COP_{corr} \tag{11}$$

Calculations of the type shows deviations lower than 4% in almost all the cases.

6.4.3 Model description

The system under analysis is presented in figure 4, the scheme shows a direct heat recovery from the net through a heat exchanger followed by a heat pump in charge of suppling the rest of the required energy.

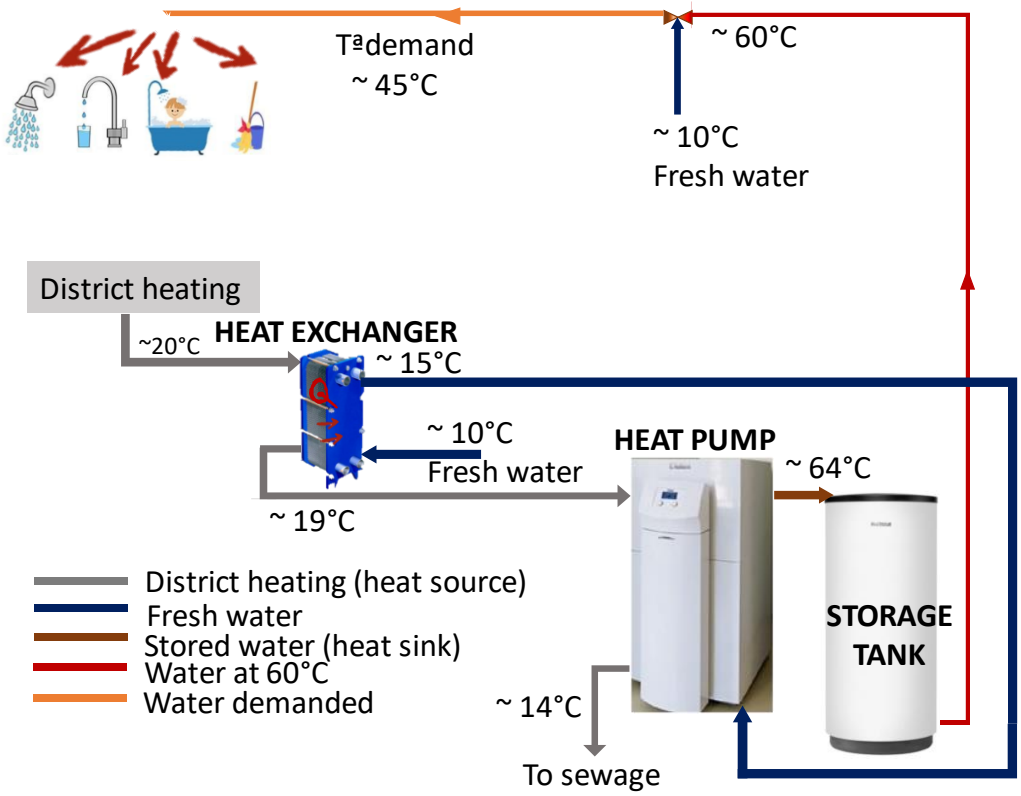

Figure 4: System layout and design conditions

The main components of the system are:

- Heat exchanger with an effectivity of 0.75 (type 5b). This heat exchanger will allow a first energy recuperation.

- The SHP model presented previously: The water evaporator mass flow rate was defined in order to have a water temperature difference in the evaporator of 4.5°C. Thi heat pump with the characteristic curve show in figure 2 is especially

indicated when a net water pre-heater (recuperator) is installed and that temperature could change significantly depending on external parameters.

- Storage tank of variable volume (type 39): with an aspect ratio of H/D=4 and a heat loss coefficient of 0.8 W/m2K (based on Spanish regulation). The storage tank assumes an ambient temperature of 20°C. The storage tank has been selected in order to maximize the efficiency of the system, therefore, contrary to the more common stratified tanks, this tank only have one inlet and outlet and maintain a uniform temperature inside of it.

- Water pumps (Type 742): used with an efficiency of 0.3. Only the pressure drop of the heat exchangers were considered in order to evaluate their consumption.

In order to define the load profile, the stochastic model described previously has been used. The service water temperature was considered at 45°C and the productions was fixed based on the target of having a minimum storage water temperature of 60°C (legionella regulation restriction for this type of systems [29]).

The simulations use a time step of 1 minute (as a consequence of the profile characteristics longer time steps could due to not size properly the system) and include 1-year simulation period.

Figure 5 collects the main inputs and outputs of the model and the optimization variables in order to minimize the CO2 emissions.

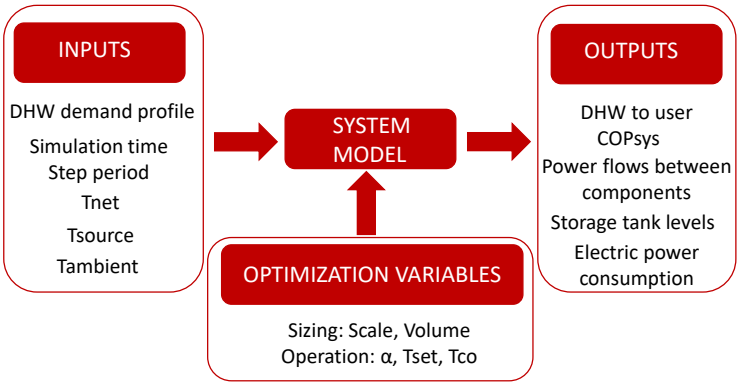

Figure 5: Main inputs and outputs of the system and optimization variables.

Figure 5 shows a scheme of the structure of the used model showing the input, the output and the optimization variables. In that scheme, scale is the size of the heat pump, volume is the size of the tank, alfa is the tank level when the heat pump

switches on, Tset is the water tank temperature and Tco is the condenser outlet temperature.

COPsys is the COP of the whole system and is defined as:

$$COP_{system} = Energy/Electric =$$

$$\int_{t=0}^{t=simulationtime} (Q_{ST\_out})/(W_{c\_corr} + \sum W_{pumps}) \quad (12)$$

One should notice that the "useful energy" introduced by the system is a result of the heat exchanged in the pre-heating HE and the heating capacity of the HP after the ST losses.

Regarding the control algorithm, the main source of irreversibility of the system arises from the addition of a ST. Thus, the control of the installation is based on the minimization of the temperature and the time that the water is stored in the ST required to satisfy the demand. As the temperature of the stored water increases, so does the irreversibility. The minimum possible temperature of stored water considered in this work is 60°C. Hence, the control set temperature is Tset = 60°C.

In order to maintain a temperature of at least 60°C at the ST, the outlet temperature of the condenser in the HP needs to be some degrees higher. Specifically, based on the simulation results, the minimum outlet temperature to achieve this requirement stably is 64°C. Thus, from all the simulations, the water outlet temperature at the condenser is set to 64°C.

The minimum time for which the water is stored is dependent on both the volume of the ST and the level of the water inside the tank. Dynamic control based on the water level inside the tank is required and both the volume and the level of the tank are parameters to be optimized. This control parameter is called α and expresses the control level as a percentage of the volume according to Eq. 13.

$$Control\_level = \alpha \cdot Volume \quad (13)$$

Where *Volume* is the capacity (size) of the tank. The determination of the optimal α is also an objective of this work.

A maximum ST level is also required to avoid overproduction; the maximum level set is based on the production capacity of the HP in one-time step as indicated in Eq. 14.

$$\max\_level = Volume - mw\_cond \cdot step \quad (14)$$

Where mw_cond is the HP water mass flow rate production for a determined scale and step the simulation time step.

Finally, to preserve the durability of the HP, a maximum of nine starts within the same hour is recommended by manufacturers and has been considered in the control. This feature is programmed in the HP type. Figure 6 summarizes the control algorithm followed.

The used comfort criteria are based in two conditions, satisfy the demand 99% of the time and do not allow more than one-minute shortage at the same hour daily. The second condition is added in order to consider the user satisfaction characteristics of this type of hot water demand.

The optimization of CO2 emissions has been performed for a system considering all these constrains.

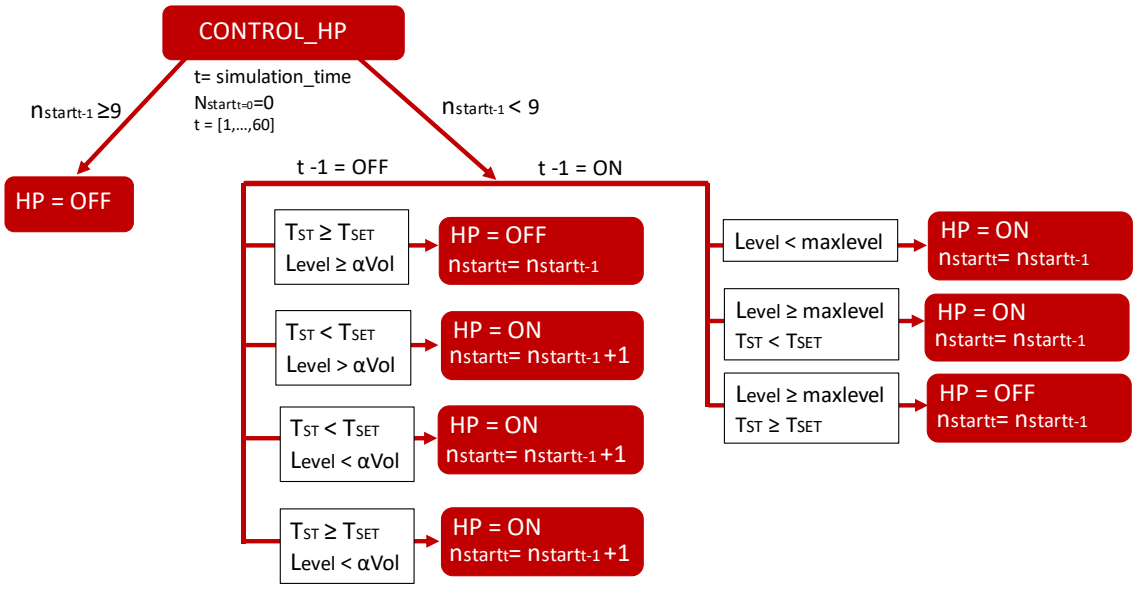

Figure 6: System control strategy implemented each hour

6.5 Performed studies

The analysis of the variation in the CO2 emissions derived from different sizing criteria of this heat recovery systems and to supply design guidelines about this kind of systems are the main outcome of this work. To this aim, the study considers four different points:

a) Optimization of the system for the nominal conditions.
b) Sensitivity analysis of the obtained solution with the external conditions
c) Analysis of the influence of each system component (SHP, Heat Exchanger and storage)
d) Comparison with other technologies

These points are described below.

(a) Optimization of the system for the nominal conditions.

The optimization of the HP size (Scale), the volume of the ST, and the control level (α) is carried out in order to minimize the CO2 emissions for the reference conditions (see table 4) has been done. The calculation of the CO2 emissions has been made using the conversion coefficients from [30].

Table 4. Considered reference conditions.

DHW demand profile	20H/10H/30H
Tnet	10°C
Tsource	20°C
Tambient	20°C

Constant values of the mains and district heating temperatures have been used as reference conditions.

The values chosen are selected from a conservative point of view, with 10 °C as the net water temperature and 20 °C as the heat source water temperature.

Due to the excessively time-consuming process resulting from long simulation periods and small-time steps, a one-year simulation timeframe with a time step of one minute was considered as a good compromise in terms of the accuracy/time ratio. As will be pointed out later on, larger time steps could lead to oversizing.

In order to find the optimum value of the different parameters and obtain information about the influence of each one a set of parametric studies were performed. Figure 7 summarizes the simulations performed in the parametric studies done for each demand size: 10H, 20H, and 30H.

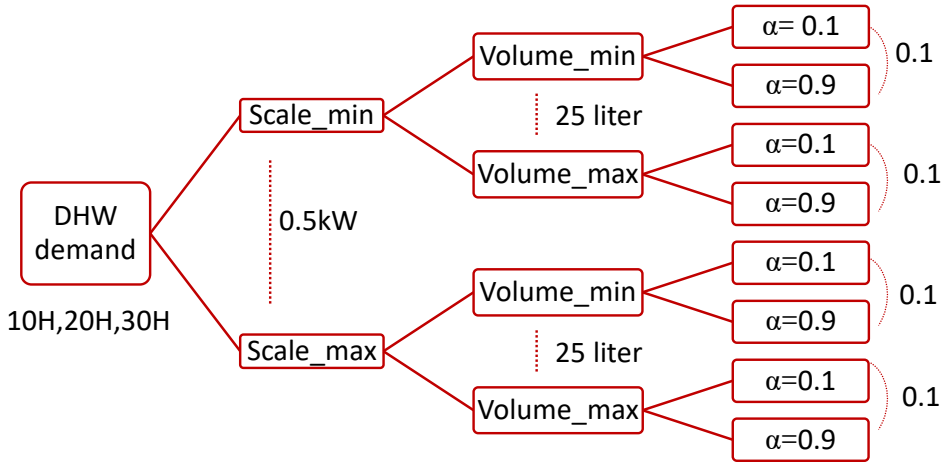

Figure 7: Parametric studies for each demand size. 0.5kW Scale increments, 25liter ST sizes increments and 0.1 increments in α.

The different parametric study performed are:

- *Scale* variation range: it is expressed in terms of heating capacity (Qcond) and goes from the minimum size that meets the discomfort requirements to the size that satisfies the demand with an operating time of a minimum of 1.5 hours per day (in 0.5-kW steps).
- *Volume* variation range: for each heating capacity, the maximum and minimum ST sizes that meet discomfort levels are investigated (in 25-liter steps).
- *Alpha* variation range: for each ST size, the variation of the control level in terms of the volume percentage, α, goes from 0.1 to 0.9 (in steps of 0.1).

The results presented in the next section have been obtained from more than 12000 simulations.

(b) Sensitivity analysis of the obtained solution with the external conditions

To verify the generality of the results obtained, a sensitivity analysis for one of the optimal solutions shown in the 20H case has been done. The sensitivity analysis has included:

•Sensitivity to the external conditions: the objective is to validate the solution with different net and wasted-heat water temperatures; hence the conclusions of

the work developed in the previous analysis could be extended to different locations and conditions.

a. Tnet variation: from 5 to 25 ºC
b. Twasted/district variation: 10–35 ºC

•Sensitivity to other DHW profiles: The target of this analysis is to analyse the validity of the solution when different peaks take place for the same average consumption (20H). This part of the study allows understanding the importance of the type of profile chosen.

c. For 20H draw-off and input characteristics of 10 consecutive years, (20HY).

(c) Analysis of the influence of each system component (SHP, Heat Exchanger and storage)

In order to analyse the impact on the energy consumption derived from the characteristics of the DHW production application and the components included in the system, the following simulations for the reference case (20H) has been performed:

-Reference HP case: calculation of the annual COPhp and associated CO2 emissions when the system is composed of the HP alone and the DHW load profile is constant in each time step.

-HP + HE: calculation of the annual COPsys and associated CO2 emissions when the system is composed of a HP with a HE keeping a constant demand profile. This case can be considered as the ideal case from the energy recovery point of view. (System with less losses).

-HP+HE+ST: calculation of the annual COPsys and associated CO2 emissions for the system with the HP, the HE and the This case can be considered as the real system as there is a variability in the demand in order to motivate the inclusion of a ST.

(d)Comparison with other technology

Finally, for the reference conditions at 20H solution, an annual comparison study with other technologies in terms of CO2 emissions is included.

Four systems are considered:

- HP: Only the HP and the ST, with COPhp = 5.74 (Table 6)

- HP + HE: the optimal system composed of HP+ST+HE

- NG Boiler: natural gas boiler with an efficiency of 0.92

- NGB + Solar: considers 50% of production from solar and 50% from a natural gas boiler with an efficiency of 0.92

CO2 emissions associated with each type of source are chosen according to the Spanish conversion rates: 0.331 kgCO2/kWh for an electric source and 0.252 kgCO2/kWh for natural gas [30].

6.6 Results

Although the analysis has been done based on a one-minute time step and yearly simulation time, due to the amount of data, the results are presented using the hourly time step. The temperature results are the integral of the minute-temperatures each hour, while the mass flow and energy hourly results are the sum of the respective variable for each minute within the hour.

Figure 8 and Figure 9 show an example of the outputs obtained in each simulation. In this example, a 20H demand, a HP heating capacity, Q_{cond} of 7.56 kW, a volume of 400 liter, and a control parameter α equal to 0.8 (control level 0.8*400 = 320 liter), have been used.

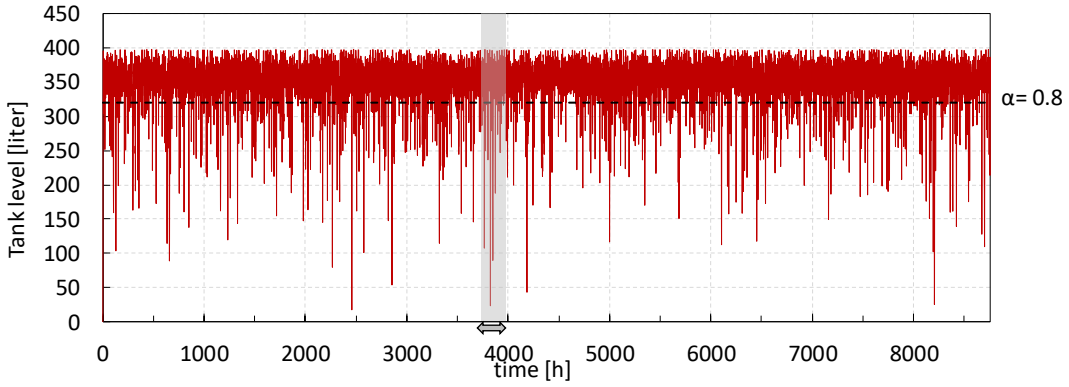

Figure 8: Hourly average tank level for 20H in a complete year, Qcond= 7.56kW, alpha=0.8 and volume=225liter

Figure gives a general view of the hourly results. However, the use of a yearly scale makes still difficult the analysis. Hence, a three-day period, represented in grey (from hour 3796-3868) is used for next figures.

Figure considers some of the most important outcomes of the model for two-days period. Figure (a) represents the water mass flow rate in the tank (in red), where mw_cond is the water mass flow rate at the outlet of the condenser (inlet of the ST), blue is used for the water mass flow rate going out the ST (mw_st) and dotted columns represent the water mass flow rate load required at the tank temperature (mw_hot). Figure (b) shows in red the hourly-average level of the tank and in blue the hourly-average temperature and Figure (c) depicts the hourly energy supplied to the user (black dotted lines) and demanded by the user (red line) within the three days.

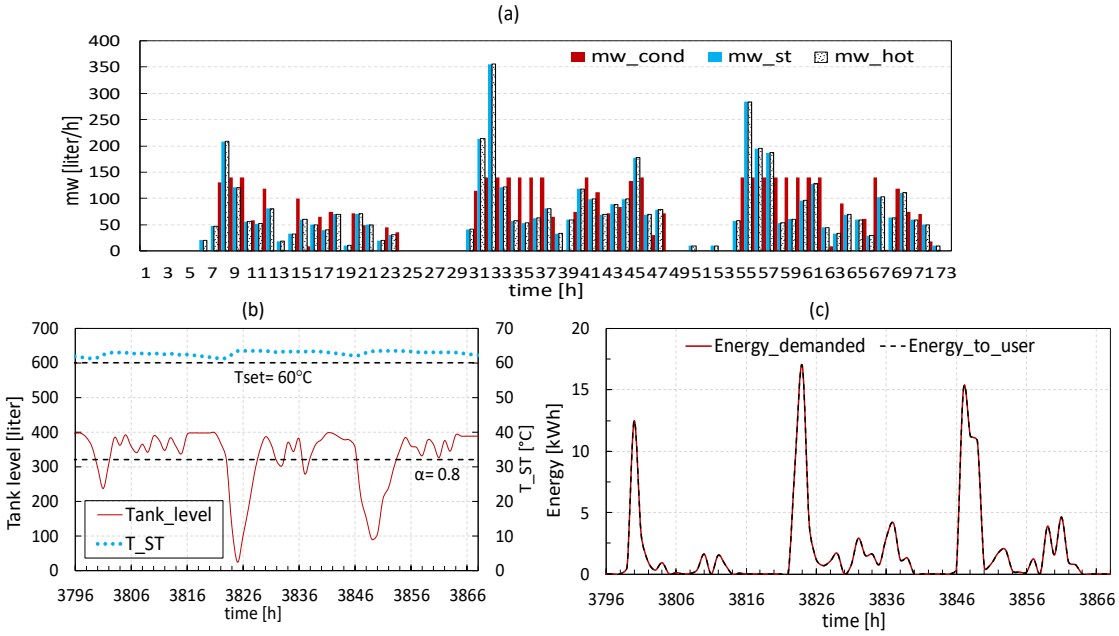

Figure 9: Hourly results for 20H throughout two days, Qcond= 7.56kW, alpha=0.8 and volume=225liter. (a) Water mass flow rate production (mw_cond), ST outlet water mass flow rate (mw_st) and water mass flow rate load required at the tank temperature, (b) average tank level and temperature and (c) Energy supply to the user according and Energy demanded by the user.

According to Figure 9(b), the tank temperature never falls below 60°C and the ST is not oversized as in some periods it is full and in others it is almost empty while remaining capable of supplying the required energy in time thanks to the α and temperature controls that manage the HP production time. As can be seen in figure 9(c), the energy supplied fulfils the requirements for the chosen sizing values and controls. The most convenient solution from the energy point of view is to produce as closely as possible to the demand, minimizing the time during which the water remains stored in the tank. Figure 9 also shows that only a few HP operating periods are required to maintain the level and temperature of the tank at the control values.

(a) Optimization of the system for the nominal conditions.

Figure and Figure give an example of the parametric studies performed with each demand size. In this case, a 20H load profile has been used. Figure shows the annual CO2 emissions associated to the system and Figure the respective HP operating hours. Each figure (a), (b) and (c), different to one HP size and for each size, the CO2 emissions of the possible solutions ST sizes and control values are

represented. The parametric studies are based on different sizes in 0.5kW steps but Figure 0 and Figure 1 outline only the three most representative. (a) minimum HP size, (b) optimal HP size and (c) maximum HP size.

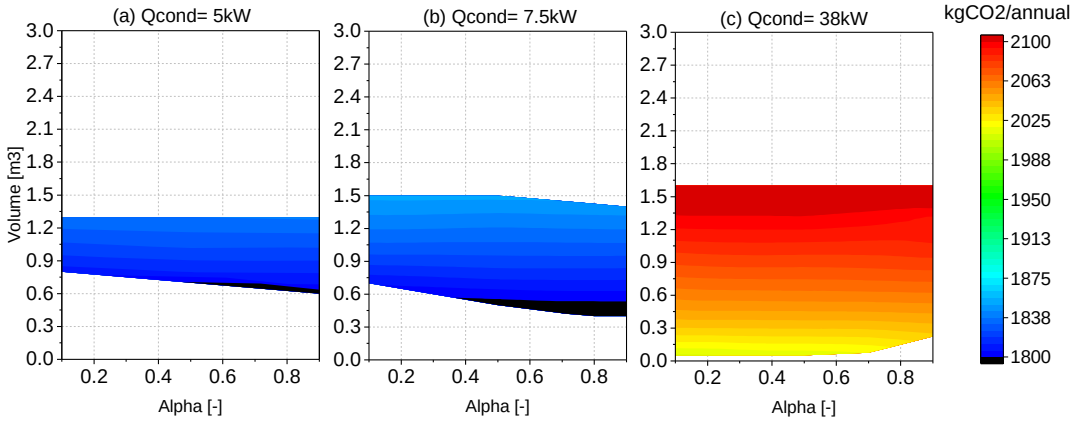

Figure 10: Annual CO2 emissions associated to the system function of the ST size (volume) and control level (alpha) for (a) minimum HP size, (b) optimal HP size and (c) Highest optimal size. Only the solutions that met discomfort standards are represented.

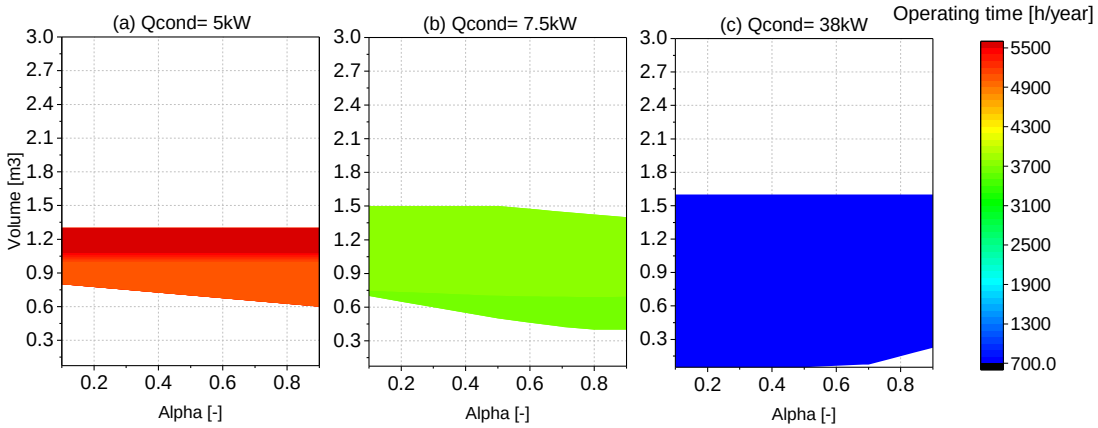

Figure 11: Annual HP operating function of the ST size (volume) and control level (alpha) for (a) minimum HP size, (b) optimal HP size and (c) Highest optimal size. Only the solutions that met discomfort standards are represented.

From Figure and Figure 11 several aspects are derived:

- Not all the combination sizes are possible solutions. In fact, there is a maximum ST size (depending on the HP size) capable to achieve the

discomfort requirements. The region of possible solutions is greater as the HP size increases.

- The operating time depends mainly on the HP size. The ST size influences more with smalls heating capacities. High volumes lead to higher operating times.
- Combinations of small HP-ST sizes lead to lower CO2 emissions. Among the solutions, the best energy combinations belong to the lowest ST size and high α but greater operating production time. The reason for that is based in two points: a) the smaller the ST the smaller the losses associated with it, b) when the heat pump is too large it produces too much water that must be stored in the tank more time than the required one.
- For a given size, CO2 emissions increase linearly with the ST size. Around 5% increase from the minimum volume to the maximum volume takes place.
- Higher HP sizes lead to significantly higher CO2 emissions (even though fewer operating hours are required). When the operating time increases from 1.5 h/day to 12 h/day, the CO2 emissions decreases by 15%.
- As a consequence of using a small time-scale and a variable volume ST, the ST sizes obtained are small. In fact, an ST of less than 400 litres for a 20H demand is obtained in optimal cases; this is smaller than the common ST used in DHW applications. For this type of systems where the peak demands could last only 5 minutes, a time steps in the simulations of one hour could change significantly the obtained solutions.
- With high ST volumes, the control of the storage tank level (α) losses importance. In these cases, the HP operating control is driven mainly by the ST temperature.
- With small ST volumes, the dominant control is alpha and widens the solution region compared to not using any control level, especially with small HP sizes (optimum). For instance, in (b), the minimum volume without level control is 700liter while a ST tank 57% smaller (400liter) is possible when high water level controls are applied.

Similar results are obtained with other demand sizes and in all parametric simulations.

Following the approach showed in Figure and Figure but taking into account only the optimal control (Alpha value), the binomial analysis of the ST-HP size is done for 10H, 20H and 30H load demands.

Figure and Figure 3 show the CO2 emissions per house and the annual operating time, respectively, for the solution maps (in terms of HP-ST size) and the optimal α value for 10H, 20H, and 30H. To distinguish the influence of the demand size, the same scale has been used in each figure. Nevertheless, a magnified view of 10H has been considered in some cases.

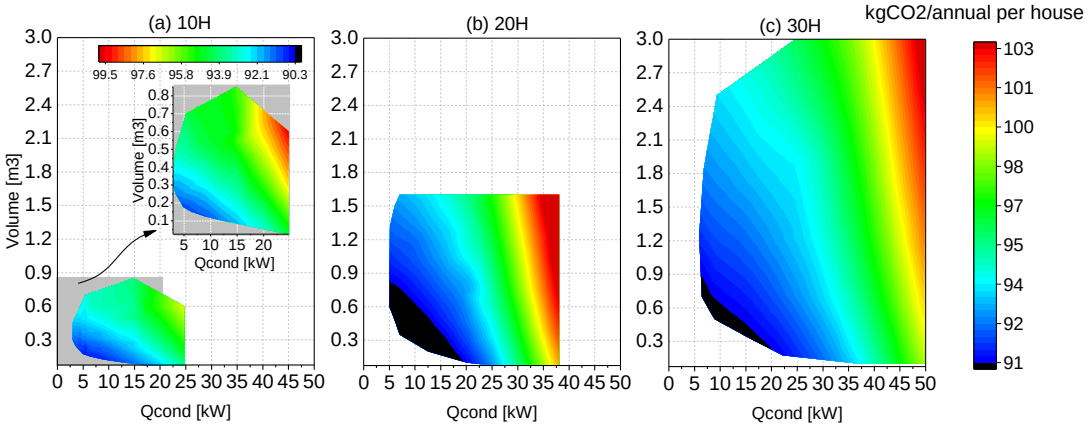

Figure 12: CO2 annual emissions per house for each HP-ST size and (a)10H demand, (b) 20H demand and (c) 30H demand

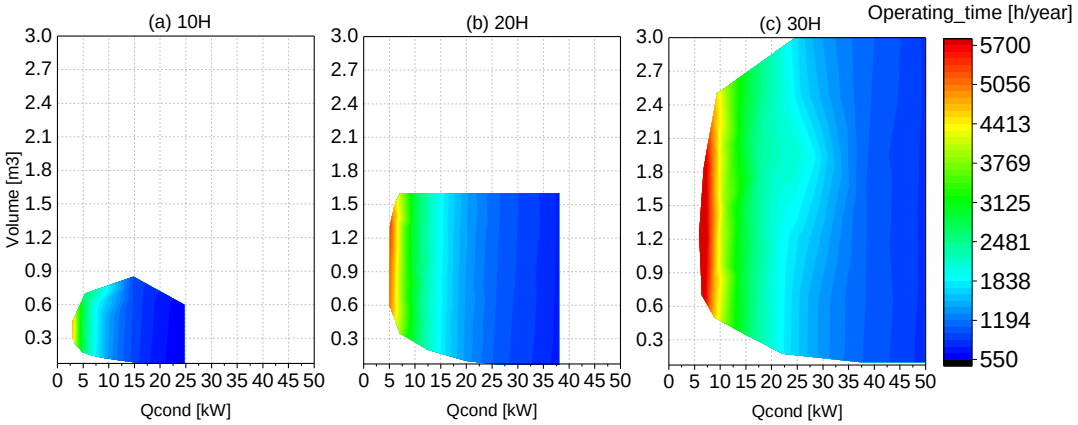

Figure 13: Annual operating time for each HP-ST size and (a)10H demand, (b) 20H demand and (c) 30H demand

The most remarkable conclusions from Figure 2 are:

- Higher aggregated demands (more houses served by the same system) lead to lower CO2 emissions per house. This could be explained considering that for the same hot water demand, the demand profile requiring less energy to satisfy it is the constant demand profile, therefore more houses are served

by the same system the profile demand will be more homogeneous and therefore the energy required per dwell will be smaller.

- There is a small optimal region of HP-ST size combinations that lead to similar annual emissions for each demand type. The minimum emissions correspond to a line of solutions with the smallest ST and HP sizes in each case.
- For a given demand, CO2 emissions can vary up to 20% from the optimal solution to the worst case.

From Figure 13 the following can be extracted:

- A bigger solutions map leads to a wide range of operating times, from 1.5 h/day to almost 16 h/day in the 30H case, while with a smaller demand, where fewer combinations are possible, the range is from around 7 h/day to 2 h/day.
- Optimal solutions appear with high to medium operating time production. These solutions imply less heat losses in the storage tank.

The COPsys is in all the cases, is higher than 5.

Figure 14 collects the optimal HP-ST sizes for each demand size presented in figure 12, the curves presented in the figure represent the different combinations of HP-ST operating with a similar efficiency in order to satisfy a given DHW demand. In addition, the required annual operating hours are also represented as a function of the optimal binomial sizes. Green color is used for 30H, blue for 20H, and orange for 10H. Dotted lines indicate the operating time and continuous lines represent ST sizes.

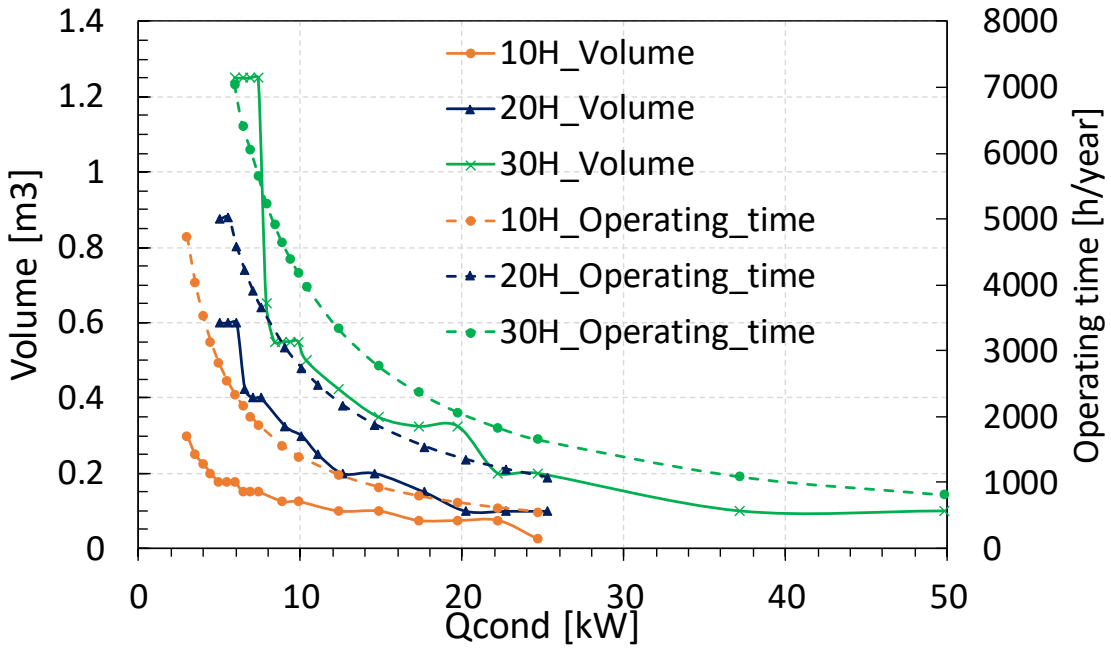

Figure 14: Optimal HP-ST size combination and its operating associated annual operating time for 10H, 20H and 30H demands.

Figure 14 is useful for sizing an HP system for DHW production with the characteristics described in this work. According to the figure, with small HP sizes, there is a minimum ST size required, while as the HP size increases, lower ST volumes are possible. In addition, increasing the heating capacity of the HP does not always lead to lower ST volumes (due to discomfort requirements).

(b) Sensitivity analysis of the obtained solution with the external conditions

A sensitivity analysis of the system considering different heat source temperatures (district heating temperature) and water mains is included for the case represented in Figure and Figure 9. This is one of the best ST-HP sizes combinations in the 20H case (minimum HP-ST size among the optimal solutions).

Figure represents the performance of the system for 20H, optimal α in each case, scale=0.15 and volume=400liter. Green lines are used for a net temperature of 15°C, red lines with 10°C and black lines with 5°C.

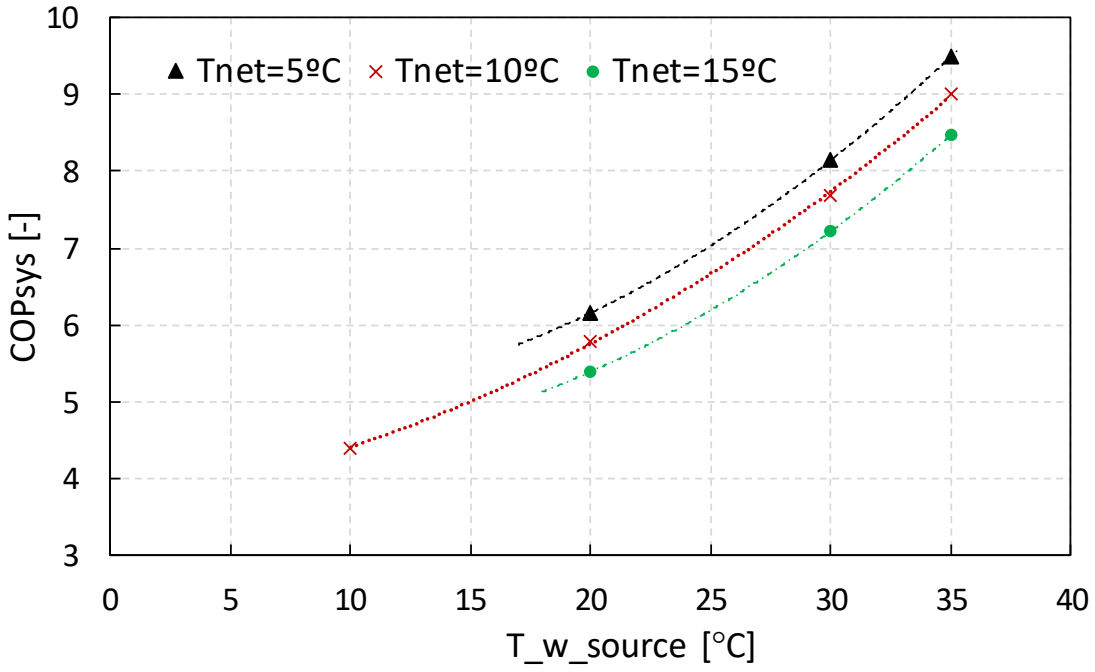

Figure 15: Performance of the system for 20H, Qcond= 7.5kW, alpha=0.8 and volume=400liter for different water source and mains temperatures

The figure 15 shows that the COPsys increases as the temperature inlet temperature of the heat sink is reduced (maintaining the outlet temperature of the heat sink constant), this is because this procedure is equivalent to effectively reduce the mean temperature of the heat sink. The COPsys also increases and the temperature of the the heat source increases.

The whole study presented in this work is based on one of the most critical conditions: 10°C of water net temperature and 20°C of water heat source temperature. However, in most heat recovery applications these conditions may underestimate the potentiality of a HP system.

From that way, if the heat source temperature changes to 35°C, which could be a representative temperature for low temperature district heating applications, COPsys can increase up to 9.

Table 5 collects the main results of the sensitivity study for the optimal solution obtained for demand of 20H working in different Tnet and Tsource conditions. Design conditions are highlighted in bold. The system capacity supply indicates the capacity of the system based on the user requirements, that is, the percentage of energy that the system is able to supply.

In all combinations, the systems can provide the required energy with an annual discomfort level below 0.6%. Thus, the proposed solution could be valid under a wide range of external conditions without compromising the level of satisfaction. The most influential variable is the temperature of the heat source.

Table 5 also shows that the adaptation of the HP-ST system to different external conditions can be done with tank control volume parameter α_opt. Favorable conditions lead to lower values of control levels and the opposite. Hence, if a system is designed following this type of approach, the optimal level of control would be adapted based on the external conditions.

Table 5: Main results of the system for 20H and different water net and source temperatures for scale= 0.15 and volume=400liter.

Tnet [°C]	Tsource [°C]	α_opt [-]	Qcond [kW]	Annual Elec. Consump [kWh]	CO2 emissions [kgCO2]	Operating time [h]	COPhp [-]	System capacity supply [%]
5	20	0.8	7.54	5079.39	1681.27	3448.15	5.15	99.95%
5	30	0.4	8.92	3838.36	1270.49	2457.41	5.76	99.94%
5	35	0.3	9.7	3291.14	1089.36	2047.18	6.1	99.98%
10	10	0.8	6.23	7085.68	2345.36	5137	4.54	99.66%
10	**20**	**0.8**	**7.56**	**5408.68**	**1790.27**	**3659.03**	**5.14**	**99.95%**
10	30	0.5	8.95	4063.54	1345.03	2592.3	5.76	99.98%
10	35	0.4	9.74	3473.65	1149.78	2153.45	6.1	99.97%
15	20	0.9	7.58	5802.68	1920.69	3911.73	5.14	99.92 %
15	30	0.5	8.99	4329.09	1432.93	2751.5	5.76	99.93%
15	35	0.4	9.77	3687.13	1220.44	2277.73	6.09	99.95%

Finally, in order to check the generality of the obtained solution, the same system solution has been used in order to satisfy an input load profile generated with DHWcalc using the same conditions but a simulation period of 10 consecutive years, with the same average consumption. In all cases, the system was able to serve the energy demand with the required satisfaction and similar CO2 emissions associated with the production. Thus, it can be stablished that the obtained solution is independent of the particular random profile generated.

(c) Analysis of the influence of each system component (SHP, Heat Exchanger and storage)

In this section, an analysis of the influence of the different components in order to satisfy the required total energy demand is performed. Three different systems able to satisfy a 20H demand load profile of DHW have been analyzed. These systems are: a standalone HP, a HP+HE and HP+HE+ST. The DHW profile is considered as constant except for the case including the ST, where the 20H profile generated with DHWcalc has been used. One should notice that the heating capacity includes the heat from the HP and the pre-heater HE (recuperator) when it is present.

Table 6: System analysis. Results for HP, HP+HE, HP+HE (30 ºC) and HP+HE+ST

System	HP	HP + HE	HP+HE+ST
Tsource [ºC]	20	20	20
Annual Energy demand [kWh]	31283.2	31283.2	31283.2
Average required heating power [kW]	3.57	3.57	3.57
Tco [ºC]	60	60	64
HE capacity [kW]	0	0.357	0.357
HP heating capacity, Qcond [kW]	3.57	3.21	3.5
COPhp	5.74	5.39	5.14
COPsys	5.71	5.95	5.2

Table 6 presents the results of the analysed cases, according to it, the addition of a pre-heating recovery HE improves the COPsys by almost 5% even though the COP of the HP decreases by around 6%. In fact, 10% of the heating energy required comes from the HE, this value that could be higher (for higher heat source temperatures) shows the relevance of this component. This is a consequence of the second law of thermodynamics, when the temperature allows the heat exchange, always is better to recover heat directly than to use a heat pump for that.Therefore

as a rule of thumb, in this type of systems, first recover energy with a HE and then pump the rest of the energy.

When a DHW non-uniform profile is used, an ST tank is required. This component increases the irreversibility significantly. Higher condenser outlet water temperatures (64 ºC) are required and heat losses take place in the ST. In fact, the COPsys of the HP+HE+ST system is 12% lower than that of the HP+HE system for the same external temperatures in the analyzed cases.

In order to understand the cases analysed in Table 6, Figure 16 shows a more detailed comparison of the results of the standalone HP system and the HP+HE+ST system. Since a one-year simulation with a one-minute step scale does not allow to visualize the results graphically, only the results for one day are shown. Figure 16(a) represents the production and hot water requirements for the reference case, HP. Figure 16(b) Shows the hot water production in red, the consumption in dotted and the ST outlet water mass flow in grey. Figure 16(c) represents the water temperature at the inlet and inside the ST if the Figure 16(b) case and Figure 16(d) represents the water level of the tank during the day of the Figure 16(b) case.

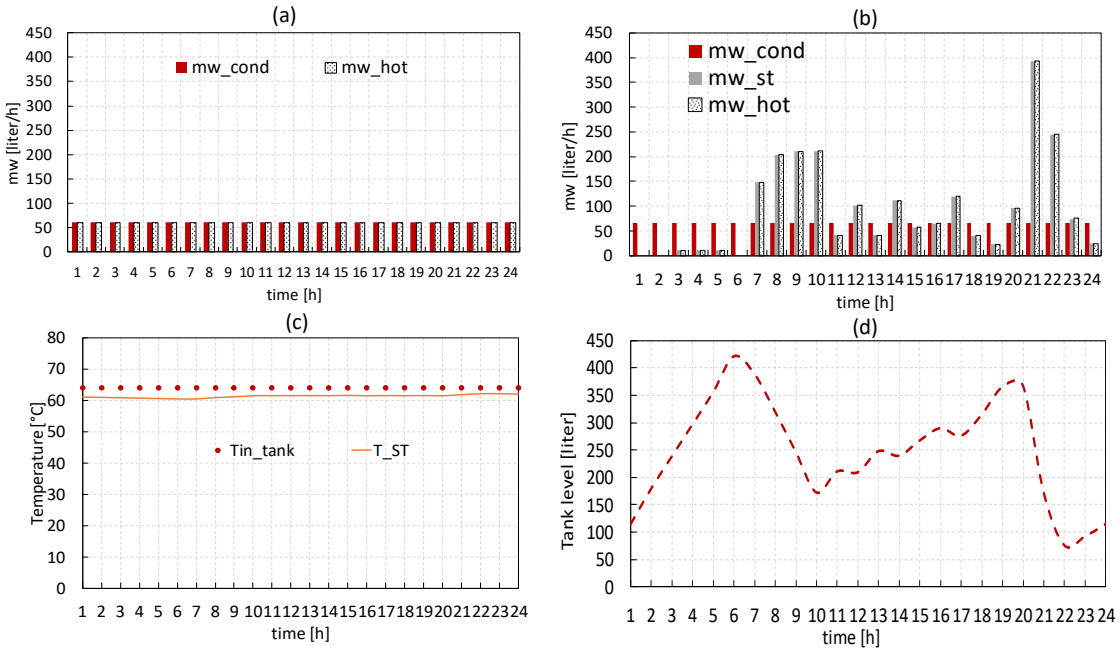

Figure 16: Results in hourly-base for one day of the year (a) water mass flow rates for the HP case (b) water mass flow rates for the HP+HE+ST case (c) ST temperatures for the HP+HE+ST case (d) ST level for the HP+HE+ST case

From the obtained results, it is worth pointing out that the variability of the DHW load profile results in a significant COP loss of the system; that is, the characteristics of the profile condition are the most influential parameter in the

efficiency of the system. This result is mentioned in [31], where the authors analyzed the efficiency of a system based on different profile shapes, numbers of peaks, and distances between peaks in addition to operating schedules. From that study, they concluded that the imposition of, for instance, "night" production leads to a 20% loss of efficiency and the position and the number of peaks have significant impacts on the final solution from the sizing of the system and form the efficiency point of view.

Therefore, the optimization of these systems could be addressed from a different perspective: instead of optimizing systems for a determined type of user, the system and the user habits could be optimized for the maximum energy efficiency.

(d) Comparison with other technology

Table 7 contains the electric consumption and the annual CO2 emissions associated to four different systems taking into account the temperatures of the design conditions (Tnet=10 ºC and Twsource=20 ºC and an annual energy demand of 31283.2kWh).

Table 7: annual CO2 emissions associated to different DHW production systems for 20H for Tnet=10 ºC and Twsource=20 ºC

Annual electric consumption [kWh]	HP (*)	5450
	HP + HE (**)	5341.5
	Gas boiler	34003.5
	Gas boiler + 50% Solar	17001.7
Associated CO2 emissions [kgCO2]	HP	1803.9
	HP + HE	1768.03
	Gas boiler	8568.9
	Gas boiler + 50% Solar	4284.4

(*)COP_{hp}= 5.74

(**) COP_{hp}= 5.14, 87.76% of the energy supplied by the HP and 12.24% by the HE

Figure 17 shows the annual CO2 emissions of the considered systems and 20 multifamily houses and highlights the potentiality of HP systems for DHW production. CO2 emissions could be reduced up to 4.5 times from the substitution of Gas Boiler to HP systems.

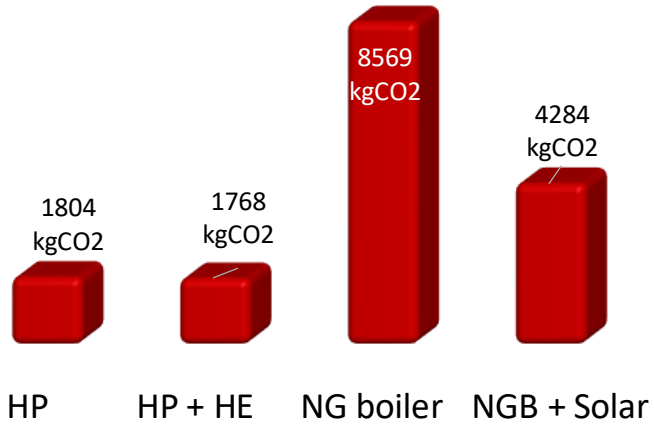

Figure 17: Annual CO2 emissions associated to a HP, HP+HE, NG Boiler and NGB + Solar systems for 20H DHW production.

6.7 Conclusions

This work analyses a system to produce DHW from the recovery of low-grade temperature sources using HPs. The study analyses the influence of the proper sizing and the operation strategy of an HP-ST system in order to satisfy DHW production within the residential sector based on the minimization of the associated CO2 emissions for a given demand profile. In addition, it could supply an indicative value about the minimum energy required to satisfy the DHW demand with current technologies.

In order to maxime the efficiency of the system, it is composed of a pre-recuperator heat exchanger installed before the heat pump, an innovative heat pump with a special dependence of the COP as a function of the condenser water inlet temperature (the SHP) and a storage tank of variable volume in which the temperature is almost constant along all the tank and no stratification is produced.

The main conclusions obtained from this work have been:

- A set of HP-ST sizes combinations with similar associated CO2 emissions exists nevertheless a significant penalty in the energy consumption, up to 20%, can be obtained from going outside this set of solutions.
- Small sizes of both components (HP+ST) are preferred, allowing to minimize the time that the water is stored in the tank.
- The net water temperature and the temperature of the water heat source do not affect critically to the design of the components.
- The water pre-heating heat exchanger significantly enhances the performance of the system, lowering annual CO2 emissions by around 15% on average.
- The need for the ST is justified in order to satisfy the variable demand curve of this type of application. It introduces a significant reduction in the annual system performance. In order to minimize that source of losses a variable volume tank with no stratification has been used in all the study. Using that type of tank, 12% of system efficiency reduction compared with no tank use (constant demand profile) has been obtained.
- More centralized DHW production system (more houses connected to the same system) leads to a flatter hot water profile demands and lower annual emissions per house.
- Derived from the previous point, it should be pointed out that for the same DHW demand, the energy consumption could change up to 12% depending on the used profile. Therefore, solutions to minimize the environmental impact associated with DHW production should take that point into account and should also imply the need for education and adoption of some habits in DHW use by the user.

Finally, it should be commented that the obtained results are independent of other factors like energy policies or prices that could be added in a second level analysis. This point gives generality to this study.

6.8 Acknowledgements

Part of the work presented was carried out by Estefanía Hervás Blasco with the financial support of a PhD scholarship from the Spanish government SFPI1500X074478XV0. The authors would like also to acknowledge the Spanish 'MINISTERIO DE ECONOMIA Y COMPETITIVIDAD', through the project "MAXIMIZACION DE LA EFICIENCIA Y MINIMIZACION DEL IMPACTO AMBIENTAL DE BOMBAS DE CALOR PARA LA DESCARBONIZACION DE LA CALEFACCION/ACS EN LOS EDIFICIOS DECONSUMO CASI NULO" with the reference ENE2017-83665-C2-1-P for the given support.

6.9 References

[1] Meyers S, Schmitt B, Vajen K. The future of low carbon industrial process heat: A comparison between solar thermal and heat pumps. Sol Energy 2018;173:893–904. doi:10.1016/J.SOLENER.2018.08.011.

[2] Energy consumption in households – Statistics Explained 2018. http://ec.europa.eu/eurostat/statistics-explained/index.php/Energy_consumption_in_households (accessed 1 August 2018).

[3] Hepbasli A, Kalinci Y. A review of heat pump water heating systems. Ren. and Sust. Ener. Rev. 2009;13:1211-1229. doi: 10.1016/j.rser.2008.08.002

[4] Stene J. Residential CO2 heat pump system for combined space heating and hot water heating.Int. J. Refrig. 2005;28:8, 1259-1265. doi: 10.1016/j.ijrefrig.2005.07.006

[5] Qi P-C, He Y-L, Wang X-L, Meng X-Z. Experimental investigation of the optimal heat rejection pressure for a transcritical CO2 heat pump water heater. Appl Therm Eng 2013;56:120–5. doi:10.1016/j.applthermaleng.2013.03.045.

[6] Gluesenkamp KR, Patel V, Abdelaziz O, Mandel B, Dealmeida V. High efficiency water heating technology development – final report, Part II: CO2 and absorption-based residential heat pump water heater development. 2017.

[7] Austin BT, Sumathy K. Transcritical carbon dioxide heat pump systems: A review. Ren. and Sust. Ener. Rev. 2011; 15:8;4013-4029. doi: 10.1016/j.rser.2011.07.021

[8] Cecchinato L, Corradi M, Fornasieri E, Zamboni L. Carbon dioxide as refrigerant for tap water heat pumps: A comparison with the traditional solution. Int. J. Refrig. 2005;28:8; 1250-1258. doi: 10.1016/j.ijrefrig.2005.05.019

[9] Pitarch M, Navarro-Peris E, Gonzálvez-Maciá J, Corberán JM. Evaluation of different heat pump systems for sanitary hot water production using natural refrigerants. Appl Energy 2017;190:911–9. doi:10.1016/j.apenergy.2016.12.166.

[10] Pottker G, Hrnjak P. Effect of the condenser subcooling on the performance of vapor compression systems. Int J Refrig 2015;50:156–64. doi:10.1016/j.ijrefrig.2014.11.003.

[11] E Fuentes E, Arce L, Salom J. A review of domestic hot water consumption profiles for application in systems and buildings energy performance analysis. Renew Sustain Energy Rev 2017. doi:10.1016/J.RSER.2017.05.229.

[12] Marini D, Buswell R, Hopfe CJ. A critical software review – how is hot water modelled in current building simulation? 14th International Conference of the International Building Performance Simulation Association, Hyderabad, India, Dec. 7-9th. 2015.

[13] Floss A, Hofmann S. Optimized integration of storage tanks in heat pump systems and adapted control strategies. Energy Build 2015;100:10–5. doi:10.1016/j.enbuild.2015.01.009.

[14] Justo M, Stene AJ. IEA heat pump programme annex 32. Umbrella report, system solutions, design guidelines. Prototype system and field testing – Norway. 2010.

[15] Hepbasli A, Biyik E, Ekren O, Gunerhan H, Araz M. A key review of wastewater source heat pump (WWSHP) systems. Energy Convers Manag 2014;88:700–22. doi:10.1016/j.enconman.2014.08.065.

[16] Shen C, Lei Z, Wang Y, Zhang C, Yao Y. A review on the current research and application of wastewater source heat pumps in China. Therm Sci Eng Prog 2018;6:140–56. doi:10.1016/J.TSEP.2018.03.007.

[17] Culha O, Gunerhan H, Biyik E, Ekren O, Hepbasli A. Heat exchanger applications in wastewater source heat pumps for buildings: A key review. Energy Build 2015;104:215–32. doi:10.1016/J.ENBUILD.2015.07.013.

[18] Liu L, Fu L, Jiang Y. Application of an exhaust heat recovery system for domestic hot water. Energy 2010;35:1476–81. doi:10.1016/j.energy.2009.12.004.

[19] Elgendy E, Schmidt J, Khalil A, Fatouh M. Performance of a gas engine driven heat pump for hot water supply systems. Energy 2011; 36:2883-2889. doi:10.1016/j.energy.2011.02.030

[20] Jiang H, Jiang Y, Wang Y, Ma Z,Yao Y. An experimental study on a modified air conditioner with a domestic hot water supply (ACDHWS). Energy 2006; 31:1789-1803. doi: 10.1016/j.energy.2005.07.004

[21] Jordan U, Vajen K. Manual DHWcalc tool for the generation of domestic hot water (DHW) profiles on a statistical basis. n.d.

[22] Fischer D, Wolf T, Scherer J, Wille-Haussmann B. A stochastic bottom-up model for space heating and domestic hot water load profiles for German households. Energy Build 2016;124:120–8. doi:10.1016/J.ENBUILD.2016.04.069.

[23] TRNSYS: Transient system simulation tool 2016

[24] Verein Deustscher Ingenieure. VDI 2067-12:2017 | Economic efficiency of building installations – effective energy requirements for heating service water. 2017.

[25] Pitarch M, Navarro-Peris, E,Gonzalvez-Macia J, Corberan JM. Experimental study of a subcritical heat pump booster for sanitary hot water production using a subcooler in order to enhance the efficiency of the system with a natural refrigerant (R290). Int. J. Refrig. 2017.73. 223-234. doi: 10.1016/j.ijrefrig.2016.08.017

[26] Hervás-Blasco E, Navarro-Peris E, Barceló-Ruescas F, Corberán JM. Optimized water to water heat pump design for low-temperature waste heat recovery based on subcooling control. Accepted to be published in Int. J. Refrig.

[27] IMST-ART (2010) Simulation Tool to Assist the Selection, Design and ptimization of Refrigeration Equipment and Components. In: Inst. Univ. Investig. en Ing. Energética, Univ. Politècnica València, Val. http://www.imst-art.com/

[28] Pitarch M, Hervas-Blasco E, Navarro-Peris E, Gonzálvez-Maciá J, Corberán JM. Evaluation of optimal subcooling in subcritical heat pump systems. Int J Refrig 2017;78:18–31. doi:10.1016/j.ijrefrig.2017.03.015.

[29] Spanish norm: UNE 100030:2017. Prevención y control de la proliferación y diseminación de Legionella en instalaciones.

[30] Factores de emisión de CO2 y coeficientes de paso a energía primaria de diferentes fuentes de energía final consumidas en el sector de edificios en España. WIT Press; 2016.

[31] Hervás-Blasco E, Marchante-Avellaneda J, Navarro-Peris E, Corberán JM. Design of a system for the production of domestic hot water from wastewater heat recovery based on a heat pump optimized to work at high water temperature lift. 5th Int High Perform Build Conf Purdue, 9–12 July 2018, West Lafayette; 2018.

Chapter 7
Closing the residential energy loop: grey-water heat recovery system for Domestic Hot Water production based on heat pumps

Estefanía Hervás-Blasco[a], Emilio Navarro-Peris[a], José Miguel Corberán[a]

[a] Institut Universitari d'Investigació d'Enginyeria Energètica, Universitat Politècnica de València, Camí de Vera s/n, València, 46022, Spain

Tel: +34 963879123

enava@ter.upv.es

7.1 Abstract

Passive houses linked to more efficient heating and cooling technologies have been one of the focus in last years. However, to close the loop of the building sector, there is still one open source: wasted heat from grey water. This paper addresses the potentiality of the wasted heat from grey water as a heat source to produce domestic hot water (DHW) based on a heat pump system (HP). A heat pump optimized for these applications, a heat recovery heat exchanger and two variable volume storage tanks compose the system. The main objective of this work is to determine the potential recuperation of the wasted heat in order to minimize the building energy consumption. Design guidelines of the components and the analysis of an optimum operation algorithm of the system have been performed in order to minimize CO2 emissions. In addition, an evaluation of the potential heat recuperation of the wasted heat is included. As an example, that methodology has been applied to 20 dwells. Results demonstrate that by recovering 60% of the available heat, the total demand of DHW can be served with high levels of comfort and efficiency.

7.2 Nomenclature

DHW: domestic hot water

ST: storage tank

HE: pre-heating heat exchanger (recuperator)

SHP: subcooled heat pump

Tei: water inlet temperature at the evaporator [°C]

Teo: water outlet temperature at the evaporator [°C]

Tci: water inlet temperature at the condenser [°C]

Tco: water outlet temperature at the condenser [°C]

Tnet: water mains/net temperature [°C]

Tgrey: water heat recovery temperature [°C]

Tsewage: grey water temperature after its recuperation (to the sewage) [°C]

TST: water stored temperature in the respective tank [°C]

Thot= water temperature at the system conditions [°C]

Tuser= water temperature supplied to the user [°C]

Tdemanded=water demand temperature [°C]

Tset= temperature control [°C]

Tamb= ambient temperature [°C]

Qcond=Heat pump heating capacity [kW]

Qevap=Heat Pump cooling capacity [kW]

COP_{hp}: Heat pump Coefficient of Performance, [-]

COP_{sys}: System Coefficient of Performance, [-]

COP_{Lorenz}: Lorenz Coefficient of Performance, [-]

mw_grey: grey water mass flow rate [kg/s]

mw_user= water mass flow rate to the user [kg/s]

m_{wc}:condenser water mass flow rate [kg/s]

m_{we}:evaporator water mass flow rate [kg/s]

Wc: Heat pump electric consumption [kW]

Scale: Relative size of the heat pump compared to the reference value

Volume= capacity of the respective tank [liter]

ρ: Water density [kg/m3]

α: Control level rate in the DHW tank[-]

β: Control level rate in the grey water tank[-]

λ: Ratio between the hot water mass flow and the grey water mass flow [-]

γ: proportion of the DHW storage tank capacity [-]

C_0: proportion of the condenser water mass flow rate [-]

Subscripts

ST: storage tank

HP: Heat pump

gw: grey water

DHW: domestic hot water

hot: hot water (at production temperature, 64°C)

7.3 Introduction

Nowadays, global policies tend to move towards a more sustainable system with a more responsible use of energy. In 2014, the European Union set the goal of reducing greenhouse gas emissions (GHG) and improving the energy efficiency up to, 40% and 27%, respectively, by 2030 [1]. Currently, the building sector accounts for nearly 40% of the annual GHG emissions [2] and for almost 27% of the final energy consumption. Therefore, the reduction of the energy consumption and the improvement of the technologies used in this sector are necessary in order to reach the 2030 targets.

In recent years, there has been a great effort in order to reduce the energy consumption in buildings. The main actions have been focused on both, the reduction of heating demand and on the improvement of the technologies used for heating and cooling ends. However, little attention has been paid to the reduction of the energy demand related to DHW production even though, in developed countries, accounts for approximately 15% [3].

Furthermore, 85-90% of the total energy dedicated to hot water production [4] is wasted to the ambient after its use. Its heat recovery has been studied in literature from the point of view of both thermodynamic potential [24] and heat pumps [36].

Based on that, the use of high efficient technologies for water heating applications as well as the heat recuperation from warm wastewater can significantly contribute to the reduction of the energy consumption and the GHG emissions associated to the building sector.

Heat pumps are the most suitable technology dealing with the mentioned two aspects: high efficiency and the use of medium-low temperature water flows as a heat source. In order to analyze the use of heat pumps in these application, the most common approach is from the system point of view is related to show the reliability of the system or is bounded to economic factors, such as electric tariffs [33] or cost functions [44][48] associating the control and design of the whole system to these parameters. The problem of these kinds of approaches is related to the fact that the obtained results depend on socio-politic parameters that could change over time.

Furthermore, the solutions obtained with those approaches may be just for a specific case. For instance, in [49] the operation of the heat pump is directly driven by the off-peak electricity period, in [10] the majority of the production also takes place in these periods or in [50] the authors analyze the impact of the operation control of a HP-photovoltaic system under an energy and economic point of view, concluding that the optimization of energy factors results in a degradation of the economic factors and vice versa.

In the open literature, although, approaches dealing with the optimization of solely the energy efficiency and based on components specifically designed for this type of application could supply a valuable information, they are not so common. This approach can be used afterwards to perform specific economic analysis outside the scope of this work.

An approach based on the maximization of the recovery potential using heat pumps from a purely energy analysis must take into account not only the heat pumps, but also the systems where they are integrated and based on that the operation of the heat pump and the rest of the system must be adapted properly to the specific characteristics of the heat sinks and heat sources. Later on, these points are going to be described more in depth.

Heat sink characteristics (DHW)

The main characteristics of DHW (sink) are high temperature lifts and high demand variability:

- High water temperature lifts have been addressed by the use of transcritical cycles [5][6][7], mixtures [8][9][10] or, more recently, by the use of subcritical cycles with the application of high degrees of subcooling [11] [12] which can have substantial advantages compared to other heat pump systems in DHW production from heat recovery applications as it allows an improvement in the temperature match between the refrigerant and the secondary fluid deriving in a higher system efficiency.
  High performances have been obtained with these solutions, in that line, the subcritical cycles with a subcooling control enhance the system efficiency at low and high temperature lifts [13][14][15][16][17], with reduced global system cost.
- To deal with high variability, the use of a variable speed compressors or storage tanks are required. The first solution penalizes HP efficiency as moving far away from the design condition could decrease the compressor efficiency and could be not enough to cover profiles with sharper peaks and intermittent production. The second alternative, storage tanks, is commonly employed. A vast literature is available on optimization studies in terms of geometry and control of the tank, especially, coupled with CO2 HPs and solar systems where stratified tanks are desired [18][19][20][21]. More limited information is available dealing with the operation and control of other types of tanks (such as variable volume or fully mixed) that are preferable under an energy point of view [22] [23][24][25].

Heat source characteristics (wastewater)

Building wastewater (grey water) is characterized by higher temperature than the ambient, stable through the year and with a high variability depending on the used source of heat:

- HPs are capable to operate under high efficiencies with medium-low temperatures within applications where there is no limitation in the water quantity [23]. Examples of these are district heating [26][27][28], sewage water [29][30][19] or industrial heat recovery processes with high demand of refrigeration applications[31][32].
- The variability is directly linked to the variability observed in other sources like DHW. To ensure the availability of waste water when it is required, the most common solution is to use storage tanks to collect waste water when it is produced. HP performance remains high if a proper design and isolation of the tank is used [24][33][34][35][36].
- The use of grey water from the building itself allows to have higher temperatures of the heat source than other sources like for instance, sewage water. In contrast, the availability of grey water produced by a building is limited. Thus, if this amount is small compared to the demand of heat, the temperature lift at the evaporator could increase so much that the resulting mean temperature in the evaporator secondary fluid could be lower than the obtained using other sources like seawage water, resulting in a decrease of the HP performance. Few studies about this topic are found in literature. Most works done in this line are focused only on the direct recovery of part of the heat available in the grey water using just a heat exchanger (mostly water from showers) [24][37][38][39][40][35][41].

  However, these kinds of systems lose an important part of the wasted energy potential and they are not capable to satisfy all the DHW demand. In [42], they address this problem acting over the control of the system but they do not address the adaptation of the heat pump components to the system characteristics. Additionally, these authors consider a grey water temperature between 40ºC and 50ºC that could overestimate the capacity of the system.

As it has been commented previously, greywater presents a large potential of recuperation [43] [44]. With the proper energy recovery strategy, it can contribute even with more energy than the required in DHW production [35]. However, not only these energy aspects are important (demand and availability),in order to maximize the benefit of the recovery, the heat pump, the system in which it is integrated, and the control parameters must be taken into account.

Adaptation of the system to the specific characteristics of the heat sink and heat source.

Most of the heat recovery applications found in the literature only take advantage of the direct heat recovery and in general they only use a limited amount of the available exergetic potential of the grey water [41][43][46][35][47]. In addition, when these applications are combined with heat pumps [10][44], the heat pumps are not adapted specifically to the operating conditions and the system is not optimized to satisfy all the DHW demand with the minimum energy consumption.

Work and contribution of this paper

The aim of this work is to analyze the potential of the grey water produced by a dwelling in order to minimize the CO2 emissions associated to DHW production in the residential sector. To do so, the system described in [45] has been used. The configuration consists of a primary recovery heat exchanger, a heat pump prototype specially designed to maximize the COP of the whole system for this application (see [15] to find a more detailed description of its characteristics, this heat pump will be called subcooled heat pump (SHP)) and two variable volume storage tanks. This configuration is considered as the one which allows a higher energy efficiency potential.

The dynamic behavior of the system has been reproduced implementing a TRNSYS [51] model.

As a proof of concept, 20 dwellings have been used as an example to develop the proposed design. In order to perform a deeper analysis of the influence of the heat source in this kind of system, the study considers first an unlimited availability of the heat source. Thereafter, a limited but constant profile of grey water has been taken into account and finally, profiles based on the grey water used in the dwellings are studied and compared to the previous cases.

Based on this analysis, the most efficient system in order to satisfy a DHW demand in the residential sector by the recovery of the heat from wastewater (grey water) has been determined. The study includes the sizing of the different components (heat pump, recuperator heat exchanger, tanks) and the definition of the optimum control strategy. The obtained results allow quantifying irreversibility added to the system by the use of variable low-grade heat sources. It also gives some guidance about its potential and supplies an estimation about

the expected differences in energy consumption associated to the system design and waste water heat availability.

7.4 Methodology

7.4.1 Heat sink characterization

This study focuses on DHW production for residential sector. Thus, the heat sink is the end-user hot water demand. A yearly profile for 20 dwellings generated with the stochastic model, DHWcalc [52], has been used. The selected time step has been of 1 minute. This profile includes an estimation of socioeconomic factors and it has been validated with SynPro[53]. The profile is the same as the one used in [23]. The reader is referred to it for further details.

The daily DHW demand is 54.1 l. of water at 45°C per person and per day. This represents an annual average energy consumption of 804kWh (for a net water temperature of 10°C). That is, an average water consumption at 45°C of 105.5 liter per apartment and a total mean water consumption of 2110l/day (for 20 dwellings).

The consideration of a constant net water temperature is a good estimation for sizing or general purposes. However, seasonal effects and the variation of the net water temperature needs to be considered for a more detailed analysis. In fact, its fluctuation (mainly seasonal) can have an impact on the energy demanded up to 10% depending on the location [54]. In this work the profile for the water temperature from the net has been determined following the methodology proposed in [54] and used in [53] based on Eq. 1.

$$T_{net} = \overline{T_{amb}} - 3 \cdot \cos\left(\frac{2\pi}{365} \cdot (n_{day} - n_{daus,offset})\right) \quad (1)$$

Where $\overline{T_{amb}}$ is the mean ambient temperature (10°C), n_{day} is the day of the year and $n_{daus,offset}$ is the offset, set according to the coldest day of the year.

7.4.2 Heat source characterization

Decentralized grey water from 20 dwellings has been considered as a heat source. Grey water includes all water consumptions in a house except that from toilets (black-water) collected before the general sewage system. Due to the scarce information about grey water in the literature, the estimation of the profiles and

its characteristics have been done based on the total average water consumption, the end-use, the typical temperatures according to its use, the characterization of the DHW load profile and data found in literature.

Germany has been considered as the reference country for the grey load profile used. Furthermore, as the consumption in this country is rather conservative compared to other developed countries, for the potential estimation of heat recovery, which will imply that the obtained results would be conservative. According to [55], the average drinking water consumption in Germany is 123liter/day and person (240 liter/day and apartment). The final end-mix for the grey water is based on [56]: 15% to shower, 25% to bath, 30% to flush the toilet, 13% to the clothes washing machine, 7% to dishwasher, 6% to hand wash, cleaning and gardening and 4% destined to cook. That is, grey water represents 70% of the total drinking water consumption (168liter/day and apartment).

Furthermore, both streams, DHW and drinking consumption, are related in terms that all DHW mass flow would be part of the grey water. Hence, as the daily average DHW consumption per household is 105.5liter at 45°C, the rest would come from the other uses except, toilets.

On the one hand, the grey water from DHW water has been considered to follow the same profile as the DHW but one-minute delayed (time considered between the hot water consumption and its availability as a grey source). It is convenient to point out that DHW is going to be produced at 60°C (legionella regulation) but its end use is at 45°C. In order to reduce the water temperature, some additional drinking water will be mixed with the DHW produced.

On the other hand, a profile representing the use of clothes and dish washing machines has been generated with DHWcalc software. Average flow rates, frequency and temperatures have been estimated according to the work presented in [35] and the mentioned drink water consumption.

Table 1 summarizes the main inputs used in DHWcalc software for the characterization load profile of the clothes and dish machines. An average consumption of 960liter/day, 20 dwellings with a daily probability function based on a step function for weekends and weekdays, a 120% probability weekday/weekend and seasonal variations are accounted by means of sinusoidal function have been considered.

Table 1: Drink water use in appliances that do not require DHW inputs for DHWcalc.

Draw-off type	End-use temperature [ºC]	Mass flow [lpm]	Duration [min]	Probability [%]
Dishwasher	65	4.8	1	11
Hot rinse	50	4.2	1.5	15
Cold rinse	45	3.6	1	9
Cloth washer	37	10.2	3	65

Literature regarding to the temperature at the drain of each type of flow rate is also very limited.

From the available data, the authors consider as good estimation the values of the hot water temperature used in the work presented in [35] which have been obtained from a wide literature review and experimental measurements. Table 2 collects the temperature of the end-user used in this work for both types of streams.

Regarding to the temperature of the grey water at the drain, a drop of 7K from the end-user temperature has been estimated regardless the nature of the consumption. This value is based on the most conservative study performed [10].

Table 2 shows the temperatures at the end-use and at the drain considered in this study.

Table 2: End-use water and drain temperatures of the different streams considered.

Draw-off type	End-use temperature [ºC]	Drain temperature [ºC]
Handwashing	38	31
Shower	40	33
Bathtub	40	33
Cooking/cleaning	45	38
Washing machine	37	30
Dishwasher	53	46

The grey water load profile is obtained aggregating the DHW profile with one-minute delay, the profiles of the clothes and dish washing machines with a thirty-

minutes delay generated with DHWcalc and mixed with cold water until the end-use temperature for an annual time-frame and one-minute step time. An average daily grey water availability of 3360liter (168liter/apartment) and an average grey water temperature of 32.8°C is obtained out of that mix.

Figure 1 depicts the daily mean temperature of the grey water. Notice that the use of mean temperatures for a daily scale hints the real temperatures used in each minute.

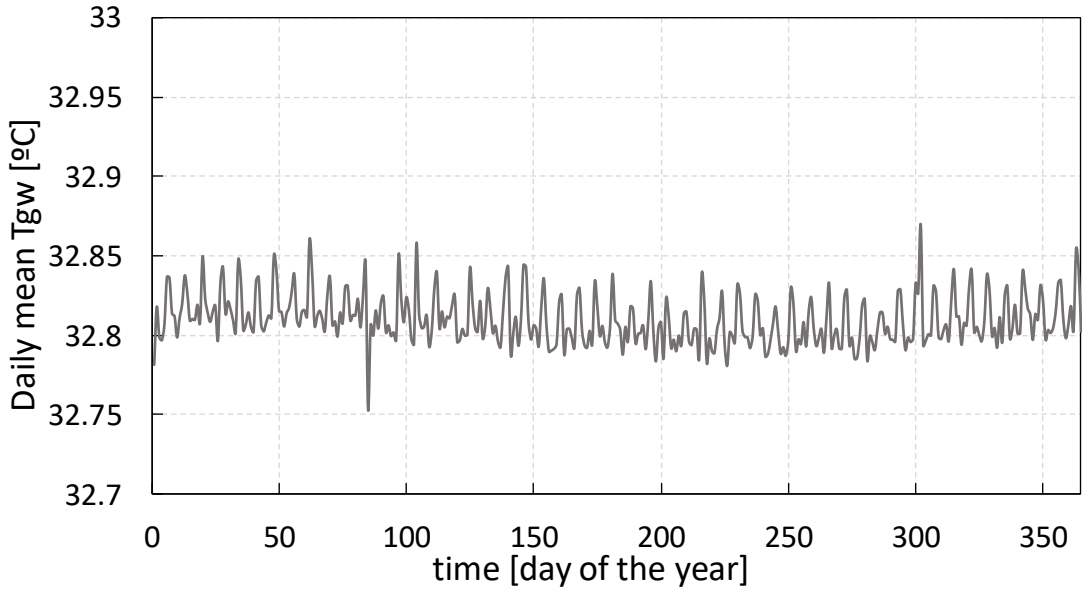

Figure 1: Daily mean grey water temperature over a year

Figure 2 represents the DHW demand load at 45°C and the grey water available profile for 20 dwellings obtained using the described methodology. Water mass flow rates are expressed under a daily scale. However, it is important to remark that the use of a minute time scale when dealing with these type of profiles based on short periods and high variability demands is strongly recommended [57] and

it has been the time step selected in order to perform all the simulations of this work.

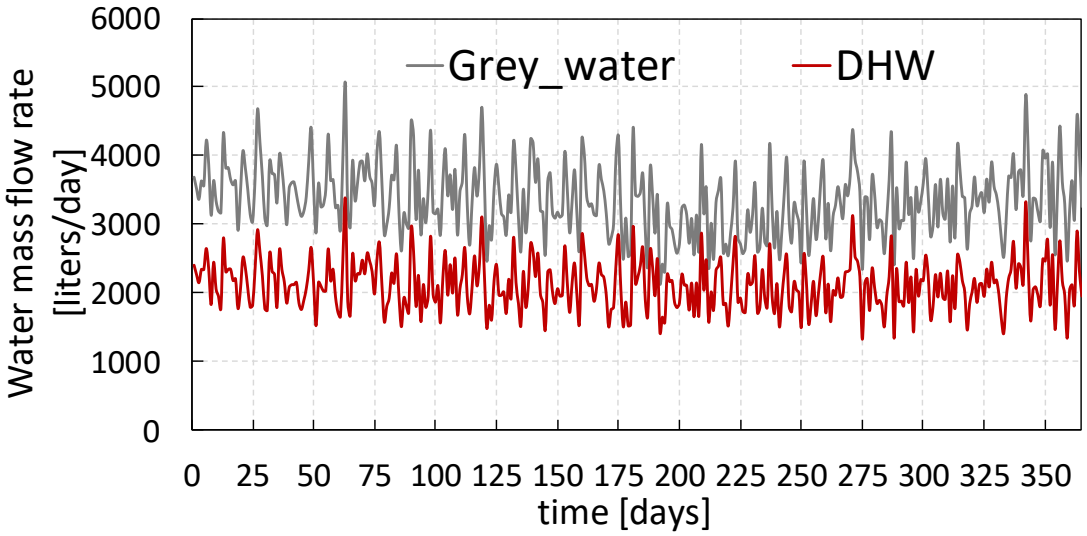

Figure 2: DHW and grey water daily- profiles for a 20 multifamily-houses DHW consumption at 45 ºC and Tmains 10 ºC

7.4.3 Model description

Figure 3 shows a scheme of the main components, water flows and average temperatures of the system. The system configuration has been selected in order to maximize the efficiency in such a way that the energy recovery from the grey water is performed in two steps: first, with a heat exchanger (recuperator) and later on the rest of the energy is extracted using th SHP. This heat pump allows to work with a good performance using a variable volume water storage tank for the DHW in such a way that the water accumulated in the tank do not need a reheat up allowing that the tank only have one inlet and one outlet.

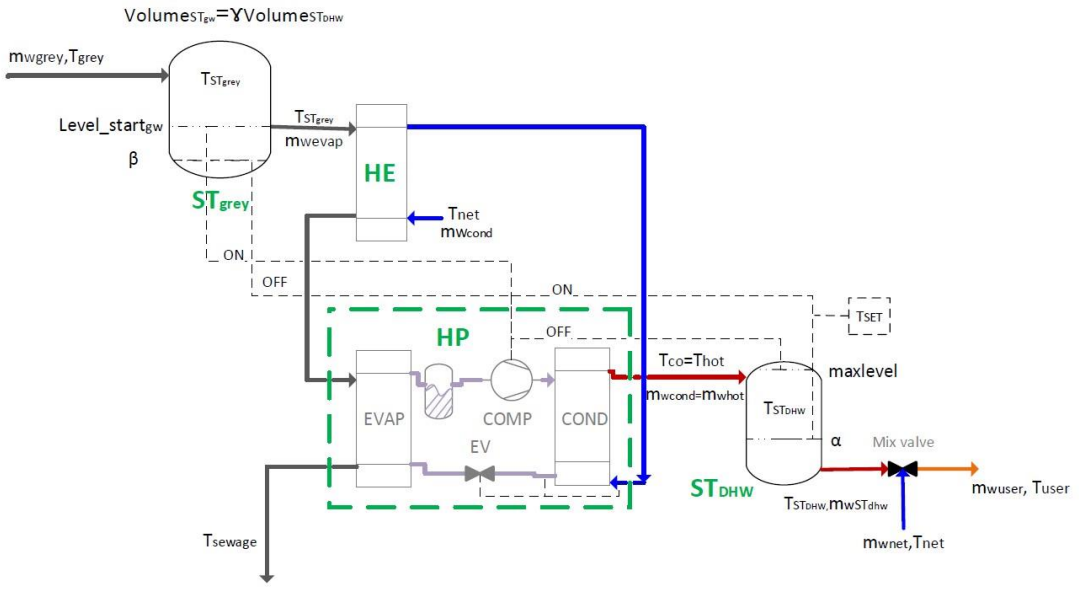

Figure 3: Lay-out of the system and average temperature conditions.

The main components of the system modelled are:

- Grey water storage tank (ST_{gw}): The variable volume storage tank modelled in Type 39 has been used. The size of the tank (Vol_{grey}) is one of the optimization parameters to minimize CO2 emissions.
  As conservative case, a geometric configuration that favours stratification has been used, that is H/D=4. The heat loss coefficient has been set to the one required by the Spanish legislation for DHW production, *RITE 07 IT 1.2.4.2.1.2,* that is 0.8W/m2K. An ambient temperature of 20°C is set for all the simulations, as it is a typical value inside the houses through the year.
- Heat recovery heat exchanger (HE): Heat exchanger with an effectivity of 0.75 (type 5b). This heat exchanger will allow a first energy recovery.
- Water to water subcooled heat pump (SHP): This type contains a validated model of the subcooled heat pump [12].Due to its especial characteristics, a common HP type does not represent its behaviour properly and a new type was required. For further details about the developed type, the reader is referred to [23].

Figure 4 shows the main inputs and outputs of the HP type.

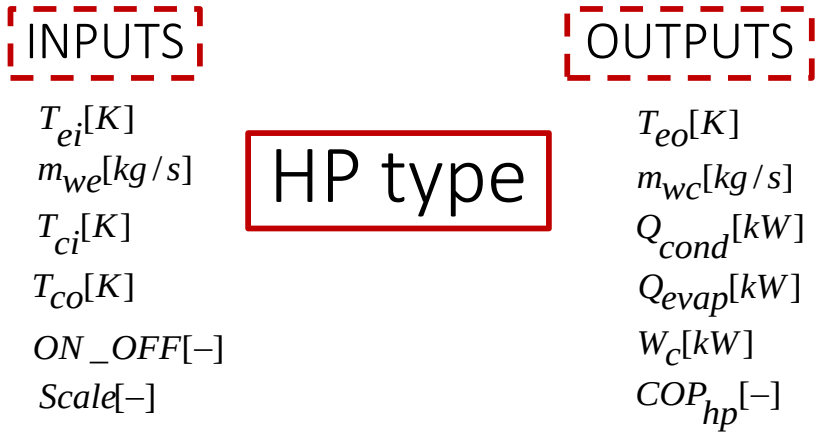

Figure 4: Inputs and outputs of the HP type

- DHW Storage tank (ST_{DHW}): For DHW Type 39 has also been used. As it is the case in STgw, the size of the tank (Vol_{DHW}) is one of the optimization parameters to minimize emissions. The same insulation, geometry and characteristics used in the storage tank for grey water have been set in this case.
- Auxiliary water pumps and circuits: Types 742 with an efficiency of 0.3. Only the pressure drop of the heat exchangers were considered in order to evaluate their consumption.

The simulations use a time step of 1 minute (because of the profile characteristics longer time steps could due to not size properly the system) and include 1-year simulation period.

Figure 5 represents the main inputs, outputs and optimization parameters of the model. In that scheme, scale is the size of the SHP, Volume is the size of the STDHW, γ indicates the proportion of the ST_{DHW} size and it is used for the STgw size ($Volume_{gw}= \gamma \cdot Volume_{DHW}$). α is the ST_{DHW} level when the heat pump switches on, Tset is the ST_{DHW} temperature, T_{co} is the condenser outlet temperature and C_0 is related to the grey water mass flow rate (evaporator water mass flow rate) as a proportional value of the condenser water mass flow rate.

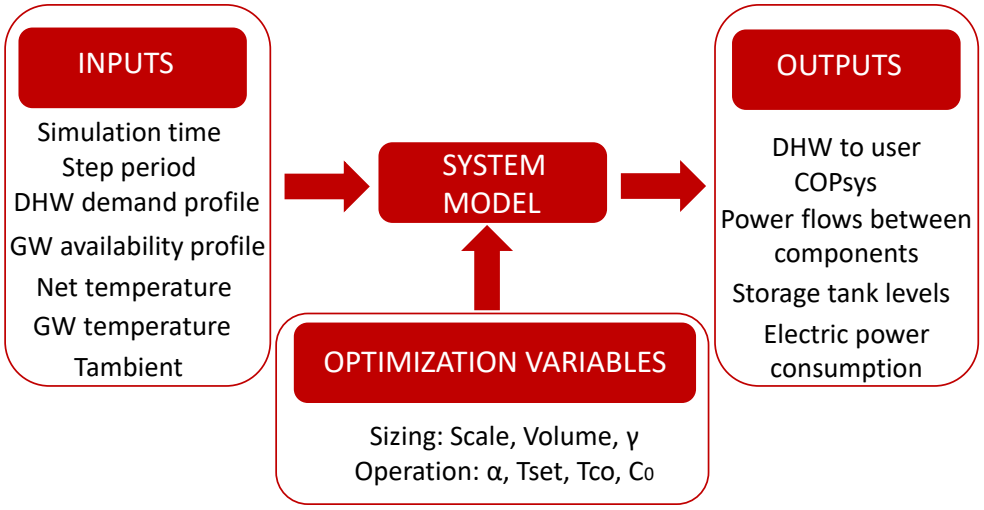

Figure 5: Main inputs, outputs and operation variables of the system.

The performance of the system (COP_{sys}) is calculated according to Eq. 2

$$COP_{sys} = Energy/Electric = \int_{t=0}^{t=simulationtime} (Q_{ST_{DHW\_out}})/(W_{c\_corr} + \sum W_{pumps}) \quad (2)$$

One should notice that the "useful energy" supplied by the system is the result of the heat exchanged in the HE and the heating capacity of the HP after the ST losses.

- *Control of the system*

As it is mentioned in [23], the main irreversibility is introduced by the ST. In this case, since there are two storage tanks, the operation control in order to minimize irreversibility (maximize efficiency) may rely on both components.

The ST_{DHW} temperature is higher than in the ST_{gw} resulting in higher losses. That is, the control is based on the minimization of the time that the water is stored in the ST_{DHW}. Hence, the ST_{gw} should have enough water in order to allow the system to operate. Based on it, the control algorithm is based in the following points:

- Switching on the HP when a minimum level of water is reached in the STDHW (α, it is the optimization parameter) or when T_{STDHW} is lower than a predefined T_{SET}. In addition, a maximum number of HP 9 starts for one hour to ensure the HP durability has been implemented.

- Once the heat pump is running it stops when the water in the ST_{DHW} reaches a predefined level (maxlevel).

- In order to do not incur in more than 9 starts per hour, to soften the peaks and to ensure at least 30 minutes of the heat pump working continuously, a minimum level of the grey water in its tank has been set according to Eq. 3. to start up the heat pump:

$$level\_start_{gw} = {30 \cdot m_{w\_evap}}/{\rho_w} = {30 \cdot C_0 \cdot m_{w\_cond}}/{\rho_w} \quad (3)$$

Where ρ_w is the water density (considered 1000 kg/m3). Notice that in this case, the initial volume is set to this level and that the one-minute scale allows introducing this type of control without significantly penalize the ST size.

- A minimum level of the ST_{gw} to guarantee the production is required, if the level in the tank is lower than this value the HP will be switched off. Therefore, the minimum volume of this tank will be limited by the production of grey water in one time-step. As safety coefficient of 3 has been employed. Eq. 4 shows the minimum volume of the ST_{gw}.

$$\beta = {3 \cdot m_{w\_evap}}/{\rho_w} = {3 \cdot C_0 \cdot m_{w\_cond}}/{\rho_w} \quad (4)$$

Therefore, the control of the heat pump is based on the tank level and temperature of the water within the ST_{DHW} (α, T_{STDHW}) and the availability of a minimum water volume to run the heat pump ($level\_start_{gw}$) and a minimum level (β) in the ST_{gw}.

Figure 6 shows the scheme of the control strategy implemented. Where t is the minute simulation time within each hour, $T_{ST,}$ *Level,* α*, Vol,* T_{SET} *and maxlevel* refer to the DHW storage tank while subscript *gw* is used for conditions related to the grey water storage tank. It should be pointed out that once the HP is operating and while there is enough availability on the grey water storage tank, it keeps in the ON mode until the maximum level of the tank is reached or, in case it was already at that level, it keeps recirculating until the set point temperature (Tset) is reached.

The used comfort criteria are based in two conditions, satisfy the demand 99% of the time and do not allow more than one-minute shortage at the same hour daily. The second condition is added in order to consider the user satisfaction characteristics of this type of hot water demand.

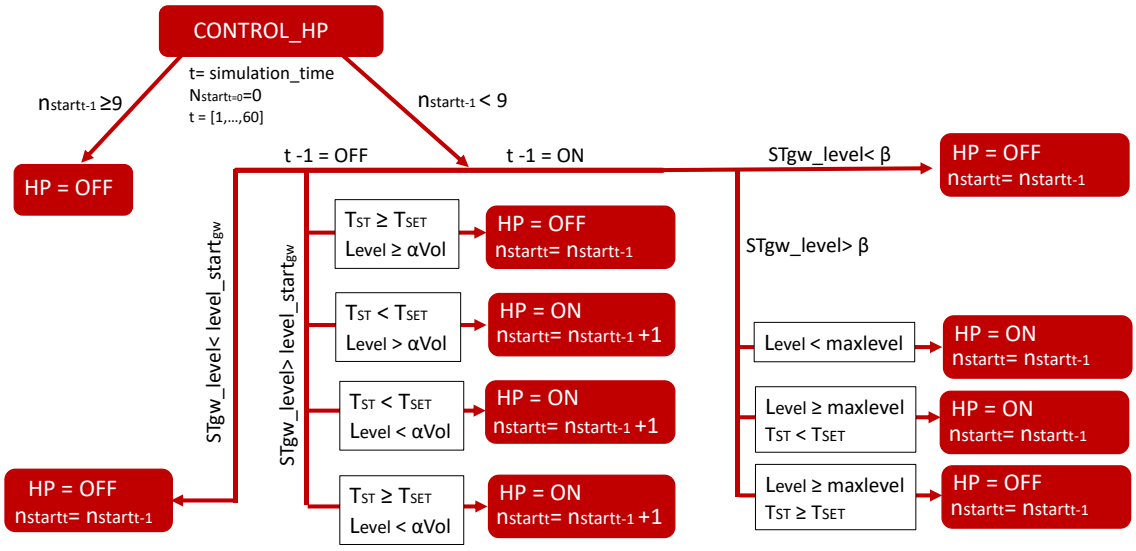

Figure 6: System control strategy implemented each hour of the simulation time. Subscript gw refers to grey water storage tank and no subscript to the DHW storage tank.

7.5 Grey water heat recovery potencial

In this work, the energy available for recovery is going to be considered as the energy that can be extracted from the grey water until it reaches the value of 0ºC (2ºC for safety). In a more precise way, only the energy extracted from the grey water until it reaches a value equal to tap water can be considered as recovered energy. However, the authors have considered that clean water can not be used as a heat source and based on that, the potential use of grey water as a heat source has been considered until it is exhausted.

Eq. 5 shows the heat recovery capacity from the grey water in terms of energy.

$$Q_{grey} = m_{w\_grey} \cdot cp \cdot (T_{grey} - T_{sewage}) \quad (5)$$

Where T_{grey} is the grey water temperature, T_{sewage} the temperature at which the water is thrown to the sewage and m_{w_grey} the grey water mass flow rate. Hence, the potential of the heat source would be function of these three variables.

DHW flow rate is the main composer of the grey water. In fact, in this work 63% of the grey water comes from DHW appliances independently of the external conditions. Therefore, the available grey water mass flow rate can be related to the hot water consumption at 45°C according to Eq. 6.

$$m_{w\_grey} \approx (1/0.63) \cdot m_{w\_user} \quad (6)$$

Furthermore, according to the first law of thermodynamics, the energy required by the user should equal the energy stored in the ST_{DHW} as it is described in Eq. 7.

$$Q_{user} = m_{w\_user} \cdot cp \cdot (T_{user} - T_{net}) = m_{w\_hot} \cdot cp \cdot (T_{ST\,DHW} - T_{net}) \quad (7)$$

Assuming a constant heating capacity of the water, the ratio of Eq. 8 is obtained.

$$\frac{m_{w\_user}}{m_{w\_hot}} = \frac{(T_{ST\,DHW} - T_{net})}{(T_{user} - T_{net})} \approx \frac{0.63 \cdot m_{w\_grey}}{m_{w\_hot}} \quad (8)$$

In general, the grey water mass flow rate can be expressed as a proportion of DHW as it is showed in Eq.9.

$$m_{w\_grey} \approx \lambda \frac{(T_{ST\,DHW} - T_{net})}{(T_{user} - T_{net})} \cdot m_{w\_hot} = C_0 \cdot m_{w\_hot} \quad (9)$$

Ideal heat recuperation with a standalone heat pump

The 2nd law of thermodynamics gives a restriction in the amount of heat that can be pumped from a heat source at a temperature T_1 to a hot sink at a temperature T_2 where $T_2 > T_1$. Based on that limit, the limits of a heating process are set by the condition $Q_{heating} = Q_{recovered} + W_{cl}$ where W_{cl} is the minimum work required calculated using as a reference the ideal Lorenz cycle (this cycle is selected as a reference because of the heat source and sink can change their temperatures). W_{cl} would be 0 only if the thermal levels of the sink and the source allow the direct heat transfer but not in general.

From this equality, the ideal limits of maximum recuperation, C_{0i}, are obtained according to Eq. 10.

$$C_{0i} = \frac{(T_{hot} - T_{net})}{(T_{grey} - T_{sewage})} \left(1 - \frac{1}{COP_{Lorenz}}\right) \quad (10)$$

Where COP_{lorenz} is the Coefficient of Performance of Lorenz, it limits the maximum efficiency of the heating process considered [58] and it is given by Eq. (11).

$$COP_{Lorenz} = \frac{1}{1 - \overline{T_C}/\overline{T_H}} \quad (11)$$

Where $\overline{T_H}$ and $\overline{T_C}$ are the entropy averaged temperatures. For a constant capacitance and pressure process, the temperatures can be written as in Eq. 12and Eq. 13.

$$\overline{T_H} = \frac{T_{hot} - T_{net}}{ln(T_{hot}/T_{net})} \quad (12)$$

$$\overline{T_C} = \frac{T_{grey} - T_{sewage}}{ln(T_{grey}/T_{sewage})} \quad (13)$$

Where T_{hot} is the hot water temperature required in the heating process, (64°C in this case).

These would be the theoretical ideal limits based on the second law of thermodynamics. Notice that from the recovery point of view it is convenient to increase as much as possible the m_{w_grey} as higher values of it result in higher values of $\overline{T_C}$. From this analysis, if the real mass flow ratio available, $C_0 \geq C_{0i}$, all the water heating can be satisfied with energy recovered from the grey source and if C_0 is < C_{0i} in order to satisfy the demand part of the energy must be generated by other alternatives.

Nevertheless, once we define the heat pump that is going to be used to recover the wasted energy, the COP of the system would be lower, and the energy balance can be expressed as $Q_{heating}=Q_{recovered} + W_{cl}+W_{ci}$. Where W_{ci} is the additional heating that is introduced by irreversibility, and it is not the result of any thermodynamic heat pumped but it is just heat produced and added to the system (or it can be seen as a heat produced with a COP=1). It can be calculated as:

$$W_{ci} = \left(\frac{1}{COP_{HP}} - \frac{1}{COP_{Lorenz}}\right) Q_{heating}$$

It is suitable to generalize the concept of $Q_{recovered}$ to $Q'_{recovered}$ where $Q'_{recovered}= Q_{recovered} + W_{cl}$ as W_{cl} is intrinsically bounded to the heat recovery process itself

Finally, the real heat recovery limit would be given by C_{0r}:

$$C_{0r} = C_{0i} \frac{\left(1 - \frac{1}{COP_{HP}}\right)}{\left(1 - \frac{1}{COP_{Lorenz}}\right)} \quad (14)$$

Where COP_{HP} is the COP of the heat pump.

Based on the values of these C parameters Figure 7 represents a design criteria for heat recovery based on heat pumps. A deeper explanation about how to obtain that scheme has been placed as appendix.

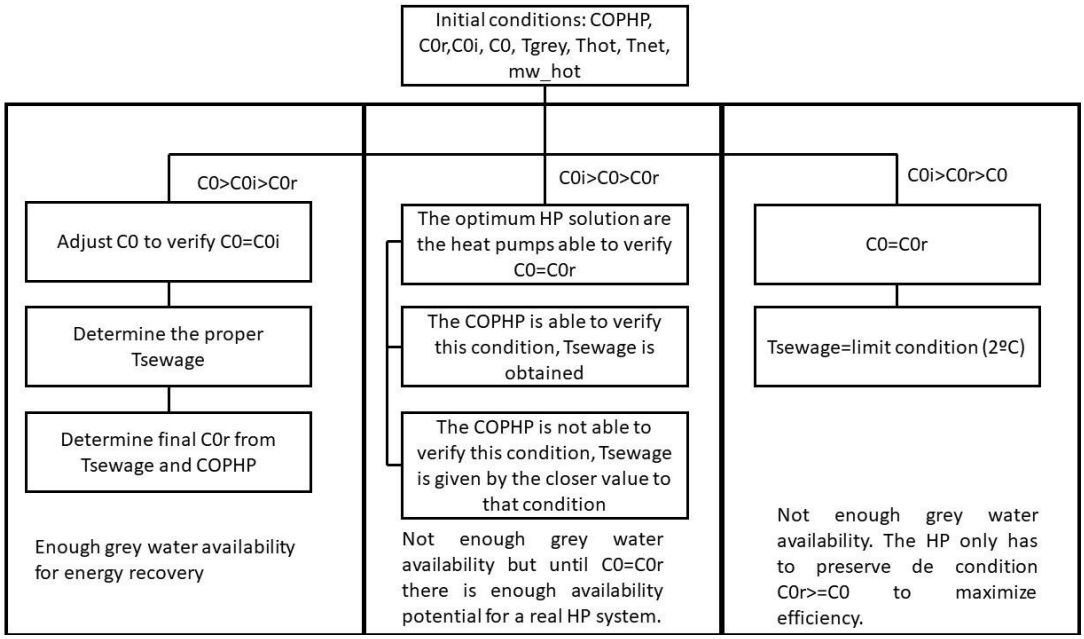

Figure 7: Design scheme developed for heat recuperation systems

According to Figure 7, when the availability of grey water is limited, the most efficient solution is not always for the maximum m_{w_grey}. In fact, if $\mathbf{C_0>C_{0i}}$ it is convenient to point out here that in order to maximize the recovery potential, the m_{w_grey} required in the real system is obtained by the temperature T_{sewage} obtained when the condition $\mathbf{C_0=C_{0i}}$ is satisfied. This point is important overall when the availability of grey water is finite/restricted as minimizes the use of grey water for the same efficiency and allows its use in other applications.

Because of the used profiles, in this work all the analyzed situations are going to be in the frame of the situations $C_0>C_{0i}$.

Optimum heat recuperation based on heat pump systems

Until this point, the potential of heat recovery has been analysed from the point of view of the 1st principle (direct recovery) and of the 2nd principle (pumping recovery). However, the most common situation is to have thermal levels that allow initially a direct heat recovery up to certain temperature level and later, a pumping heat recovery must be applied to satisfy the demand requirements. Therefore, the most efficient configuration in this type of application is to install a heat exchanger + heat pump.

In order to gain insight in the order of magnitude of the relative importance of each component and to obtain a first estimation of the potential energy savings, for

the application under study, the percentage of heat produced by each component has been evaluated.

The heat recovery potential of the HE can be obtained by:

$$Q_{heating\_from\_rec}[\%] = \frac{m_{w\_hot} \cdot cp \cdot (T_{ci} - T_{net})}{m_{w\_hot} \cdot cp \cdot (T_{hot} - T_{net})} = \frac{(T_{grey} - 5 - T_{net})}{(64 - T_{net})} \quad (15)$$

Where T_{ci} is the inlet water temperature at the condenser and has been obtained from the design assumption of 5K as the temperature approach (temperature difference between the grey water temperature and the cold-water outlet temperature).

In a heat exchanger with a temperature approach of 5K, Figure 8 depicts the maximum percentage of the energy supplied by the HE in order to heat a water stream from Tnet to 64°C from the recovery of a heat source at T_{grey}.

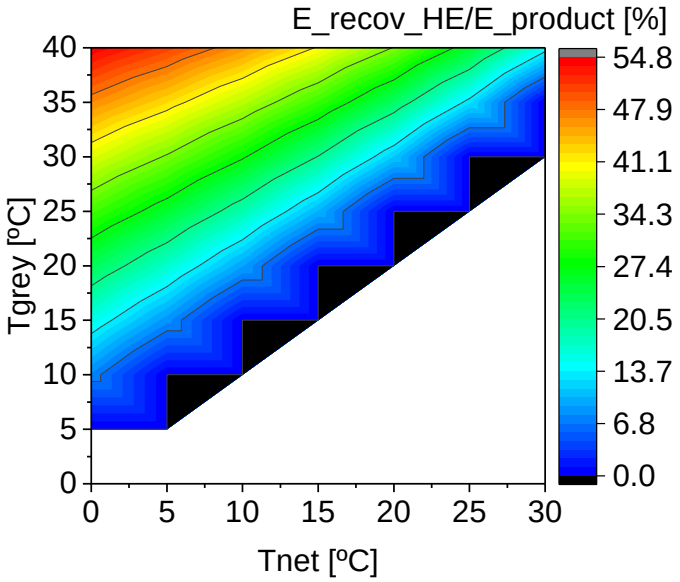

Figure 8: Maximum % of demand energy recuperated from the available grey water in the HE

According to Figure 8, the pre-heater HE represents a significant portion of total energy supplied to the system. For instance, for an average condition of T_{net}=10°C and T_{grey}=33°C, the demanded energy that can be obtained from the HE is 33%.

7.6 Performed study

Three cases based on the grey water conditions have been investigated and compared:

1. Infinite availability of grey water.
2. Finite availability of grey water and constant in time
3. Finite availability of grey water and no constant in time

According to [23], there is a set of system combination (size of the system components) resulting in similar performances. Among all the optimal combinations, the solution corresponding to the smaller heat pump size (scale) and the solution with the smaller ST sizes (ST_{DHW}) will be analyzed in more detail. Grey water amount available along the year is considered the same for the case 2 and 3 but in the case 2 the grey water is distributed uniformly for all the hours of the year and in the case 3 it is distributed according the profiles defined in section 7.2. Table 3 shows the main inputs, variables used for limited mwgr availability based on the profiles of T_{net}, T_{grey} and mw_{grey} presented in the methodology section.

CASE 1: Infinite availability of grey water

This case will define the base case in order to evaluate constrains imposed by limitations in the heat availability for the rest of the analysis. The methodology followed in [23] has been used. Notice that infinite availability of the heat source leads to the absence of the ST_{grey} and its derived variables.

The greywater mass flow rate (m_{wgrey}) used has been calculated according to the methodology of the previous section, C_0. Considering mean water temperatures of: T_{grey}=33ºC and T_{net}=10ºC, COP_{hp} is 5.96 (T_{co} =64ºC), $C_0=\infty$, (Eq. 14) C_{0i}=10.4 and C_{0r}= 8.9 for T_{sewage}=2ºC. That is, $C_0>C_{0i}>C_{0r}$ what indicates enough availability according to Figure 7 and C_0 is adjusted to 10 in order to have a grey water temperature lift at the evaporator of 4.5K.

With these definitions for m_{wgrey} , parametric studies have been done in order to obtain the map of possible solutions and the set of optimal combinations (heat pump size, capacity of the ST_{DHW}, alpha) that lead to minimum CO2 emissions satisfying the DHW demand under the comfort levels and operating constrains required.

Figure 9 shows the parametric studies performed over the different design alternatives (heat pump size, storage tank size and control algorithm) for the

available grey heat source (optimal m_{wevap}). This matrix comprises more than 4000 simulations.

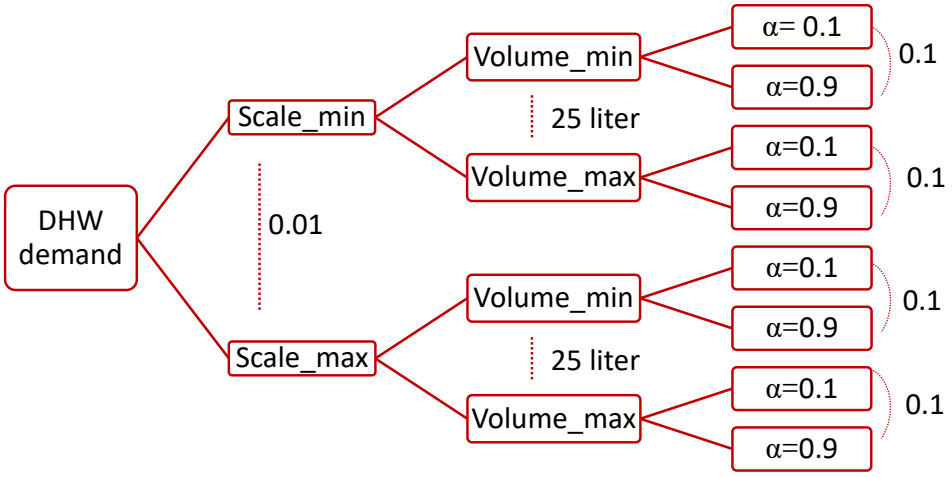

Figure 9: Parametric studies performed for available grey heat source based on variations of 0.01 in the scale of heating capacity, of 25liter in the ST_{DHW} tank and of 0.1 in α.

Where:

- *Scale* variation range: has been expressed in terms of heating capacity (Q_{cond}) in results. It ranges from the minimum size that meets discomfort requirements to the size that belongs a minimum of 1.5 hour per day operating time. In 0.01 steps.
- *Volume* variation range: for each heating capacity, the maximum and minimum ST size that meet discomfort levels are investigated. In 25 liter steps.
- *Alpha (α)* variation range: for each ST size, the variation of the control level in terms of a volume percentage, goes from 0.1 to 0.9. In 0.1 steps.

CASE 2: Finite availability of grey water and constant in time

In the case studied, the limitation of the grey water availability corresponds to a mean average ratio of C_0=2.27 (Eq. 9), C_{0i}=1.63 and C_{0r}=1.45 obtained from the mean net water temperature, T_{net}=10°C and the mean grey water temperature of T_{gw}=33ºC, T_{sewage}= 2°C calculated in the same way as in the previous case. In this case, the situation is $C_0 > C_{0i} > C_{0r}$, hence, there should be enough energy from grey water to satisfy the DHW demand.

The same parametric studies shown in Figure 9 have been performed.

In order to compare this case with the case 1, two situations have been analysed quantitatively.

1. Case 2a: Solution with minimum heat pump size (scale factor).
2. Case 2b: Solution with minimum ST_{DHW}.

CASE 3: Finite and not constant availability of grey water

Real applications introduce variability in three ways: time, temperature and quantity. This situation adds complexity to the system and require the introduction of a new element, the ST_{gw}.

The main target of this study consists of, on the one hand, the definition of the coupling of all the system components considering dynamic and real conditions from the system point of view and on the other hand, of the determination of the impact on the system efficiency of these restrictions in the available energy compared to the previous cases.

Based on the design criteria used to size the different components, two subcases will be analysed in this part:

1. *System design based on a constant profile of waste water*

The system designed for the case 2 is not able to satisfy the DHW demand under the variable m_{gw} conditions. Hence, the size of the system is performed following the same methodology of case 2 but in this case, the design temperatures correspond to the worst expected conditions along the year (T_{net}=7ºC and T_{grey}=25ºC). The available m_{gw} is the mean value of the grey water produced along the day.

The tandem HP-ST_{DHW} is sized according to these conditions. In this case, it is necessary to include in the design the ST_{gw} in order to respond to the variable m_{wgr} production. This component is dimensioned as: $Volume_{STgw}=\gamma \cdot Volume_{STDHW}$. The design conditions were changed from the considered in case 2 as with those conditions the system was not able to satisfy the confort criteria when the system was working with variable m_{wgr}.

The worst condition for $Volume_{STgw}$ is obtained with highest minimum level of ST_{gw} and lowest *minimum_level* of ST_{DHW}. In this case, the critical conditions to size the ST_{gw} are: C_0=2.33, α=0 and a 30 min of availability according to Eq. 9. That is, γ=2.5.

Two solutions are analyzed for this case:

1. Case 3a: Solution with minimum heat pump size (scale factor).
2. Case 3b: Solution with minimum ST_{dhw}.

System design based on a real profile of waste water

The system has been optimized in order to satisfy the real profiles of the waste water and of the net water temperature. This optimization is based mainly on:

- C_0 control:

  According to Figure 7, heating processes based on finite sinks/sources have better performance with greater heat source mass flow rates (m_{wgrey}) when (C_0>C_{0i}>C_{0r}) as it is the case. Thus, C_0 is optimized in order to maximize the use of m_{wgrey}.

- α control:

The minimum α capable to satisfy the demand is the one that ensures that the water remains the shortest time in the DHW tank. Thus, this value has been determined out of simulation parametric cases for the components size and α.

Table 3: Main inputs used in each case. Grey cases correspond to cases where the conditions used for the design/size of the different components of the system where different from the conditions used for the simulations.

		T_{net} [°C]	T_{gw} [°C]	GW_{avail}	C_0 [-]
1	Infinite grey	10	33	∞	10
2a	Finite, $Scale_{min}$	10	33	Constant	2.27
2b	Finite, ST_{dhwmin}	10	33	Constant	2.27
3a	Design cond. $Scale_{min}$	7	25	Constant	2.33
3b	Design cond. ST_{dhwmin}	7	25	Constant	2.33
3c	Real cond. $Scale_{min}$	Profile	Profile	Profile	Opt.
3d	Real cond. ST_{dhwmin}	Profile	Profile	Profile	Opt.

7.7 Results

This section shows the results obtained from the study of the cases explained in the previous section. The section has been structured in three parts in such a way that, first, the feasible set of combinations for each case are detailed, then, the most representative results are collected in Table 4 hence a comparison among them can be performed in a clear way, and finally, a detailed analysis of the obtained results for the case 3 is presented.

- **CASE 1: Infinite availability of grey water**

Figure 10 depicts the possible sizes combinations for the optimal α that meet the discomfort standards described in the methodology section. Figure 10a refers at the operating hours, Figure 10b to the COP of the system and Figure 10c to the associated CO_2 emissions.

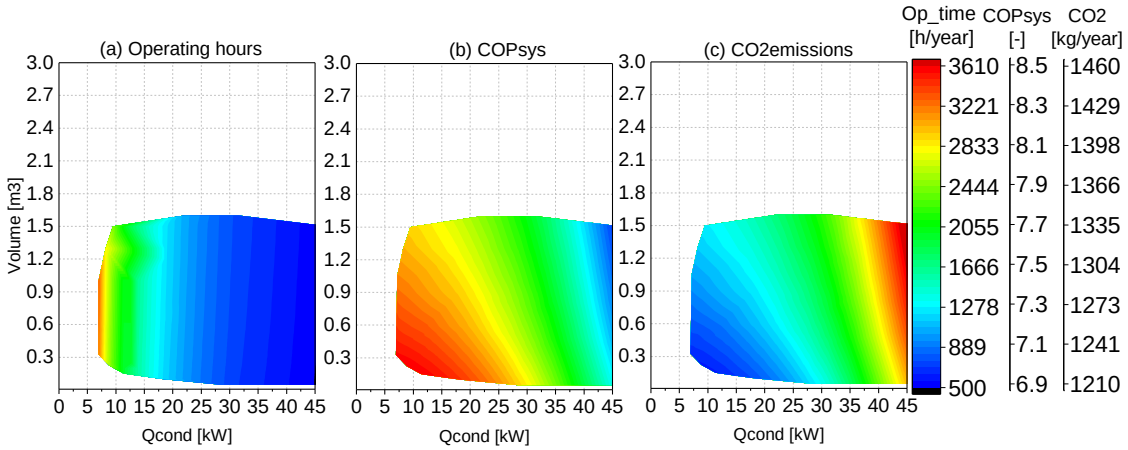

Figure 10: Annual operating hours, COP of the system and CO2 emissions associated to an infinite available grey water heat source and the optimal alpha.

According to Figure 11, low-temperature heat sources recuperation has a great potential to DHW production applications. There is a wide range of combination HP-ST_{DHW} that result in similar CO_2 emissions (around 1230kg/year) and that are capable to operate under COPs up to 8.5 with operating hours around 2200 hours (6h/day). According to figures 10 b) and c) best combinations are found for small heat pumps and small DHW storage tanks. The figure also shows that as the size of the heat pump is reduced, the size of the storage tank increases and there is a minimum size for the tank and for the heat pump which allows to satisfy the DHW

demand. From all these combinations, the minimum CO_2 emissions value is obtained for α=0.5, Scale=0.15 (heating capacity of 9.42kW) and a ST_{DHW}=250liter.

To be able to compare numerically the results obtained for each case, that case has been taken as a base case out of all the possible best combinations. These results are presented in table 4.

- **CASE 2: Finite availability of grey water**

This case corresponds with the assumption that grey water is generated uniformly during the year and the total amount generated is the same that the one obtained using the grey water profiles defined in section 7.2. Additionally, the water temperature conditions are the same as case 1.

Figure 11 shows the possible ST-HP combinations for the optimal α that meet the discomfort standards described in the methodology section when limiting grey water to the considered availability. Figure 11a refers at the operating hours, Figure 11b to the COP of the system and Figure 11c to the associated CO_2 emissions.

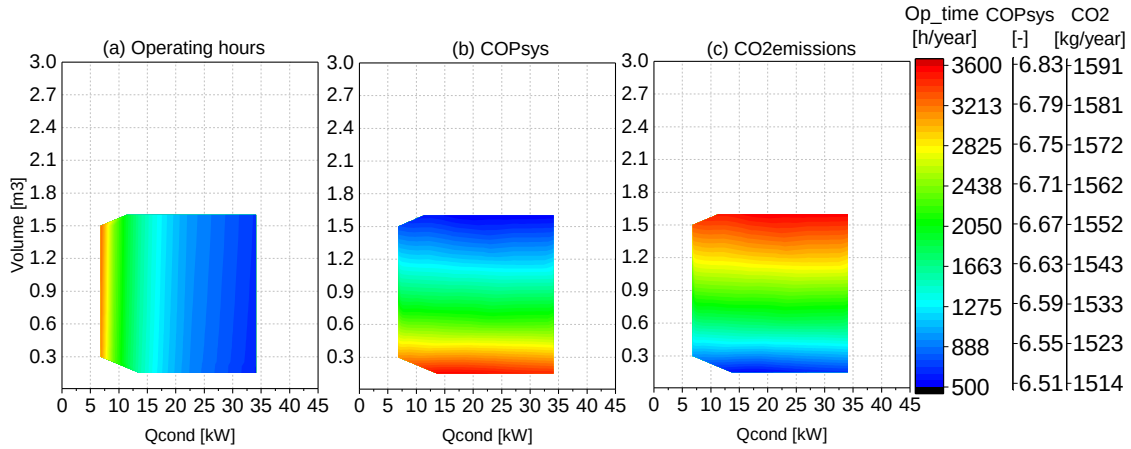

Figure 11 Annual operating hours, COP of the system and CO2 emissions associated to a finite available grey water heat source and the optimal alpha.

In this case, the reference combination obtained with optimal m_{wgrey} does not meet comfort standards. Instead, higher ST and/or heating capacities are required. Furthermore, the limitation of m_{wgrey}, lead to small COP variations with the increase of the heating capacity (for a given ST_{DHW} size). The ST_{DHW} size the most influent variable on the performance.

According to Figure 11 and Figure 12, from the comparison of the optimal solutions in both systems (the combination with minimum CO_2 strictly), the

limitation of the available grey water results in a reduction in the COP of the system up to 20%.

In order to compare from a quantitative point of view the obtained results. Table 4 presents the numerical values for case 2a (solution with the minimum heat pump size) and case 2b (solution with the minimum ST size). In this table, for the case 2a the heating capacity is reduced due to a COP_{hp} loss and the solution results in higher ST_{DHW} and CO_2 emissions. For case 2b, the heat pump size is significantly bigger, and a 23% increase of CO_2 emissions is obtained.

- **CASE 3: Finite and variable availability of grey water**

In order to design these systems, similar results to the ones shown in Figures 11 and 12 were obtained from the parametric studies performed in cases 3a and 3b. The same situation is found once the system is adapted to the real profiles and results considering the adaptation to the profiles for the minimum HP size (case 3c) and the minimum ST_{DHW} and STgw sizes (case 3d). Table 4 collects the most important results of each case.

Table 4: STgw-HP-STdhw optimal combinations for infinite availability of the heat source, finite availability but constant, and finite and variable availability.

		Scale [-]	Heating capacity [kW]	ST_{DHW} [liter]	ST_{gw} [liter]	α [-]	COPsys [-]	Annual Operating hours [h]	Annual emissions [kgCO2]
1	Infinite grey	0.15	9.42	250	-	0.5	8.49	2310	1219.4
2a	Finite, $Scale_{min}$	0.15	6.9	300	-	0.9	6.85	3100	1510.9
2b	Finite, ST_{dhwmin}	0.2	9.08	250	-	0.9	6.8	2351	1522.6
3a	Design cond. $Scale_{min}$	0.15	6.06	500	1250	0.9	5.68	4261	1970.6
3b	Design cond. ST_{dhwmin}	0.25	10.09	350	875	0.9	5.73	2541	1959.6
3c	Real cond. $Scale_{min}$	0.15	6.81	500	1250	0.9	6.67	3175	1540.3
3d	Real cond. ST_{dhwmin}	0.25	11.38	350	875	0.5	6.72	1890	1529.1

According to Table 4, the consideration of real profiles (demand, temperatures and grey water availability) with a design based on extreme constant conditions, cases 3a-3b leads to a solution with higher sizes of the main components and the performance of the system decreases in more than 30% compared to case 1 and 20% compared to case 2. However, once the design is dynamically adapted to the variable conditions (cases 3c-3d), the loss of efficiency diminishes to 2% compared to Case 2. As it has been commented previously it is convenient to remark that the system of the case 2 is not able to satisfy the DHW demand under the variable m_{gw} conditions of the case 3. However, once the design is dynamically adapted to the variable conditions (cases 3c-3d), the difference in COPsys between case 2 and case 3 is lower than 2%. This fact reveals that with a proper system design, the variability in the availability of m_{gw} does not have a huge impact on the final system efficiency.

High values of optimal α allow the reduction of the ST_{gw} γ_{min} parameter, while low-medium values require the design condition of γ_{min}.

In order to understand properly the dynamics of a real optimized system, later, the results of case 3d are going to be analyzed deepply:

Figure 12 shows the levels and temperatures of the water stored in both tanks for a one-minute time scale and annual simulation. Figure 12a represents in grey the evolution of the level of the grey water with time within the ST_{gw} and in red the evolution of the level of the hot water with time within the ST_{DHW}. Figure 12b represents in grey the evolution of the stored grey water temperature with time within the ST_{gw} and in blue the stored grey water temperature evolution of the level of the hot water with time within the ST_{DHW}.

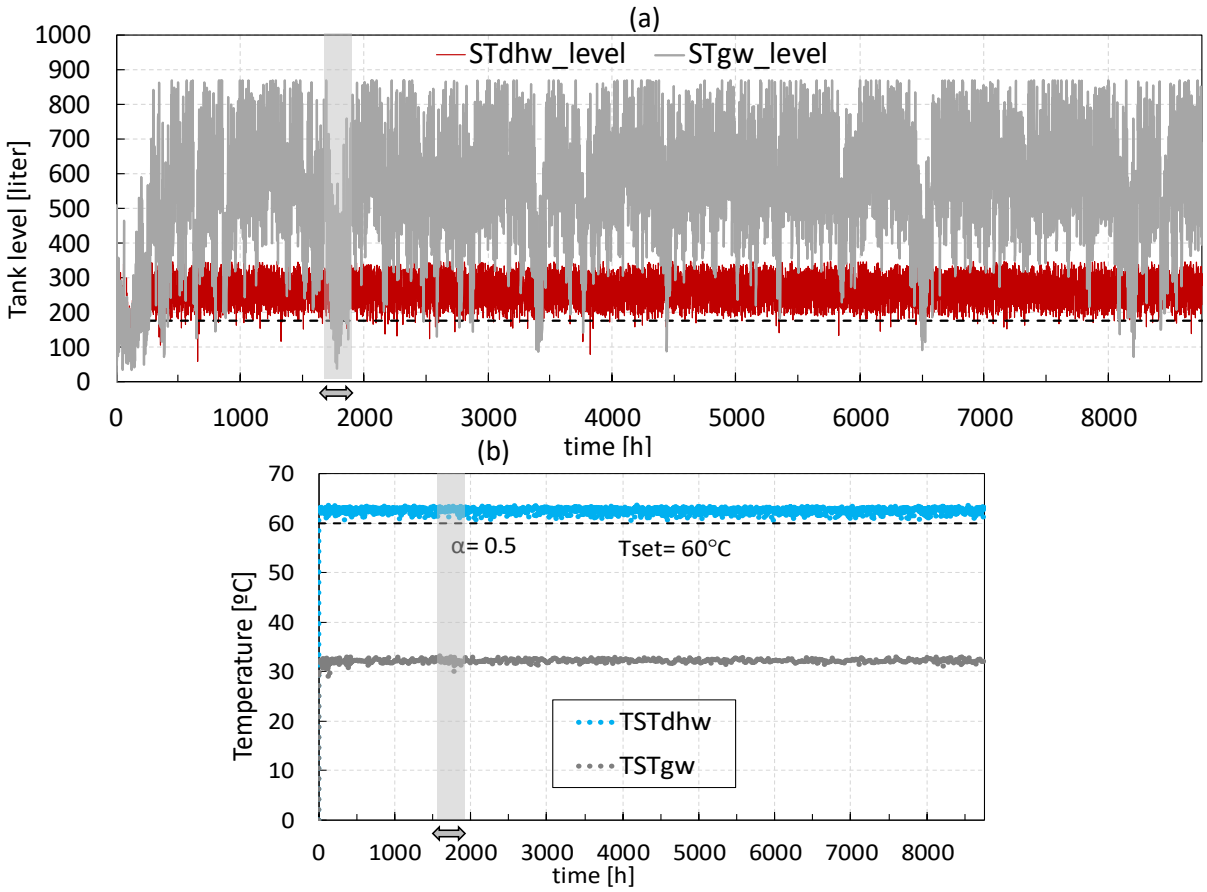

Figure 12: STgw, ST_{DHW}, Tstgw, Tstdhw for one-minute time scale annual simulations and the optimal solution (case 3d).

As it can be seen in Figure 12 the temperature on the ST_{DHW} never falls below 60°C (design requirement) and the temperature of ST_{gw} never falls from 25°C (non-stationary design requirement).

In order to appreciate in more detail the behaviour of both ST, Figure 13 shows for period of 48h, the levels, temperatures and mass flow rates inlets/outlets. Figure 13a represents the stored water mass flow rate balance in the ST_{DHW}. Red color indicates the inlet water temperature (from the condenser), blue color represents the required water flow rate from the demand and dotted-filled black patter is employed in order to represent the water mass flow rate leaving the ST_{DHW}. Figure 13b represents the temperature and the level evolution of the stored water mass in the ST_{DHW}. Red color corresponds to the level and blue dotes are used for the hourly-average temperature. Figure 13c represents the stored water mass flow rate balance in the ST_{gw}. Orange color indicates the inlet water temperature (from the drain), line-filled black patter is employed represents the required water flow rate from the heat pump operation and grey color represent the water mass

flow rate leaving the ST_{DHW}. Figure 13d represents the temperature and level evolution of the stored water mass in the ST_{gw}. Grey color corresponds to the level and green dotes are used for the hourly-average temperature.

From Figure 13a, one can see how the demand is always satisfied. The level of the stored water in STD_{HW} does not fall below the control (α, T_{set}=60°C) and the operation is driven by ST_{DHW} even with the most critical conditions of grey water availability.

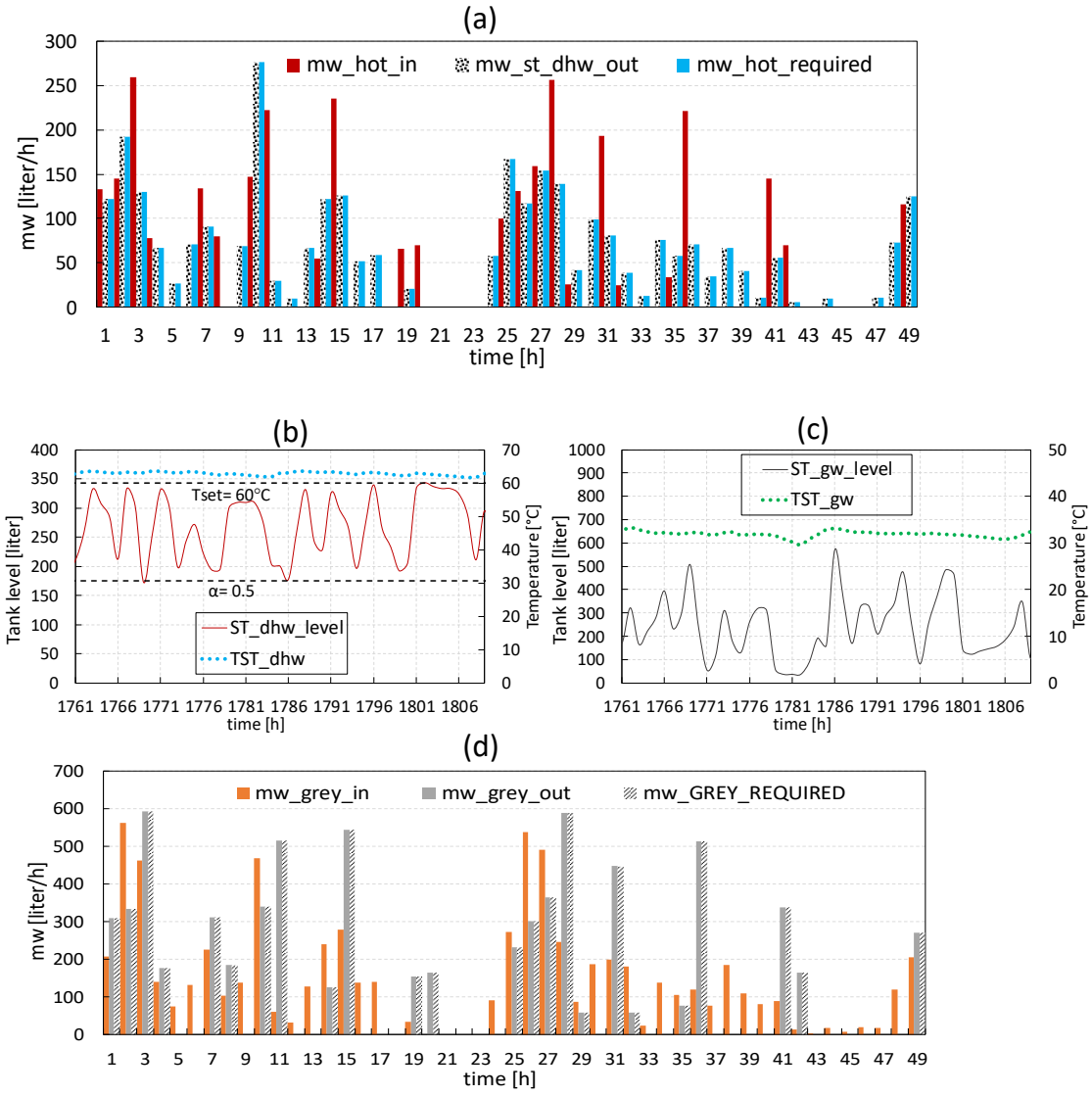

Figure 13: 48h STs Behavior in terms of mass flow rates, temperatures and level of the water stored.

Figure 14 represents monthly energy and efficiency values. Figure 14a contains the energy information. Columns in red represent the monthly heating energy supplied by the HP, columns in line-filled black pattern represent the heating energy supplied by the HE. Grey line represents the energy demanded by the user and dotted blue lines has been used to represent the final energy supplied to the user. Figure 14b shows the monthly average efficiency. Blue dotes are used for the system (COP_{sys}) and red triangles for the heat pump (COP_{hp}).

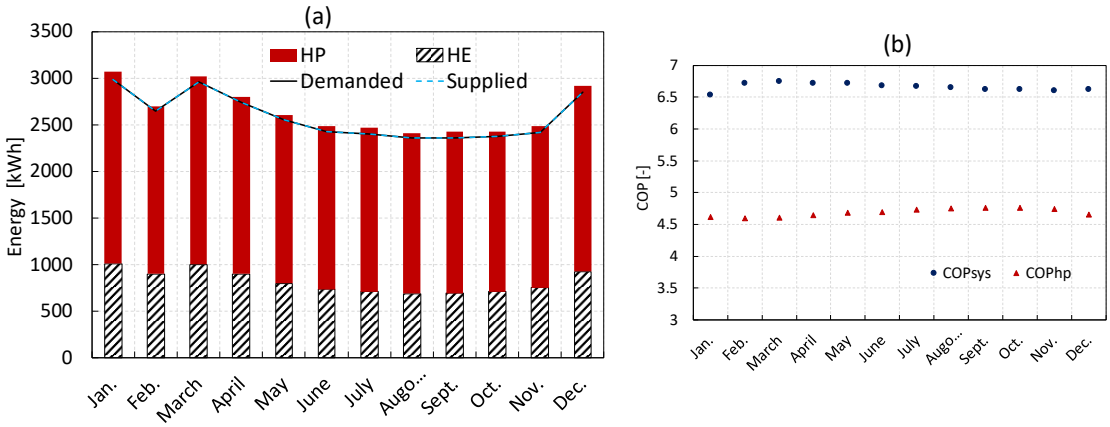

Figure 14: Monthly energy consumption, demand and supply in addition to average heat pump and system performances.

As it can be seen in Figure 14, a significant proportion of the energy used for heating is obtained from HE. The energy obtained from the HE is greater during cold months (results in line to the potentiality seen in Figure). The energy demanded and supplied are superposed indicating that the demand is satisfied by the system in terms of energy. The difference between the energy employed to satisfy the demand and the energy supplied to the user indicate the system losses. The efficiency of the system remains above 6.5 through the year with highest values in cold months, this is a consequence of the fact that the temperature of the grey water does not depend on the season and there is more recovery potential when the tap water is colder. It is also noticeable the fact that in Figure 14b, the optimum in COP_{sys} does not match with the COP_{hp} showing the relevance in the system design of adopting a holistic approach to the system.

Figure 15 contains the main characteristics of the grey water heat source Figure 15a represents the monthly grey water energy extracted by the HP (grey column) and by the HE (line-filled column), the grey energy available in light brown and the percentage of energy extracted from the total available. Figure 15b shows the

temperature of the grey water at the outlet of the evaporator (grey water temperature to the sewage) through the year.

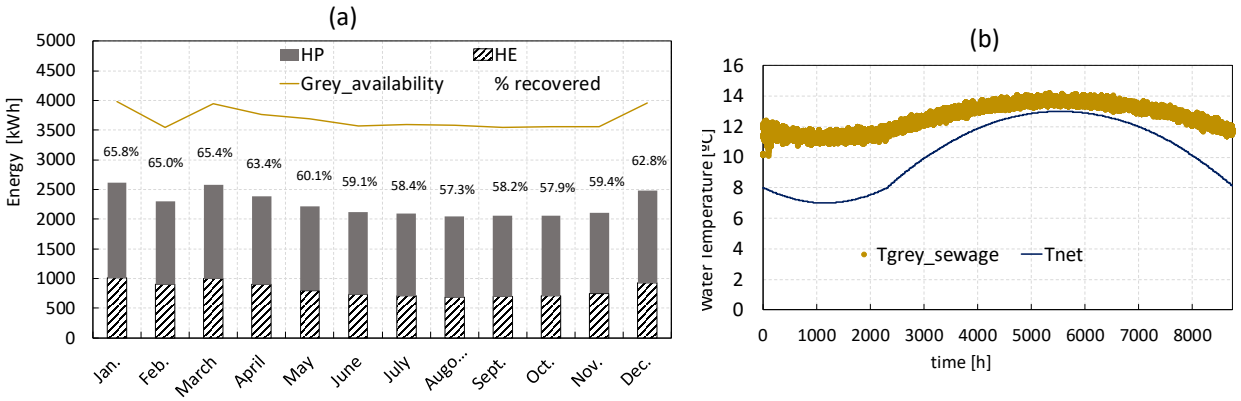

Figure 15: Monthly grey energy recovered and available and final annual grey water outlet temperature (to the sewage).

As it can be seen in Figure 15, a significant heat extraction is done by the HE with slightly seasonal fluctuations. From the available energy to extract (considering the minimum water temperature of the sewage as 2°C), an average extraction of 60% has been enough for the DHW supply. In addition, Figure 15b represents the net water temperature and the temperature of the grey water at the outlet of the SHP, it can be seen that always the $T_{grey\_sewage} > T_{net}$, therefore the system is able to satisfy the DHW demand only with recovered energy from the dwells, in addition Figure 15b also shows that the energy recovery system is more effective during the colder months.

Results highlight the great potential of grey water heat recovery as a heat source for DHW production based on a HE and a HP.

7.8 Conclusions

In this work, the influence of having a limited (and variable) availability of heat source at a given temperature in order to satisfy the demand of DHW has been addressed. In order to do that, a system configuration has been defined to maximize the efficiency of the recovery potential, this configuration includes not only the system topology which includes a heat exchanger plus a heat pump but also the right design of the heat pump and the accumulation strategy in the water storage tanks.

The obtained results have been systematically compared with the results obtained when this restriction is not present and an optimum system configuration (HE (recuperator)+SHP+ST_{dhw}+ST_{gw}) have been proposed.

This analysis has allowed estimating the variations in energy consumption that could be expected from different design criteria. Finally, a system in order to satisfy the DHW demand of 20 dwellings using their grey water production as a heat source has been analysed in detail.

Regarding to the obtained results, the main conclusions can be summarized as:

- A decrease of 20% in the efficiency could be derived when there is a limitation of the available grey water in terms of average quantity compared with a system in which that availability of heat source water is not limited.

- When there is a not constant availability of grey water, and the system is sized according to the most critical conditions, the energy efficiency of the system could be reduced up to 17%.

- In the previous situation, significantly larger sizes of the components are required in order to satisfy the user comfort levels (for instance, double ST_{DHW} capacities for the minimum HP_{size}).

- The grey water temperature at the outlet of the evaporator is always higher than the net water temperature. Hence, the system is able to satisfy the DHW demand only with energy recovered from the grey water. It should be pointed out that to obtain this result, all the grey water produced by the dwellings must be used and not only the grey water coming from the DHW.

- The advantage of this type of system is higher when the ambient temperatures are lower.

A great potential of grey water used as a heat source for DHW production based on SHP has been demonstrated. When the system is properly designed and adapted to real availability and demand profiles, it is able to supply the required energy for water heating purpose only using only the grey water produced by the dwell with high efficiency. In fact, only with the extraction of 60% of the available energy all the production can be satisfied for the example analyzed in this work and all the used energy is energy recovered from the grey water source.

Finally, it can be said that the defined system topology of the energy recovery system based on heat pumps has been used in this work for the particular case of satisfying the DHW demand using the grey water production in dwellings can be extended to other energy recovery applications as the followed principles are common to other situations and the control algorithm of the used heat pump allows the adaptation of its performance to the temperature differences in the secondary fluids.

7.9 Appendix

In section 7.5, a scheme in order to size properly recovery systems based on heat pumps were supplied in Figure 7. In this appendix, the way in which that scheme was obtained is supplied. Nevertheless, in order to understand properly the different situations that could appear in this kind of systems, a conceptual example based on fixed temperatures is analyzed.

From Equation14, C_{0r} is always lower than C_{0i} (equal only in the ideal case). For a given demand, m_{w_hot} is constant, and in a real system three situations can be found related to m_{w_grey} when the inlet and outlet temperatures of the heat sink and heat source are fixed:

a) **$C_0 > C_{0i} > C_{0r}$:** In this case, there is enough grey water mass flow rate available to recover the required energy to satisfy the demand. m_{w_grey} used would be $m_{w\_grey} = C_{0r} m_{w\_hot}$. The rest of the grey water would not be required by the system to satisfy the demand. Regarding the energy consumption, the additional heat W_{cah} that the user must supply to the system directly (COP=1), is in this case $W_{cah} = W_{ci} = Q_{heating} - Q'_{recovered}$. Even though there is an excess of grey water available it cannot be used to satisfy part of the demand.

b) **$C_{0i} > C_{0r} > C_0$:** In this case there is not enough grey water available to recoverenough energy to satisfy the heating demand. The amount of water that can be heated by heat recovery is given by $m_{w\_hot} = \frac{m_{w\_grey}}{C_{0r}}$ and the rest of the water heating demand must be supplied by other methods. In this case the additional heat that the user has to supply to the system directly is $W_{cah} = W_{ci} + W_{Res}$. Where W_{Res} is a heating capacity that can be supplied by an electrical heater or other alternatives and its value is given by:

$$W_{Res} = (m_{w_{hot}} - \frac{m_{wgrey}}{C_{0r}})(T_{hot} - T_{net}) \quad \text{(A.1)}$$

It is important to point out here that in this case, while the COP_{HP} maintains the condition $\mathbf{C_{0r} > C_0}$, it will not have an influence in the energy consumption of the system. A change in the COP of the heat pump only changes the ratio between W_{ci} and W_{Res} but not the total consumption, at least while the condition $\mathbf{C_{0r} > C_0}$ is preserved, that is:

$$COP_{HP} > \frac{1}{1-\frac{C_0}{C_{0i}}\left(1-\frac{1}{COP_{Lorenz}}\right)} \quad \text{(A.2)}$$

c) $\mathbf{C_{0i} > C_0 > C_{0r}}$**:** In this case there is not enough grey water availability to ideally recover enough energy to satisfy the heating demand but there is enough grey water availability to satisfy the demand with the used heat pump. The situation would be very similar to the first case and there would be a fraction of the grey water that cannot be used. Nevertheless, in this situation the room for improvement in the COP of the heat pump is limited by the condition $\mathbf{C_0 > C_{0r}}$, which means that the user can improve the COP of the heat pump (reducing the total consumption of the system) until it reaches a limit value:

$$COP_{HP} = \frac{1}{1-\frac{C_0}{C_{0i}}\left(1-\frac{1}{COP_{Lorenz}}\right)} \quad \text{(A.3)}$$

From there, any improvement in the COP of the heat pump will not have any effect on the energy consumption of the system.

It should be pointed out that, in this analysis, the inlet and outlet temperatures of the source and the sink have been considered constant. The water inlet temperatures for a predefined application are fixed, the outlet temperature of the user is fixed, but the outlet temperature of the wastewater is a parameter that we can change when there is an excess of grey water availability. Those cases are very relevant from the point of view of the system control and design and are going to be analysed. The following situations can be found:

- $\mathbf{C_0 > C_{0i} > C_{0r}}$**:** In this case, in order to improve the system performance C_{0i} can be increased up to verify the condition $C_0=C_{0i}$. This situation will imply that T_{sewage} increases and therefore $\overline{T_C}$ will also increase which implies a higher COP_{Lorenz}. For the real system, C_{0r} has also to increase until its corresponding T_{sewage} will be the same as the one obtained for the ideal system. Therefore, when there is enough grey water availability, this argument supplies a design criterium in order to define the used m_{w_grey}.

- **$C_{0i}>C_{0r}>C_0$:** In this case there is not enough grey water available to recover enough energy to satisfy the heating demand, the outlet temperature would be the minimum value, in this case 2 °C and the situation will be equivalent to the explained in the previous analysis.

- **$C_{0i}>C_0>C_{0r}$:** This case represents the situation in which the ideal system is not able to satisfy the demand with the available grey water, but the real heat pump is able to do it. In this case, for the real heat pump, T_{sewage} will be the one corresponding to the condition $C_0=C_{0r}$. It is convenient to remark that here it is the value of C_{0r} the one used to determine T_{sewage} and on the first case it was in the other way around. This condition also imposes that any HP with a COP higher than that one will not have any impact on the energy consumption of the system.

From all this analysis, the optimum T_{sewage} temperature (or m_{w_grey}) can be determined for a specific application. For instance, Figure A.1. represents ideal T_{sewage} as a function of C_{0i} for T_{hot}=64 °C, T_{grey}=30 °C and T_{net}= 10 °C. The figure shows that depending on C_{0i}, there will br an optimum T_{sewage} which maximizes the recuperation. Later on, for a real case, this T_{sewage} with the COP_{HP} can be used to determine the C_{0r} using the Equation 14. Resulting that the total m_{w_grey} used is given by:

$$m_{w\_grey} = m_{w\_greyavailable} \frac{\left(1-\frac{1}{COP_{HP}}\right)}{\left(1-\frac{1}{COP_{Lorenz}}\right)} \quad (A.4)$$

Where $m_{w\_greyavailable}$ is the total mass flow rate of grey water available to recover (the one used by the ideal Lorenz system)

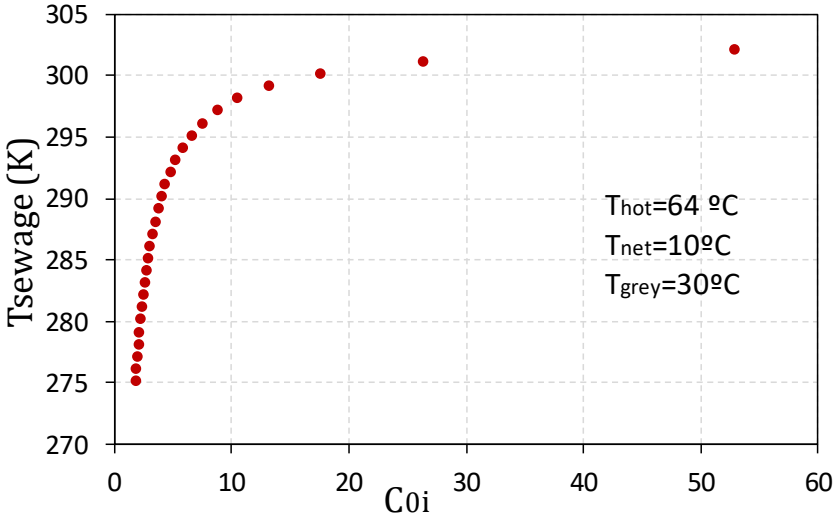

Figure A.1: T_{sewage} as a function of C_{0i} assuming a heating recovery based on a Lorenz ideal cycle in which the value of the rest of the cycle points are: Thot=64°C, Tnet= 10°C and Tgrey=30°C.

7.10 Acknowledgements

Part of the work presented was carried out by Estefanía Hervás Blasco with the financial support of a PhD scholarship from the Spanish government SFPI1500X074478XV0. The authors would like also to acknowledge the Spanish 'MINISTERIO DE ECONOMIA Y COMPETITIVIDAD', through the project "MAXIMIZACION DE LA EFICIENCIA Y MINIMIZACION DEL IMPACTO AMBIENTAL DE BOMBAS DE CALOR PARA LA DESCARBONIZACION DE LA CALEFACCION/ACS EN LOS EDIFICIOS DECONSUMO CASI NULO" with the reference ENE2017-83665-C2-1-P for the given support.

7.11 References

[1] García-Álvarez MT, Moreno B, Soares I. Analyzing the sustainable energy development in the EU-15 by an aggregated synthetic index. Ecol Indic 2016;60:996–1007. doi:10.1016/J.ECOLIND.2015.07.006.

[2] News and Developments – Architecture 2030 2018. https://architecture2030.org/news-and-developments/ (accessed November 29, 2018).

[3] Energy consumption in households - Statistics Explained 2018. http://ec.europa.eu/eurostat/statistics-explained/index.php/Energy_consumption_in_households (accessed August 1, 2018).

[4] Technical | Passive House energy reduection and efficiency 2017. http://recoupwwhrs.co.uk/technical/passive-house/ (accessed August 1, 2018).

[5] Stene J. INTEGRATED CO 2 HEAT PUMP SYSTEMS FOR SPACE HEATING AND HOT WATER HEATING IN LOW-ENERGY HOUSES AND PASSIVE HOUSES. Int Energy Agency 2007.

[6] Zehnder M. Efficient Air-Water pumps for high temperature lift residential heating, including oil migration aspects. ÉCOLE POLYTECHNIQUE FÉDÉRALE DE LAUSANNE, 2004.

[7] Cecchinato L, Corradi M, Fornasieri E, Zamboni L. Carbon dioxide as refrigerant for tap water heat pumps: A comparison with the traditional solution. Int J Refrig 2005;28:1250–8. doi:10.1016/J.IJREFRIG.2005.05.019.

[8] Kharagpur Indian Institute of Technology. Lesson 10 - Vapour Compression Refrigeration Systems. Refrig Air Cond Lect 2005:1–18.

[9] Gluesenkamp KR, Patel V, Abdelaziz O, Mandel B, Dealmeida V. High Efficiency Water Heating Technology Development-Final Report, Part II: CO 2 and Absorption-Based Residential Heat Pump Water Heater Development. 2017.

[10] Nehm G, Nehme G, Palandre L, Clodic D. Purdue e-Pubs High Efficiency Heat Pump for Domestic Hot Water Generation 2008.

[11] Miquel Pitarch i Mocholí. High capacity heat pump development for sanitary hot water production. 2017.

[12] Hervás-Blasco E, Navarro-Peris E, Barceló-Ruescas F, Corberán JM. Improved water to water heat pump design for low-temperature waste heat recovery based on subcooling control. Int J Refrig 2019. doi:10.1016/J.IJREFRIG.2019.06.030.

[13] Tammaro M, Montagud C, Corberán JM, Mauro AW, Mastrullo R. Seasonal performance assessment of sanitary hot water production systems using propane and CO2 heat pumps. Int J Refrig 2017;74:222–37. doi:10.1016/j.ijrefrig.2016.09.026.

[14] Jensen, J. B., & Skogestad, S. (2007). Optimal operation of simple refrigeration cycles: Part I: Degrees of freedom and optimality of sub-cooling. Computers & chemical engineering, 31(5-6), 712-721.

[15] Pitarch M, Navarro-Peris E, Gonzálvez-Maciá J, Corberán JM. Evaluation of different heat pump systems for sanitary hot water production using natural refrigerants. Appl Energy 2017;190:911–9. doi:10.1016/j.apenergy.2016.12.166.

[16] Koeln JP, Alleyne AG. Optimal subcooling in vapor compression systems via extremum seeking control: Theory and experiments. Int J Refrig 2014;43:14–25. doi:10.1016/j.ijrefrig.2014.03.012.

[17] Hervas-Blasco E, Pitarch M, Navarro-Peris E, Corberán JM. Study of different subcooling control strategies in order to enhance the performance of a heat pump. Int J Refrig 2018. doi:10.1016/J.IJREFRIG.2018.02.003.

[18] Chow TT, Pei G, Fong KF, Lin Z, Chan ALS, He M. Modeling and application of direct-expansion solar-assisted heat pump for water heating in subtropical Hong Kong. Appl Energy 2010;87:643–9. doi:10.1016/j.apenergy.2009.05.036.

[19] Baek NC, Shin UC, Yoon JH. A study on the design and analysis of a heat pump heating system using wastewater as a heat source 2004. doi:10.1016/j.solener.2004.07.009.

[20] REULENS, W., 'Natural Refrigerant CO2 EDITED BY WALTER REULENS OCTOBER 2009 (Leonardo project)' http://www.atmosphere2009.com/files/NaReCO2-handbook-2009.pdf.

[21] Tammaro M, Montagud C, Corberán JM, Mauro AW, Mastrullo R. A propane water-to-water heat pump booster for sanitary hot water production: Seasonal performance analysis of a new solution optimizing COP. Int J Refrig 2015;51:59–69. doi:10.1016/j.ijrefrig.2014.12.008.

[22] Spriet J, McNabola A. Decentralized drain water heat recovery: A probabilistic method for prediction of wastewater and heating system interaction. Energy & Buildings. 2019.183; 684-696. doi:10.1016/j.enbuild.2018.11.036

[23] Hervás-Blasco E, Navarro-Peris E, Corberán JM. Optimal design and operation of a central domestic hot water heat pump system for a group of dwellings employing low temperature waste heat as a source. Energy 2019;In Press.

[24] Meggers F, Leibundgut H. The potential of wastewater heat and exergy: Decentralized high-temperature recovery with a heat pump. Energy Build 2010;43:879–86. doi:10.1016/j.enbuild.2010.12.008.

[25] Ferrantelli A, Ahmed K, Pylsy P, Kurnitski J. Analytical modelling and prediction formulas for domestic hot water consumption in residential Finnish apartments. Energy Build 2017;143:53–60. doi:10.1016/J.ENBUILD.2017.03.021.

[26] Zhen L, Lin DM, Shu HW, Jiang S, Zhu YX. District cooling and heating with seawater as heat source and sink in Dalian, China. vol. 32. 2007. doi:10.1016/j.renene.2006.12.015.

[27] Torío H, Schmidt D. Development of system concepts for improving the performance of a waste heat district heating network with exergy analysis. Energy Build 2010;42:1601–9. doi:10.1016/j.enbuild.2010.04.002.

[28] Lund H, Werner S, Wiltshire R, Svendsen S, Thorsen JE, Hvelplund F, et al. 4th Generation District Heating (4GDH): Integrating smart thermal grids into future sustainable energy systems. Energy 2014;68:1–11. doi:10.1016/j.energy.2014.02.089.

[29] Alnahhal S, Spremberg E. Contribution to Exemplary In-House Wastewater Heat Recovery in Berlin , 2016;40:35–40. doi:10.1016/j.procir.2016.01.046.

[30] Baek NC, Shin UC, Yoon JH. A study on the design and analysis of a heat pump heating system using wastewater as a heat source 2004. doi:10.1016/j.solener.2004.07.009.

[31] Nidup, J. (2009). Investigation of Heat Recovery in Different Refrigeration System Solutions in Supermarkets. Unpublished MSc, Royal Institute of Technology (KTH), Stockholm

[32] Fricke, B. A. (2011). Waste Heat Recapture from Supermarket Refrigeration Systems (No. ORNL/TM-2011/239). Oak Ridge National Lab.(ORNL), Oak Ridge, TN (United States); Building Technologies Research and Integration Center.

[33] Hervas, Estefania, et al. "Design of a System for the Production of Domestic Hot Water from Wastewater Heat Recovery Based on a Heat Pump Optimized to Work at High Water Temperature Lift." Purdue Conference (2018). 2018:1–10.

[34] Ni L, Lau SK, Li H, Zhang T, Stansbury JS, Shi J, et al. Feasibility study of a localized residential grey water energy-recovery system. Appl Therm Eng 2012;39:53–62. doi:10.1016/J.APPLTHERMALENG.2012.01.031.

[35] Bertrand A, Aggoune R, Maréchal F. In-building waste water heat recovery: An urban-scale method for the characterisation of water streams and the assessment of energy savings and costs. Appl Energy 2017;192:110–25. doi:10.1016/J.APENERGY.2017.01.096.

[36] Hepbasli A, Biyik E, Ekren O, Gunerhan H, Araz M. A key review of wastewater source heat pump (WWSHP) systems. Energy Convers Manag 2014;88:700–22. doi:10.1016/j.enconman.2014.08.065.

[37] Liu L, Fu L, Jiang Y. Application of an exhaust heat recovery system for domestic hot water. Energy 2009;35:1476–81. doi:10.1016/j.energy.2009.12.004.

[38] Chen W, Liang S, Guo Y, Cheng K, Gui X, Tang D. Investigation on the thermal performance and optimization of a heat pump water heater assisted by shower waste water. Energy Build 2013;64:172–81. doi:10.1016/j.enbuild.2013.04.021.

[39] Baek NC, Shin UC, Yoon JH. A study on the design and analysis of a heat pump heating system using wastewater as a heat source. Sol Energy 2005;78:427–40. doi:10.1016/j.solener.2004.07.009.

[40] Mekdache, Amine, Assaad Zoughaib, and Denis Clodic. "Heat Pump Driven by a Gas Engine for Heating and Domestic Hot Water Generation." Purdue conferences (2016).

[41] McNabola, Shields K. Efficient drain water heat recovery in horizontal domestic shower drains. Energy & Buildings. 2013; 59:44-49. doi:10.1016/j.enbuild.2012.12.026

[42] Meggers F, Leibundgut H. The potential of wastewater heat and exergy: Decentralized high-temperature recovery with a heat pump. Energy Build 2011;43:879–86. doi:10.1016/j.enbuild.2010.12.008.

[43] Eslami-nejad, Parham, and Michel Bernier. "Impact of grey water heat recovery on the electrical demand of domestic hot water heaters." 11th IBPSA Conference, Glasgow. 2009

[44] Spriet J, McNabola. Decentralized drain water heat recovery from commercial kitchens in the hospital sector. Energy & Buildings 2019; 194:247-259. doi:10.106/j.enbuild.2019.04.032.

[45] Hervas-Blasco E, Pitarch M, Navarro-Peris E, Corberán JM. Optimal sizing of a heat pump booster for sanitary hot water production to maximize benefit for the substitution of gas boilers. Energy 2017;127:558–70. doi:10.1016/j.energy.2017.03.131.

[46] Wong LT, Mui KW, Guan Y. Shower water heat recovery in high-rise residential buildings of Hong Kong. Appl Energy 2010;87:703–9. doi:10.1016/J.APENERGY.2009.08.008.

[47] Postrioti L, Baldinelli G, Bianchi F, Buitoni G, Maria F Di, Asdrubali F. An experimental setup for the analysis of an energy recovery system from wastewater for heat pumps in civil buildings. Appl Therm Eng 2016;102:961–71. doi:10.1016/J.APPLTHERMALENG.2016.04.016.

[48] Hendrick P, Spriet J. Wastewater as a heat source for individual residential heating: a thermoeconomic feasibility study in Brusels capital region. J. of develop. of En, Water and Envir Systems. 2017;5:3:289-308. doi:10.1304/j.swdewes.d5.0148.

[49] Baek NC, Shin UC, Yoon JH. A study on the design and analysis of a heat pump heating system using wastewater as a heat source. Sol Energy 2005;78:427–40. doi:10.1016/j.solener.2004.07.009.

[50] Dar UI, Sartori I, Georges L, Novakovic V. Advanced control of heat pumps for improved flexibility of Net-ZEB towards the grid. Energy Build 2014;69:74–84. doi:10.1016/J.ENBUILD.2013.10.019.

[51] TRNSYS 17. 2009.

[52] Jordan U, Vajen K. Realistic Domestic Hot-Water Profiles in Different Time Scales 2001.

[53] Fischer D, Wolf T, Scherer J, Wille-Haussmann B. A stochastic bottom-up model for space heating and domestic hot water load profiles for German households. Energy Build 2016;124:120–8. doi:10.1016/J.ENBUILD.2016.04.069.

[54] Dott, Ralf, et al. "The reference framework for system simulations of the IEA SHC Task 44/HPP Annex 38 Part B: buildings and space heat load." International Energy Agency (2013).

[55] A stochastic bottom-up model for space heating and domestic hot water load profiles for German households. Energy Build 2016;124:120–8. doi:10.1016/J.ENBUILD.2016.04.069.

[56] Federal Ministry for the Environment Nature Conservation and Nuclear Safety. Wasserverbrauch im Haushalt | Media | BMU 2013. https://www.bmu.de/media/wasserverbrauch-im-haushalt/ (accessed November 15, 2018).

[57] Saker D, Vahdati M, Coker PJ, Millward S. Assessing the benefits of domestic hot fill washing appliances. Energy Build 2015;93:282–94. doi:10.1016/J.ENBUILD.2015.02.027.

[58] Hasan AA, Goswami DY, Vijayaraghavan S. First and second law analysis of a new power and refrigeration thermodynamic cycle using a solar heat source. Sol Energy 2002;73:385–93. doi:10.1016/S0038-092X(02)00113-5.

Chapter 8
Discussion of the main results, general conclusions and future work

This chapter gives a general view of the findings and insights earned from this research. The main objectives presented in the first chapter are contrasted with the main obtained results, in Section 8.1. General conclusions can be found in Section 8.2. A topic as large, novel and dynamic as heat pumps for DHW within heat recovery applications offers more possibilities for future research; Section 8.3 contains some suggestions about future research that have been identified.

8.1 Discussion of the main results

The main objectives dealing with the design of a highly efficient vapor compression (subcritical) heat pump for DHW based on heat recovery applications are now fulfilled:

a) **Theoretically study the most efficient heat pump working with a subcritical cycle based on the heat sink and source characteristics.**
b) **Study the dependency of the optimal subcooling with superheat.**
c) **Analyze the role of superheat in applications where temperature lifts take place in the heat source (i.e. heat recovery applications).**
d) **Evaluate the consequences on the performance derived from the loss of one control variable (superheat) that could take place in the proposed heat pump configuration in the PhD [1] based only on common HP components.**
e) **Identify possible room for improvement taking into account subcooling and superheat from a heat pump system point of view based on the heat sink and source characteristics.**

An exergetic analysis of the vapor compression cycle in a heat pump based on the water temperature lift in the condenser and the water temperature glide in the

evaporator has been performed. From this analysis, the relative influence of each component on the performance of the system has been identified.

Furthermore, the existence of an optimal degree of subcooling based on the temperature lift at the condenser was found. This point becomes especially important in applications where high (or variable) temperature lifts take place (as it is the case in DHW applications).

Similarly, an optimal degree of superheat dependent on the temperature glide of the secondary fluid at the evaporator was determined. In heat recovery applications, this point becomes important as it enhances the performance maximizing the recovered heat.

Working with optimal degrees of subcooling can enhance up to 30% the efficiency of the heat pump while optimal degrees of superheat could contribute to 3% of upturn.

With high temperature lifts at the secondary fluid of the condenser, the compressor and the condenser are the components with highest irreversibilities. Thus, they are the first ones to look at for improvement in vapor compression systems with subcooling.

With small temperature lifts at the secondary fluid of the condenser, the compressor and the expansion valve are the most influent components to look at for improvement in vapor compression systems with subcooling. Possibly, considering doing mechanical subcooling as well as using a liquid to suction heat exchanger could help improving the efficiency.

With superheat, the compressor is the most important component for improvement. Furthermore, if operating with lower degrees of superheat than the optimal, the relative irreversibility of each component are not affected due to they are mainly dependent on the conditions at the condenser.

From the theoretical point of view, the capability of controlling both, superheat and subcooling, at the same time, is recommended. The control of these variables does not imply major changes on the vapor compression system and allows for improvement of the cycle under variable external conditions.

These recommendations can be useful for any vapor compression system and they are not limited to heat pumps for DHW applications with heat recovery. For instance, a dryer or dynamic heat recuperator technologies could also benefit from this outcome.

f) Design and test a subcooling control methodology based on the findings found in the PhD [1].

Two strategies were theoretically assessed based on the dependence of the optimal subcooling with external temperatures found in the PhD [1]:

- One proposes a linear fitting, directly relating the secondary temperature lift with the optimal subcooling, that theoretically leads to a very accurate correlation (errors lower than 0.04%).
  This methodology depends on the refrigerant and the fitting found cannot be generalized to other refrigerants.
- Another one proposes setting a constant temperature approach as a control value.
  This approach is based on the analysis of the optimal subcooling for real heat exchangers. It was known that for infinite heat exchangers, optimal subcooling takes place with two pinch point condition (dew point and approach). In finite heat exchangers, the zero-temperature difference at both pinch point situation does not occur. However, according to the study performed, the optimum can be approximated in a similar way, when two pinch points situation takes place with maximum theoretical deviations of approximately 1%.
  This assumption allows the control of optimal subcooling with a constant temperature approach (maintaining constant the temperature difference between the secondary fluid and the refrigerant at the outlet of the condenser). This approach seems to be generalizable for a given condenser size, refrigerant and approaches lower than 5K.

Due to the independency from the working fluid, the control based on a constant temperature approach was chosen out of both methods. Its stability was experimentally proved and deviations from the optimal COP were lower than 0.2%.

Both control strategies rely on “simple” algorithms without compromising accuracy what extends its application. Only a PID and two thermocouples are required what does not represent an economic barrier for its implementation in commercial heat pumps working with subcritical cycles.

g) **Develop a new heat pump concept composed only by one expansion valve, one compressor, an evaporator, a condenser and a liquid receiver.**
h) **Experimentally evaluate the reliability of the concept developed and compare the performance with the performance obtained from the existing designs. Determine the most convenient configuration of the heat pump out of the three designs.**

A new design composed only by the typical components of a heat pump was developed and experimentally tested (so called 0K1V). In this design, the liquid receiver is placed at the outlet of the evaporator and subcooling is made inside the condenser.

Subcooling is controlled by the expansion valve, which has shown to be stable and reliable. At the same time, superheat control is automatically performed by the existence of a vapor to liquid interface in the liquid receiver forcing saturated conditions at the outlet of the evaporator.

The main potential problems of null superheat are: deterioration of the compressor reliability due to the possible presence of some liquid at the inlet of the compressor, and the loss of a possible improvement when the temperature glide at the secondary fluid in the evaporator is large. However, vapor conditions were always observed at the inlet of the compressor and there was not malfunctioning detected in the compressor from the beginning of the experimental campaign to the end.

To analyze the effect of null superheat control, experimental measurements of 0K1V and 10K2V were compared. As a reminder, 10K2V concept was developed in [1] and the configuration is capable to control both, superheat and subcooling at the expense of placing an extra expansion valve (throttling valve) at the outlet of the condenser. The liquid receiver is located between both expansion valves allowing independent control: the throttling valve controls the subcooling and the expansion valve, the superheat.

Performances are always better (around 5%) in 0K1V than in 10K2V concept, independently from the secondary temperature glides at the evaporator. Optimal degrees of subcooling, 5K greater, and compressor discharge temperatures around 10K lower, were found in 0K1V. The decrease in the discharge temperaure limits the application range of 0K1V to a maximum hot water production of 70°C-80°C

unless, for instance, a liquid to suction heat exchanger was placed after the receiver (this has not been evaluated).

Slightly higher evaporating pressures take place with 0K1V due to smaller vapor qualities occuring at the inlet of the evaporator and null superheat

Controlling subcooling with the expansion valve based on the temperature approach proposed from objective (f) was also stable and accurate. Furthermore, optimal values were found with DT=3K as it was the case in 10K2V.

These results did not completely agree with theoretical results obtained in Chapter 2 and a qualitative analysis of the fluid distribution in the evaporator was performed. From it, thermography observations pointed out the existence of a mal distribution of the refrigerant in the evaporator, possibly, due to an unbalanced pressure drop. The effect was more important with the increase of superheat. It could be the reason for obtaining always a better performance with the 0K1V configuration. However, time is limited and going deeper into this topic was out of the scope of this thesis.

Therefore, based on the experimental results, the configuration with highest performance was the 0K1V configuration. Hence, it was chosen as the most suitable for DHW production.

Nevertheless, the three heat pump concepts working with a subcritical cycle show a potential operation with high efficiencies under a wide range of external conditions (not only DHW) thanks to the subcooling control. This opens a new market for subcritical systems since they can be used as alternative to current technologies employed in water heating applications.

The main targets related to the integration of this heat pump (called subcooled heat pump, SHP) within a system for DHW production and heat recovery have been met as well:

i) **Determine a proper sizing of a heat recovery heat exchanger (recuperator) to maximize energy efficiency from the coupling with the subcooled heat pump.**

From an energy point of view, the addition of a heat recovery heat exchanger before the heat pumping is always profitable compared to conventional DHW production alternatives. The only disadvantage could be economics. However, the use of a pre-heating heat exchanger (recuperator) has demonstrated a great potential compared to gas boilers even under pessimistic operating and investment costs estimations.

Operating strategies and external conditions of the system are the most influent on the optimal size of the combination heat exchanger-heat pump. However, as a guideline for designing, 5K approach in the heat exchanger could be a proper assumption for preliminary sizing.

j) Define and design the components required to maximize the efficiency of a system for DHW production in the residential sector.

The most efficient heat recovery system that satisfies actual DHW demand in the residential sector should include, apart from the heat pump, a pre-heater heat exchanger (recuperator) and a storage tank with variable volume.

If instantaneous production could be reached by a heat pump itself, storage tanks would not be required.

The optimal sizing and operation for different demand sizes was obtained concluding that a unique optimal design does not exist. Instead, there are a set of size combinations that result in similar efficiencies of the system.

Sizing is highly dependent on the demand of DHW while operating strategies are similar at any case (they depend more on external conditions).

For a given demand size and infinite heat source reservoir, the successful integration of the subcooled heat pump within these systems depends on both factors: sizing and operating strategies. The main control variables are the temperature and the level of the water in the storage tank. The minimization of the CO_2 emissions is obtained for solutions that minimize the time that the water is stored while guaranteeing the standard levels of comfort.

Levels of comfort should include not only the mismatch between the demand and the availability of hot water, but also the moment when the shortfall takes place. Optimum solutions differ if this second aspect is not considered in the evaluation.

The temperature of the water stored should be kept as lowest as possible and the signal control associated to the level may be set at high values (80% - 90% of the storage tank size).

The use of a pre-heater heat exchanger (recuperator) confirms the conclusions from the previous chapter since it enhances the performance of the system up to

15% even with low heat source temperatures regardless the heat pump performance diminution.

The best potential from the heat exchanger-heat pump tandem on the overall performance is obtained for maximum differences between the inlet temperatures of the heat sink and source, being the temperature of the heat source the most influent condition. For instance, an annual COP_{sys} of the system up to 9.5 could be reached with net water temperatures of 5°C and 35 °C in the heat source. $COPs_{sys}$ of the system around 8.3 are obtained with net water temperatures of 15°C and 35°C in the heat source or annual performances of 7.1 are obtained with net water temperatures of 5°C and 25°C in the heat source.

High efficiencies, and important potential reductions of the CO_2 emissions associated, were obtained. In fact, almost 5 times CO_2 emissions reduction from the substitution of conventional gas boiler by heat pumps is showed. Small sizes and greater annual operating hours are preferable (as closest as possible to instantaneous production). The minimum size optimal solution for 20 multifamily building results in a storage tank of 400liter and a heating capacity of the heat pump of 7.5 kW and approximately 10h/day of production time.

Dynamic models and a holistic approach are required to address this type of problems. DHW is characterized by sharp and short peaks, therefore, using hourly-basis demand and time steps lead to miss the real behavior of the system, what is usually translated into a component oversizing. Furthermore, parametric studies are required to obtain the solutions range. Optimization algorithms find a possible solution but not all “good” solutions.

DHW consumption has a intrinsically random characteristic as a large amount of factors (from socio-economics to location) play an important role in the final use of hot water (the pattern of the consumption becomes more predictable as DHW production is centralized agregating a great number of dwellings). Hence, the generalization of the results are difficult and most of the design strategies rely on worst cases what results in high oversizing of the components entailing a significant loss of efficiency. For instance, an oversized tank can lead to 12% higher CO2 annual emissions than a proper sized one.

Obtaining representative profiles in a small-time scale is an uphill work that has been and is the focus of many researches. However, to have an efficient energy production of hot water, solutions could come from a change on the driver factor: defining energyally efficient systems for the user to adapt its behavior instead of the opposite. This approach is already followed in other contexts such as recycling

or having a committed attitude towards environment (‘do not throw garbage to the floor’).

The solution found was validated for other demand sizes and external conditions.

k) Design the most energy efficient system for DHW production in the residential sector based on heat recovery from low temperature sources capable to satisfy a residential sector demand with high comfort

l) Analyze the potential energy available in wastewater heat sources at low temperature and determine a control strategy to maximize the efficiency of the DHW production system from waste heat recovery.

The most efficient heat recovery system that satisfies DHW demand in the residential sector should include, apart from the heat pump, a pre-heater heat exchanger (recuperator) and two storage tanks with variable volume.

With infinite heat source availability and instantaneous production by the heat pump, storage tanks are not required. However, the lack of one condition leads to the need of energy accumulation. This introduces irreversibility to the system. Thus, the control strategy should minimize the energy accumulated.

The integration of the grey water side with the DHW side can be done by means of a proportion between the grey water mass flow rate and the hot water mass flow rate. This criterion is used to control the greywater mass flow rate extracted from the storage tank and to size the grey water storage tank. This insight can facilitate the design of these type of systems.

For a given demand size and finite heat source, the main control variables influencing the design are: the temperatures and levels of the water in the storage tanks.The minimization of the CO2 emissions is obtained for solutions that minimize the energy stored while guaranteeing the standard levels of comfort. That is, whenever possible, the DHW side must be the driver of the operation since the DHW tank is at higher temperatures and heat loses become more important. To this aim, a minimum level of water in the greywater storage tank should be considered.

With finite heat sources, the maximization of the wastewater mass flow rate used leads to the highest performance. The control of the grey water mass flow rate

is defined in order to maximize the mass flow rate following the proportion of the availability function of the hot water production, grey water temperature, and net water temperature.

Based on stochastic models and the available information with regards to the characterization of greywater characteristics, an estimation of a greywater availability profile has been obtained (temperature and water flows). From it, and a variable net water temperature, the optimization of the system has been performed following a methodology that could be useful in future works dealing with similar applications.

For a 20 Multifamily building DHW demand, a drop of the COP of the system from 8.5 to 6.8 is obtained because of the waste mass flow rate limitation. Furthermore, greater optimal sizes are required. If additionally, grey water variability is accounted (hence, a grey water storage tank is required) optimum performance decreases 17% extra, although this value can be reduced to 2% if a dynamic adaptation to real conditions is implemented.

The optimal solution with real profiles that belongs to the minimum storage tank sizes results in a heating capacity of 11.4 kW, a DHW storage tank of 350 liter and a grey water storage tank of 875 liter. Annual COPs of the system upto6.7 are obtained. A 60% of the available grey water energy is recovered (97% of the grey water mass flow rate and an average of 12 °C in the grey water temperature leaving to the sewage).

Scarce information is available dealing with grey water characteristics and the estimation of representative profiles (temperature and wastewater mass flow rate). Further work on this topic is encouraged.

8.2 General conclusions

An optimized heat pump for DHW applications based on low temperature heat sources has been developed, experimentally tested and theoretically studied. Thereafter, a study and a model of the most efficient system that integrates this heat pump has been conducted. The main general conclusions extracted from the work are presented below.

8.2.1 From the HP design point of view

- The performance of a subcritical heat pump strongly depends on the on the correct match between subcooling and water temperature lift. Improvements up to 30% with high temperature lifts and optimum degrees of subcooling have been achieved.
- The performance of a subcritical heat pump also depends on the optimization of the superheat. Improvements up to 3% have been theoretically found for optimum degrees of superheat in comparison with usual values of superheat.
- The performance of a subcritical heat pump with optimal subcooling is comparable to transcritical heat pumps for high temperature water lifts.
- For DHW production and heat recovery applications, subcritical heat pumps present greater potential than transcritical cycles due to their capacity of adaptation to different temperature lifts without compromising efficiency.
- It is possible to control the subcooling based on the temperature at the outlet of the condenser. That is, from a temperature difference controlled by a PID. This control has demonstrated stability in both prototypes tested: by means of throttling valve and by means of the expansion valve.
- A heat pump design only with a single expansion valve that controls subcooling and ensures saturated conditions at the inlet of the compressor by the placement of a liquid receiver, is the most efficient configuration among the different solutions tested.

8.2.2 From the system point of view

- The most efficient system for hot water production based on heat recovery is composed by a primary heat recovery heat exchanger (recuperator), the optimized heat pump and two variable volume storage tanks (only one storage tank is required if the heat source has infinite capacity).
- The use of a recuperator placed before the heat pump is always desired. It should always be placed upstream the heat pump. More than 30% of the required energy required can be obtained from the recuperator.
- The sizing of the recuperator is a topic for the optimization of these systems. A temperature approach of 5K seems a good preliminary sizing criterium.
- High variability on the DHW demand or grey water availability leads to the necessity of a grey water storage tank.
- Irreversibility introduced by the storage tanks is minimum with the right control strategy (minimization of the energy stored).
- Variable volume storage tanks allow the minimization of the water energy stored leading to lower energy losses
- The DHW characterization profile is a critical task that needs further research. The user behavior has a strong influence on the global energy consumption of this kind of application.
- Aggregating DHW demands lead always to flatter profiles what results in more efficient systems.
- There is not an optimal sizing solution, instead, a set of size combinations result in similar energy performances. However, inadequate sizing could lead up to 20% lower efficiency.
- An oversized tank sizing could result in 5-10% lower system efficiency.
- Smaller heat pump sizes and higher running times are always preferable from an energy point of view (constant production).
- The temperature of grey water (or heat source) significantly impacts the efficiency. For applications, as for instance district heating (35 °C), COPs of the system greater than 8.5 are possible.
- From the system point of view, the most favorable conditions are low city water temperatures and high recovery temperatures (winter conditions and cold climates).
- The limitation in terms of available mass flow rate as a heat source lead to the need of a waste water storage tank with a control (temperature/mass flow rate control).

- Significant water temperature glides take place in the evaporator with heating recovery applications and the limitation of the available waste water.
- The quality of the energy for recovery is crucial: quantity and temperature.
- According to the results obtained from an example of 20 multifamily building, there is enough grey water heat recovery energy in their daily water consumption to produce the required DHW demand with high levels of comfort based on a heat pump, without the need of any backup technology.

The study demonstrates, in any case, the interest of subcritical heat pumps systems for DHW production based on heat recovery of wastewater. Findings of this work, based on energy aspects, remain the same regardless specific conditions or politics and may be useful for coupling with for instance economic factors specific for each case.

8.3 Future work

The results obtained in this thesis encourage to continue working on the application of heat pumps for DHW production and its integration in buildings.

8.3.1 Heat pump design

- Study of the subcooling control with a variable speed compressor.
- Investigation of the evaporator mal-distribution problem in the 10K2V mode.
- Comparison of the results with a CO2 heat pump for heat recovery applications.

8.3.2 System integration

- Comparison of the results with a stratified storage tank.
- Comparison of the results with present alternatives for water heating systems applications.
- DHW profiles estimation.
- Grey water profiles characterization.
- Other heat recovery applications: industrial or commercial.
- Coupling of the results with economic aspects.
- Field applications.

8.4 Publications

8.4.1 In peer-reviewed journals

Pitarch, M., Hervas-Blasco, E., Navarro-Peris, E., & Corberán, J. M. (2019). Exergy analysis on a heat pump working between a heat sink and a heat source of finite heat capacity rate. International Journal of Refrigeration, 99, 337–350. http://doi.org/10.1016/J.IJREFRIG.2018.11.044

Hervas-Blasco, E., Pitarch, M., Navarro-Peris, E., & Corberán, J. M. (2018). Study of different subcooling control strategies in order to enhance the performance of a heat pump. International Journal of Refrigeration. http://doi.org/10.1016/J.IJREFRIG.2018.02.003

Hervás-Blasco, E., Navarro-Peris, E., Barceló-Ruescas, F., & Corberán, J. M. (2019). Improved water to water heat pump design for low-temperature waste heat recovery based on subcooling control. International Journal of Refrigeration. http://doi.org/10.1016/J.IJREFRIG.2019.06.030

Hervas-Blasco E, Pitarch M, Navarro-Peris E, Corberán JM. Optimal sizing of a heat pump booster for sanitary hot water production to maximize benefit for the substitution of gas boilers. Energy 2017;127:558–70. doi:10.1016/j.energy.2017.03.131.

Hervás-Blasco, E., Navarro-Peris, E., & Corberán, J. M. (2019). Optimal design and operation of a central domestic hot water heat pump system for a group of dwellings employing low temperature waste heat as a source. Energy, 115979. http://doi.org/10.1016/J.ENERGY.2019.115979

Hervás-Blasco,E., Navarro-Peris, E., & Corberán, J. M. (2019). Closing the residential energy loop: grey-water heat recovery system for Domestic Hot Water production based on heat pumps. Energy and Buildings. Accepted.

8.4.2 In conference proceedings

10º Congreso Nacional Ingeniería Termodinámica y 1º Internacional celebrated in Lleida, del 28 al 30 of June de 2017 with papers:

Title:"Optimal sizing of a heat pump booster to maximize benefit from the substitution of the production of sanitary hot water with gas boilers"

Authors: Estefanía Hervás-Blasco, Miguel Pitarch, Laetitia Bardoulet, Emilio Navarro-Peris

Title:"Control of the optimal subcooling"

Estefanía Hervás-Blasco, Miquel Pitarch, Alejandro López-Navarro, Emilio Navarro-Peris, José Gonzalvez-Maciá, José Miguel Corberán

Title:"Optimal subcooling in subcritical systems"

Miquel Pitarch, Estefanía Hervás-Blasco, Emilio Navarro-Peris, José Gonzalvez-Maciá, José Miguel Corberán

- *CYTEF 2018 CIENCIAS Y TÉCNICAS DEL FRÍO – IX Congreso Ibérico / VII Congreso Iberoamericano (Junio 2018)*

"ANALYSIS OF THE STORAGE TANK-HEAT PUMP PERFORMANCE BASED ON EXTERNAL CONDITIONS UNDER A THERMAL POINT OF VIEW"

Estefania Hervas-Blasco, Emilio Navarro-Peris, José Miguel Corberán

-13th IIR-GUSTAV LORENTZEN CONFERENCE ON NATURAL REFRIGERANTS (Junio 2018)

"Experimental comparison between different heat pump designs working with propane to control subcooling for sanitary hot water production"

Estefania Hervás Blasco, Miquel Pitarch Mocholi, Emilio Navarro Peris, José M. Corberán Salvador

-5th International High Performance Buildings Conference (Julio 2018)

"Design of a System for the Production of Domestic Hot Water from Wastewater Heat Recovery Based on a Heat Pump Optimized to Work at High Water Temperature Lift"

Estefanía Hervas-Blasco, Javier Marchante-Avellaneda, Emilio Navarro-Peris, José Miguel Corberán

References

[1] Miquel Pitarch i Mocholí, “High capacity heat pump development for sanitary hot water production,” 2017.

[2] L. Doman, “EIA projects 28% increase in world energy use by 2040 - Today in Energy - U.S. Energy Information Administration (EIA),” 2017. [Online]. Available: https://www.eia.gov/todayinenergy/detail.php?id=32912. [Accessed: 01-Aug-2018].

[3] J. Cook, N. Oreskes, P. T. Doran, W. R. L. Anderegg, B. Verheggen, E. W. Maibach, J. S. Carlton, S. Lewandowsky, A. G. Skuce, S. A. Green, D. Nuccitelli, P. Jacobs, M. Richardson, B. Winkler, R. Painting, and K. Rice, “Consensus on consensus: a synthesis of consensus estimates on human-caused global warming,” *Environ. Res. Lett.*, vol. 11, no. 4, p. 048002, Apr. 2016.

[4] P. Nejat, F. Jomehzadeh, M. M. Taheri, M. Gohari, and M. Z. Abd. Majid, “A global review of energy consumption, CO2 emissions and policy in the residential sector (with an overview of the top ten CO2 emitting countries),” *Renew. Sustain. Energy Rev.*, vol. 43, pp. 843–862, Mar. 2015.

[5] “Energy consumption in households - Statistics Explained,” 2018. [Online]. Available: http://ec.europa.eu/eurostat/statistics-explained/index.php/Energy_consumption_in_households. [Accessed: 01-Aug-2018].

[6] “Sectoral greenhouse gas emissions by IPCC sector — European Environment Agency,” 2014. [Online]. Available: https://www.eea.europa.eu/data-and-maps/daviz/change-of-co2-eq-emissions-2#tab-chart_4. [Accessed: 01-Aug-2018].

[7] M. T. García-Álvarez, B. Moreno, and I. Soares, “Analyzing the sustainable energy development in the EU-15 by an aggregated synthetic index,” *Ecol. Indic.*, vol. 60, pp. 996–1007, Jan. 2016.

[8] “Technical | Passive House energy reduection and efficiency,” 2017. [Online]. Available: http://recoupwwhrs.co.uk/technical/passive-house/. [Accessed: 01-Aug-2018].

[9] K. Dawson and B. Wmi, “Trends in the World Traditional & Renewable Heating Markets,” 2014.

[10] “BSRIA World Market Intelligence Industry Briefing - AHR Expo 2016.” [Online]. Available: https://www.slideshare.net/BSRIA/bsria-world-market-intelligence-industry-briefing-ahr-expo-2016. [Accessed: 13-Jun-

2017].

[11] D. Fischer, “Integrating Heat Pumps into Smart Grids,” 2017.

[12] “EUROPA - EHPA Secretary General Thomas Nowak talks to SETIS | SETIS - European Commission.” [Online]. Available: https://setis.ec.europa.eu/newsroom/interviews/ehpa-secretary-general-thomas-nowak-talks-setis. [Accessed: 13-Jun-2017].

[13] K. Brodowicz and T. Dyakowski, *Heat pumps*. 1993.

[14] S. C. Kaushik, S. K. Tyagi, and P. Kumar, *Finite time thermodynamics of power and refrigeration cycles*. Springer, 2017.

[15] C. (Claus) Borgnakke and R. E. Sonntag, *Fundamentals of thermodynamics*. 2013.

[16] J. Berghmans, *Heat Pump Fundamentals : Proceedings of the NATO Advanced Study Institute on Heat Pump Fundamentals, Espinho, Spain, September 1-12, 1980*. Springer Netherlands, 1983.

[17] A. A. Hasan, D. Y. Goswami, and S. Vijayaraghavan, “First and second law analysis of a new power and refrigeration thermodynamic cycle using a solar heat source,” *Sol. Energy*, vol. 73, no. 5, pp. 385–393, Nov. 2002.

[18] United States of Labor, “Safety and Health Topics | Legionellosis (Legionnairesâ€™ Disease and Pontiac Fever) - Control and Prevention | Occupational Safety and Health Administration,” 2016. [Online]. Available: https://www.osha.gov/SLTC/legionnairesdisease/control_prevention.html #hotwater. [Accessed: 06-Dec-2018].

[19] R. Slim, A. Zoughaib, and D. Clodic, “Modeling of a solar and heat pump sludge drying system,” *Int. J. Refrig.*, vol. 31, no. 7, pp. 1156–1168, 2008.

[20] D. Fischer, T. Wolf, J. Scherer, and B. Wille-Haussmann, “A stochastic bottom-up model for space heating and domestic hot water load profiles for German households,” *Energy Build.*, vol. 124, pp. 120–128, Jul. 2016.

[21] A. Bertrand, R. Aggoune, and F. Maréchal, “In-building waste water heat recovery: An urban-scale method for the characterisation of water streams and the assessment of energy savings and costs,” *Appl. Energy*, vol. 192, pp. 110–125, Apr. 2017.

[22] L. Cecchinato, M. Corradi, and S. Minetto, “Energy performance of supermarket refrigeration and air conditioning integrated systems,” *Appl. Therm. Eng.*, vol. 30, no. 14–15, pp. 1946–1958, Oct. 2010.

[23] B. A. Fricke, “Waste Heat Recapture from Supermarket Refrigeration Systems,” 2011.

[24] A. Mekdache, A. Zoughaib, and D. Clodic, “Purdue e-Pubs Heat Pump Driven by a Gas Engine for Heating and Domestic Hot Water Generation Heat pump driven by a gas engine for heating and domestic hot water generation.”

[25] S. H. Noie-Baghban and G. R. Majideian, “Waste heat recovery using heat pipe heat exchanger (HPHE) for surgery rooms in hospitals,” *Appl. Therm. Eng.*, vol. 20, no. 14, pp. 1271–1282, Oct. 2000.

[26] Y. Pericault, E. Kärrman, M. Viklander, A. Hedström, Y. Pericault, E. Kärrman, M. Viklander, and A. Hedström, “Expansion of Sewer, Water and District Heating Networks in Cold Climate Regions: An Integrated Sustainability Assessment,” *Sustainability*, vol. 10, no. 10, p. 3743, Oct. 2018.

[27] D. Schmidt, A. Kallert, M. Blesl, S. Svendsen, H. Li, N. Nord, and K. Sipilä, “Low Temperature District Heating for Future Energy Systems,” *Energy Procedia*, vol. 116, pp. 26–38, Jun. 2017.

[28] X. Guo and M. Hendel, “Urban water networks as an alternative source for district heating and emergency heat-wave cooling,” *Energy*, vol. 145, pp. 79–87, Feb. 2018.

[29] P. Nekså, H. Rekstad, G. R. Zakeri, and P. A. Schiefloe, “CO2-heat pump water heater: characteristics, system design and experimental results,” *Int. J. Refrig.*, vol. 21, no. 3, pp. 172–179, May 1998.

[30] L. Cecchinato, M. Corradi, E. Fornasieri, and L. Zamboni, “Carbon dioxide as refrigerant for tap water heat pumps: A comparison with the traditional solution,” *Int. J. Refrig.*, vol. 28, pp. 1250–1258, 2005.

[31] C. J. Pitarch. M., Navarro-Peris. E., Gonzálvez-Maciá. J., Montagud. C., “Influence of Water Lift Temperature in Transcritical and Subcritical Refrigerants,” in *VII Congreso Ibérico de Ciencias y Técnicas del Frío, Tarragona, Spain.*, 2014.

[32] J. Stene, “INTEGRATED CO 2 HEAT PUMP SYSTEMS FOR SPACE HEATING AND HOT WATER HEATING IN LOW-ENERGY HOUSES AND PASSIVE HOUSES,” *Int. Energy Agency*, 2007.

[33] C. Chaichana, L. Aye, and W. W. . Charters, “Natural working fluids for solar-boosted heat pumps,” *Int. J. Refrig.*, vol. 26, no. 6, pp. 637–643, Sep. 2003.

[34] M. Pitarch, E. Hervas-Blasco, E. Navarro-Peris, J. Gonzálvez-Maciá, and J. M. Corberán, “Evaluation of optimal subcooling in subcritical heat pump systems,” *Int. J. Refrig.*, vol. 78, pp. 18–31, Jun. 2017.

[35] J. Choi and Y. Kim, "Influence of the expansion device on the performance of a heat pump using R407C under a range of charging conditions," *Int. J. Refrig.*, vol. 27, no. 4, pp. 378–384, 2004.

[36] J. M. Corberá, I. O. Martínez, and J. Gonzá, "Charge optimisation study of a reversible water-to-water propane heat pump Etude sur l'optimisation de la charge d'une pompe à chaleur ré versible eau-eau au propane," 2007.

[37] T. Hjerkinn, "Analysis of Heat Pump Water Heater Systems for Low-Energy Block of Flats," Master thesis at the Norwegian University of Science and Technology (NTNU), Dept. of Energy and Process Engineering. EPT-M-2007-24, 2007.

[38] G. Pottker and P. Hrnjak, "Experimental investigation of the effect of condenser subcooling in R134a and R1234yf air-conditioning systems with and without internal heat exchanger," *Int. J. Refrig.*, vol. 50, pp. 104–113, Feb. 2015.

[39] J. B. Jensen and S. Skogestad, "Optimal operation of simple refrigeration cycles: Part I: Degrees of freedom and optimality of sub-cooling," *Comput. Chem. Eng.*, vol. 31, no. 5, pp. 712–721, 2007.

[40] J. B. Jensen and S. Skogestad, "Optimal operation of simple refrigeration cycles: Part II: Selection of controlled variables," *Comput. Chem. Eng.*, vol. 31, no. 12, pp. 1590–1601, 2007.

[41] L. Xu, "POTENTIAL OF CONTROLLING SUBCOOLING IN RESIDENTIAL AIR CONDITIONING SYSTEM," 2014.

[42] J. P. Koeln and A. G. Alleyne, "Optimal subcooling in vapor compression systems via extremum seeking control: Theory and experiments," *Int. J. Refrig.*, vol. 43, pp. 14–25, 2014.

[43] M. Pitarch, E. Navarro-Peris, J. Gonzálvez-Maciá, and J. M. Corberán, "Experimental study of a subcritical heat pump booster for sanitary hot water production using a subcooler in order to enhance the efficiency of the system with a natural refrigerant (R290)," *Int. J. Refrig.*, vol. 73, pp. 226–234, 2017.

[44] M. Pitarch-Mocholí-, E. Navarro-Peris, J. Gonzalvez-Maciá, and J. M. Corberán, "High Efficiency Heat Pump with Subcooling for Sanitary Hot Water Production Working with Propane," *Int. Refrig. Air Cond. Conf.*, 2016.

[45] M. Pitarch, E. Navarro-Peris, J. Gonzálvez-Maciá, and J. M. Corberán, "Evaluation of different heat pump systems for sanitary hot water production using natural refrigerants," *Appl. Energy*, vol. 190, pp. 911–919, 2017.

[46] G. Nehm, G. Nehme, L. Palandre, and D. Clodic, "Purdue e-Pubs High Efficiency Heat Pump for Domestic Hot Water Generation High Efficiency Heat Pump for Domestic Hot Water Generation," 2008.

[47] O. Culha, H. Gunerhan, E. Biyik, O. Ekren, and A. Hepbasli, "Heat exchanger applications in wastewater source heat pumps for buildings: A key review," *Energy Build.*, vol. 104, pp. 215–232, Oct. 2015.

[48] P. G. Jolly, C. P. Tso, P. K. Chia, and Y. W. Wong, "Intelligent Control to Reduce Superheat Hunting and Optimize Evaporator Performance in Container Refrigeration," *HVAC&R Res.*, vol. 6, no. 3, pp. 243–255, Jul. 2000.

[49] F. Meggers and H. Leibundgut, "The potential of wastewater heat and exergy: Decentralized high-temperature recovery with a heat pump," *Energy Build.*, vol. 43, no. 4, pp. 879–886, 2011.

[50] T. Q. Qureshi and S. A. Tassou, "Variable-speed capacity control in refrigeration systems," *Appl. Therm. Eng.*, vol. 16, no. 2, pp. 103–113, Feb. 1996.

[51] S. . Tassou and T. . Qureshi, "Comparative performance evaluation of positive displacement compressors in variable-speed refrigeration applications," *Int. J. Refrig.*, vol. 21, no. 1, pp. 29–41, Jan. 1998.

[52] S. K. Chaturvedi, D. T. Chen, and A. Kheireddine, "Thermal performance of a variable capacity direct expansion solar-assisted heat pump," *Energy Convers. Manag.*, vol. 39, no. 3–4, pp. 181–191, Feb. 1998.

[53] S. Shao, W. Shi, X. Li, and J. Ma, "A new inverter heat pump operated all year round with domestic hot water," *Energy Convers. Manag.*, vol. 45, no. 13–14, pp. 2255–2268, Aug. 2004.

[54] C. Vasile, "International data on successfully demonstrated Residential waste water heat-recovery System: GFX."

[55] U.S. Department of energy, "Drain-Water Heat Recovery | Department of Energy," 2017. [Online]. Available: https://www.energy.gov/energysaver/water-heating/drain-water-heat-recovery. [Accessed: 07-Dec-2018].

[56] L. Hua, "Heat exchanger development for waste water heat recovery," University of Canterbury. Mechanical Engineering, 2005.

[57] L. T. Wong, K. W. Mui, and Y. Guan, "Shower water heat recovery in high-rise residential buildings of Hong Kong," *Appl. Energy*, vol. 87, no. 2, pp. 703–709, Feb. 2010.

[58] T. Veijola, A. Thesis Supervisor Veijola, and T. M. Ruusunen, "DOMESTIC

DRAIN WATER HEAT RECOVERY Process engineering Domestic drain water heat recovery," 2016.

[59] L. Liu, L. Fu, and Y. Jiang, "Application of an exhaust heat recovery system for domestic hot water," *Energy*, vol. 35, no. 3, pp. 1476–1481, 2010.

[60] "How Does it Work – Quantum." [Online]. Available: http://quantumenergy.com.au/how-does-it-work/. [Accessed: 07-Dec-2018].

[61] "NIBE PRODUCT RANGE Exhaust Air Heat Pumps Ground Source Heat Pumps Air/Water Heat Pumps Air/Air Heat Pumps Solar Programme Water Heaters Thermal Storage Tanks Domestic Boilers."

[62] K. Ahmed, P. Pylsy, and J. Kurnitski, "Hourly consumption profiles of domestic hot water for different occupant groups in dwellings," *Sol. Energy*, vol. 137, pp. 516–530, Nov. 2016.

[63] T. T. Chow, G. Pei, K. F. Fong, Z. Lin, A. L. S. Chan, and M. He, "Modeling and application of direct-expansion solar-assisted heat pump for water heating in subtropical Hong Kong," *Appl. Energy*, vol. 87, no. 2, pp. 643–649, 2010.

[64] "Q-ton is a heat pump for the production of domestic hot water up to 90° C with refrigerant gas R744 (CO2)."

[65] N. C. Baek, U. C. Shin, and J. H. Yoon, "A study on the design and analysis of a heat pump heating system using wastewater as a heat source," 2004.

[66] M. Tammaro, C. Montagud, J. M. Corberán, A. W. Mauro, and R. Mastrullo, "A propane water-to-water heat pump booster for sanitary hot water production: Seasonal performance analysis of a new solution optimizing COP," *Int. J. Refrig.*, vol. 51, pp. 59–69, 2015.

[67] P. Eslami-Nejad and M. Bernier, "IMPACT OF GREY WATER HEAT RECOVERY ON THE ELECTRICAL DEMAND OF DOMESTIC HOT WATER HEATERS."

[68] U. I. Dar, I. Sartori, L. Georges, and V. Novakovic, "Advanced control of heat pumps for improved flexibility of Net-ZEB towards the grid," *Energy Build.*, vol. 69, pp. 74–84, Feb. 2014.

[69] M. Tammaro, C. Montagud, J. M. Corberán, A. W. Mauro, and R. Mastrullo, "Seasonal performance assessment of sanitary hot water production systems using propane and CO2 heat pumps," *Int. J. Refrig.*, vol. 74, pp. 222–237, 2017.

[70] C. Shen, Z. Lei, Y. Wang, C. Zhang, and Y. Yao, "A review on the current research and application of wastewater source heat pumps in China," *Therm. Sci. Eng. Prog.*, vol. 6, pp. 140–156, Jun. 2018.

[71] A. Hepbasli, E. Biyik, O. Ekren, H. Gunerhan, and M. Araz, "A key review of wastewater source heat pump (WWSHP) systems," *Energy Convers. Manag.*, vol. 88, pp. 700–722, 2014.

[72] "Method for producing a flow of hot water and associated system," Apr. 2012.

[73] J. G.-M. José Miguel Corberán, "Refrigeration Technologies Software IMST-ART." Universidad Politécnica de Valencia, Valencia, 2009.

[74] K. SA., "Engineering equation Solver. F-Chart Software." 2003.

[75] "TRNSYS : Transient System Simulation Tool 2016." .

[76] J. M. Corberan, J. Gonzalvez, P. Montes, R. Blasco, J. M. Corberán, J. Gonzálvez, P. Montes, and R. Blasco, "Purdue e-Pubs ' ART' A Computer Code To Assist The Design Of Refrigeration and A/C Equipment R9-4 'ART' A COMPUTER CODE TO ASSIST THE DESIGN OF REFRIGERATION AND A/C EQUIPMENT," 2002.

[77] P. F. de C. J. G. F. A. José M. Corberán, Pedro Fernández d, "SEMIEXPLICIT METHOD FOR WALL TEMPERATURE LINKED EQUATIONS (SEWTLE): A GENERAL FINITE-VOLUME TECHNIQUE FOR THE CALCULATION OF COMPLEX HEAT EXCHANGERS," *Numer. Heat Transf. Part B Fundam.*, vol. 40, no. 1, pp. 37–59, Jul. 2001.

[78] M. Pitarch, E. Navarro-Peris, J. Gonzálvez-Maciá, and J. M. Corberán, "Experimental study of a heat pump with high subcooling in the condenser for sanitary hot water production," *Sci. Technol. Built Environ.*, vol. 24, no. 1, pp. 105–114, Jan. 2018.

[79] J. L. Yang, Y. T. Ma, M. X. Li, and H. Q. Guan, "Exergy analysis of transcritical carbon dioxide refrigeration cycle with an expander," *Energy*, vol. 30, no. 7, pp. 1162–1175, Jun. 2005.

[80] A. Bahman, D. Ziviani, and E. Groll, "Development and Validation of a Mechanistic Vapor-Compression Cycle Model." 2018.

[81] SWEP, "SWEP. (s.f.). SSP G7 version 7.0.3.53." .

[82] A. F. Mills, *Heat Transfer*. Concord, MA 01742: Richard D. Irwnin Inc.

[83] "gasnaturalfenosa." [Online]. Available: http://www.gasnaturalfenosa.es/es/Empresas/Electricidad_o_gas/Contratar_electricidad_o_gas/Tarifa_Fija.html. [Accessed: 06-Feb-2016].

[84] IDAE, "Regulated tariffs in Spain, IDAE," 2016.

[85] M. Y. Haller, R. Dott, J. Ruschenburg, F. Ochs, and J. Bony, "The Reference

Framework for System Simulations of the IEA SHC Task 44 / HPP Annex 38 Part A: General Simulation Boundary Conditions A technical report of subtask C Report C1 Part A, Final-Revised."

[86] "A stochastic bottom-up model for space heating and domestic hot water load profiles for German households," *Energy Build.*, vol. 124, pp. 120–128, Jul. 2016.

[87] Federal Ministry for the Environment Nature Conservation and Nuclear Safety, "Wasserverbrauch im Haushalt | Media | BMU," 2013. [Online]. Available: https://www.bmu.de/media/wasserverbrauch-im-haushalt/. [Accessed: 15-Nov-2018].

[88] E. Hervas-Blasco, M. Pitarch, E. Navarro-Peris, and J. M. Corberán, "Optimal sizing of a heat pump booster for sanitary hot water production to maximize benefit for the substitution of gas boilers," *Energy*, vol. 127, pp. 558–570, 2017.

[89] A. A. Hasan, D. Y. Goswami, and S. Vijayaraghavan, "First and second law analysis of a new power and refrigeration thermodynamic cycle using a solar heat source," *Sol. Energy*, vol. 73, no. 5, pp. 385–393, Nov. 2002.

[90] Miquel Pitarch i Mocholí, "High capacity heat pump development for sanitary hot water production," 2017.

[91] M. P. i Mocholí, "High capacity heat pump development for sanitary hot water production," UPV, 2017.

Appendix A

Experimental setup and test conditions

The 1V0K heat pump prototype is tested in the same test rig that the one designed and built in the thesis [1]. The information provided in this appendix is the same as in that thesis. Only updates related to the 1V0K heat pump design have been added to the description of the [1] thesis.

This appendix describes the three heat pump designs tested, the experimental setup (test rig) used to test the prototype in addition to the sensors and the error analysis used in the three configurations. Furthermore, the test conditions of the experimental campaigns performed with both configurations are described in Chapter 2 and Chapter 3.

A.1 Heat pump designs

The liquid receiver (LR) is a common accessory in heat pumps and refrigeration systems. Not only to accommodate an excess of refrigerant to recover from losses along time, but also to control the active refrigerant charge in order to work with the optimal subcooling'. Nevertheless, in the scientific literature, not many authors have paid attention to the influence of liquid receiver characteristics on the system performance, and none of them has studied its influence during transient behavior due to changes in the operating conditions.

This work compares the effect of two different configurations designs of the inlet port for the liquid receiver experimentally. The differences are found in the shape of the inlet and outlet port inside the liquid receiver. The LR is installed in a heat pump for producing domestic hot water and working with propane, in such a systems the distribution of the charge is very important to obtain great performance.

Results have shown that transient behavior differs highly depending on which LR configuration is used. For instance, the transient period last 35 minutes in one configuration, while in the other one takes less than 5 minutes.

A.2 Experimental setup

Figure A. 1 depicts the lay-out of the test rig. The test rig is able to test water-to-water heat pumps with a heating capacity up to 70 kW. The unit to be tested is inside the dashed line, where points 1 and 2 are the inlet/outlet of the heat sink (demand side), and points 3 and 4 are the inlet/outlet of the heat source (waste heat side). The test rig is able to maintain constant the water temperature at these points.

The test rig consists of five loops:

1. The main loop is the propane refrigerant cycle (inside of dash line)
2. The water loop for the heat source (Evaporator). It simulates the heat recovery from a water source.
3. The water loop for the heat sink (Condenser). It simulates the DHW production.
4. The water/glycol loop.
5. The chiller. Works with R410A

Regarding to the security measures derived from the use of Propane: the laboratory is equipped with gas sensors and an alarm system able to detect a propane leakage in order to start with a security routine. The heat pump has a total refrigerant charge of 6.5 kg. This charge is the refrigerant required to work with any of the three designs at all considered conditions. This charge is use for testing purposes and it could be reduced up to 5kg if commercialized.

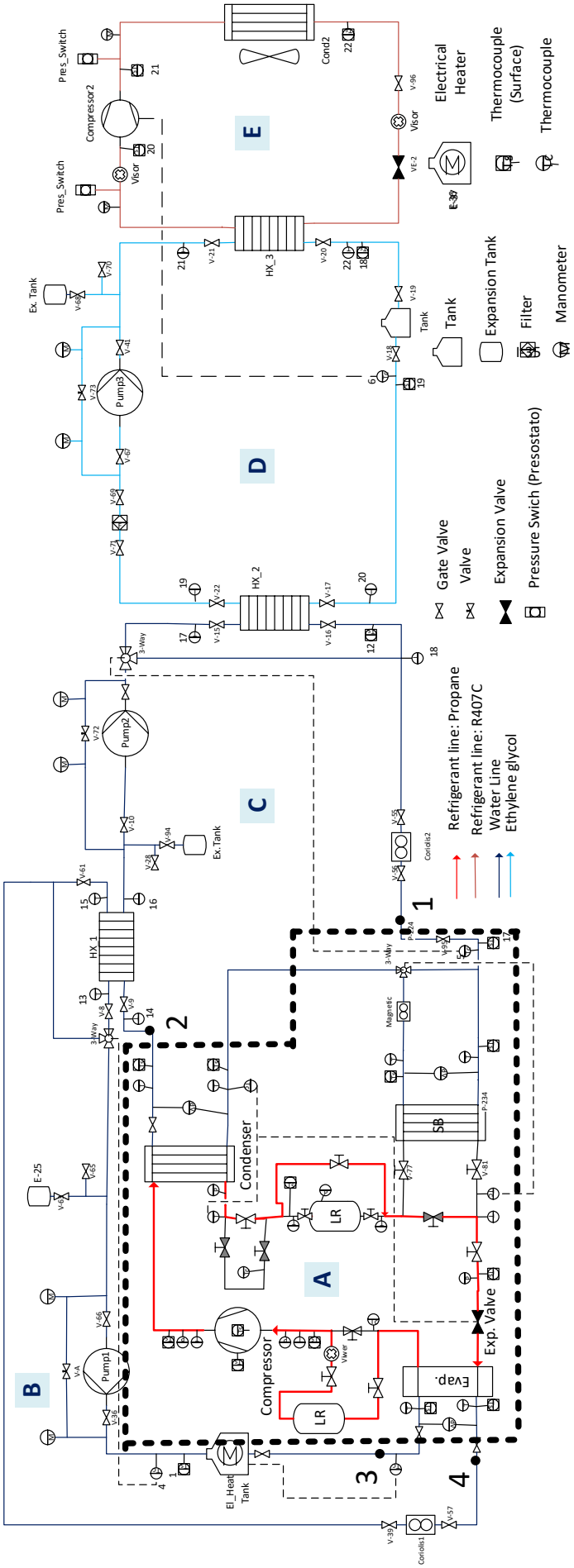

Figure A.1: Lay-out of the test rig including sensors

A.2.1 Propane cycle (Prototype configurations)

Figure A.2 represents the main features, general layouts and refrigerant cycles of the three heat pump concepts developed in the test rig. Figure A.2.(1) shows the characteristics of the 10K1K configuration. Figure A.2.(2) belongs to the 10K2V configuration and the third configuration shows the characteristics of the 0K1V configuration.

About the nomenclature, the first number is the superheat degree while the second part of the name means the number of control expansion valves.

The 10K1V configuration, for instance, "10K means the superheat degree set point and 1V means the number of control valves, in this case, one". In this configuration we make the subcooling in a heat exchanger dedicated to it. Its control is not possible and the expansion valve controls the superheat, which is set to 10K. By placing the liquid receiver at the outlet of the condenser, we ensure saturated conditions in that point.

In 10K2V, that is 10K of superheat and 2 control valves, subcooling is made in the condenser and the throttling valve controls it. The liquid receiver ensures saturated conditions at the outlet of the valve and the expansion valve is used to control superheat.

Both configurations were developed in the frame of the thesis [90]. Please refer to it in order to obtain a further details. The 0K1V is the new configuration and it has been one of the objectives of this work.

In the 0K1V configuration, subcooling is made in the condenser as well and the expansion valve controls it. Zero superheat and no liquid at the inlet of the compressor are possible thanks to the liquid receiver which is placed at the inlet of the compressor. A comprehensive study of this configuration is presented in Chapter 3.

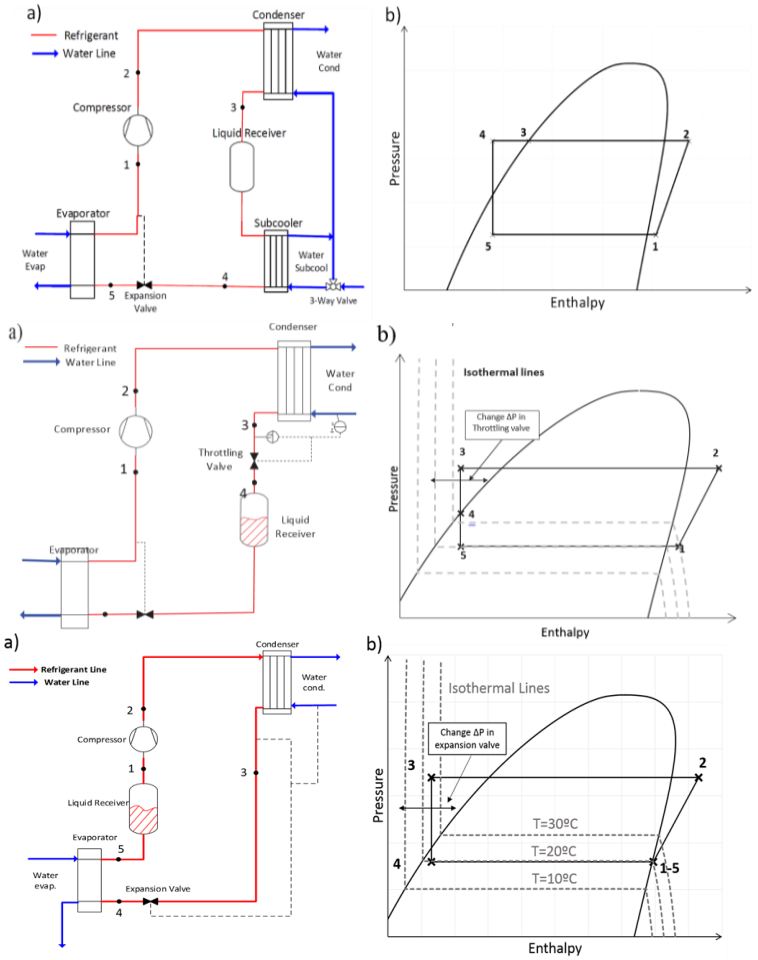

(1)

10K1V

- ❑Superheat = 10 K
- ❑ 1 control valve: Superheat
- ❑Subcooling in subcooler fix

(2)

10K2V

- ❑Superheat = 10 K
- ❑ 2 control valves: Superheat and subcooling

(3)

0K1V

- ❑Superheat = 0 K
- ❑ 1 control valve: Subcooling

Figure A.2: Main features, general layouts and refrigerant cycles of the three heat pump concepts developed in the test rig.

A.2.2 Water loop for the heat source (Evaporator)

Figure A.2 shows the scheme of the evaporator water loop with typical temperatures at the most representative points. This loops ensures the desired water temperature at the inlet and outlet of the evaporator. A frequency variable water pump adjusts the water mass flow rate, which will determine the temperature at the outlet of the evaporator. Furthermore, a bypass with a needle valve connecting the outlet and inlet of the water pump can be used for a more precise water mass flow rate control. In order to achieve the target temperature at the inlet of the evaporator, the water loop includes:

- A recovery heat exchanger that interacts with the condensing water loop to recover part of the energy in the condenser

- A three-way valve controlled by a PID in order to adjust the desired temperature at the outlet of the recovery HX.
- An electrical heater controlled by a PID to add the rest of the needed energy in case it is necessary.

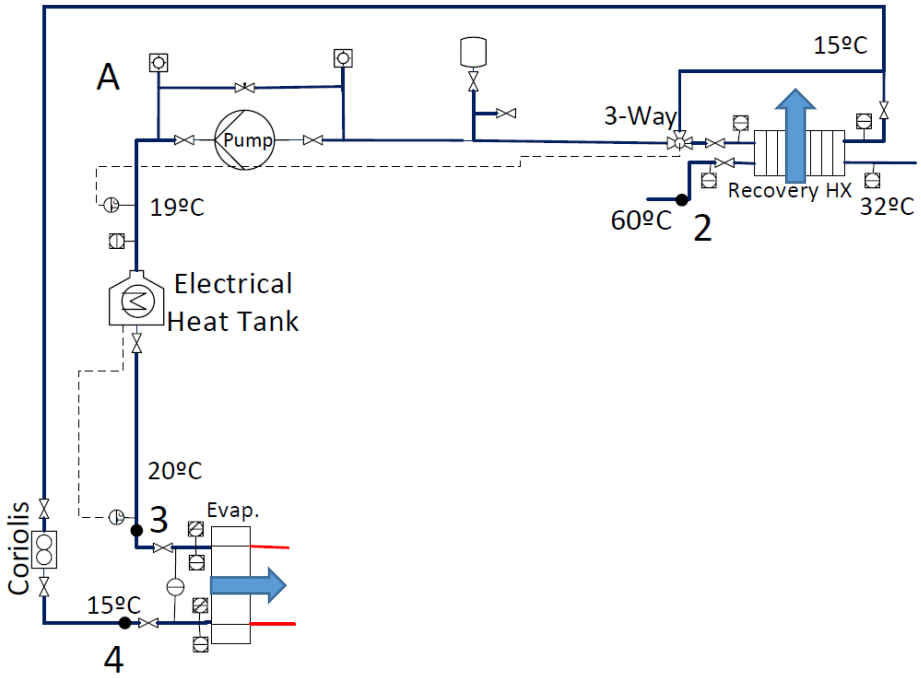

Figure A.3: Scheme of the heat source water loop with typical temperatures

A.2.3 Water loop for the heat sink (Condenser)

Figure A.3 shows the scheme of the condenser water loop with representative temperatures at different points. The condensing water loop maintains at the desired value the temperature of the water the outlet of the condenser (2) (usually 60 °C), and the inlet water temperature of the system fixed to a value ranging from 5°C to 55°C. A frequency variable water pump adjusts the water mass flow rate, which will determine the temperature at the outlet of the condenser. Furthermore, a bypass with a needle valve connecting the outlet and inlet of the water pump can be used for a more precise water mass flow rate control. In order to achieve the target temperature at the inlet of the heat pump prototype, this water loop consists of:

- A recovery heat exchanger that interacts with the evaporator water loop to recover. The heat transfer will depend on the evaporator water loop control.
- A heat exchanger that interacts with the water/glycol loop, which is used to cool down the water at the condenser loop.
- A three-way valve controlled by a PID in order to adjust the desired temperature at inlet of the heat pump prototype (5°C to 55°C)

The three-way valve controlling the water mass flow rate through the subcooler is part of the heat pump prototype. Figure 4.4 shows a picture of the evaporator and condenser water loops.

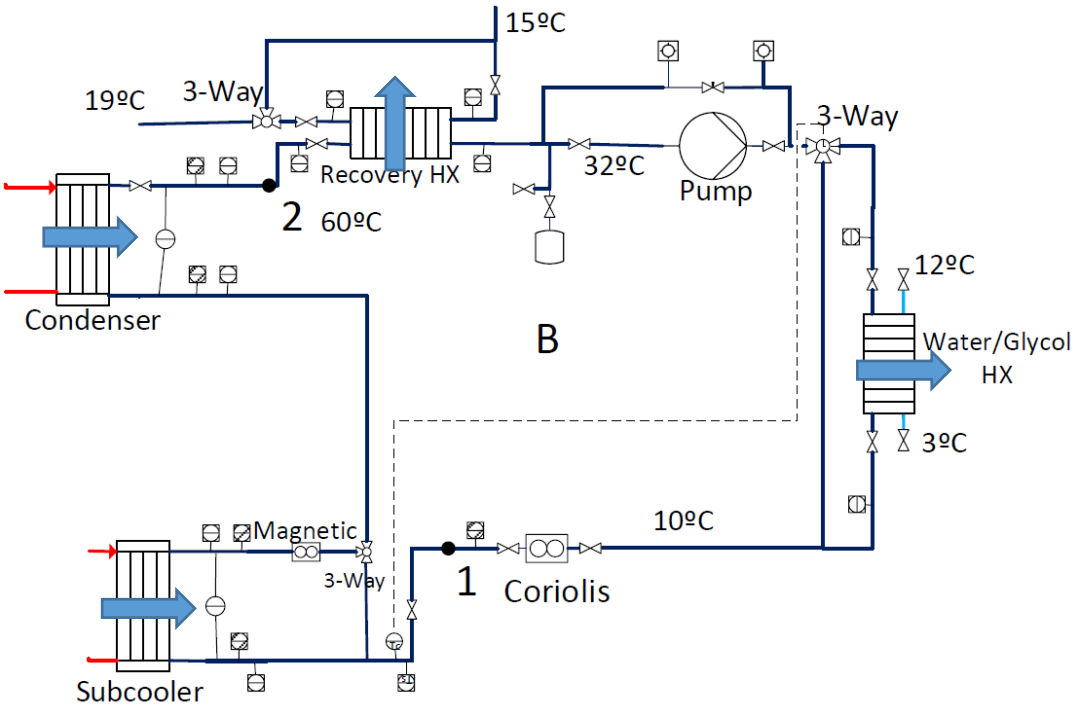

Figure A.4: Scheme of the heat sink water loop with representative temperatures

Figure A.5: Picture of the heat sink and source water loops on the test rig

A.2.4 Water/glycol and chiller working with R410A loops

Figure A.5 shows the scheme and the picture of the water/glycol and the chiller working with R410A loops. The chiller is in charge to pump out to the ambient the heat remaining in the water of the condenser loop after passing through the recovery heat exchanger. The capacity of the chiller is not controlled; hence, it does not match exactly with the required heat to be removed. To solve this issue, the water/glycol loop is equipped with an inertia tank that connects the condenser water loop and the chiller. With this configuration, the overall needed capacity is achieved by an ON-OFF control of the compressor (chiller). It starts or stops depending on the demand of cold of the system.

The ON/OFF control of the compressor is connected to the temperature at the outlet of the inertia tank (500 liters). The chiller is started when the controlled water/glycol temperature is above 4.5°C and stopped when this temperature is below 2°C.

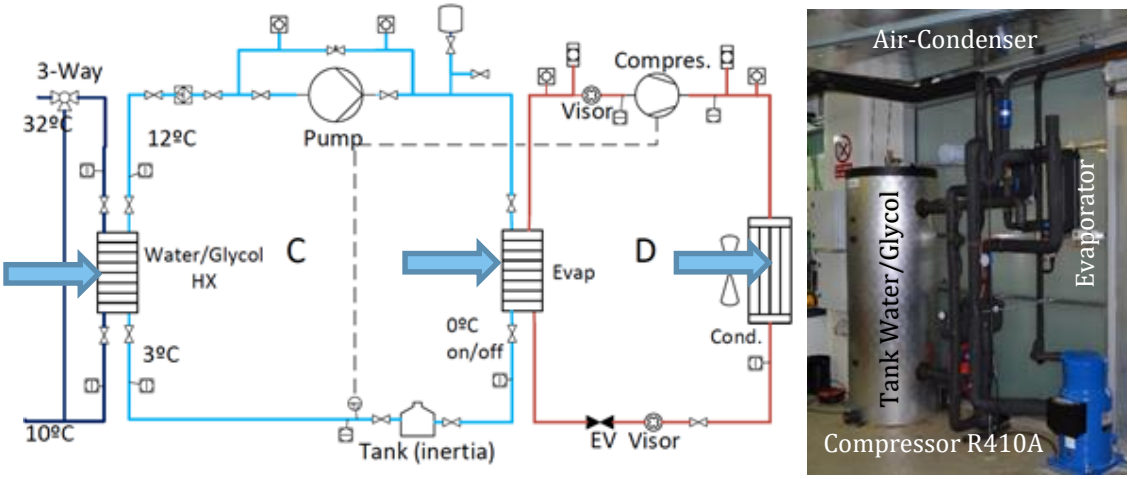

Figure A.6: Scheme and picture of the water/glycol and chiller loops

A.3 Sensors and error analysis

The evaporator and condenser capacities of the heat pump were measured from the waterside. In order to measure them as accurate as possible, six thermoresistances were located at inlet/outlet of each heat exchanger directly in contact with the water. In order to monitor and measure temperature in other points, a total number of 27 T-type thermocouples were used. The water mass flow rate through the evaporator and the condenser were measured with Coriolis mass flow meters. For control reasons, a magnetic mass flow meter was measuring the water mass flow through subcooler, which in most of the cases was the same as in the condenser. For the pressure, on the refrigerant side, there were three high accuracy Rosemount sensors. In the water side, there were 3 differential pressure sensors to measure the pressure drop in the heat exchangers. With these measurements and according to the norm EN 14511-3 “Test methods” (DIN EN 14511-3, 2013), the auxiliary consumption of the water pumps was calculated (Appendix B).

In order to monitor and measure those key parameters to evaluate the performance of the heat pump, all the sensors were connected to a data acquisition system “Agilent 34970A”, where all parameters were monitored.

Table A.1 shows the main sensors with the relative and absolute accuracy for the sensor. The reader can refer to Appendix B to find details about uncertainties and other information of the experimental results.

Table A.1: Sensors and their uncertainity

Magnitude	Model	Relative Accuracy	Absolute Accuracy	Units
Pressure	Differential 1151 Smart Rosemount	0.13 % of Span	5 E-04	bar
	Differential p Siemens Sitrans	0.14 % of Span	4 E-04	bar
	Differential p Setra	0.3 % of Span	1.7 E-03	bar
	P 1151 Smart GP7 Rosemount	0.12 % of Span	0.03	bar
	P 1151 Smart GP8 Rosemount	0.15 % of Span	0.08	bar
	P 3051 TG3 Rosemount	0.14 % of Span	0.04	bar
Temperature	Thermocouple T-Type		1	°C
	RTD Class 1/10 DIN		0.06	°C
Flow	Coriolis SITRANS F C MASS 2100	0.3 % of Reading		
	Magnetic SITRANS FM MAG5100 W	0.4 % of Reading		
Power	DME 442	0.3 % of Reading		

A.4 Performed tests

This section describes the experimental measurements performed with 0K1V and 10K2V configurations and presented in Chapter 3.

The data acquisition of each test is recorded every 10 seconds during 30 minutes starting once the system is stabilized on the set conditions. In order to ensure a steady state behavior, all the measured points were checked to lie under the limits marked by the norm EN 14511-3 “Test methods” (DIN EN 14511-3, 2013).

A first campaign in order to characterize the 0K1V configuration and compare its performance with the 10K2V configuration was carried out. Hence, a similar test matrix that the one already available with the 10K2V [91] was measured.

The matrix was defined in order to cover most of the typical temperature conditions of the DHW application. That is, 60°C as water outlet temperature at the condenser, a variation of the inlet water temperature at the condenser from 10-50°C and 60°C.

In the evaporator, the inlet water temperatures ranged from 10°C to 30°C, which corresponds to the waste heat recovery application. The water mass flow through the evaporator was adjusted in order to obtain a 5 K water temperature decrease at the nominal point (water 20°C/15°C at the evaporator and 10°C to 60°C for the hot water production). The water mass flow rate adjusted in the nominal point was kept constant for the rest of test points (around 7000 kgh^{-1}). This procedure is described in the European Standard EN 14825 (EN 14825, 2011).

Table A2 shows the test matrix with a total number of 86 measured points with the 0K1V configuration. Superheat was kept lower than 2°C at any condition.

Table A.2: Test matrix with a total number of 86 measured points with 0K1V configuration used to compare the results from 10K2V and to validate the IMST-ART model employed in the Chapter 3.

$T_{w,ei}$ [°C]	$T_{w,ci}$ [°C]	$T_{w,co}$ [°C]	Refrigerant *Sc* range [K]
10	10	60	From 4 to 54
	30		From 4 to 36
	50		From 4 to 16
20	10		From 4 to 54
	30		From 4 to 36
	50		From 4 to 16
30	10		From 4 to 54
	30		From 4 to 36
	50		From 4 to 16

A second campaign in order to characterize both configurations for other possible water heating applications (industrial, commercial) was performed. Tests with higher water temperatures at the outlet of the condenser were carried out (up to 90°C). In this case, the water inlet temperature at the evaporator was ranged from 20 to 30°C simulating water heating recovery applications while the water

inlet temperature at the condenser was set to 30 and 40°C (typical values of the water from the net obtained within heat recovery applications after passing through a pre-heater heat exchanger or recuperator). The evaporator water mass flow rate was kept around 7000 kgh^{-1} according to the designed conditions explained for the first campaign.

Table A.3 shows the test matrix with 18 measured points with each of the configurations (0K1V and 10K2V). Superheat was kept lower than 2°C at any condition in the 0K1V mode while 10K were maintained in the tests performed with 10K2V configuration.

Table A.3: Test matrix with a total number of 18 measured points in each 0K1V and 10K2V configurations used to analyze the performance under limit conditions used in Chapter 3.

$T_{w,ei}$ [°C]	$T_{w,ci}$ [°C]	$T_{w,co}$ [°C]	$DT_{control}$ [K]
20	30	70	3 and 5
		80	5 and 7
		90	5 and 9
	40	70	3 and 5
		80	5 and 7
		90	5 and 9
30	30	70	3 and 5
		80	5 and 7
		90	5 and 9

The third campaign had the objective of evaluating both configurations under different evaporating conditions (common within heat recovery applications with limited heat source). In this case, the water conditions at the condenser were kept constant (20-60°C). The water inlet temperature at the evaporator ranged from 15°C to 35°C (simulating heat recovery temperatures) and the water mass flow rate through the evaporator was varied from the minimum water mass flow rate to the maximum according to the auxiliary pump capacity.

Table A.4 shows the test matrix with a total number of 54 measured points with each of the configurations (0K1V and 10K2V). Superheat was kept lower than 2°C at any condition in the 0K1V mode while 10K were maintained in the tests performed with 10K2V configuration

Table A.4: Test matrix with 54 measured points in each of the configurations (0K1V and 10K2V) used to analyze and compare the influence on the performance of the water temperature lift at the evaporator used in Chapter 3.

$T_{w,ei}$ [ºC]	$DT_{w,evap}$ [K]	$T_{w,ci}$ and $T_{w,co}$ [ºC]	Refrigerant *Sc* range [K]
15	From 3.5-9		
20	From 4-12.5	20 - 60	From 28-39
35	From 5-21		

Appendix B

Refrigerant distribution in the evaporator

This appendix presents the qualitative analysis performed in order to find possible reasons regarding to the mismatch obtained from theoretical expectations (the existence of an optimal degree of superheat based on the secondary temperature glide at the evaporator) and experimental results (higher performances are obtained always with low/zero superheats, that is, configuration 0K1V has greater performance than configuration 10K2V regardless the secondary conditions at the evaporator). First, a comparison between the heat pump performances calculated and experimentally measured, are depicted. Second, an analysis of the refrigerant distribution in the evaporator is shown and possible reasons of the experimental results are pointed out.

B.1 Experimental and theoretic heat pump performance

Figure B.1. shows the experimental and theoretic performance variation with the secondary temperature lift at the evaporator for zero superheat (0K1V) and for 10K of superheat (10K2V) for water inlet temperatures at the evaporator of 35 °C, 20 °C and 15 °C and constant conditions at the secondary fluid of the condesnser (Tw_ci=20 °C and Tw_co=60 °C). Dash green lines represents theoretical performances without superheat while in orange dots the experimental results are represented. Blue lines belong to theoretic performances with 10K of superheat and triangles are used to represent experimental results with 10K of superheat. Experimental results were obtained from the campaign described in Chapter 3, Figure 8 and theoretic performances were calculated from the model of the heat pump developed with the IMST-ART software (validated for the design condition

at the evaporator since experimental measures related to the evaporator side were not performed before).

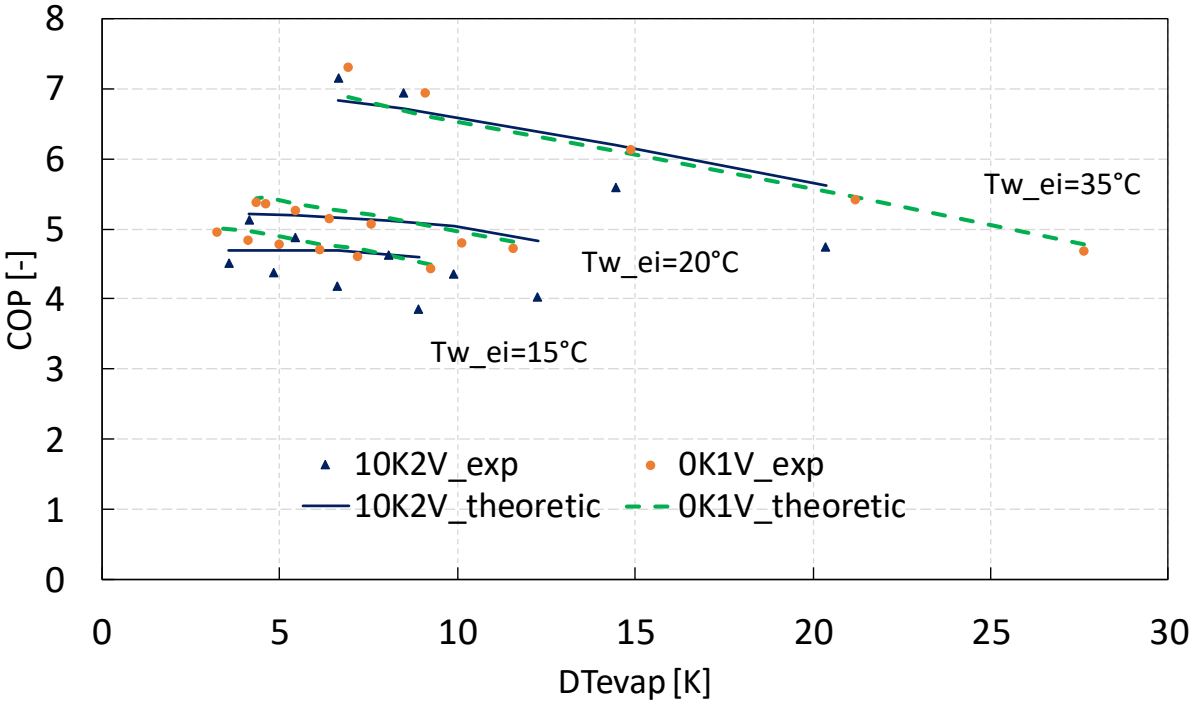

Figure B.1: Experimental and theoretic performance variation with the secondary temperature lift at the evaporator for zero superheat (0K1V) and 10K of superheat (10K2V) for different evaporating temperatures.

According to Figure B.1 and to the calculations realized in Chapter 4, having high degrees of superheat contributes to enhance the performance of the heat pump from a certain degree of temperature lifts at the secondary fluid of the evaporator. In fact, approximately from 8 K – 10 K of water temperature glides in the evaporator, having 10 K of superheat entails a better efficiencies than not having superheat.

Similar discrepancies were obtained for evaporating pressures, evaporating temperatures, and the main refrigerant cycle characteristics in the evaporator.

Therefore, the looking for an explanation, the observation of the refrigerant distribution in the evaporator was performed.

B.2 Distribution of the refrigerant in the evaporator

A qualitative investigation of the distribution of the refrigerant within the evaporator based on thermography was realized.

Water conditions in the condenser side were 20 °C at the inlet of the condenser and 60 °C at the outlet of the condenser as well as 20 °C is the water temperature at the inlet of the evaporator in all the pictures taken. Different evaporating pressures and temperatures as well as degrees of superheat were considered.

Figure B.2. shows a picture of the evaporator (frontal view as it is captured in the thermography) and a transversal sketch with the location of the water and refrigerant input/output ports and depicts the distribution of the refrigerant in the evaporator for different superheat values, evaporating temperatures and temperature glides of the water in the evaporator.

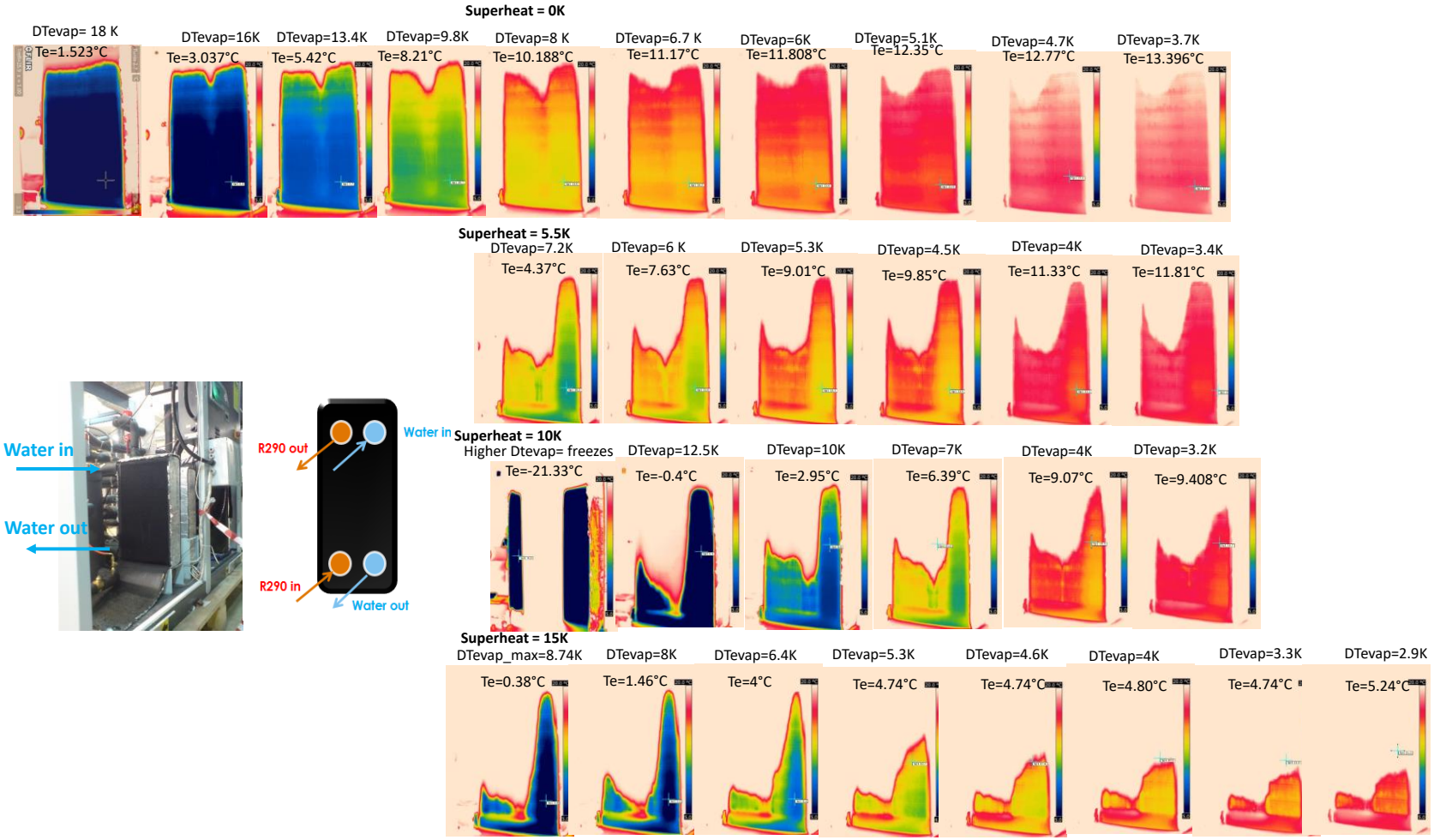

Figure B.2: Picture of a frontal view of the evaporator (face used for thermography) and a transversal view with the location of the refrigerant and water inlet/outlet ports. Thermography of the evaporator at different superheats and water temperature glides for the same water inlet temperature at the evaporator and water conditions in the condenser.

Figure B.3. represents the evaporating pressure and temperature variation with the water temperature glide at the evaporator for different superheats and the measured points of Figure B.2

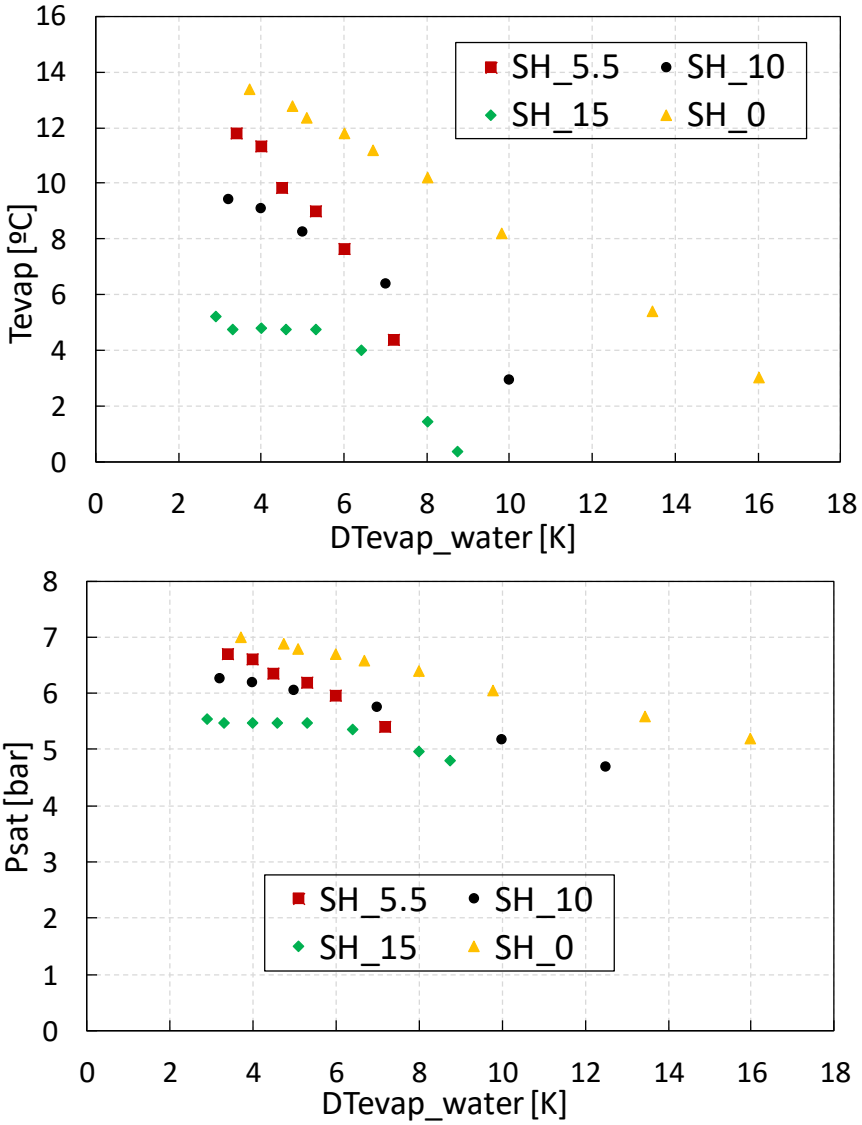

Figure B.3: Evaporating pressure and temperature variation with the water temperature glide at the evaporator for different superheats and the measured points of Figure B.2

As it can be seen figure B.2., a clear mal-distribution of the refrigerant in the evaporator takes place. This effect is magnified as superheat increases. In fact, for low/zero superheat values, the mal-distribution is not observed. The effect affects the evaporating temperature and pressure in the same manner.

Therefore, part of the evaporator area is not used when high degrees of superheat are applied. It could be the explanation of the theoretic and experimental discrepancies highlighted in Figure B.1.

A possible pressure drop imbalance in the plates could be the reason for the mal-distribution effect. However, this study was qualitative and had led to understand the discrepancies observed. A deeper study based on more detailed experimental analysis is required in order to find an explanation of the mal-distribution but it is out of the scope of this thesis. A new research line was opened in order to further work on this topic and it is currently being carried out by our Institut Universitari d'Investigació d'Enginyeria Energètica in collaboration with the Fraunhofer-Institut für Solare Energiesysteme ISE.

Appendix C

This appendix first presents the equations to calculate the heating COP and capacity accounting with the auxiliary consumption as it is indicated in EN 14511-3 "Test methods" (DIN EN 14511-3, 2013). Thereafter, the procedure to calculate the total uncertainty of the measured parameters and calculated variables is described according to the methodology followed in [91]. Finally, two tables include the main parameters and its total uncertainty for all measured points.

All the physical properties of propane and water are calculated using the software REFPROP 9.0 (Lemmon et al., 2007)

C.1 Auxiliary consumption

The heating COP and the heating capacity for the heat pump can be calculated as the heating capacity divided by the compressor energy input:

$$COP_{\mathrm{h}} = \frac{\dot{Q}_{\mathrm{h}}}{\dot{W}_{comp}} \tag{C.1}$$

$$\dot{Q}_{\mathrm{h}} = \dot{m}_{w,c} \cdot c_{p,w} \cdot \left(T_{w,co} - T_{w,ci}\right) \tag{C.2}$$

Where $\dot{m}_{w,c}$ is the water mass flow rate through the condenser, and $c_{p,w}$ is the specific heat for the water.

The auxiliary consumption of the water pumps to drive the water through the heat pump, can be added to the COP calculation as it is indicated in EN 14511-3 "Test methods" (DIN EN 14511-3, 2013) when the water pump is located outside the unit (as it is the case):

$$COP_{\mathrm{h},aux} = \frac{\dot{Q}_{\mathrm{h}} + \dot{W}_{aux,c}}{\dot{W}_{comp} + \dot{W}_{aux,c} + \dot{W}_{aux,e}} \tag{C.3}$$

$\dot{W}_{aux,c}$ accounts with the auxiliary consumption due to the condenser and subcooler (kW), and it is added to the heating capacity because part of this losses goes to the water that wants to be heated up. This term is also added to the compressor power input, together with the consumption due to the evaporator ($\dot{W}_{aux,e}$).

The auxiliary consumption is calculated with the hydraulic power (due to pressure drop, in kW) and a predefined pump efficiency defined by the norm:

$$\dot{W}_{aux} = \frac{\dot{W}_{\mathrm{h}ydraulic}}{\eta_{\mathrm{h}ydraulic}} = \frac{\dot{W}_{\mathrm{h}ydraulic}}{0.0721 \cdot (\dot{W}_{\mathrm{h}ydraulic} \cdot 1000)^{0.3183}} \tag{C.4}$$

The hydraulic power depends on the pressure drop (in kPa) at the heat pump components and the volumetric mass flow rate (for water in this case, in m^3/s):

$$\dot{W}_{\mathrm{h}ydraulic} = \Delta p \cdot \dot{V}_w \tag{C.5}$$

One should notice that, if the heating COP is given with the auxiliary consumption, the heating capacity must also include the auxiliary of the condenser. Then the heating capacity accounting with auxiliary:

$$Q_{\mathrm{h},aux} = \dot{Q}_{\mathrm{h}} + \dot{W}_{aux,c} \tag{C.6}$$

In this thesis, all the experimental results account for the auxiliary consumption unless the contrary is indicated. Therefore, for simplicity, the heating COP and capacity are always named as COP_h and Q_h.

C.2 Uncertainty

Once the steady state is reached, the physical properties are measured during half an hour every ten seconds. The mean value of each variable is used for the calculations. The total uncertainties include the systematic uncertainty of the sensor, the acquisition data (data logger), and the standard deviation of the mean value, which was calculated from the measured sequence during 30 minutes. The method described by Moffat (1988) and used in [91] was followed to calculate the uncertainties.

The uncertainty analysis for each of the measured variables is calculated as:

$$U_{0.95} = \{(B_{Xi})^2 + (tS_{\overline{Xi}})^2\}^{1/2} \tag{C.7}$$

Where B_{Xi} is the systematic uncertainty of the sensor and the acquisition data (at 95% of confidence), t is the Student's multiplier, which for 95% confidence and large sample data is equal to 1.96. $S_{\overline{X}i}$ is the sample standard deviation of the mean for the variable X

$$S_{\overline{Xi}} = \frac{S_{Xi}}{\sqrt{N}} \tag{C.8}$$

Where S_{Xi} is the sample standard deviation and N the number of observations at the test.

If the function R is calculated from several independent variables (X_i), the propagation error for the calculated parameters such as heating COP, the equation of propagating error is used.

$$\delta R = \left\{ \sum_{i=1}^{n} \left(\frac{\partial R}{\partial X_i} \, \delta X_i \right)^2 \right\}^{1/2} \tag{C.9}$$

For instance, in Eq.B.2, the heating capacity would be the variable R, while the water mass flow rate and temperatures would be the variables X_i, which have been measured directly with the Coriolis and the thermoresistances respectively.

C.3 Experimental results for the 0K1V design

Table C.1: Experimental results and uncertainties for the 0K1V design

$T_{w,ei}$ [°C]	$T_{w,ci}$ [°C]	$T_{w,co}$ [°C]	$m_{w,e}$ [kg/h]	$m_{w,c}$ [kg/h]	p_c [bar]	p_{LR} [bar]	Wc [kW]	Tc [°C]	Sc [K]	COP_h [-]	Q_h [kW]
20.03 ±0.08	10.06 ±0.08	60.01 ±0.08	1.948 ±0.004	0.2343 ±0.0008	21.95 ±0.05	7.84 ±0.03	8.97 ±0.06	61.77 ±0.12	44.4 ±0.2	5.42 ±0.03	48.92 ±0.02
20.06 ±0.08	10.02 ±0.08	60.01 ±0.09	1.945 ±0.004	0.2336 ±0.0008	21.56 ±0.05	7.86 ±0.03	8.84 ±0.06	60.88 ±0.12	43.3 ±0.2	5.49 ±0.03	48.81 ±0.02
19.97 ±0.08	10.03 ±0.08	59.99 ±0.09	1.943 ±0.004	0.2301 ±0.0007	20.85 ±0.05	8.02 ±0.03	8.61 ±0.05	59.26 ±0.12	41.0 ±0.2	5.54 ±0.04	48.03 ±0.02
19.93 ±0.08	9.97 ±0.08	59.94 ±0.09	1.945 ±0.004	0.2257 ±0.0008	20.45 ±0.05	8.61 ±0.03	8.51 ±0.06	58.32 ±0.13	37.3 ±0.2	5.51 ±0.04	47.15 ±0.02
20.03 ±0.08	9.93 ±0.08	59.94 ±0.09	1.948 ±0.004	0.2184 ±0.0008	20.27 ±0.05	9.57 ±0.03	8.46 ±0.06	57.90 ±0.13	32.7 ±0.2	5.36 ±0.04	45.64 ±0.02
19.98 ±0.08	9.94 ±0.08	60.02 ±0.09	1.953 ±0.004	0.2125 ±0.0007	20.16 ±0.05	10.79 ±0.03	8.43 ±0.06	57.66 ±0.13	27.6 ±0.2	5.24 ±0.03	44.483 ±0.015
19.93 ±0.08	9.92 ±0.08	60.08 ±0.09	1.961 ±0.004	0.1987 ±0.0006	20.02 ±0.05	13.25 ±0.03	8.40 ±0.06	57.32 ±0.13	18.6 ±0.2	4.93 ±0.03	41.655 ±0.011
19.96 ±0.08	9.93 ±0.08	60.03 ±0.09	1.967 ±0.004	0.1885 ±0.0006	19.95 ±0.05	14.64 ±0.03	8.36 ±0.06	57.14 ±0.13	14.1 ±0.2	4.69 ±0.03	39.465 ±0.01
19.97 ±0.08	9.93 ±0.08	60.09 ±0.09	1.971 ±0.004	0.1782 ±0.0006	19.91 ±0.05	16.04 ±0.03	8.36 ±0.05	57.04 ±0.13	9.9 ±0.2	4.44 ±0.03	37.357 ±0.01
19.95 ±0.08	10.01 ±0.08	59.95 ±0.08	1.977 ±0.004	0.1669 ±0.0006	19.78 ±0.05	17.98 ±0.03	8.31 ±0.05	56.72 ±0.13	4.41 ±0.14	4.17 ±0.03	34.847 ±0.009
19.95 ±0.08	29.99 ±0.08	59.98 ±0.08	1.999 ±0.004	0.3717 ±0.0014	27.00 ±0.05	10.94 ±0.03	10.52 ±0.05	72.19 ±0.1	41.58 ±0.14	4.40 ±0.02	46.59 ±0.03
19.97 ±0.08	29.96 ±0.08	59.96 ±0.08	1.999 ±0.004	0.3712 ±0.0014	27.00 ±0.05	10.94 ±0.03	10.53 ±0.05	72.21 ±0.1	41.60 ±0.14	4.40 ±0.02	46.55 ±0.03
19.95 ±0.08	29.90 ±0.08	60.03 ±0.08	1.998 ±0.004	0.3608 ±0.0014	22.19 ±0.05	11.19 ±0.03	9.00 ±0.05	62.31 ±0.12	30.8 ±0.2	5.01 ±0.03	45.43 ±0.03
20.01 ±0.08	29.93 ±0.08	59.93 ±0.08	1.998 ±0.004	0.3579 ±0.0013	21.44 ±0.05	11.52 ±0.03	8.75 ±0.05	60.63 ±0.12	27.9 ±0.2	5.09 ±0.03	44.87 ±0.02
20.03 ±0.08	29.88 ±0.08	59.97 ±0.08	1.998 ±0.004	0.3566 ±0.0013	21.45 ±0.05	11.53 ±0.03	8.77 ±0.05	60.66 ±0.12	27.9 ±0.2	5.08 ±0.03	44.84 ±0.02
20.06 ±0.08	29.89 ±0.08	60.03 ±0.08	1.999 ±0.004	0.3571 ±0.0015	21.41 ±0.05	11.61 ±0.03	8.76 ±0.05	60.56 ±0.12	27.5 ±0.2	5.10 ±0.03	44.99 ±0.03
20.02 ±0.08	29.89 ±0.08	59.91 ±0.08	1.999 ±0.004	0.356 ±0.002	21.19 ±0.05	11.91 ±0.03	8.69 ±0.05	60.05 ±0.12	25.9 ±0.2	5.10 ±0.03	44.68 ±0.03
19.95 ±0.08	29.90 ±0.08	59.99 ±0.08	1.999 ±0.004	0.3513 ±0.0014	21.08 ±0.05	12.30 ±0.03	8.65 ±0.05	59.80 ±0.12	24.3 ±0.2	5.07 ±0.03	44.18 ±0.02

20.10 ±0.08	19.98 ±0.08	59.99 ±0.09	0.767 ±0.002	0.2410 ±0.0006	22.19 ±0.05	8.73 ±0.03	8.70 ±0.06	62.30 ±0.12	40.8 ±0.2	4.61 ±0.03	40.301 ±0.01
20.13 ±0.08	19.97 ±0.08	59.99 ±0.09	0.767 ±0.002	0.2396 ±0.0006	20.94 ±0.05	9.15 ±0.03	8.33 ±0.06	59.48 ±0.12	36.1 ±0.2	4.79 ±0.03	40.077 ±0.01
20.01 ±0.08	20.00 ±0.08	59.91 ±0.08	0.710 ±0.002	0.2223 ±0.0006	20.30 ±0.05	11.71 ±0.03	8.20 ±0.06	57.99 ±0.13	24.5 ±0.2	4.50 ±0.03	37.070 ±0.009
20.04 ±0.08	20.03 ±0.08	59.95 ±0.09	0.556 ±0.002	0.1823 ±0.0006	20.05 ±0.05	15.34 ±0.03	8.11 ±0.06	57.38 ±0.13	12.3 ±0.2	3.74 ±0.03	30.416 ±0.007
20.11 ±0.08	19.96 ±0.08	59.98 ±0.09	1.102 ±0.002	0.2577 ±0.0007	21.76 ±0.07	9.00 ±0.03	8.63 ±0.06	61.35 ±0.15	38.6 ±0.2	4.97 ±0.03	43.101 ±0.012
20.10 ±0.08	19.98 ±0.08	59.87 ±0.08	1.102 ±0.002	0.2545 ±0.0006	20.76 ±0.05	9.71 ±0.03	8.36 ±0.05	59.07 ±0.12	33.3 ±0.2	5.05 ±0.03	42.416 ±0.01
20.00 ±0.08	19.99 ±0.08	60.09 ±0.08	1.045 ±0.002	0.2386 ±0.0006	20.46 ±0.05	11.62 ±0.03	8.29 ±0.05	58.36 ±0.13	25.3 ±0.2	4.80 ±0.03	39.982 ±0.01
15.16 ±0.08	19.96 ±0.08	59.96 ±0.08	0.754 ±0.002	0.2187 ±0.0006	21.07 ±0.05	8.56 ±0.03	8.24 ±0.05	59.77 ±0.12	39.0 ±0.2	4.42 ±0.03	36.564 ±0.008
15.04 ±0.08	19.99 ±0.08	59.88 ±0.08	0.755 ±0.002	0.2142 ±0.0006	20.51 ±0.05	9.24 ±0.03	8.08 ±0.05	58.47 ±0.12	34.7 ±0.2	4.40 ±0.03	35.725 ±0.008
14.92 ±0.08	19.96 ±0.08	60.06 ±0.08	0.635 ±0.002	0.1834 ±0.0006	20.18 ±0.05	11.91 ±0.03	8.04 ±0.06	57.70 ±0.13	23.6 ±0.2	3.81 ±0.03	30.734 ±0.007
20.12 ±0.08	19.97 ±0.08	60.03 ±0.08	0.670 ±0.002	0.2385 ±0.0006	22.50 ±0.05	8.65 ±0.03	8.79 ±0.05	62.99 ±0.12	41.8 ±0.2	4.53 ±0.03	39.931 ±0.01
20.19 ±0.08	20.04 ±0.08	60.05 ±0.08	0.657 ±0.002	0.2345 ±0.0006	20.85 ±0.05	9.16 ±0.03	8.29 ±0.05	59.27 ±0.12	35.8 ±0.2	4.71 ±0.03	39.207 ±0.009
20.03 ±0.08	20.05 ±0.08	59.91 ±0.08	0.631 ±0.002	0.2261 ±0.0006	20.45 ±0.05	10.20 ±0.03	8.18 ±0.06	58.33 ±0.13	30.6 ±0.2	4.59 ±0.03	37.676 ±0.009
20.02 ±0.08	20.06 ±0.08	60.01 ±0.08	0.537 ±0.002	0.1981 ±0.0006	20.23 ±0.05	12.43 ±0.03	8.11 ±0.06	57.80 ±0.13	21.8 ±0.2	4.06 ±0.03	33.066 ±0.008
19.99 ±0.08	30.05 ±0.08	60.00 ±0.08	2.006 ±0.004	0.316 ±0.002	20.62 ±0.05	16.38 ±0.03	8.57 ±0.05	58.73 ±0.12	10.63 ±0.14	4.59 ±0.03	39.60 ±0.05
14.91 ±0.08	20.07 ±0.08	60.10 ±0.09	0.577 ±0.002	0.1737 ±0.0006	20.13 ±0.05	12.80 ±0.03	8.00 ±0.05	57.56 ±0.13	20.4 ±0.2	3.62 ±0.02	29.060 ±0.007
15.04 ±0.08	19.95 ±0.08	60.01 ±0.08	1.033 ±0.002	0.2302 ±0.0006	21.94 ±0.05	8.58 ±0.03	8.56 ±0.05	61.74 ±0.12	40.9 ±0.2	4.48 ±0.03	38.538 ±0.009
15.05 ±0.08	19.96 ±0.08	59.86 ±0.08	1.012 ±0.002	0.2267 ±0.0006	20.70 ±0.05	9.11 ±0.03	8.20 ±0.05	58.91 ±0.12	35.7 ±0.2	4.59 ±0.03	37.807 ±0.009
15.06 ±0.08	19.99 ±0.08	60.06 ±0.08	0.960 ±0.002	0.2148 ±0.0006	20.44 ±0.05	10.44 ±0.03	8.14 ±0.05	58.30 ±0.13	29.6 ±0.2	4.40 ±0.03	35.968 ±0.009
14.97 ±0.08	20.07 ±0.08	60.09 ±0.08	0.773 ±0.002	0.1747 ±0.0006	20.09 ±0.05	14.41 ±0.03	8.08 ±0.05	57.49 ±0.13	15.13 ±0.15	3.60 ±0.02	29.219 ±0.006
15.11	19.95	60.03	1.235	0.2365	22.49	8.63	8.77	62.97	41.9	4.49	39.619

±0.08	±0.08	±0.08	±0.003	±0.0006	±0.05	±0.03	±0.06	±0.12	±0.2	±0.03	±0.01
15.05 ±0.08	19.94 ±0.08	59.97 ±0.09	1.236 ±0.003	0.2341 ±0.0006	21.01 ±0.05	8.95 ±0.03	8.32 ±0.06	59.63 ±0.12	37.1 ±0.2	4.68 ±0.03	39.175 ±0.01
15.02 ±0.08	19.96 ±0.09	60.04 ±0.08	1.236 ±0.003	0.2261 ±0.0006	20.54 ±0.05	10.07 ±0.03	8.22 ±0.06	58.53 ±0.13	31.3 ±0.2	4.58 ±0.03	37.870 ±0.009
14.85 ±0.08	19.93 ±0.08	60.10 ±0.08	0.990 ±0.002	0.1859 ±0.0006	20.17 ±0.05	13.83 ±0.03	8.15 ±0.06	57.66 ±0.13	17.1 ±0.2	3.81 ±0.03	31.209 ±0.007
19.98 ±0.08	29.89 ±0.09	60.20 ±0.09	2.010 ±0.004	0.2701 ±0.0008	20.59 ±0.05	18.65 ±0.03	8.54 ±0.05	58.65 ±0.13	4.61 ±0.15	3.98 ±0.02	34.226 ±0.011
20.06 ±0.08	29.87 ±0.09	60.01 ±0.08	2.001 ±0.004	0.3540 ±0.0009	21.85 ±0.05	11.36 ±0.03	8.87 ±0.06	61.54 ±0.12	29.4 ±0.2	4.99 ±0.03	44.60 ±0.02
20.04 ±0.08	29.89 ±0.08	60.19 ±0.08	2.001 ±0.004	0.3466 ±0.0008	21.44 ±0.05	11.85 ±0.03	8.76 ±0.05	60.62 ±0.12	26.7 ±0.2	4.98 ±0.03	43.918 ±0.014
19.97 ±0.08	29.87 ±0.09	59.99 ±0.08	2.001 ±0.004	0.3453 ±0.0008	21.22 ±0.05	12.14 ±0.03	8.66 ±0.06	60.13 ±0.12	25.2 ±0.2	4.98 ±0.03	43.473 ±0.015
20.03 ±0.08	29.95 ±0.09	59.95 ±0.09	2.003 ±0.004	0.3348 ±0.0009	20.95 ±0.05	13.31 ±0.03	8.61 ±0.05	59.50 ±0.12	20.6 ±0.2	4.84 ±0.03	41.978 ±0.014
20.03 ±0.08	29.95 ±0.09	60.07 ±0.08	2.003 ±0.004	0.3310 ±0.0008	20.97 ±0.05	13.53 ±0.03	8.60 ±0.05	59.53 ±0.12	19.94 ±0.15	4.81 ±0.03	41.671 ±0.013
20.03 ±0.08	29.86 ±0.09	60.17 ±0.08	2.006 ±0.004	0.3110 ±0.0008	20.83 ±0.05	14.98 ±0.03	8.59 ±0.05	59.22 ±0.12	15.13 ±0.15	4.56 ±0.03	39.401 ±0.012
20.01 ±0.08	29.90 ±0.09	60.14 ±0.09	2.006 ±0.004	0.3117 ±0.0008	20.80 ±0.05	14.95 ±0.03	8.57 ±0.05	59.16 ±0.12	15.16 ±0.15	4.56 ±0.03	39.400 ±0.013
20.02 ±0.08	29.92 ±0.09	59.85 ±0.09	2.006 ±0.004	0.3055 ±0.0008	20.66 ±0.05	15.85 ±0.03	8.52 ±0.05	58.82 ±0.13	12.20 ±0.15	4.45 ±0.03	38.227 ±0.013
19.95 ±0.08	29.86 ±0.09	59.93 ±0.08	2.008 ±0.004	0.2918 ±0.0008	20.60 ±0.05	16.97 ±0.03	8.53 ±0.05	58.68 ±0.12	8.99 ±0.14	4.27 ±0.03	36.670 ±0.011
19.97 ±0.08	29.88 ±0.09	60.13 ±0.08	2.009 ±0.004	0.2782 ±0.0008	20.61 ±0.05	17.99 ±0.03	8.54 ±0.05	58.70 ±0.12	6.32 ±0.14	4.09 ±0.03	35.182 ±0.01
15.03 ±0.08	19.96 ±0.08	59.92 ±0.08	1.545 ±0.003	0.2426 ±0.0006	22.52 ±0.05	8.67 ±0.03	8.80 ±0.06	63.02 ±0.12	41.8 ±0.2	4.58 ±0.03	40.527 ±0.01
14.99 ±0.08	20.00 ±0.08	59.95 ±0.08	1.545 ±0.003	0.2366 ±0.0006	20.69 ±0.05	9.47 ±0.03	8.27 ±0.06	58.89 ±0.12	34.1 ±0.2	4.75 ±0.03	39.504 ±0.01
15.02 ±0.08	19.99 ±0.08	59.99 ±0.09	1.336 ±0.003	0.2113 ±0.0006	20.29 ±0.05	12.22 ±0.03	8.16 ±0.05	57.94 ±0.13	22.7 ±0.2	4.30 ±0.03	35.321 ±0.008
14.97 ±0.08	20.06 ±0.08	59.92 ±0.08	1.153 ±0.004	0.1817 ±0.0006	20.05 ±0.05	15.19 ±0.03	8.13 ±0.06	57.37 ±0.13	12.68 ±0.15	3.70 ±0.02	30.259 ±0.007
15.09 ±0.08	19.89 ±0.08	60.00 ±0.08	1.921 ±0.004	0.2477 ±0.0006	23.07 ±0.05	8.71 ±0.03	9.01 ±0.06	64.23 ±0.12	42.8 ±0.2	4.58 ±0.03	41.520 ±0.01
15.06 ±0.08	19.89 ±0.09	60.05 ±0.09	1.921 ±0.004	0.2406 ±0.0007	20.75 ±0.05	9.60 ±0.03	8.33 ±0.06	59.02 ±0.13	33.7 ±0.2	4.81 ±0.03	40.376 ±0.011
15.00	19.90	60.03	1.832	0.2186	20.33	12.32	8.21	58.04	22.5	4.43	36.663

±0.08	±0.08	±0.08	±0.004	±0.0006	±0.05	±0.03	±0.05	±0.13	±0.2	±0.03	±0.009
14.93 ±0.08	19.89 ±0.08	59.92 ±0.08	1.504 ±0.004	0.1850 ±0.0006	20.06 ±0.05	15.44 ±0.03	8.15 ±0.05	57.40 ±0.13	11.98 ±0.15	3.78 ±0.02	30.949 ±0.007
15.00 ±0.08	19.90 ±0.08	60.01 ±0.08	1.906 ±0.009	0.1887 ±0.0006	20.11 ±0.05	15.61 ±0.03	8.19 ±0.05	57.53 ±0.13	11.62 ±0.15	3.84 ±0.02	31.643 ±0.007
19.90 ±0.08	50.17 ±0.08	59.91 ±0.08	2.007 ±0.004	0.933 ±0.002	22.59 ±0.05	16.08 ±0.03	9.16 ±0.05	63.18 ±0.12	15.87 ±0.14	4.10 ±0.02	38.03 ±0.06
19.93 ±0.08	50.15 ±0.08	59.23 ±0.13	2.010 ±0.004	0.926 ±0.002	21.91 ±0.09	16.2 ±0.3	8.98 ±0.06	61.7 ±0.2	13.9 ±0.8	3.87 ±0.03	35.18 ±0.13
19.93 ±0.08	50.12 ±0.08	59.98 ±0.08	2.002 ±0.004	0.922 ±0.002	22.45 ±0.05	16.35 ±0.03	9.14 ±0.05	62.88 ±0.12	14.82 ±0.14	4.11 ±0.02	38.04 ±0.06
19.93 ±0.08	50.12 ±0.08	59.92 ±0.08	2.003 ±0.004	0.910 ±0.002	22.23 ±0.05	16.89 ±0.03	9.08 ±0.05	62.41 ±0.12	12.86 ±0.14	4.06 ±0.02	37.30 ±0.06
19.95 ±0.08	50.12 ±0.08	59.75 ±0.08	2.004 ±0.004	0.909 ±0.002	22.07 ±0.05	17.38 ±0.03	9.04 ±0.05	62.04 ±0.12	11.19 ±0.14	4.00 ±0.02	36.60 ±0.06
15.12 ±0.08	19.85 ±0.08	59.96 ±0.08	2.529 ±0.005	0.2539 ±0.0006	23.07 ±0.05	8.84 ±0.03	9.04 ±0.05	64.23 ±0.11	42.2 ±0.2	4.67 ±0.03	42.559 ±0.01
15.10 ±0.08	19.93 ±0.08	60.10 ±0.08	2.529 ±0.005	0.2492 ±0.0006	21.10 ±0.05	9.27 ±0.03	8.44 ±0.05	59.84 ±0.12	35.9 ±0.2	4.92 ±0.03	41.822 ±0.01
15.14 ±0.08	20.05 ±0.08	60.13 ±0.08	2.454 ±0.004	0.2374 ±0.0006	20.57 ±0.05	10.81 ±0.03	8.30 ±0.05	58.61 ±0.13	28.5 ±0.2	4.75 ±0.03	39.755 ±0.01
19.88 ±0.08	50.15 ±0.08	59.68 ±0.08	2.009 ±0.004	0.845 ±0.002	21.78 ±0.05	19.38 ±0.03	8.93 ±0.05	61.39 ±0.12	5.50 ±0.13	3.73 ±0.02	33.66 ±0.05
19.90 ±0.08	50.15 ±0.08	59.62 ±0.08	2.010 ±0.004	0.844 ±0.002	21.74 ±0.05	19.57 ±0.03	8.91 ±0.05	61.30 ±0.12	4.95 ±0.13	3.72 ±0.02	33.47 ±0.05
20.03 ±0.08	50.04 ±0.08	60.04 ±0.08	2.006 ±0.004	0.930 ±0.002	23.05 ±0.05	15.88 ±0.03	9.28 ±0.05	64.19 ±0.11	17.44 ±0.14	4.14 ±0.02	38.89 ±0.06
20.02 ±0.08	50.04 ±0.08	59.90 ±0.08	2.006 ±0.004	0.929 ±0.002	22.54 ±0.05	16.24 ±0.03	9.13 ±0.05	63.07 ±0.12	15.30 ±0.14	4.15 ±0.02	38.32 ±0.06
20.03 ±0.08	50.04 ±0.08	60.09 ±0.08	2.006 ±0.004	0.899 ±0.002	22.40 ±0.05	16.65 ±0.03	9.09 ±0.05	62.77 ±0.12	13.88 ±0.14	4.11 ±0.03	37.78 ±0.06
20.03 ±0.08	50.04 ±0.08	60.19 ±0.08	2.007 ±0.004	0.876 ±0.002	22.30 ±0.05	17.06 ±0.03	9.05 ±0.05	62.55 ±0.12	12.55 ±0.14	4.06 ±0.02	37.19 ±0.05
20.02 ±0.08	50.06 ±0.08	60.07 ±0.08	2.007 ±0.004	0.875 ±0.002	22.18 ±0.05	17.46 ±0.03	9.02 ±0.05	62.29 ±0.12	11.23 ±0.14	4.01 ±0.02	36.63 ±0.05
19.99 ±0.08	50.09 ±0.08	60.01 ±0.08	2.007 ±0.004	0.875 ±0.002	22.13 ±0.05	17.63 ±0.03	9.00 ±0.05	62.18 ±0.12	10.66 ±0.14	3.99 ±0.02	36.32 ±0.06
20.01 ±0.08	50.11 ±0.08	59.94 ±0.08	2.008 ±0.004	0.875 ±0.002	22.08 ±0.05	17.84 ±0.03	8.99 ±0.05	62.07 ±0.12	10.03 ±0.14	3.96 ±0.02	36.02 ±0.05
20.18 ±0.08	30.09 ±0.08	60.07 ±0.08	2.023 ±0.004	0.3504 ±0.0009	21.35 ±0.05	11.87 ±0.03	8.70 ±0.05	60.42 ±0.12	26.4 ±0.2	5.01 ±0.03	43.895 ±0.014

20.04 ±0.08	39.97 ±0.1	79.95 ±0.09	1.949 ±0.004	0.2513 ±0.0007	30.06 ±0.05	14.13 ±0.03	11.42 ±0.05	77.82 ±0.1	36.16 ±0.13	3.66 ±0.02	42.033 ±0.012
30.11 ±0.08	50.13 ±0.08	60.36 ±0.08	1.988 ±0.004	1.158 ±0.002	24.60 ±0.05	17.36 ±0.03	10.06 ±0.06	67.44 ±0.11	16.55 ±0.13	4.86 ±0.03	49.54 ±0.09
30.17 ±0.08	50.06 ±0.08	60.00 ±0.08	1.989 ±0.004	1.157 ±0.002	22.73 ±0.05	18.33 ±0.03	9.43 ±0.06	63.50 ±0.12	10.16 ±0.13	5.03 ±0.03	48.10 ±0.09
30.14 ±0.08	50.07 ±0.08	60.03 ±0.08	1.989 ±0.004	1.158 ±0.002	22.81 ±0.05	18.19 ±0.03	9.45 ±0.06	63.66 ±0.12	10.67 ±0.13	5.03 ±0.03	48.25 ±0.09
30.15 ±0.08	50.05 ±0.08	59.92 ±0.08	1.989 ±0.004	1.157 ±0.002	22.61 ±0.05	18.58 ±0.03	9.38 ±0.06	63.23 ±0.12	9.26 ±0.13	5.02 ±0.03	47.77 ±0.09
30.17 ±0.08	50.04 ±0.08	59.83 ±0.08	1.989 ±0.004	1.157 ±0.002	22.49 ±0.05	18.90 ±0.03	9.33 ±0.05	62.96 ±0.12	8.20 ±0.13	5.00 ±0.03	47.38 ±0.09
30.19 ±0.08	50.04 ±0.08	59.79 ±0.08	1.989 ±0.004	1.156 ±0.002	22.42 ±0.05	19.11 ±0.03	9.31 ±0.05	62.83 ±0.12	7.56 ±0.13	4.98 ±0.03	47.13 ±0.09
30.15 ±0.08	50.04 ±0.08	59.89 ±0.08	1.990 ±0.004	1.125 ±0.002	22.34 ±0.05	19.69 ±0.03	9.29 ±0.05	62.64 ±0.12	5.98 ±0.13	4.92 ±0.03	46.36 ±0.09
30.07 ±0.08	50.05 ±0.08	59.78 ±0.08	1.990 ±0.004	1.125 ±0.002	22.24 ±0.05	20.05 ±0.03	9.25 ±0.05	62.42 ±0.12	4.91 ±0.13	4.87 ±0.03	45.78 ±0.09
10.00 ±0.08	9.87 ±0.08	59.90 ±0.08	0.850 ±0.002	0.1076 ±0.0005	19.44 ±0.05	16.57 ±0.03	7.79 ±0.05	55.92 ±0.13	7.36 ±0.15	2.88 ±0.02	22.497 ±0.006
10.01 ±0.08	9.88 ±0.08	59.99 ±0.08	1.968 ±0.004	0.1149 ±0.0005	19.55 ±0.05	17.14 ±0.03	7.89 ±0.05	56.17 ±0.13	6.06 ±0.15	3.03 ±0.02	24.062 ±0.007
9.98 ±0.08	9.88 ±0.08	59.80 ±0.08	1.966 ±0.004	0.1377 ±0.0005	19.67 ±0.05	13.78 ±0.03	7.87 ±0.05	56.48 ±0.13	16.1 ±0.2	3.63 ±0.02	28.715 ±0.007
9.93 ±0.08	9.91 ±0.08	60.00 ±0.08	1.967 ±0.004	0.1271 ±0.0005	19.67 ±0.05	15.16 ±0.03	7.89 ±0.05	56.47 ±0.13	11.9 ±0.2	3.35 ±0.02	26.611 ±0.007
35.01 ±0.08	19.97 ±0.08	60.03 ±0.08	1.972 ±0.004	0.3933 ±0.0009	23.86 ±0.05	11.52 ±0.03	9.90 ±0.05	65.91 ±0.11	33.15 ±0.14	6.60 ±0.04	65.84 ±0.02
34.96 ±0.08	19.89 ±0.08	60.03 ±0.08	1.971 ±0.004	0.3837 ±0.0009	21.79 ±0.05	11.65 ±0.03	9.10 ±0.05	61.42 ±0.12	28.2 ±0.2	7.03 ±0.04	64.38 ±0.02
35.00 ±0.08	19.94 ±0.08	60.00 ±0.08	1.972 ±0.004	0.3874 ±0.0009	21.65 ±0.05	12.05 ±0.03	9.07 ±0.05	61.09 ±0.12	26.46 ±0.15	7.10 ±0.04	64.86 ±0.02
34.93 ±0.08	19.92 ±0.08	59.96 ±0.08	1.972 ±0.004	0.3864 ±0.0009	21.54 ±0.05	12.14 ±0.03	8.94 ±0.05	60.85 ±0.12	25.90 ±0.15	7.18 ±0.04	64.67 ±0.02
20.12 ±0.08	29.93 ±0.08	87.03 ±0.09	1.952 ±0.004	0.1855 ±0.0006	32.72 ±0.06	12.37 ±0.03	12.20 ±0.05	82.34 ±0.09	46.52 ±0.13	3.62 ±0.02	44.328 ±0.012
20.02 ±0.08	39.98 ±0.09	80.02 ±0.08	1.955 ±0.004	0.2465 ±0.0006	29.90 ±0.05	14.51 ±0.03	11.30 ±0.05	77.53 ±0.1	34.71 ±0.12	3.64 ±0.02	41.307 ±0.01
29.99 ±0.08	29.98 ±0.08	87.02 ±0.08	1.943 ±0.004	0.2290 ±0.0006	33.18 ±0.05	13.48 ±0.03	12.74 ±0.05	83.10 ±0.09	43.50 ±0.12	4.27 ±0.02	54.656 ±0.015
20.04 ±0.08	30.03 ±0.09	70.00 ±0.08	1.945 ±0.004	0.2655 ±0.0007	25.62 ±0.05	11.76 ±0.03	10.05 ±0.05	69.51 ±0.11	35.86 ±0.14	4.39 ±0.02	44.365 ±0.011

20.06 ±0.08	29.99 ±0.08	80.00 ±0.08	1.950 ±0.004	0.2126 ±0.0006	29.87 ±0.05	12.15 ±0.03	11.33 ±0.05	77.48 ±0.1	42.44 ±0.13	3.91 ±0.02	44.464 ±0.011
20.06 ±0.08	30.00 ±0.08	80.03 ±0.08	1.950 ±0.004	0.2126 ±0.0006	29.89 ±0.05	12.15 ±0.03	11.34 ±0.05	77.51 ±0.09	42.48 ±0.13	3.91 ±0.02	44.497 ±0.011
18.6 ±0.08	26.00 ±0.08	53.05 ±0.03	1.851 ±0.008	0.3212 ±0.13	21.23 ±0.05	12.03 ±0.03	8.58 ±0.04	60.14 ±0.12	25.6 ±0.2	5.015 ±0.15	45.05 ±0.012
30.04 ±0.08	29.97 ±0.08	60.02 ±0.08	1.977 ±0.004	0.4416 ±0.001	22.41 ±0.05	11.91 ±0.03	9.26 ±0.05	62.79 ±0.12	28.65 ±0.15	5.95 ±0.04	55.46 ±0.02
30.01 ±0.08	29.94 ±0.08	59.77 ±0.08	1.978 ±0.004	0.4391 ±0.001	21.57 ±0.05	12.41 ±0.03	8.95 ±0.05	60.91 ±0.12	25.02 ±0.15	6.07 ±0.04	54.74 ±0.02
30.01 ±0.08	29.94 ±0.08	60.26 ±0.08	1.980 ±0.004	0.4236 ±0.0009	21.39 ±0.05	13.21 ±0.03	8.90 ±0.06	60.52 ±0.12	21.95 ±0.15	5.99 ±0.04	53.69 ±0.02
29.6 ±0.2	29.81 ±0.14	41.3 ±0.2	1.907 ±0.004	1.124 ±0.002	17.92 ±0.09	11.62 ±0.04	7.55 ±0.06	52.1 ±0.2	19.0 ±0.3	7.04 ±0.07	54.2 ±0.4
30.01 ±0.08	29.91 ±0.08	60.27 ±0.08	1.982 ±0.004	0.4130 ±0.0009	21.20 ±0.05	14.13 ±0.03	8.83 ±0.05	60.07 ±0.12	18.55 ±0.15	5.89 ±0.04	52.42 ±0.02
29.99 ±0.08	29.93 ±0.08	59.85 ±0.08	1.983 ±0.004	0.4083 ±0.0009	20.91 ±0.05	15.15 ±0.03	8.72 ±0.06	59.41 ±0.12	14.81 ±0.14	5.81 ±0.04	51.07 ±0.02
29.92 ±0.08	29.95 ±0.08	60.00 ±0.08	1.987 ±0.004	0.3853 ±0.0009	20.79 ±0.05	17.19 ±0.03	8.69 ±0.06	59.13 ±0.12	8.84 ±0.14	5.53 ±0.04	48.41 ±0.02
30.05 ±0.08	50.12 ±0.08	59.73 ±0.08	1.990 ±0.004	1.132 ±0.002	22.20 ±0.05	20.26 ±0.03	9.24 ±0.06	62.33 ±0.12	4.33 ±0.13	4.85 ±0.03	45.48 ±0.09
10.01 ±0.08	9.83 ±0.08	60.14 ±0.09	0.844 ±0.002	0.1399 ±0.0005	19.86 ±0.05	10.97 ±0.03	7.77 ±0.06	56.92 ±0.13	26.2 ±0.2	3.77 ±0.03	29.416 ±0.008
9.99 ±0.08	9.86 ±0.08	60.01 ±0.08	0.845 ±0.002	0.1361 ±0.0005	19.75 ±0.05	11.70 ±0.03	7.80 ±0.05	56.66 ±0.13	23.3 ±0.2	3.64 ±0.03	28.525 ±0.007
9.95 ±0.08	9.92 ±0.08	60.13 ±0.08	0.846 ±0.002	0.1251 ±0.0005	19.70 ±0.05	13.32 ±0.03	7.82 ±0.06	56.53 ±0.13	17.6 ±0.2	3.34 ±0.02	26.256 ±0.007
9.99 ±0.08	29.93 ±0.08	60.03 ±0.09	0.844 ±0.002	0.2508 ±0.0007	21.75 ±0.05	9.42 ±0.03	8.37 ±0.05	61.32 ±0.12	36.8 ±0.2	3.76 ±0.02	31.556 ±0.008
29.95 ±0.08	30.04 ±0.08	59.76 ±0.08	1.987 ±0.004	0.3767 ±0.0009	20.62 ±0.05	18.44 ±0.03	8.61 ±0.05	58.73 ±0.12	5.22 ±0.14	5.39 ±0.03	46.79 ±0.02
29.93 ±0.08	30.09 ±0.08	60.15 ±0.08	1.987 ±0.004	0.3768 ±0.0009	20.79 ±0.05	17.98 ±0.03	8.67 ±0.05	59.14 ±0.12	6.78 ±0.14	5.42 ±0.03	47.35 ±0.02
9.94 ±0.08	29.99 ±0.08	59.95 ±0.08	0.845 ±0.002	0.2315 ±0.0006	20.54 ±0.05	11.56 ±0.03	8.05 ±0.06	58.53 ±0.12	25.7 ±0.2	3.59 ±0.03	28.992 ±0.007
9.86 ±0.08	29.97 ±0.08	60.02 ±0.08	0.848 ±0.002	0.2045 ±0.0006	20.36 ±0.05	14.16 ±0.03	8.07 ±0.06	58.11 ±0.13	16.53 ±0.15	3.17 ±0.02	25.687 ±0.006
9.99 ±0.08	49.99 ±0.08	60.09 ±0.08	0.847 ±0.002	0.6703 ±0.0015	22.72 ±0.05	12.72 ±0.03	8.69 ±0.05	63.48 ±0.12	26.51 ±0.14	3.24 ±0.02	28.32 ±0.03
9.98	49.98	60.04	0.847	0.6564	22.08	13.21	8.49	62.06	23.47	3.23	27.63

±0.08	±0.08	±0.08	±0.002	±0.0014	±0.05	±0.03	±0.06	±0.12	±0.14	±0.02	±0.03
9.90 ±0.08	50.04 ±0.08	60.07 ±0.08	0.849 ±0.002	0.6086 ±0.0014	21.76 ±0.05	14.99 ±0.03	8.44 ±0.06	61.36 ±0.12	17.21 ±0.14	3.01 ±0.02	25.52 ±0.03
9.99 ±0.08	50.02 ±0.08	59.95 ±0.08	0.852 ±0.002	0.5079 ±0.0014	21.28 ±0.05	18.66 ±0.03	8.44 ±0.06	60.25 ±0.12	6.14 ±0.14	2.49 ±0.02	21.10 ±0.02
34.92 ±0.08	20.04 ±0.08	59.96 ±0.08	1.426 ±0.003	0.3723 ±0.0009	21.81 ±0.05	11.44 ±0.03	9.07 ±0.05	61.45 ±0.12	29.0 ±0.2	6.81 ±0.04	62.11 ±0.02
34.97 ±0.08	20.06 ±0.08	60.06 ±0.08	1.426 ±0.003	0.3711 ±0.0009	21.50 ±0.05	11.87 ±0.03	8.93 ±0.05	60.77 ±0.12	26.7 ±0.2	6.90 ±0.04	62.04 ±0.02
34.94 ±0.08	20.06 ±0.08	60.13 ±0.08	1.426 ±0.003	0.3687 ±0.0009	21.35 ±0.05	12.29 ±0.03	8.92 ±0.05	60.42 ±0.12	24.94 ±0.15	6.88 ±0.04	61.76 ±0.02
35.15 ±0.08	20.07 ±0.08	60.04 ±0.08	1.967 ±0.004	0.3873 ±0.0009	21.36 ±0.05	12.79 ±0.03	8.85 ±0.05	60.43 ±0.12	23.24 ±0.15	7.25 ±0.04	64.70 ±0.02
35.07 ±0.08	20.06 ±0.08	60.04 ±0.09	1.966 ±0.004	0.3836 ±0.0009	21.25 ±0.05	13.20 ±0.03	8.83 ±0.05	60.19 ±0.12	21.64 ±0.15	7.20 ±0.04	64.09 ±0.02
30.05 ±0.08	29.98 ±0.08	80.02 ±0.08	1.934 ±0.004	0.2641 ±0.0007	30.33 ±0.05	13.14 ±0.03	11.87 ±0.05	78.30 ±0.09	39.84 ±0.13	4.63 ±0.02	55.281 ±0.014
30.05 ±0.08	29.98 ±0.08	85.98 ±0.08	1.939 ±0.004	0.2333 ±0.0006	32.95 ±0.05	13.86 ±0.03	12.72 ±0.05	82.73 ±0.09	41.92 ±0.12	4.28 ±0.02	54.653 ±0.015
10.01 ±0.08	9.89 ±0.08	60.17 ±0.09	1.931 ±0.004	0.1838 ±0.0006	23.13 ±0.05	6.85 ±0.03	8.94 ±0.05	64.37 ±0.11	52.0 ±0.2	4.29 ±0.03	38.630 ±0.01
9.96 ±0.08	9.92 ±0.08	59.90 ±0.09	1.931 ±0.004	0.1836 ±0.0006	21.61 ±0.05	6.92 ±0.03	8.48 ±0.05	61.01 ±0.12	48.2 ±0.2	4.49 ±0.03	38.346 ±0.01
9.96 ±0.08	9.95 ±0.08	60.00 ±0.09	1.931 ±0.004	0.1826 ±0.0006	21.22 ±0.05	6.97 ±0.03	8.35 ±0.05	60.13 ±0.12	47.1 ±0.2	4.54 ±0.03	38.183 ±0.01
9.95 ±0.08	9.96 ±0.08	60.07 ±0.08	1.931 ±0.004	0.1761 ±0.0006	20.24 ±0.05	7.95 ±0.03	8.06 ±0.05	57.83 ±0.13	39.9 ±0.2	4.54 ±0.03	36.873 ±0.009
20.14 ±0.08	29.93 ±0.08	60.05 ±0.08	0.836 ±0.002	0.3230 ±0.0008	24.13 ±0.05	10.57 ±0.03	9.39 ±0.06	66.48 ±0.11	37.31 ±0.15	4.31 ±0.03	40.666 ±0.013
20.12 ±0.08	29.94 ±0.08	60.01 ±0.09	0.839 ±0.002	0.2944 ±0.0008	20.76 ±0.05	13.10 ±0.03	8.38 ±0.06	59.05 ±0.12	20.9 ±0.2	4.40 ±0.03	36.995 ±0.011
20.03 ±0.08	29.91 ±0.08	60.10 ±0.08	0.845 ±0.002	0.2462 ±0.0006	20.46 ±0.05	17.65 ±0.03	8.36 ±0.05	58.36 ±0.12	6.87 ±0.14	3.70 ±0.02	31.072 ±0.007
20.13 ±0.08	29.94 ±0.08	60.09 ±0.08	0.837 ±0.002	0.3093 ±0.0008	21.05 ±0.05	11.62 ±0.03	8.44 ±0.06	59.74 ±0.12	26.6 ±0.2	4.60 ±0.03	38.988 ±0.012
20.09 ±0.08	50.05 ±0.08	60.00 ±0.08	0.843 ±0.002	0.817 ±0.002	22.19 ±0.05	15.91 ±0.03	8.88 ±0.05	62.31 ±0.12	15.49 ±0.14	3.80 ±0.02	33.99 ±0.05
20.14 ±0.08	50.03 ±0.08	59.95 ±0.09	0.844 ±0.002	0.790 ±0.003	21.99 ±0.05	16.89 ±0.03	8.84 ±0.05	61.86 ±0.12	12.33 ±0.14	3.68 ±0.02	32.80 ±0.05
20.12 ±0.08	49.98 ±0.08	59.95 ±0.08	0.846 ±0.002	0.7366 ±0.0015	21.76 ±0.05	18.73 ±0.03	8.80 ±0.05	61.34 ±0.12	7.04 ±0.13	3.46 ±0.02	30.71 ±0.04
35.11	20.13	60.06	0.435	0.2763	21.07	9.54	8.61	59.78	34.7	5.34	46.113

±0.08	±0.08	±0.08	±0.002	±0.0007	±0.05	±0.03	±0.05	±0.12	±0.2	±0.03	±0.012
35.17 ±0.08	20.17 ±0.08	59.82 ±0.12	0.435 ±0.002	0.2798 ±0.0009	20.85 ±0.05	9.98 ±0.03	8.57 ±0.05	59.27 ±0.12	32.4 ±0.2	5.39 ±0.03	46.37 ±0.02
35.07 ±0.08	20.10 ±0.08	60.03 ±0.08	0.734 ±0.002	0.3243 ±0.0008	21.31 ±0.05	10.05 ±0.03	8.83 ±0.05	60.32 ±0.12	33.2 ±0.2	6.10 ±0.04	54.12 ±0.02
35.11 ±0.08	20.16 ±0.08	60.13 ±0.08	0.735 ±0.002	0.3200 ±0.0008	21.08 ±0.05	10.33 ±0.03	8.72 ±0.05	59.80 ±0.12	31.6 ±0.2	6.10 ±0.04	53.47 ±0.02
35.05 ±0.08	20.13 ±0.08	59.89 ±0.08	0.2702 ±0.014	0.2331 ±0.0006	20.73 ±0.05	9.03 ±0.03	8.28 ±0.05	58.99 ±0.12	36.1 ±0.2	4.67 ±0.03	38.738 ±0.009
20.04 ±0.08	9.91 ±0.08	60.02 ±0.09	0.832 ±0.002	0.2035 ±0.0006	22.04 ±0.05	7.24 ±0.03	8.70 ±0.06	61.98 ±0.12	47.5 ±0.2	4.88 ±0.03	42.613 ±0.011
20.17 ±0.08	9.95 ±0.08	59.84 ±0.08	0.832 ±0.002	0.1937 ±0.0006	20.09 ±0.05	9.72 ±0.03	8.09 ±0.06	57.47 ±0.13	31.7 ±0.2	4.97 ±0.03	40.387 ±0.01
20.20 ±0.08	10.01 ±0.08	60.02 ±0.08	0.841 ±0.002	0.1540 ±0.0005	19.79 ±0.05	16.35 ±0.03	8.11 ±0.06	56.76 ±0.13	8.77 ±0.15	3.95 ±0.03	32.182 ±0.008
20.18 ±0.08	9.95 ±0.08	60.05 ±0.08	0.831 ±0.002	0.1986 ±0.0006	20.41 ±0.05	8.18 ±0.03	8.19 ±0.06	58.24 ±0.13	39.2 ±0.2	5.05 ±0.04	41.581 ±0.01
29.86 ±0.08	9.88 ±0.08	59.99 ±0.09	0.838 ±0.002	0.2492 ±0.0007	23.16 ±0.05	8.22 ±0.03	9.37 ±0.05	64.43 ±0.11	45.2 ±0.2	5.55 ±0.03	52.182 ±0.014
20.09 ±0.08	30.00 ±0.08	70.05 ±0.08	1.937 ±0.004	0.2695 ±0.0007	26.64 ±0.06	11.09 ±0.03	10.37 ±0.05	71.51 ±0.11	40.33 ±0.14	4.33 ±0.02	45.145 ±0.011
30.09 ±0.08	30.00 ±0.08	70.06 ±0.08	1.928 ±0.004	0.3306 ±0.0008	25.98 ±0.05	12.21 ±0.03	10.47 ±0.05	70.22 ±0.1	35.00 ±0.14	5.26 ±0.03	55.38 ±0.02
30.09 ±0.08	30.06 ±0.08	69.99 ±0.08	1.928 ±0.004	0.3272 ±0.0008	25.56 ±0.05	12.75 ±0.03	10.31 ±0.05	69.39 ±0.11	32.28 ±0.14	5.27 ±0.03	54.63 ±0.02
29.84 ±0.08	9.95 ±0.08	59.99 ±0.09	0.836 ±0.002	0.2404 ±0.0007	20.38 ±0.05	9.59 ±0.03	8.40 ±0.05	58.16 ±0.13	32.9 ±0.2	5.96 ±0.04	50.280 ±0.014
30.00 ±0.08	9.95 ±0.08	60.02 ±0.09	0.847 ±0.002	0.2493 ±0.0007	21.33 ±0.05	8.41 ±0.03	8.74 ±0.05	60.37 ±0.12	40.3 ±0.2	5.94 ±0.04	52.182 ±0.014
29.74 ±0.08	9.90 ±0.08	59.98 ±0.08	0.840 ±0.002	0.1941 ±0.0006	19.86 ±0.05	17.95 ±0.03	8.29 ±0.05	56.93 ±0.13	4.68 ±0.14	4.88 ±0.03	40.626 ±0.01
30.18 ±0.08	29.97 ±0.08	60.05 ±0.08	0.823 ±0.002	0.3951 ±0.0009	25.43 ±0.06	11.30 ±0.03	10.10 ±0.05	69.13 ±0.11	37.17 ±0.14	4.90 ±0.03	49.67 ±0.02
30.15 ±0.08	29.92 ±0.08	60.00 ±0.08	0.825 ±0.002	0.3649 ±0.0009	20.96 ±0.05	14.11 ±0.03	8.61 ±0.06	59.51 ±0.12	18.08 ±0.15	5.30 ±0.04	45.88 ±0.02
30.18 ±0.08	29.93 ±0.08	60.05 ±0.08	0.823 ±0.002	0.3842 ±0.0009	21.60 ±0.05	11.93 ±0.03	8.81 ±0.05	60.99 ±0.12	26.76 ±0.15	5.46 ±0.03	48.37 ±0.02
30.22 ±0.08	29.87 ±0.08	60.00 ±0.08	0.831 ±0.002	0.3239 ±0.0009	20.62 ±0.05	18.63 ±0.03	8.53 ±0.06	58.73 ±0.12	4.73 ±0.14	4.76 ±0.03	40.785 ±0.013
20.01 ±0.08	30.15 ±0.09	59.88 ±0.08	1.979 ±0.004	0.3235 ±0.0008	19.82 ±0.05	19.63 ±0.03	8.31 ±0.06	56.83 ±0.13	0.45 ±0.14	4.80 ±0.03	40.211 ±0.013

20.02 ±0.08	30.07 ±0.08	60.12 ±0.12	1.981 ±0.004	0.3240 ±0.0011	21.66 ±0.06	11.16 ±0.03	8.97 ±0.05	61.11 ±0.13	29.7 ±0.2	4.50 ±0.03	40.69 ±0.02
20.04 ±0.08	30.09 ±0.08	59.69 ±0.09	1.982 ±0.004	0.3134 ±0.0008	19.88 ±0.05	13.35 ±0.03	8.38 ±0.05	56.98 ±0.13	18.0 ±0.2	4.59 ±0.03	38.773 ±0.013
20.01 ±0.1	50.05 ±0.1	59.5 ±0.2	1.986 ±0.004	0.820 ±0.002	21.56 ±0.07	20.53 ±0.1	8.6 ±0.2	60.9 ±0.2	2.3 ±0.3	3.72 ±0.07	32.3 ±0.3
30.05 ±0.08	50.01 ±0.08	60.04 ±0.08	0.577 ±0.002	0.968 ±0.002	23.30 ±0.05	16.19 ±0.03	9.41 ±0.05	64.72 ±0.11	17.07 ±0.13	4.27 ±0.02	40.61 ±0.07
30.07 ±0.08	50.01 ±0.08	59.91 ±0.08	0.578 ±0.002	0.948 ±0.002	22.32 ±0.05	17.43 ±0.03	9.11 ±0.05	62.60 ±0.12	11.61 ±0.13	4.27 ±0.03	39.24 ±0.06
30.04 ±0.08	50.03 ±0.08	59.89 ±0.08	0.579 ±0.002	0.927 ±0.002	22.14 ±0.05	18.41 ±0.03	9.07 ±0.06	62.20 ±0.12	8.69 ±0.13	4.18 ±0.03	38.25 ±0.06
30.08 ±0.08	50.06 ±0.08	60.00 ±0.08	0.580 ±0.002	0.890 ±0.002	22.02 ±0.05	19.72 ±0.03	9.03 ±0.06	61.92 ±0.12	5.20 ±0.13	4.06 ±0.03	36.99 ±0.06
29.90 ±0.08	50.12 ±0.08	60.06 ±0.08	0.831 ±0.002	1.053 ±0.002	24.11 ±0.05	16.67 ±0.03	9.73 ±0.05	66.43 ±0.11	17.43 ±0.13	4.45 ±0.03	43.80 ±0.08
29.94 ±0.08	50.10 ±0.08	59.86 ±0.08	0.832 ±0.002	1.047 ±0.002	22.62 ±0.05	17.45 ±0.03	9.24 ±0.05	63.25 ±0.12	12.20 ±0.13	4.57 ±0.03	42.74 ±0.08
29.96 ±0.08	50.09 ±0.08	59.82 ±0.08	0.834 ±0.002	1.003 ±0.002	22.16 ±0.05	19.21 ±0.03	9.12 ±0.05	62.25 ±0.12	6.76 ±0.13	4.43 ±0.03	40.81 ±0.07
29.97 ±0.08	50.07 ±0.08	59.84 ±0.08	0.834 ±0.002	0.979 ±0.002	22.08 ±0.05	19.94 ±0.03	9.10 ±0.06	62.06 ±0.12	4.80 ±0.13	4.35 ±0.03	40.03 ±0.07
30.07 ±0.08	9.95 ±0.08	60.02 ±0.09	0.587 ±0.002	0.2340 ±0.0006	22.67 ±0.06	7.74 ±0.03	9.30 ±0.05	63.35 ±0.12	46.4 ±0.2	5.25 ±0.03	48.953 ±0.013
30.03 ±0.08	9.96 ±0.08	60.02 ±0.08	0.586 ±0.002	0.2292 ±0.0007	21.15 ±0.05	7.80 ±0.03	8.73 ±0.05	59.95 ±0.13	42.7 ±0.2	5.48 ±0.03	47.967 ±0.013
30.07 ±0.08	10.03 ±0.08	59.96 ±0.08	0.593 ±0.002	0.1822 ±0.0006	19.83 ±0.05	17.56 ±0.03	8.32 ±0.05	56.84 ±0.13	5.61 ±0.15	4.55 ±0.03	38.007 ±0.009
30.09 ±0.08	9.98 ±0.08	59.98 ±0.09	0.586 ±0.002	0.2228 ±0.0006	20.39 ±0.05	8.87 ±0.03	8.41 ±0.05	58.19 ±0.13	36.0 ±0.2	5.52 ±0.03	46.558 ±0.012
30.15 ±0.08	30.07 ±0.08	59.93 ±0.08	0.597 ±0.002	0.3689 ±0.0009	23.69 ±0.05	11.20 ±0.03	9.51 ±0.05	65.54 ±0.11	33.96 ±0.15	4.82 ±0.03	46.05 ±0.02
30.04 ±0.08	30.05 ±0.08	60.03 ±0.08	0.599 ±0.002	0.3377 ±0.0008	20.85 ±0.05	14.24 ±0.03	8.61 ±0.05	59.27 ±0.12	17.43 ±0.15	4.89 ±0.03	42.305 ±0.013
30.02 ±0.08	30.04 ±0.08	59.86 ±0.08	0.602 ±0.002	0.3056 ±0.0008	20.53 ±0.05	18.16 ±0.03	8.55 ±0.05	58.51 ±0.12	5.71 ±0.14	4.44 ±0.03	38.098 ±0.011
30.17 ±0.08	30.17 ±0.08	59.95 ±0.08	0.597 ±0.002	0.3600 ±0.0009	21.27 ±0.05	12.06 ±0.03	8.72 ±0.05	60.23 ±0.12	25.5 ±0.2	5.12 ±0.03	44.806 ±0.014
20.02 ±0.08	30.03 ±0.09	59.95 ±0.08	1.940 ±0.004	0.3447 ±0.0009	21.12 ±0.05	12.12 ±0.03	8.64 ±0.05	59.90 ±0.12	25.0 ±0.2	4.95 ±0.03	43.11 ±0.02
10.00 ±0.08	10.08 ±0.08	60.01 ±0.09	1.955 ±0.004	0.1867 ±0.0006	23.03 ±0.05	6.89 ±0.03	8.90 ±0.06	64.14 ±0.12	51.5 ±0.2	4.35 ±0.03	38.957 ±0.01

10.00 ±0.08	9.97 ±0.08	60.04 ±0.09	1.955 ±0.004	0.1858 ±0.0006	22.52 ±0.05	6.89 ±0.03	8.73 ±0.05	63.04 ±0.12	50.4 ±0.2	4.43 ±0.03	38.872 ±0.01
10.04 ±0.08	9.98 ±0.08	59.91 ±0.08	1.956 ±0.004	0.1779 ±0.0006	20.22 ±0.05	7.90 ±0.03	8.00 ±0.05	57.78 ±0.13	40.1 ±0.2	4.61 ±0.03	37.119 ±0.009
10.01 ±0.08	9.96 ±0.08	60.02 ±0.09	1.955 ±0.004	0.1855 ±0.0006	22.02 ±0.05	6.91 ±0.03	8.58 ±0.05	61.92 ±0.12	49.2 ±0.2	4.50 ±0.03	38.819 ±0.01
10.01 ±0.08	9.96 ±0.08	60.04 ±0.09	1.955 ±0.004	0.1843 ±0.0006	21.02 ±0.05	7.04 ±0.03	8.27 ±0.05	59.67 ±0.12	46.2 ±0.2	4.64 ±0.03	38.582 ±0.01
10.00 ±0.08	10.05 ±0.08	60.01 ±0.09	1.955 ±0.004	0.1816 ±0.0006	20.45 ±0.05	7.37 ±0.03	8.09 ±0.06	58.34 ±0.13	43.2 ±0.2	4.65 ±0.03	37.919 ±0.01
10.05 ±0.08	9.98 ±0.08	59.98 ±0.09	1.957 ±0.004	0.1775 ±0.0006	20.23 ±0.05	7.93 ±0.03	8.00 ±0.05	57.82 ±0.13	40.0 ±0.2	4.60 ±0.03	37.082 ±0.01
10.03 ±0.08	9.96 ±0.08	60.03 ±0.09	1.956 ±0.004	0.1801 ±0.0006	20.38 ±0.05	7.51 ±0.03	8.07 ±0.05	58.17 ±0.13	42.4 ±0.2	4.64 ±0.03	37.691 ±0.01
10.04 ±0.08	10.03 ±0.08	59.95 ±0.09	1.957 ±0.004	0.1741 ±0.0006	20.09 ±0.05	8.75 ±0.03	7.99 ±0.05	57.47 ±0.13	35.8 ±0.2	4.52 ±0.03	36.332 ±0.009
9.88 ±0.08	10.15 ±0.08	60.07 ±0.09	1.930 ±0.004	0.1782 ±0.0006	20.33 ±0.05	7.72 ±0.03	8.03 ±0.05	58.05 ±0.13	41.2 ±0.2	4.60 ±0.03	37.183 ±0.009
9.96 ±0.08	10.12 ±0.08	59.92 ±0.09	1.930 ±0.004	0.1789 ±0.0006	20.29 ±0.05	7.69 ±0.03	8.02 ±0.05	57.94 ±0.13	41.2 ±0.2	4.61 ±0.03	37.243 ±0.01
10.00 ±0.08	10.09 ±0.08	60.03 ±0.09	1.931 ±0.004	0.1738 ±0.0006	20.12 ±0.05	8.69 ±0.03	8.00 ±0.05	57.56 ±0.13	36.2 ±0.2	4.50 ±0.03	36.278 ±0.009
10.01 ±0.08	29.94 ±0.09	60.02 ±0.09	1.933 ±0.004	0.2817 ±0.0008	23.69 ±0.05	9.89 ±0.03	9.09 ±0.05	65.55 ±0.11	39.1 ±0.2	3.87 ±0.02	35.421 ±0.011
10.02 ±0.08	29.93 ±0.09	60.05 ±0.09	1.933 ±0.004	0.2779 ±0.0008	21.81 ±0.05	10.03 ±0.03	8.53 ±0.05	61.45 ±0.12	34.4 ±0.2	4.07 ±0.03	34.988 ±0.011
10.03 ±0.08	29.88 ±0.08	60.20 ±0.08	1.933 ±0.004	0.2688 ±0.0007	21.01 ±0.05	10.65 ±0.03	8.29 ±0.05	59.65 ±0.12	30.1 ±0.2	4.08 ±0.03	34.070 ±0.008
10.04 ±0.08	29.91 ±0.09	59.92 ±0.08	1.934 ±0.004	0.2633 ±0.0007	20.73 ±0.05	11.31 ±0.03	8.21 ±0.05	58.99 ±0.12	27.0 ±0.2	3.99 ±0.03	33.029 ±0.009
10.01 ±0.08	29.90 ±0.09	60.04 ±0.08	1.934 ±0.004	0.2437 ±0.0006	20.57 ±0.05	12.86 ±0.03	8.19 ±0.05	58.62 ±0.12	21.2 ±0.2	3.72 ±0.02	30.701 ±0.008
20.06 ±0.09	9.97 ±0.08	60.00 ±0.1	1.966 ±0.004	0.2340 ±0.0009	23.71 ±0.06	23.54 ±0.03	9.71 ±0.05	65.59 ±0.12	0.34 ±0.14	5.01 ±0.03	48.92 ±0.02
19.96 ±0.08	10.01 ±0.08	60.24 ±0.09	1.960 ±0.004	0.2185 ±0.0008	20.41 ±0.06	20.18 ±0.03	8.44 ±0.05	58.23 ±0.13	0.54 ±0.15	5.40 ±0.03	45.86 ±0.02
20.01 ±0.08	9.95 ±0.08	59.94 ±0.09	1.963 ±0.004	0.2077 ±0.0006	20.01 ±0.05	19.77 ±0.03	8.29 ±0.05	57.28 ±0.13	0.56 ±0.14	5.20 ±0.03	43.402 ±0.012
19.98 ±0.08	10.10 ±0.08	60.06 ±0.09	1.964 ±0.004	0.1972 ±0.0007	19.89 ±0.05	19.66 ±0.03	8.28 ±0.05	57.00 ±0.13	0.55 ±0.15	4.94 ±0.03	41.174 ±0.013
19.99	10.04	59.98	1.964	0.1949	19.83	19.56	8.26	56.86	0.64	4.89	40.679

±0.08	±0.08	±0.09	±0.004	±0.0006	±0.05	±0.03	±0.05	±0.13	±0.15	±0.03	±0.012
20.02 ±0.08	9.99 ±0.08	60.01 ±0.09	1.967 ±0.004	0.1891 ±0.0006	19.77 ±0.05	19.50 ±0.03	8.25 ±0.05	56.71 ±0.13	0.64 ±0.15	4.76 ±0.03	39.528 ±0.011
20.03 ±0.08	9.95 ±0.08	60.33 ±0.08	1.969 ±0.004	0.1854 ±0.0006	19.85 ±0.05	19.59 ±0.03	8.29 ±0.05	56.90 ±0.13	0.60 ±0.14	4.68 ±0.03	39.032 ±0.01
20.02 ±0.08	9.96 ±0.08	60.02 ±0.09	1.969 ±0.004	0.1837 ±0.0006	19.71 ±0.05	19.43 ±0.03	8.24 ±0.05	56.57 ±0.13	0.66 ±0.15	4.63 ±0.03	38.449 ±0.01
20.03 ±0.08	9.96 ±0.08	60.00 ±0.08	1.970 ±0.004	0.1817 ±0.0006	19.68 ±0.05	19.40 ±0.03	8.23 ±0.05	56.49 ±0.13	0.66 ±0.14	4.59 ±0.03	38.000 ±0.01
20.02 ±0.09	10.00 ±0.08	60.19 ±0.12	1.981 ±0.004	0.577 ±0.002	19.70 ±0.06	17.49 ±0.04	8.27 ±0.05	56.55 ±0.14	5.5 ±0.2	14.50 ±0.09	121.08 ±0.1
20.08 ±0.08	10.00 ±0.08	60.07 ±0.09	1.955 ±0.004	0.747 ±0.002	20.11 ±0.05	10.34 ±0.03	8.34 ±0.05	57.52 ±0.13	29.2 ±0.2	18.52 ±0.12	156.3 ±0.2
20.00 ±0.08	9.99 ±0.08	59.98 ±0.09	1.959 ±0.004	0.724 ±0.002	20.00 ±0.05	11.40 ±0.03	8.32 ±0.05	57.25 ±0.13	25.0 ±0.2	17.97 ±0.11	151.33 ±0.12
20.02 ±0.08	9.99 ±0.08	60.00 ±0.09	1.962 ±0.004	0.697 ±0.002	19.89 ±0.05	13.11 ±0.03	8.31 ±0.05	56.99 ±0.13	18.8 ±0.2	17.33 ±0.11	145.62 ±0.09
20.00 ±0.08	9.97 ±0.08	60.04 ±0.09	1.963 ±0.004	0.679 ±0.002	19.85 ±0.05	13.87 ±0.03	8.30 ±0.05	56.90 ±0.13	16.2 ±0.2	16.94 ±0.11	142.10 ±0.09
20.01 ±0.08	9.98 ±0.08	60.07 ±0.09	1.967 ±0.004	0.662 ±0.002	19.84 ±0.05	14.41 ±0.03	8.29 ±0.05	56.87 ±0.13	14.5 ±0.2	16.54 ±0.11	138.61 ±0.08
20.01 ±0.08	9.98 ±0.08	60.05 ±0.09	1.967 ±0.004	0.640 ±0.002	19.81 ±0.05	14.74 ±0.03	8.29 ±0.05	56.81 ±0.13	13.5 ±0.2	15.99 ±0.1	133.95 ±0.09
19.99 ±0.08	9.97 ±0.08	59.86 ±0.09	1.967 ±0.004	0.6501 ±0.0014	19.73 ±0.05	14.92 ±0.03	8.27 ±0.05	56.61 ±0.13	12.7 ±0.2	16.22 ±0.1	135.54 ±0.07
19.97 ±0.08	9.96 ±0.08	60.00 ±0.08	1.968 ±0.004	0.6452 ±0.0014	19.77 ±0.05	15.13 ±0.03	8.29 ±0.05	56.70 ±0.13	12.2 ±0.2	16.11 ±0.1	134.95 ±0.07
19.94 ±0.08	9.95 ±0.08	60.04 ±0.08	1.969 ±0.004	0.6395 ±0.0014	19.77 ±0.05	15.33 ±0.03	8.29 ±0.05	56.70 ±0.13	11.61 ±0.15	15.99 ±0.1	133.87 ±0.07
19.92 ±0.08	9.94 ±0.08	59.96 ±0.08	1.970 ±0.004	0.6356 ±0.0014	19.73 ±0.05	15.51 ±0.03	8.27 ±0.05	56.61 ±0.13	10.99 ±0.15	15.90 ±0.1	132.87 ±0.07
19.93 ±0.08	9.95 ±0.08	59.97 ±0.08	1.970 ±0.004	0.6279 ±0.0014	19.71 ±0.05	15.84 ±0.03	8.26 ±0.05	56.57 ±0.13	10.01 ±0.15	15.72 ±0.1	131.24 ±0.07
9.97 ±0.08	30.09 ±0.09	59.90 ±0.08	1.934 ±0.004	0.2271 ±0.0006	20.41 ±0.05	14.50 ±0.03	8.14 ±0.05	58.23 ±0.13	15.60 ±0.15	3.45 ±0.02	28.307 ±0.007
10.01 ±0.08	30.04 ±0.09	60.10 ±0.08	1.936 ±0.004	0.2032 ±0.0006	20.32 ±0.05	16.52 ±0.03	8.13 ±0.05	58.03 ±0.13	9.57 ±0.15	3.12 ±0.02	25.522 ±0.006
10.00 ±0.08	50.13 ±0.08	59.93 ±0.08	1.934 ±0.004	0.748 ±0.002	23.54 ±0.05	13.43 ±0.03	9.05 ±0.06	65.24 ±0.11	25.92 ±0.14	3.36 ±0.02	30.68 ±0.04
9.98 ±0.08	50.09 ±0.08	59.90 ±0.08	1.934 ±0.004	0.748 ±0.002	23.46 ±0.05	13.43 ±0.03	9.03 ±0.05	65.07 ±0.11	25.76 ±0.14	3.37 ±0.02	30.66 ±0.04
10.03	50.09	59.85	1.934	0.742	22.50	13.62	8.73	62.99	23.07	3.44	30.30

±0.08	±0.08	±0.08	±0.004	±0.002	±0.05	±0.03	±0.06	±0.12	±0.14	±0.02	±0.04
10.00 ±0.08	50.08 ±0.08	59.78 ±0.08	1.935 ±0.004	0.7278 ±0.0015	22.05 ±0.05	14.09 ±0.03	8.61 ±0.06	62.00 ±0.12	20.60 ±0.14	3.39 ±0.02	29.52 ±0.04
10.04 ±0.08	50.08 ±0.08	59.91 ±0.08	1.935 ±0.004	0.6907 ±0.0015	21.90 ±0.05	14.86 ±0.03	8.58 ±0.06	61.66 ±0.12	17.91 ±0.14	3.28 ±0.02	28.39 ±0.04
10.03 ±0.08	50.07 ±0.08	60.01 ±0.08	1.935 ±0.004	0.6681 ±0.0014	21.86 ±0.05	15.27 ±0.03	8.56 ±0.06	61.58 ±0.12	16.62 ±0.14	3.21 ±0.02	27.79 ±0.03
29.72 ±0.08	9.77 ±0.08	60.03 ±0.08	1.939 ±0.004	0.2843 ±0.0008	21.63 ±0.05	9.60 ±0.03	9.00 ±0.05	61.05 ±0.12	35.8 ±0.2	6.59 ±0.04	59.71 ±0.02
29.62 ±0.08	9.85 ±0.08	59.97 ±0.08	1.939 ±0.004	0.2788 ±0.0008	20.74 ±0.05	9.75 ±0.03	8.64 ±0.06	59.00 ±0.12	33.1 ±0.2	6.71 ±0.04	58.39 ±0.02
20.15 ±0.08	19.95 ±0.08	59.95 ±0.09	2.063 ±0.004	0.2813 ±0.0008	22.38 ±0.05	9.17 ±0.03	9.00 ±0.05	62.72 ±0.12	39.3 ±0.2	5.19 ±0.03	47.023 ±0.014
20.15 ±0.08	19.96 ±0.08	59.99 ±0.09	2.063 ±0.004	0.2782 ±0.0008	21.34 ±0.05	9.49 ±0.03	8.66 ±0.05	60.40 ±0.12	35.5 ±0.2	5.34 ±0.03	46.544 ±0.014
19.92 ±0.08	19.94 ±0.08	59.87 ±0.08	2.063 ±0.004	0.2626 ±0.0007	20.51 ±0.05	11.56 ±0.03	8.41 ±0.05	58.47 ±0.12	25.6 ±0.2	5.17 ±0.03	43.824 ±0.011
29.75 ±0.08	9.79 ±0.08	60.00 ±0.09	1.943 ±0.004	0.2214 ±0.0006	19.92 ±0.05	17.92 ±0.03	8.33 ±0.06	57.07 ±0.13	4.91 ±0.15	5.54 ±0.04	46.459 ±0.012
29.86 ±0.08	9.90 ±0.08	60.19 ±0.08	1.941 ±0.004	0.2833 ±0.0008	21.28 ±0.05	9.70 ±0.03	8.82 ±0.06	60.26 ±0.12	34.6 ±0.2	6.70 ±0.04	59.52 ±0.02
30.04 ±0.08	9.94 ±0.08	59.99 ±0.08	1.942 ±0.004	0.2776 ±0.0007	20.54 ±0.05	10.20 ±0.03	8.54 ±0.06	58.54 ±0.13	30.8 ±0.2	6.76 ±0.04	58.06 ±0.02
29.79 ±0.08	9.86 ±0.08	59.85 ±0.09	1.942 ±0.004	0.2723 ±0.0007	20.34 ±0.05	10.67 ±0.03	8.46 ±0.06	58.08 ±0.13	28.5 ±0.2	6.68 ±0.04	56.90 ±0.02
29.76 ±0.08	9.80 ±0.08	59.95 ±0.09	1.942 ±0.004	0.2483 ±0.0007	20.11 ±0.05	13.58 ±0.03	8.40 ±0.06	57.53 ±0.13	17.8 ±0.2	6.16 ±0.04	52.054 ±0.014
19.93 ±0.08	19.89 ±0.09	60.02 ±0.08	1.633 ±0.003	0.2668 ±0.0007	20.96 ±0.05	9.75 ±0.03	8.51 ±0.05	59.52 ±0.12	33.6 ±0.2	5.22 ±0.03	44.749 ±0.011
19.86 ±0.08	19.87 ±0.08	59.96 ±0.08	1.634 ±0.003	0.2604 ±0.0007	20.63 ±0.05	10.72 ±0.03	8.42 ±0.06	58.74 ±0.13	29.0 ±0.2	5.15 ±0.03	43.622 ±0.011
19.89 ±0.08	19.90 ±0.08	59.97 ±0.09	1.460 ±0.003	0.2353 ±0.0006	20.31 ±0.05	13.69 ±0.03	8.34 ±0.06	58.00 ±0.13	17.9 ±0.2	4.70 ±0.03	39.406 ±0.01
19.96 ±0.08	19.91 ±0.08	60.04 ±0.09	1.189 ±0.003	0.2044 ±0.0006	20.16 ±0.05	16.39 ±0.03	8.30 ±0.06	57.65 ±0.13	9.55 ±0.15	4.11 ±0.03	34.289 ±0.008
20.03 ±0.08	20.03 ±0.08	59.77 ±0.08	1.932 ±0.004	0.2780 ±0.0008	21.52 ±0.05	9.34 ±0.03	8.71 ±0.05	60.81 ±0.12	36.6 ±0.2	5.27 ±0.03	46.174 ±0.013
20.05 ±0.08	19.98 ±0.08	59.96 ±0.08	1.967 ±0.004	0.2730 ±0.0007	20.96 ±0.05	9.83 ±0.03	8.52 ±0.05	59.51 ±0.12	33.3 ±0.2	5.32 ±0.03	45.611 ±0.011
20.00 ±0.08	19.97 ±0.08	59.94 ±0.09	1.923 ±0.004	0.2621 ±0.0007	20.56 ±0.05	11.27 ±0.03	8.43 ±0.06	58.59 ±0.13	26.8 ±0.2	5.16 ±0.03	43.776 ±0.011

19.84 ±0.08	19.91 ±0.08	59.93 ±0.08	1.579 ±0.003	0.2117 ±0.0006	20.14 ±0.05	16.53 ±0.03	8.32 ±0.06	57.60 ±0.13	9.11 ±0.14	4.23 ±0.03	35.405 ±0.008
19.97 ±0.08	20.12 ±0.08	60.07 ±0.08	1.635 ±0.003	0.2093 ±0.0006	20.17 ±0.05	17.03 ±0.03	8.35 ±0.06	57.68 ±0.13	7.84 ±0.14	4.16 ±0.03	34.941 ±0.008
20.03 ±0.08	20.01 ±0.08	59.96 ±0.08	1.949 ±0.004	0.2788 ±0.0008	21.27 ±0.05	9.60 ±0.03	8.66 ±0.05	60.24 ±0.12	34.9 ±0.2	5.34 ±0.03	46.560 ±0.014
20.11 ±0.08	9.95 ±0.08	60.06 ±0.09	1.952 ±0.004	0.748 ±0.002	20.12 ±0.05	10.25 ±0.03	8.35 ±0.05	57.54 ±0.13	29.6 ±0.2	18.52 ±0.12	156.58 ±0.13
20.10 ±0.08	9.96 ±0.08	60.00 ±0.09	1.955 ±0.004	0.731 ±0.002	20.00 ±0.05	11.46 ±0.03	8.33 ±0.05	57.26 ±0.13	24.7 ±0.2	18.14 ±0.12	152.88 ±0.13
19.95 ±0.08	9.98 ±0.08	60.04 ±0.08	1.958 ±0.004	0.701 ±0.002	19.93 ±0.05	12.66 ±0.03	8.32 ±0.05	57.09 ±0.13	20.4 ±0.2	17.43 ±0.11	146.70 ±0.1
19.81 ±0.08	10.01 ±0.08	60.06 ±0.08	1.964 ±0.004	0.682 ±0.002	19.88 ±0.05	13.51 ±0.03	8.31 ±0.05	56.97 ±0.13	17.4 ±0.2	16.98 ±0.11	142.66 ±0.09
19.92 ±0.08	19.91 ±0.08	60.01 ±0.08	0.776 ±0.002	0.1853 ±0.0006	20.06 ±0.05	16.99 ±0.03	8.23 ±0.05	57.39 ±0.13	7.67 ±0.14	3.76 ±0.02	31.063 ±0.007
20.04 ±0.08	20.06 ±0.08	60.09 ±0.08	1.350 ±0.003	0.2658 ±0.0007	21.93 ±0.05	9.13 ±0.03	8.80 ±0.05	61.74 ±0.12	38.4 ±0.2	5.03 ±0.03	44.475 ±0.011
19.94 ±0.08	20.04 ±0.08	59.90 ±0.08	1.350 ±0.003	0.2622 ±0.0006	20.92 ±0.05	9.64 ±0.03	8.48 ±0.05	59.42 ±0.12	34.0 ±0.2	5.12 ±0.03	43.678 ±0.01
19.84 ±0.08	19.97 ±0.08	59.92 ±0.08	1.272 ±0.003	0.2442 ±0.0006	20.42 ±0.05	11.84 ±0.03	8.35 ±0.05	58.25 ±0.12	24.4 ±0.2	4.86 ±0.03	40.780 ±0.01
19.92 ±0.08	19.94 ±0.08	59.85 ±0.08	0.921 ±0.002	0.1921 ±0.0006	20.02 ±0.05	17.02 ±0.03	8.25 ±0.05	57.31 ±0.13	7.51 ±0.14	3.87 ±0.02	32.051 ±0.007
19.95 ±0.08	20.15 ±0.08	59.90 ±0.09	1.635 ±0.003	0.2740 ±0.0007	22.35 ±0.05	9.14 ±0.03	8.96 ±0.05	62.66 ±0.12	39.3 ±0.2	5.05 ±0.03	45.530 ±0.012
20.05 ±0.08	9.96 ±0.08	60.03 ±0.08	1.956 ±0.004	0.2112 ±0.0007	20.05 ±0.05	10.77 ±0.03	8.34 ±0.05	57.38 ±0.13	27.4 ±0.2	5.26 ±0.03	44.200 ±0.014
19.99 ±0.08	9.97 ±0.08	59.98 ±0.09	1.958 ±0.004	0.2098 ±0.0007	20.01 ±0.05	11.09 ±0.03	8.33 ±0.05	57.29 ±0.13	26.1 ±0.2	5.23 ±0.03	43.849 ±0.013
20.02 ±0.08	9.97 ±0.08	60.04 ±0.09	1.958 ±0.004	0.2076 ±0.0007	20.01 ±0.05	11.50 ±0.03	8.33 ±0.05	57.28 ±0.13	24.6 ±0.2	5.18 ±0.03	43.442 ±0.013
20.05 ±0.09	9.99 ±0.08	59.98 ±0.08	1.958 ±0.004	0.2070 ±0.0008	19.97 ±0.05	11.66 ±0.03	8.29 ±0.05	57.18 ±0.13	23.9 ±0.2	5.18 ±0.03	43.23 ±0.02
20.04 ±0.08	10.03 ±0.08	60.01 ±0.08	1.954 ±0.004	0.2359 ±0.0008	22.79 ±0.05	7.81 ±0.03	9.27 ±0.06	63.62 ±0.12	46.4 ±0.2	5.28 ±0.03	49.26 ±0.02
20.00 ±0.08	9.99 ±0.08	60.00 ±0.08	1.955 ±0.004	0.2358 ±0.0007	22.80 ±0.05	7.80 ±0.03	9.28 ±0.06	63.64 ±0.12	46.4 ±0.2	5.28 ±0.03	49.28 ±0.02
19.97 ±0.08	10.00 ±0.08	60.01 ±0.09	1.953 ±0.004	0.2323 ±0.0008	21.58 ±0.05	7.59 ±0.03	9.01 ±0.06	60.94 ±0.12	44.7 ±0.2	5.35 ±0.03	48.55 ±0.02
20.00 ±0.08	9.97 ±0.08	60.01 ±0.08	1.949 ±0.004	0.2302 ±0.0008	20.73 ±0.05	7.71 ±0.03	8.72 ±0.06	58.99 ±0.12	42.2 ±0.2	5.48 ±0.03	48.15 ±0.02

20.02 ±0.08	9.96 ±0.08	59.99 ±0.08	1.951 ±0.004	0.2276 ±0.0007	20.37 ±0.05	7.96 ±0.03	8.50 ±0.06	58.15 ±0.13	40.2 ±0.2	5.56 ±0.04	47.58 ±0.02

C.4 Results for the 10K2Vdesign

Table C.2: Experimental results and uncertainties for the 10K2V design

$T_{w,ei}$ [°C]	$T_{w,ci}$ [°C]	$T_{w,co}$ [°C]	$m_{w,e}$ [kg/h]	$m_{w,c}$ [kg/h]	p_c [bar]	p_{LR} [bar]	Wc [kW]	Tc [°C]	Sc [K]	COP_h [-]	Q_h [kW]
20.01 ±0.1	50.05 ±0.1	59.5 ±0.2	1.986 ±0.004	0.820 ±0.002	21.56 ±0.07	20.53 ±0.1	8.6 ±0.2	60.9 ±0.2	2.3 ±0.3	3.72 ±0.03	32.3 ±0.3
20.02 ±0.08	30.07 ±0.08	60.12 ±0.12	1.981 ±0.004	0.3240 ±0.0011	21.66 ±0.06	11.16 ±0.03	8.97 ±0.05	61.11 ±0.13	29.7 ±0.2	4.50 ±0.03	40.69 ±0.02
20.06 ±0.08	19.92 ±0.08	60.00 ±0.09	1.964 ±0.004	0.2530 ±0.0007	20.03 ±0.06	9.32 ±0.03	8.40 ±0.05	57.34 ±0.13	33.2 ±0.2	5.01 ±0.03	42.373 ±0.012
20.07 ±0.08	-0.03 ±0.09	59.96 ±0.09	1.964 ±0.004	0.2518 ±0.0007	19.91 ±0.05	9.45 ±0.03	8.34 ±0.05	57.04 ±0.13	32.4 ±0.2	5.11 ±0.03	42.83 ±0.02
20.04 ±0.08	20.05 ±0.08	60.00 ±0.09	1.965 ±0.004	0.2472 ±0.0007	19.68 ±0.05	9.98 ±0.03	8.26 ±0.05	56.50 ±0.13	29.6 ±0.2	4.96 ±0.03	41.265 ±0.01
20.04 ±0.08	19.95 ±0.08	60.02 ±0.08	0.669 ±0.002	0.2112 ±0.0006	19.60 ±0.05	9.21 ±0.03	8.15 ±0.05	56.29 ±0.13	34.7 ±0.2	4.32 ±0.03	35.364 ±0.008
20.01 ±0.08	19.96 ±0.08	59.96 ±0.08	0.669 ±0.002	0.2103 ±0.0006	19.35 ±0.05	9.68 ±0.03	8.07 ±0.05	55.68 ±0.13	32.1 ±0.2	4.34 ±0.03	35.149 ±0.008
20.03 ±0.08	19.95 ±0.08	60.01 ±0.08	0.892 ±0.002	0.2250 ±0.0006	19.79 ±0.05	9.19 ±0.03	8.26 ±0.05	56.76 ±0.13	33.2 ±0.2	4.54 ±0.03	37.674 ±0.009
19.93 ±0.08	19.97 ±0.08	59.99 ±0.08	0.892 ±0.002	0.2255 ±0.0006	19.55 ±0.05	9.67 ±0.03	8.17 ±0.05	56.17 ±0.13	30.6 ±0.2	4.60 ±0.03	37.723 ±0.009
20.04 ±0.08	19.96 ±0.08	59.99 ±0.08	1.424 ±0.003	0.2434 ±0.0007	20.00 ±0.05	9.18 ±0.03	8.37 ±0.05	57.26 ±0.13	33.7 ±0.2	4.84 ±0.03	40.727 ±0.01
20.00 ±0.08	20.00 ±0.09	59.96 ±0.08	1.425 ±0.003	0.2384 ±0.0007	19.61 ±0.05	9.79 ±0.03	8.23 ±0.05	56.33 ±0.13	30.2 ±0.2	4.81 ±0.03	39.822 ±0.011
20.01 ±0.08	19.95 ±0.09	59.97 ±0.08	0.481 ±0.003	0.1891 ±0.0007	19.24 ±0.05	9.23 ±0.03	7.93 ±0.05	55.42 ±0.13	34.0 ±0.2	3.97 ±0.03	31.636 ±0.011
20.01 ±0.08	19.95 ±0.08	59.97 ±0.09	0.481 ±0.002	0.1891 ±0.0006	19.24 ±0.05	9.23 ±0.03	7.93 ±0.05	55.42 ±0.13	34.0 ±0.2	3.97 ±0.03	31.636 ±0.007
20.00 ±0.08	19.98 ±0.08	59.97 ±0.08	0.480 ±0.002	0.1906 ±0.0006	19.09 ±0.05	9.69 ±0.03	7.91 ±0.05	55.04 ±0.13	31.5 ±0.2	4.02 ±0.03	31.867 ±0.007
14.98 ±0.08	19.93 ±0.08	59.98 ±0.09	1.386 ±0.003	0.2127 ±0.0006	19.46 ±0.05	9.42 ±0.03	8.13 ±0.05	55.95 ±0.13	33.6 ±0.2	4.36 ±0.03	35.612 ±0.009

15.02 ±0.08	19.97 ±0.09	59.97 ±0.09	1.386 ±0.003	0.2120 ±0.0006	19.36 ±0.05	9.65 ±0.03	8.09 ±0.05	55.71 ±0.13	32.2 ±0.2	4.36 ±0.03	35.441 ±0.009
15.03 ±0.08	20.00 ±0.08	60.00 ±0.08	1.960 ±0.004	0.2200 ±0.0006	19.54 ±0.05	9.42 ±0.03	8.18 ±0.05	56.14 ±0.13	33.6 ±0.2	4.47 ±0.03	36.793 ±0.009
15.01 ±0.08	20.04 ±0.09	60.02 ±0.09	1.961 ±0.004	0.2182 ±0.0006	19.45 ±0.05	9.69 ±0.03	8.13 ±0.05	55.92 ±0.13	32.3 ±0.2	4.45 ±0.03	36.464 ±0.009
14.97 ±0.08	19.92 ±0.08	60.01 ±0.08	0.619 ±0.002	0.1795 ±0.0006	18.99 ±0.05	9.46 ±0.03	7.84 ±0.05	54.80 ±0.13	32.2 ±0.2	3.82 ±0.03	30.073 ±0.007
14.98 ±0.08	19.93 ±0.08	59.97 ±0.08	0.619 ±0.002	0.1804 ±0.0006	18.93 ±0.05	9.70 ±0.03	7.83 ±0.06	54.66 ±0.13	31.1 ±0.2	3.84 ±0.03	30.193 ±0.007
14.99 ±0.08	19.97 ±0.08	60.00 ±0.08	0.940 ±0.002	0.2003 ±0.0006	19.30 ±0.05	9.43 ±0.03	8.02 ±0.06	55.57 ±0.13	33.2 ±0.2	4.16 ±0.03	33.514 ±0.008
15.07 ±0.08	19.96 ±0.08	60.00 ±0.08	0.940 ±0.002	0.1995 ±0.0006	19.21 ±0.05	9.70 ±0.03	8.00 ±0.06	55.35 ±0.13	31.8 ±0.2	4.15 ±0.03	33.388 ±0.008
34.96 ±0.08	19.98 ±0.08	60.02 ±0.08	1.946 ±0.004	0.3659 ±0.0009	20.59 ±0.05	9.80 ±0.03	8.62 ±0.05	58.66 ±0.12	34.2 ±0.2	7.06 ±0.04	61.24 ±0.02
35.00 ±0.08	20.02 ±0.08	60.02 ±0.08	1.946 ±0.004	0.3662 ±0.0009	20.49 ±0.05	10.06 ±0.03	8.55 ±0.05	58.43 ±0.12	32.9 ±0.2	7.11 ±0.04	61.22 ±0.02
35.02 ±0.09	19.99 ±0.08	60.00 ±0.09	0.650 ±0.002	0.2817 ±0.0008	20.01 ±0.05	9.85 ±0.03	8.42 ±0.05	57.29 ±0.13	32.9 ±0.2	5.57 ±0.04	47.09 ±0.02
34.98 ±0.08	20.00 ±0.08	60.01 ±0.08	0.650 ±0.002	0.2785 ±0.0008	19.89 ±0.05	10.08 ±0.03	8.40 ±0.05	57.00 ±0.13	31.5 ±0.2	5.52 ±0.03	46.562 ±0.015
35.00 ±0.08	19.98 ±0.08	60.06 ±0.08	1.472 ±0.003	0.3558 ±0.0009	20.50 ±0.05	9.80 ±0.03	8.60 ±0.05	58.46 ±0.13	34.0 ±0.2	6.89 ±0.04	59.59 ±0.02
35.08 ±0.08	20.07 ±0.08	60.00 ±0.08	1.472 ±0.003	0.3541 ±0.0009	20.40 ±0.05	10.10 ±0.03	8.54 ±0.05	58.22 ±0.13	32.6 ±0.2	6.88 ±0.04	59.09 ±0.02
35.02 ±0.08	20.06 ±0.08	59.91 ±0.08	0.3682 ±0.0015	0.2338 ±0.0006	19.59 ±0.05	9.74 ±0.03	8.22 ±0.05	56.28 ±0.13	32.7 ±0.2	4.72 ±0.03	38.937 ±0.01
34.93 ±0.08	19.97 ±0.08	59.98 ±0.08	0.3053 ±0.0014	0.2044 ±0.0006	19.22 ±0.05	9.91 ±0.03	8.02 ±0.05	55.37 ±0.13	30.9 ±0.2	4.25 ±0.03	34.180 ±0.008
20.08 ±0.08	30.07 ±0.08	59.98 ±0.09	1.936 ±0.004	0.3156 ±0.0008	20.12 ±0.05	12.31 ±0.03	8.47 ±0.05	57.54 ±0.13	22.0 ±0.2	4.56 ±0.03	39.446 ±0.012
20.08 ±0.08	30.06 ±0.09	60.15 ±0.09	1.937 ±0.004	0.3113 ±0.0008	20.06 ±0.05	12.90 ±0.03	8.45 ±0.05	57.41 ±0.13	19.9 ±0.2	4.56 ±0.03	39.147 ±0.013
20.04 ±0.08	30.07 ±0.09	59.84 ±0.09	1.937 ±0.004	0.3115 ±0.0008	19.88 ±0.05	13.51 ±0.03	8.36 ±0.05	56.98 ±0.13	17.5 ±0.2	4.56 ±0.03	38.768 ±0.012
20.05 ±0.08	49.91 ±0.08	60.02 ±0.08	1.940 ±0.004	0.855 ±0.002	22.25 ±0.05	17.49 ±0.03	9.17 ±0.05	62.44 ±0.12	11.30 ±0.14	3.87 ±0.02	36.17 ±0.05
20.03 ±0.08	49.94 ±0.08	60.06 ±0.08	1.941 ±0.004	0.834 ±0.002	21.86 ±0.05	18.30 ±0.03	9.04 ±0.05	61.58 ±0.12	8.34 ±0.14	3.83 ±0.02	35.33 ±0.05
20.05 ±0.08	49.89 ±0.08	59.87 ±0.08	1.941 ±0.004	0.831 ±0.002	21.66 ±0.05	19.05 ±0.03	8.97 ±0.05	61.12 ±0.12	6.04 ±0.14	3.79 ±0.02	34.70 ±0.05

20.10 ±0.08	49.94 ±0.08	60.02 ±0.08	1.942 ±0.004	0.809 ±0.002	21.61 ±0.05	19.90 ±0.03	8.94 ±0.06	61.02 ±0.12	3.91 ±0.13	3.74 ±0.02	34.10 ±0.05
19.95 ±0.08	49.97 ±0.08	60.02 ±0.08	1.943 ±0.004	0.795 ±0.002	21.55 ±0.05	20.60 ±0.03	8.92 ±0.06	60.87 ±0.12	2.13 ±0.13	3.67 ±0.02	33.43 ±0.04
20.05 ±0.08	9.98 ±0.08	60.09 ±0.09	1.920 ±0.004	0.2207 ±0.0006	20.70 ±0.06	6.91 ±0.03	8.67 ±0.05	58.92 ±0.13	46.2 ±0.2	5.25 ±0.03	46.217 ±0.012
20.08 ±0.08	9.98 ±0.08	60.05 ±0.09	1.921 ±0.004	0.2112 ±0.0006	19.28 ±0.06	8.04 ±0.03	8.17 ±0.05	55.50 ±0.14	39.0 ±0.2	5.32 ±0.03	44.184 ±0.012
20.07 ±0.08	10.10 ±0.08	60.69 ±0.08	1.922 ±0.004	0.2054 ±0.0006	19.37 ±0.05	8.36 ±0.03	8.17 ±0.05	55.73 ±0.13	35.8 ±0.2	5.22 ±0.03	43.424 ±0.011
20.03 ±0.08	30.20 ±0.09	60.01 ±0.09	1.933 ±0.004	0.3225 ±0.0008	20.79 ±0.06	11.22 ±0.03	8.65 ±0.05	59.13 ±0.13	27.5 ±0.2	4.57 ±0.03	40.192 ±0.013
20.02 ±0.08	30.25 ±0.08	60.50 ±0.09	1.933 ±0.004	0.3139 ±0.0008	20.48 ±0.05	11.79 ±0.03	8.53 ±0.05	58.40 ±0.13	24.7 ±0.2	4.57 ±0.03	39.688 ±0.013
19.99 ±0.08	10.08 ±0.08	59.95 ±0.09	1.936 ±0.004	0.2171 ±0.0006	19.67 ±0.05	7.35 ±0.03	8.28 ±0.05	56.47 ±0.13	41.4 ±0.2	5.38 ±0.03	45.252 ±0.012
20.03 ±0.08	10.01 ±0.08	60.05 ±0.09	1.942 ±0.004	0.2130 ±0.0006	19.43 ±0.05	7.70 ±0.03	8.21 ±0.05	55.88 ±0.13	39.1 ±0.2	5.33 ±0.03	44.545 ±0.011
20.03 ±0.08	10.01 ±0.08	60.05 ±0.09	1.942 ±0.004	0.2130 ±0.0006	19.43 ±0.05	7.70 ±0.03	8.21 ±0.05	55.88 ±0.13	39.0 ±0.2	5.33 ±0.03	44.545 ±0.011